High-Capacity Hybrid Optical Fiber-Wireless Communications Links in Access Networks

Xiaodan Pang
Ph.D. Thesis
June 2013

DTU Fotonik
Department of Photonics Engineering

High-Capacity Hybrid Optical Fiber-Wireless Communications Links in Access Networks

Xiaodan Pang

Supervisors:

Professor Idelfonso Tafur Monroy

Professor Søren Forchhammer and

Assistant Professor Juan José Vegas Olmos

Delivery Date: 30th June 2013

DTU Fotonik
Department of Photonics Engineering
Technical University of Denmark
2800 Kgs. Lyngby
DENMARK

DTU Fotonik
Institut for Fotonik

Abstract

Integration between fiber-optic and wireless communications systems in the "last mile" access networks is currently considered as a promising solution for both service providers and users, in terms of minimizing deployment cost, shortening upgrading period and increasing mobility and flexibility of broadband services access. To realize the seamless convergence between the two network segments, the lower capacity of wireless systems need to be increased to match the continuously increasing bandwidth of fiber-optic systems. The research works included in this thesis are devoted to experimental investigations of photonic-wireless links with record high capacities to fulfill the requirements of next generation hybrid optical fiber-wireless access networks. The main contributions of this thesis have expanded the state-of-the-art in two main areas: high speed millimeter-wave (mm-wave) communication links and radio-over-fiber (RoF) systems employing wireless multi-input multi-output (MIMO) multiplexing technologies.

Regarding high speed mm-wave links, this thesis focuses on high capacity fiber-wireless transmissions in both the V-band (50-75 GHz) and the W-band (75-110 GHz). Photonic mm-wave signal generation techniques with both coherent and incoherent optical sources are studied and demonstrated. Employments of advanced modulation formats including phase-shift keying (PSK), M-quadrature amplitude modulation (QAM) and orthogonal frequency-division multiplexing (OFDM) for high speed photonic-wireless transmission are experimentally investigated. Furthermore, this thesis also studies the implementation of bidirectional operations in hybrid optical fiber-wireless systems.

In addition, this thesis proposes and demonstrates the seamless translation of both fiber wavelength division multiplexing (WDM) and polarization multiplexing (PolMux) RoF systems into wireless MIMO links, to increase the spectral efficiency and overall throughput of bandwidth lim-

ited fiber-wireless systems. Two different modulation formats: MIMO-OFDM and MIMO-quadrature PSK (QPSK), are experimentally investigated based on different channel estimation techniques.

In conclusion, the results presented in the thesis show the feasibility of employing mm-wave signals, advanced modulation formats and spatial multiplexing technologies in next generation high capacity hybrid optical fiber-wireless access systems.

Resumé

Integrationen mellem fiberoptiske og trådløse kommunikationssystemer i "last mile" acces-net betragtes på nuværende tidspunkt som en lovende løsning for både leverandører og brugere i forhold til lavere implementeringsomkostninger, kortere opgraderingstider samt højere mobilitet og fleksibilitet for adgang til bredbåndsservice. For at realisere den sømløse konvergens mellem to netværkssegmenter, må den lavere kapacitet af trådløse systemer øges for at tilpasses den stigende båndbredde i fiberoptiske systemer. Forskningen, som indgår i denne afhandling, fokuserer på eksperimentelle undersøgelser af hybride trådløse/fiberoptiske forbindelser med rekordhøj kapacitet. De væsentlige bidrag for denne afhandling har udvidet state-of-the-art indenfor især to hovedområder: Højhastighed millimeter-bølge (mm-bølger) kommunikationsforbindelser og radio-over-fiber (RoF) systemer, som anvender trådløs multipel input multipel output (MIMO) multiplexningsteknologi.

I forbindelse med højhastigheds- mm-bølge forbindelser fokusere denne afhandling på høj kapacitets fiber-trådløs transmission i både V-båndet (50-75 GHz) og W-båndet (75-110 GHz). Optisk mm-bølge signal generationsteknik med både kohærente og inkohærente optiske kilder er undersøgt og demonstreret. Anvendelsen af avancerede modulationsformater (faseskift keying (PSK), M-kvadratur amplitude modulation (QAM) og ortogonale frekvens division multiplexning (OFDM)) for højhastigheds hybride fiberoptisk/trådløs transmission er eksperimentelt undersøgt. Ydermere undersøges der også i denne afhandling implementeringen af tovejs operationer i optiske hybride fiberoptiske/trådløse systemer.

Endvidere foreslår og demonstrerer denne afhandling den sømløse oversættelse af både fiber bølgelængde division multiplexning (WDM) og polarisation multiplexing (PolMux) RoF systemer i trådløse MIMO forbindelser for at øge den spektrale effektivitet og den samlede kapacitet

på båndbredde begrænsede fiber-trådløse systemer. To forskellige modulationsformater: MIMO-OFDM og MIMO-kvadratur PSK (QPSK), er eksperimentelt undersøgt baseret på forskellige kanal estimerings teknikker.

Som konklusion viser resultaterne i afhandlingen muligheden for at anvende mm-bølge signaler, avancerede modulationsformater og rumlige multiplexning teknologi i næste generations med høj kapacitet hybride fiberoptiske/trådløse acces systemer.

Acknowledgements

First of all, I would like to thank my main supervisor, Professor Idelfonso Tafur Monroy from Metro-Access & Short Range Systems group, for his guidance, encouragement and support along the way. Idelfonso shows me the importance of both optimism and courage to grasp opportunities by taking risks and challenges. There are and will always be ups and downs in life, and these values I learned from Idelfonso are priceless to my future.

I am very grateful to my co-supervisor, J.J. Vegas Olmos for all the interesting discussions, valuable advices and patient helps. I really have learned a lot from J.J about his professional way of doing things in all aspects.

I must give my special thanks to my co-supervisor Professor Søren Forchhammer from Coding and Visual Communication group, for his kindness and great understanding of my research interests and work, even though they are not quite related to video and coding. Here I sincerely hope that this thesis could provide a common platform for future researchers from both Metro-Access group and Coding group to perform better collaborations in more exciting topics on top of my work.

I am grateful to Professor Roberto Llorente, for accepting me into his research group in Nanophotonics Technology Center in Valencia, Spain and providing me the opportunity to work with the excellent researchers there. I must express my gratitude to Marta, Maria, Eloy and family, José, Pau and Luis for helping me to survive and enjoy a lot of my life across the barrier of language. You people are my most valuable memory I have in Spain.

My sincerely gratitude is to Xianbin, who patiently guided me off a smooth start of my PhD since the first day. The time we discussed ideas together, took challenges together and worked in the lab together, is unforgettable experience of mine.

I would like to give my warmest thanks to my "comrades-in-arms" Lei, Ying, Xu, Alexander, Maisara and Anton. We were spending days and nights, weekends after weekends, Christmas and even New Year's Eve in the lab. Nothing in this thesis can be done without their great efforts. I would also like to thank all my former and current colleagues at Metro-Access group, Darko, Jesper, Antonio, Robert, Valeria, Bomin, Miguel, Xema, Silvia, Roberto, Thang, Neil, Kamau and also my dearest friends in DTU Fotonik, Yunhong, Tianwu, Francesco, Bobo, Evarist, Stanley, Yiyu, Hao... I am honored getting to know you wonderful people here.

I want to thank all my Chinese friends in Denmark. We have been like a family all the time. As one Chinese poetry says, as we are friends, no matter wherever we are in this world, we are always closest neighbors.

The last, and foremost, to my family: Mom Mingling Dong, Dad Xingwu Pang, and my sister Huifeng, thank you for always being with me. The distance brings us even closer than ever. My special thanks to my wife, Xiaofen Zhang, for the sharing and caring, for everything that beyond the reach of my words.

Denmark, 28 June, 2013

Xiaodan Pang

Summary of Original Work

This thesis is based on the following original publications:

PAPER 1 Xiaodan Pang, Xianbin Yu, Ying Zhao, Lei Deng, Darko Zibar, and Idelfonso Tafur Monroy, "Experimental characterization of a hybrid fiber-wireless transmission link in the 75 to 110 GHz band," *Optical Engineering*, vol. 51, pp. 045004, 2012.

PAPER 2 Xiaodan Pang, Antonio Caballero, Anton Dogadaev, Valeria Arlunno, Lei Deng, Robert Borkowski, Jesper S. Pedersen, Darko Zibar, Xianbin Yu, and Idelfonso Tafur Monroy, "25 Gbit/s QPSK Hybrid Fiber-Wireless Transmission in the W-Band (75-110 GHz) With Remote Antenna Unit for In-Building Wireless Networks," *IEEE Photonics Journal*, vol. 4, pp. 691-698, 2012.

PAPER 3 Xiaodan Pang, Antonio Caballero, Anton Dogadaev, Valeria Arlunno, Robert Borkowski, Jesper S. Pedersen, Lei Deng, Fotini Karinou, Fabien Roubeau, Darko Zibar, Xianbin Yu, and Idelfonso Tafur Monroy, "100 Gbit/s hybrid optical fiber-wireless link in the W-band (75-110 GHz)," *Optics Express*, vol. 19, pp. 24944-24949, 2011.

PAPER 4 Lei Deng, Marta Beltrán, **Xiaodan Pang**, Xu Zhang, Valeria Arlunno, Ying Zhao, Antonio Caballero, Anton Dogadaev, Xianbin Yu, Roberto Llorente, Deming Liu, Idelfonso Tafur Monroy, "Fiber Wireless Transmission of 8.3 Gb/s/ch QPSK-OFDM Signals in 75-110 GHz Band," *IEEE Photonics Technology Letters*, vol. 24, pp. 383-385, 2012.

PAPER 5 Marta Beltrán, Lei Deng, **Xiaodan Pang**, Xu Zhang, Valeria Arlunno, Ying Zhao, Xianbin Yu, Roberto Llorente, Deming Liu, Idelfonso Tafur Monroy, "Single- and Multiband OFDM Photonic Wireless Links in the 75-110 GHz Band Employing Optical Combs," *IEEE Photonics Journal*, vol. 4, pp. 2027-2036, 2012.

PAPER 6 Lei Deng, Deming Liu, **Xiaodan Pang**, Xu Zhang, Valeria Arlunno, Ying Zhao, Antonio Caballero, Anton Dogadaev, Xianbin Yu, Idelfonso Tafur Monroy, Marta Beltrán, Roberto Llorente, "42.13 Gbit/s 16QAM-OFDM Photonics-Wireless Transmission in 75-110 GHz Band," *Progress In Electromagnetics Research*, vol. 126, pp. 449-461, 2012.

PAPER 7 Xiaodan Pang, Lei Deng, Anton Dogadaev, Xu Zhang, Xianbin Yu, Idelfonso Tafur Monroy, "Uplink transmission in the W-band (75-110 GHz) for hybrid optical fiber-wireless access networks," *Microwave and Optical Technology Letters*, vol. 55, pp. 1033-1036, 2013.

PAPER 8 Xiaodan Pang, Marta Beltrán, José Sánchez, Eloy Pellicer, J.J. Vegas Olmos, Roberto Llorente, Idelfonso Tafur Monroy, "DWDM Fiber-Wireless Access System with Centralized Optical Frequency Comb-based RF Carrier Generation," *The Optical Fiber Communication Conference and Exposition and the National Fiber Optic Engineers Conference, OFC/NFOEC'13*, Anaheim, CA, USA, 2013, paper JTh2A.56.

PAPER 9 Xiaodan Pang, J.J. Vegas Olmos, Alexander Lebedev, Idelfonso Tafur Monroy, "A Multi-gigabit W-Band Bidirectional Seamless Fiber-Wireless Transmission System with Simple Structured Access Point," *39th European Conference on Optical Communication, ECOC'13*, accepted for presentation.

PAPER 10 Xiaodan Pang, J.J. Vegas Olmos, Alexander Lebedev, Idelfonso Tafur Monroy, "A 15-meter Multi-Gigabit W-band Bidirectional Wireless Bridge in Fiber-Optic Access Networks," *IEEE*

International Topical Meeting on Microwave Photonics, MWP'13, 2013, accepted for presentation.

PAPER 11 Maisara B. Othman, Lei Deng, **Xiaodan Pang**, Josu Caminos, W. Kozuch, K. Prince, Xianbin Yu, Jesper B. Jensen, and Idelfonso Tafur Monroy, "MIMO-OFDM WDM PON with DM-VCSEL for Femtocells Application," *Optics Express*, vol. 19, pp. B537-B542, 2011.

PAPER 12 Xiaodan Pang, Lei Deng, Ying Zhao, Maisara B. Othman, Xianbin Yu, Jesper B. Jensen, Darko Zibar, and Idelfonso Tafur Monroy, "Seamless Translation of Optical Fiber PolMux-OFDM into a 2×2 MIMO Wireless Transmission Enabled by Digital Training-Based Fiber-Wireless Channel Estimation," *In Proc. Asia Communications and Photonics Conference and Exhibition, ACP'11*, Shanghai, China, 2011, paper 83090C-1.

PAPER 13 Lei Deng, **Xiaodan Pang**, Ying Zhao, Maisara B. Othman, Jesper B. Jensen, Darko Zibar, Xianbin Yu, Deming Liu, and Idelfonso Tafur Monroy, "2×2 MIMO-OFDM Gigabit Fiber-Wireless Access System Based on Polarization Division Multiplexed WDM-PON," *Optics Express*, vol. 20, pp. 4369-4375, 2012.

PAPER 14 Xiaodan Pang, Lei Deng, Ying Zhao, Maisara B. Othman, Jesper B. Jensen, Darko Zibar, Xianbin Yu, Deming Liu, and Idelfonso Tafur Monroy, "A Spectral Efficient PolMux-QPSK-RoF System with CMA-Based Blind Estimation of a 2×2 MIMO Wireless Channel," *In Proc. IEEE Photonics Conference, IPC'11*, Arlington, VA, USA, 2011, paper TuM2.

Other scientific reports associated with the project:

[PAPER 15] **Xiaodan Pang**, Xianbin Yu, Ying Zhao, Lei Deng, Darko Zibar, and Idelfonso Tafur Monroy, "Channel Measurements for a Optical Fiber-Wireless Transmission System in the 75-110 GHz Band," *IEEE Topical Meeting on Microwave Photonics, MWP'11*, Singapore, 2011, paper 2151.

[PAPER 16] Darko Zibar, Antonio Caballero, Xianbin Yu, **Xiaodan Pang**, Anton Dogadaev, Idelfonso Tafur Monroy, "Hybrid optical fibre-wireless links at the 75-110 GHz band supporting 100 Gbps transmission capacities," *IEEE Topical Meeting on Microwave Photonics, MWP'11*, pp. 445-449, Singapore, 2011, (Invited).

[PAPER 17] Marta Beltrán, Lei Deng, **Xiaodan Pang**, Xu Zhang, Valeria Arlunno, Ying Zhao, Xianbin Yu, Roberto Llorente, Deming Liu, Idelfonso Tafur Monroy, "38.2-Gb/s Optical-Wireless Transmission in 75-110 GHz Based on Electrical OFDM with Optical Comb Expansion," *The Optical Fiber Communication Conference and Exposition and the National Fiber Optic Engineers Conference, OFC/NFOEC'12*, Los Angeles, CA, USA, 2012, paper OM2B.2.

[PAPER 18] Lei Deng, **Xiaodan Pang**, Xu Zhang, Xianbin Yu, Deming Liu, Idelfonso Tafur Monroy, "Nonlinearity and Phase Noise Tolerant 75-110 GHz Signal over Fiber System Using Phase Modulation Technique," *The Optical Fiber Communication Conference and Exposition and the National Fiber Optic Engineers Conference, OFC/NFOEC'13*, Anaheim, CA, USA, 2013, JTh2A.55.

[PAPER 19] **Xiaodan Pang**, Alexander Lebedev, J.J. Vegas Olmos, Marta Beltrán, Roberto Llorente, Idelfonso Tafur Monroy, "Performance Evaluation for DFB and VCSEL-based 60 GHz Radio-over-Fiber System," *7th International Conference on Optical Network Design and Modeling, ONDM'13*, pp. 251-255, Brest, France, 2013.

[PAPER 20] **Xiaodan Pang**, Alexander Lebedev, J.J. Vegas Olmos, Idelfonso Tafur Monroy, "Seamless Optical Fiber-Wireless Millimeter-Wave Transmission Link for Access Networks," *CLEO-PR& OECC/ PS 2013*, Kyoto, Japan, 2013, paper TuPP-12.

[PAPER 21] J.J. Vegas Olmos, **Xiaodan Pang**, Alexander Lebedev, Idelfonso Tafur Monroy, "VCSEL sources for optical fiber-wireless composite data links at 60GHz," *CLEO-PR&OECC/PS 2013*, Kyoto, Japan, 2013, paper TuPP-10.

[PAPER 22] Alexander Lebedev, **Xiaodan Pang**, J.J. Vegas Olmos, Idelfonso Tafur Monroy, Søren Forchhammer "Tunable photonic RF generator for dynamic allocation and multicast of 1.25 Gbps channels in the 60 GHz unlicensed band," *IEEE MTT International Microwave Symposium, IMS'13*, Seattle, WA, USA, 2013, paper THPP-1.

[PAPER 23] **Xiaodan Pang**, Xianbin Yu, Ying Zhao, Lei Deng, Darko Zibar, Idelfonso Tafur Monroy, "A Novel Reconfigurable Ultra - Broadband Millimeter-wave Photonic Harmonic Down-converter," *IEEE Topical Meeting on Microwave Photonics, MWP'11*, Singapore, 2011, paper 2152.

[PAPER 24] Ying Zhao, **Xiaodan Pang**, Lei Deng, Xianbin Yu, Xiaoping Zheng, Idelfonso Tafur Monroy, "Ultra-Broadband Photonic Harmonic Mixer Based on Optical Comb Generation," *IEEE Photonics Technology Letters*, vol. 24, pp. 16-18, 2012.

[PAPER 25] Alexander Lebedev, J.J. Vegas Olmos, **Xiaodan Pang**, Søren Forchhammer, Idelfonso Tafur Monroy, "Demonstration and Comparison Study for V- and W-Band Real-Time High-Definition Video Delivery in Diverse Fiber-Wireless Infrastructure," *Fiber and Integrated Optics*, vol. 32, pp. 93-104, 2013.

[PAPER 26] Ying Zhao, Lei Deng, **Xiaodan Pang**, Xianbin Yu, Xiaoping Zheng, Hanyi Zhang, Idelfonso Tafur Monroy, "Digital Predistortion of 75-110 GHz W-Band Frequency Multiplier for Fiber

Wireless Short Range Access Systems," *37th European Conference on Optical Communication, ECOC'11*, Geneva, Switzerland, 2011, paper Tu.5.A.3.

[PAPER 27] Ying Zhao, Lei Deng, **Xiaodan Pang**, Xianbin Yu, Xiaoping Zheng, Hanyi Zhang, Idelfonso Tafur Monroy, "Digital predistortion of 75-110 GHz W-band frequency multiplier for fiber wireless short range access systems," *Optics Express*, vol. 19, pp. B18-B25, 2011.

[PAPER 28] Alexander Lebedev, **Xiaodan Pang**, J.J. Vegas Olmos, Marta Beltrán, Roberto Llorente, Søren Forchhammer, Idelfonso Tafur Monroy, "Fiber-supported 60 GHz mobile backhaul links for access/ metropolitan deployment," *17th International Conference on Optical Network Design and Modeling, ONDM'13*, pp. 189-192, Brest, France, 2013.

[PAPER 29] Maisara Binti Othman, Lei Deng, **Xiaodan Pang**, Josu Caminos, W. Kozuch, K. Prince, Xianbin Yu, Jesper B. Jensen, and Idelfonso Tafur Monroy, "Directly modulated VCSELs for 2×2 MIMO-OFDM radio over fiber in WDM-PON," in *37th European Conference and Exhibition on Optical Communication, ECOC'11*, Geneva, Switzerland, 2011, paper We.10.P1.119.

[PAPER 30] Ying Zhao, **Xiaodan Pang**, Lei Deng, Xianbin Yu, Xiaoping Zheng, Hanyi Zhang, Idelfonso Tafur Monroy, "Experimental Demonstration of 5-Gb/s Polarization-Multiplexed Fiber-Wireless MIMO Systems", *IEEE Topical Meeting on Microwave Photonics, MWP'11*, Singapore, 2011, paper 2144.

Other scientific reports:

[C1] Xu Zhang, **Xiaodan Pang**, Anton Dogadaev, Idelfonso Tafur Monroy, Darko Zibar, Richard Younce, "High Spectrum Narrowing Tolerant 112 Gb/s Dual Polarization QPSK Optical Communication Systems Using Digital Adaptive Channel Estimation," *The Optical Fiber Communication Conference and Exposition and the National Fiber Optic Engineers Conference, OFC/NFOEC'12,* Los Angeles, CA, USA, 2012, paper JW2A.49.

[C2] Xu Zhang, **Xiaodan Pang**, Lei Deng, Darko Zibar, Idelfonso Tafur Monroy, Richard Younce, "High phase noise tolerant pilot-tone-aided DP-QPSK optical communication systems," *Optics Express,* vol. 20, pp. 19990-19995, 2012.

[C3] Xianbin Yu, Ying Zhao, Lei Deng, **Xiaodan Pang**, Idelfonso Tafur Monroy, "Existing PON Infrastructure Supported Hybrid Fiber - Wireless Sensor Networks," *The Optical Fiber Communication Conference and Exposition and the National Fiber Optic Engineers Conference, OFC/NFOEC'12*, Los Angeles, CA, USA, 2012, paper JTh2A.32.

[C4] Ying Zhao, **Xiaodan Pang**, Lei Deng, Xianbin Yu, Xiaoping Zheng, Bingkun Zhou, Idelfonso Tafur Monroy, "High Accuracy Microwave Frequency Measurement Based on Single-Drive Dual-Parallel Mach-Zehnder Modulator," *37th European Conference on Optical Communication, ECOC'11*, Geneva, Switzerland, 2011, We.10.P1.118.

[C5] Ying Zhao, **Xiaodan Pang**, Lei Deng, Xianbin Yu, Xiaoping Zheng, Bingkun Zhou, Idelfonso Tafur Monroy, "High accuracy microwave frequency measurement based on single-drive dual-parallel Mach-Zehnder modulator," *Optics Express*, vol. 19, pp. B681-B686, 2011.

[C6] Xu Zhang, Maisara B. Othman, **Xiaodan Pang**, Jesper B. Jensen, Idelfonso Tafur Monroy, "Bi-directional Multi Dimension CAP Transmission for Smart Grid Communication Services," Asia Com-

munications and Photonics Conference (ACP), Guangzhou, China, 2012, paper AS3CA.

[C7]   G.A. Rodes Lopez, J.J. Vegas Olmos, Fotini Karinou, I. Roudas, Lei Deng, **Xiaodan Pang**, Idelfonso Tafur Monroy, "Optical Switching for Dynamic Distribution of Wireless-over-Fiber Signals," *16th International Conference on Optical Network Design and Modeling, ONDM'12*, pp. 1-4, Colchester, UK, 2012.

[C8]   Lei Deng, Ying Zhao, **Xiaodan Pang**, Xianbin Yu, Jesper B. Jensen, Deming Liu and Idelfonso Tafur Monroy, "Colorless ONU Based on All-VCSEL Sources with Remote Optical Injection for WDM-PON", *IEEE Photonics Conference, IPC'11*, Arlington, USA, 2011, paper TuE3.

[C9]   Lei Deng, Ying Zhao, **Xiaodan Pang**, Xianbin Yu, Deming Liu, Idelfonso Tafur Monroy, "Intra and Inter-PON ONU to ONU Virtual Private Networking using OFDMA in a Ring Topology", *IEEE Topical Meeting on Microwave Photonics, MWP'11*, Singapore, 2011, paper 2147.

Contents

Chapter 1

Introduction

1.1   Outline of the thesis

The overall objective of this thesis is to develop ultra-broadband hybrid optical fiber-wireless communication links with record capacities employing photonic technologies. The thesis is organized in 3 chapters as follows: Chapter 1 introduces the context of the main research papers included in this thesis. Section 1.2 provides a short overview of the application scenarios of the hybrid optical fiber-wireless systems with emphasis on the motivation of converging fiber-optic access and wireless networks and the necessity of increasing the wireless-link capacity. In section 1.3, high capacity millimeter-wave (mm-wave) photonic-wireless links for hybrid fiber-wireless access networks are presented, where different photonic up-conversion schemes for mm-wave signal generation are particularly highlighted. Section 1.4 presents the idea of adopting multi-input multi-output (MIMO) technology in the optical fiber-wireless system, which combines multiple parallel channels into the system hence achieving higher overall transmission throughput. Section 1.5 analyzes the state-of-the-art in both the high capacity mm-wave communication links and MIMO multiplexing technology. Finally, Section 1.6 describes the main contributions of this thesis and how they have extended the state-of-the-art.

Chapter 2 describes the main contributions of each publication included in this thesis. To conclude, Chapter 3 summarizes the main achievements of this thesis and provides an outlook to the future advancement of hybrid optical fiber-wireless communication links.
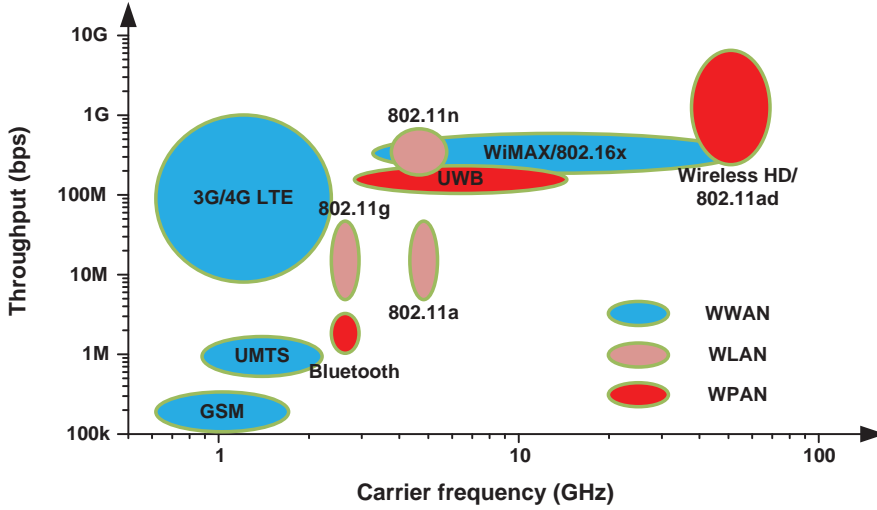
1.2   Hybrid optical fiber-wireless communication links for next generation access networks

Over the last decades, driven by the increasing number of internet users, the worldwide demand for data communication has been growing with enormous rates. By 2012, the internet users as a percentage of total population had reached 34.3%, among which in Europe and North America, this number was as high as 63.2% and 78.6%, respectively [1]. As a consequence, the global internet protocol (IP) traffic has increased more than fourfold from 2007 to 2012, while an increase of threefold is predicted over the year from 2012 to 2017, resulting in 1.4 zettabytes by the end of 2017 [2]. A recent study shows that the global mobile data traffic is growing in a speed of three times faster than fixed data traffic, with a conservative estimation of 13-fold increase between 2012 and 2017, reaching 11.2 exabytes/month [3]. Such growing demand has put severe pressure on the communication network infrastructures. Therefore, in order to meet the future capacity requirements, the developments of so called next generation networks (NGN) have attracted tremendous research attentions in recent years [4].

NGN can be separated into two segments: the next generation core networks and the next generation access (NGA) networks [5]. For core networks, transmission capacity has been increasing in a rapid pace due to the photonic technology advancements and worldwide deployment of fibers. However, in the NGA networks, which bridge the users and the core networks, mass deployment of fiber-optic infrastructure to reach numerous end users will result in significant investment for operators. In addition, future long-term upgrading of fiber-optic access networks is expected to be difficult and time consuming [6].

In contrast, wireless access networks require less and fast infrastructure deployment and can be easily upgraded over time [7]. Figure 1.1 presents examples of some current wireless standards in terms of throughput versus carrier frequency, for different application scenarios. For example, long term evolution (LTE) is for wireless wide area network (WWAN), WiFi (802.11) is for wireless local area network (WLAN) and Bluetooth is for wireless personal area network (WPAN). From the users point of view, an exponentially growing number of laptops, multifunctional smartphones and tablets in the recent years indicates that mobility is a very desirable functionality and connections via wireless

Figure 1.1: Throughput and allocated frequency of selected wireless standards.
GSM: Global System for Mobile Communications. UMTS: Universal Mobile Telecom-
munications System. LTE: Long Term Evolution. UWB: ultra-wide band. WiMAX:
Worldwide Interoperability for Microwave Access. WWAN: wireless wide area net-
work. WLAN: wireless local area network. WPAN: wireless personal area network.

media are preferred compared to fixed wireline connections, provided
that the two have the same communication speeds. In this context,
a hybrid optical fiber-wireless access network architecture can be envi-
sioned by converging the fiber-optic networks and the wireless networks.
The optical networks can provide high capacity backhaul by delivering
data from the central office (CO) to the wireless access points (WAP) or
base stations (BS), while the wireless networks can maintain the mobility
and flexibility of providing broadband services to the end users. Such a
hybrid architecture has the potential to provide a viable solution for the
'last mile' access networks. For implementation, radio-over-fiber (RoF)
technology is considered as a promising candidate for signal delivery and
BS simplification, and the technical details of this technology are well
explained in [8].

Figure 1.2 shows some typical application scenarios of next gen-
eration hybrid optical fiber-wireless systems in access and in-building
networks, supporting applications such as high-definition TV (HDTV),
video conferencing, interactive online gaming, e-learning, e-health care
services and others. In addition, a high capacity wireless system can

Figure 1.2: Application scenarios of next generation hybrid optical fiber-wireless systems in access and in-building networks. RN: remote node. P2P: point-to-point.

serve as a backup link to protect and recover transmission in case of breakdown of the primary optical fiber link. Furthermore, a wireless link can be established to bridge two spans of fiber networks for users in either metropolitan areas or rural areas, where full deployment of optical fibers is impractical.

Currently, the capacity and coverage of optical systems is advancing at a remarkable speed. On the contrary, the transmission speed of current wireless systems is highly limited by the available bandwidth in the RF spectrum. Therefore, the capacity bottleneck of the hybrid optical fiber-wireless system is the wireless section. To support bandwidth-intensive services, e.g. Super Hi-Vision / Ultra HDTV data (24 Gbit/s - 72 Gbit/s), OC-768/STM-256 data (43 Gbit/s), and 100 GbE (100 Gbit/s), there is a conceivable demand in the coming years for wireless links with capacity of Gbit/s, tens of Gbit/s or even up to 100 Gbit/s, in order to realize the seamless convergence with the fiber-optic networks [9]. Current wireless technologies operating in low frequency bands are highly congested and no longer capable of supporting such capacity requirements. There are mainly three approaches where research efforts can be made to take on the challenge: (1) moving the carrier frequency to mm-wave range where a broader bandwidth is available; (2) employing advanced modulation formats to increase the

signal spectral efficiency to improve the data throughput over the limited
bandwidth; (3) applying spatial division multiplexing (SDM) schemes to
combine more parallel channels into one system.

1.3 High capacity photonic-wireless mm-wave links

In order to solve the congestion in current frequency bands and allow the development of broadband wireless communications, moving the wireless signal carrier to mm-wave bands was proposed as a straightforward solution. The mm-wave band, by its definition, is a range of electromagnetic waves with frequencies between 30 GHz and 300 GHz, or the wavelength of one to ten millimeter in free space. Currently, the frequency bands below 60 GHz have limited unlicensed bandwidth left for wireless transmission. In 60 GHz band, or more specifically, the V-band (50-75 GHz), regulatory agencies have allocated up to 7 GHz bandwidth for unlicensed use in North America and South Korea (57-64 GHz), as well as in Japan (59-66 GHz), while up to 9 GHz in European Union (57-66 GHz) [11]. 60 GHz band communication has been standardized by several working groups such as WirelessHD, ECMA-387 and IEEE 802.15.3c for WPAN scenarios, for short-range wireless applications like high-definition multimedia interface (HDMI) cable replacement [10–12]. Furthermore, there are more proposals to adopt the 60 GHz technology for WPAN [13], WLAN [14] and data center interconnects [15].

In order to further increase the wireless capacity to reach and exceed 100 Gbit/s, an even broader bandwidth is required. Consequently, the under-exploited higher frequency range at 100 GHz and above is becoming a timely relevant research topic for its wider bandwidth availability. Recently, the W-band (75-110 GHz) is attracting increasing attention due to its potential to provide the requested high capacity [16]. In US, the Federal Communications Commission (FCC) has opened the commercial use of spectra in the 71-75.5 GHz, 81-86 GHz, 92-100 GHz, and 102-109.5 GHz bands, which are recommended for high-speed wireless communications [17]. All these facts drive industrial considerations of including the mm-wave communication links into the next generation hybrid optical fiber-wireless networks. However, there are still technical challenges in terms of mm-wave generation, spectral efficiency and detection.
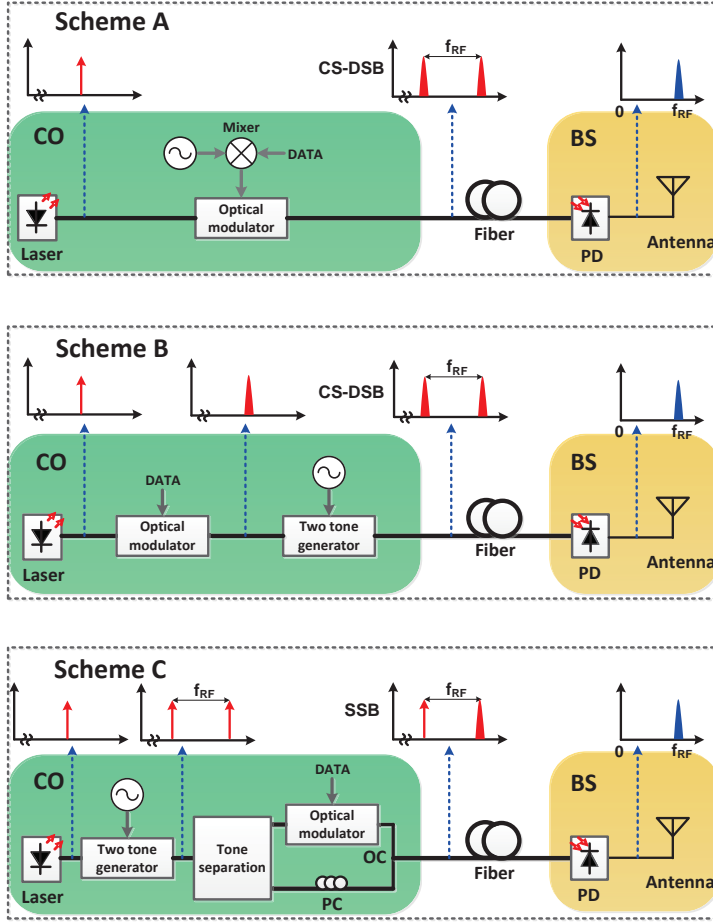
1.3.1   Photonic up-conversion techniques for mm-wave generation

Due to the high free space loss and atmospheric attenuation for mm-wave signals, the coverage of each wireless transmitter is reduced to few 10s to few 100s meters, meaning that a large number of BSs will be required to provide extensive geographical coverage in mm-wave link-based hybrid fiber-wireless networks [18]. Consequently, cost-effective and simplified BS designs are essential to make the systems commercially viable. The generation of mm-wave signals with high output power, broad bandwidth while maintaining high phase noise performance is desirable to carry high-speed wireless signals. Conventional approaches using the electrical up-conversion method to generate mm-wave signal requires high frequency RF source, mixer or cascaded frequency multipliers [19, 20]. This method can normally meet the transmission requirements in terms of the phase noise and power performance of the generated signals. However, considering the trade-off between further extension of the signal bandwidth and the increasing of system complexity, this approach is not regarded to be an optimal solution. The report of the experimental analysis of a W-band wireless link based on electrical up-conversion is included in **PAPER 1**, which shows that the wireless data rate is highly limited by the system bandwidth.

On the other hand, the generation of wireless signal using photonic techniques has the advantage of the broad bandwidth that optoelectronic components can achieve. The principle of this approach is based on photonic heterodyning mixing [18, 21, 22]. Various techniques for the mm-wave signals generation have been proposed and can be generally categorized into two main groups. The first kind employs coherent optical sources for the heterodyne mixing, which can be achieved by using a Mach-Zehnder modulator (MZM) [23], a dual-mode distributed-feedback laser (DFB) [24], a sub-harmonic mode-locked lasers [25, 26], or using a optical frequency comb (OFC) generator [27]. Figure 1.3 illustrates three common coherent up-conversion schemes employing a single wavelength laser source for photonic-wireless communication links.

Scheme A is similar to a conventional double sideband (DSB) RoF system, where the data is firstly modulated to the RF carrier before being fed to the optical modulator. The difference is that a carrier suppressed-DSB (CS-DSB) scheme is used to eliminate chromatic dispersion induced periodic radio frequency (RF) power fading in the fiber and to reduce the RF source requirement by half [28]. Simi-

Figure 1.3: mm-wave generation schemes based on coherent photonic heterodyne up-conversion technique using a single optical source. CO: central office. BS: base station. CS-DSB: carrier suppressed-double sideband. SSB: single sideband. PC: polarization controller. OC: optical coupler.

larly, scheme B also applies the CS-DSB modulation technique. In this scheme, instead of modulating the data to an RF carrier, the data is directly modulated onto the lightwave forming a optical baseband signal, before being fed to a two tone generator for frequency up-conversion. By doing this, the bandwidth limitation of the RF devices such as the mixer can be taken away. Both scheme A and B can up-convert amplitude modulation formats such as on-off keying (OOK) and pulse amplitude modulation (PAM) signals. However, as both the upper- and
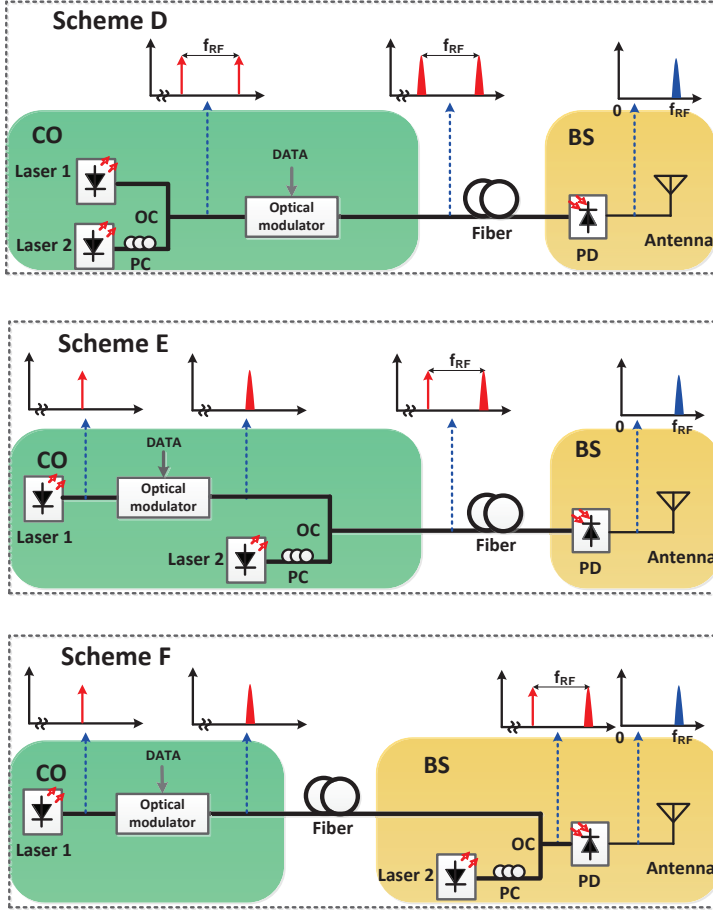
lower-sidebands contain the modulated signal, the heterodyne mixing can cause the loss of phase information. As a result, they are not suitable for complex signal formats containing phase modulation, e.g. phase-shift keying (PSK), quadrature amplitude modulation (QAM) and complex-valued orthogonal frequency-division multiplexing (OFDM) signals. Research efforts were made to accommodate the schemes to transmit complex signals. By shifting the baseband signal to an intermediate frequency (IF) before mixing with the RF in scheme A, after heterodyne beating, the up-converted complex signal can move aside from the frequency component generated by direct mixing the data-contained sidebands, or so called "beating noise", so that both intensity and phase information can be preserved [29, 85].

Different from scheme A and B, scheme C separates the upper- and lower-sidebands after the two tone generator, as shown in Fig. 1.3. The data is modulated onto one sideband and the other sideband serves as a carrier signal during the heterodyne up-conversion. In this scheme, the signal and the carrier are combined before transmitting through the fiber link, forming a single sideband (SSB) RoF signal, which can preserve complex signal formats after the heterodyne mixing while eliminating the RF power fading effect in the fiber. In this thesis, **PAPER 9** and **PAPER 10** report on experimental demonstrations of W-band transmissions based on this scheme.

Unlike the first kind of mm-wave generation based on coherent spectral lines, the second approach employs two separate free-running light sources performing a incoherent frequency up-conversion. As shown in Fig. 1.4, there are also mainly three schemes to be considered. In scheme D, both optical carriers are modulated while scheme E and F only modulate data onto one branch, leaving the other laser as the RF carrier generating signal during the up-conversion process. Similar to scheme A and B in the coherent up-conversion cases, scheme D can only applies to amplitude modulation formats with the same reasons explained before, if not being further modified. Scheme E and F working with the same principle, only differ from a architectural point of view: combine the carrier generating laser in the CO or in the BS, or in another words, remote up-conversion or local up-conversion. As the the typical coverage of access networks are within 20 km, the difference between the transmission performance of the two schemes are negligible [31]. Both the two schemes have their own advantages, depending the specific application scenarios. For example, if we want to simplify all BSs and maximize the

Figure 1.4: mm-wave generation schemes based on incoherent photonic heterodyne up-conversion technique employing two free running lasers.

centralized functionalities in the CO, scheme E is preferable. Nevertheless, in certain cases we want to establish a wireless bridge as a relay for optical baseband connections, or in a wavelength division multiplexing (WDM) system where spectral resources are all taken by transmitted signals, the local up-conversion scheme, or scheme F is more suitable. For example, **PAPER 2 - PAPER 7** in this thesis apply the remote up-conversion method to centralize both the signal laser and the carrier laser in the CO, while in **PAPER 8** we employ the local up-conversion scheme in a dense wavelength division multiplexing (DWDM) access network for the convergence of the wireline and wireless systems.

1.3.2 Spectrally efficient modulation formats for photonic-wireless communications

In conventional intensity modulation / direct detection (IM/DD) RoF systems, amplitude-shift keying (ASK) modulation is the most commonly used data format. However, ASK can only achieve an RF spectral efficiency of 0.5 bit/Hz, considering the full spectral width of the RF signal. This means 200 GHz overall bandwidth will be required for 100 Gbit/s ASK signal transmission, which is very unlikely to realize without moving the carrier frequency to terahertz (THz) range. For this reason, in order to transmit higher capacity signal within limited bandwidth, more advanced modulation formats are needed to provide higher spectral efficiency. Thanks to the recent advances in digital signal processing (DSP)-based coherent receiver technologies, complex modulation formats such as PSK, M-QAM and O-OFDM signals have been considered in fiber-wireless systems [32–34]. We can divide these modulations into single carrier and multi-carrier formats.

For single carrier signals, quadrature PSK (QPSK) and 16-QAM signals possess 1 bit/Hz and 2 bit/Hz spectral efficiencies, respectively. It means that to transmit the same data capacity, QPSK and 16-QAM only take half and a quarter spectral bandwidth compared with ASK. **PAPER 2**, **PAPER 9** and **PAPER 10** employ QPSK formats for fiber-wireless transmission in the W-band. Transmission of a single- and dual-channel of 16-QAM signal over a photonic-wireless link is presented in **PAPER 3**.

OFDM is a common multi-carrier modulation format with highest spectral density between the subcarriers and has been widely adopted for wireless communications [35, 36]. Complex modulation formats like M-QAM can be used to modulate each subcarrier, resulting in higher overall spectral efficiencies than single carrier signals with the same modulation orders. OFDM provides a very good solution for hybrid optical fiber-wireless systems as it is robust against fiber dispersion effects (chromatic dispersion and polarization mode dispersion) in optical fiber channels and frequency-selective multipath fading in wireless channels, as well as efficient DSP-based implementation [37, 38]. Furthermore, as the OFDM signal is normally generated in the digital domain, it has extra flexibility to maximize the spectral utilization efficiency, by applying bit-loading and/or power-loading techniques depending on the frequency response of the transmission channels [39, 40]. In this thesis, our works of high capacity W-band wireless transmission of complex OFDM signals

are reported in **PAPER 4**, **PAPER 5**, and **PAPER 6**. A W-band fiber-wireless transmission in the uplink direction employing intensity modulation OFDM is presented in **PAPER 7**.

1.3.3   Detection of mm-wave signals

The up-converted mm-wave signal can be radiated into the air by different types of antennas. Due to the limited signal power after opto/electro (O/E) up-conversion, we employ high directivity standard horn antennas with 24/25 dBi gain in the works of this thesis. As a result, wireless links fulfilling the line-of-sight (LOS) requirement are investigated. After the wireless transmission, another high gain antenna picks up the mm-wave signal and forwards it to a receiver for further transmission performance evaluation. In order to overcome the impediment of using conventional low frequency electronic devices and equipment for the mm-wave signal acquisition and processing, it is necessary to perform a frequency down-conversion.

Figure 1.5: mm-wave receiver architectures: (a). down-conversion with envelope detector (ED) and (b). coherent down-conversion based-on an electrical mixer and a local oscillator (LO).

Two different mm-wave receiver architectures are presented in Fig. 1.5. Figure 1.5(a) shows a frequency down-conversion using a Schottky diode-based envelope detector (ED). Because the mm-wave carrier frequency is out of the bandwidth of the detector, only the desired envelope of the signal is recovered. As this scheme can not detect the phase of the transmitted signal, only amplitude modulations like ASK and PAM can be recovered by this receiver structure. Additionally, as the operational bandwidth of the ED is closely related to the impedance which effects the reflections, it is difficult to reach high bandwidth while matching the 50Ω impedance. Therefore, bandwidth of most current commercially available EDs are limited to a few GHz, making high speed transmission

over 10 Gbit/s difficult to achieve using this scheme.

Figure. 1.5(b) presents a coherent down-conversion structure using an electrical mixer. By mixing the incident signal with the local oscillator (LO) signal, the mm-wave can be directly down-converted to baseband or to an IF that is within the operational bandwidth of the equipment, while the phase information is simultaneously detected. Meanwhile, compared with the ED, electrical mixers normally have less constrains in operational bandwidth, which brings possibility to transmit wireless signals occupying wide bandwidth. To evaluate complex signal formats, the down-converted signals are first fed into a digital storage oscilloscope (DSO) for the analogue-to-digital conversion (ADC), before being processed and demodulated by offline DSP. With the help of DSP, it is possible to compensate the phase and frequency offset caused by the free-running laser beating and other impairments induced by transmission, such as chromatic dispersion, imbalances in the transmitter and receiver, etc [41, 42].

We use the coherent down-conversion scheme combined with DSP-based receiver in most of the mm-wave transmission works that are included in this thesis, namely, **PAPER 1-10**. The ED-based receiver scheme is employed in our bi-directional mm-wave transmissions reported in **PAPER 9** and **PAPER 10**, for the wireless signal detection in the uplink direction.
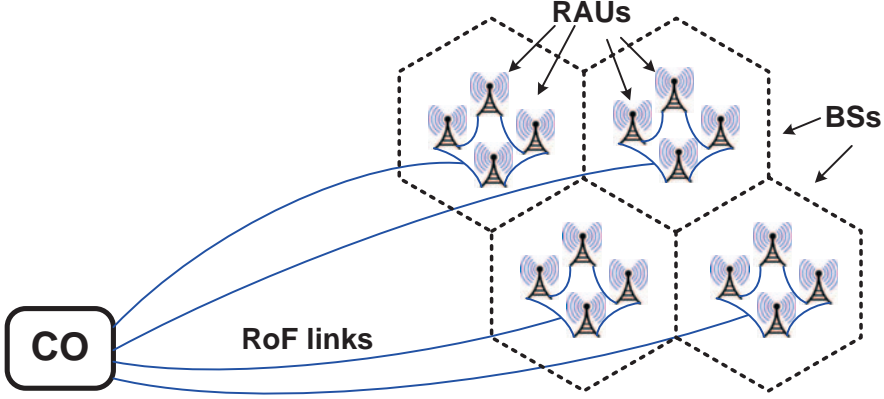
1.4 Wireless MIMO technology for hybrid optical fiber-wireless access networks

In optical fibers, WDM and polarization multiplexing (PolMux) are two typical multiplexing schemes to provide more dimensions to simultaneously transmit multiple parallel channels. On the other hand, in bandwidth limited wireless systems, a comparably more straightforward solution to apply the "parallelism" is to use SDM, by physically combining multiple low capacity point-to-point wireless links. Recently, multi-antenna technologies such as MIMO are widely put into service in wireless radio systems for highly reliable communications [43–45]. Furthermore, MIMO technology has improved transmission distances and data rates supported by modern wireless networks without adding power or bandwidth expenditure [46]. Under those circumstances, a RoF system combining optical WDM and/or PolMux or other types of multiplexing technologies together with wireless MIMO offers a viable solution providing higher system throughput and bandwidth utilization efficiency in bandwidth limited systems [47–49].

Figure 1.6 displays a RoF access network enabled by wireless MIMO technology. Optical fiber links distribute the WDM/PolMux RoF signals from the CO to a number of BSs. Within the coverage of each BS locate N remote antenna units (RAU), which translate the multiplexed RoF signals into a wireless N×N MIMO system. The wireless channel capacity can be increased by the factor of N without additional transmitting power or spectral resources. Technically, the key issue for a MIMO system is to adaptively demodulate the received spatial-correlated radio signals in the case of various resolvable and irresolvable wireless paths interfering each other. For implementation, accurate channel estimation is indispensable for designing the channel equalizer in the DSP receiver. In this thesis, two types of channel estimation methods are investigated targeting diverse signal formats. A channel estimation method based on training symbols is used for multi-carrier signals like OFDM. Instead, for single carrier signals with a constant envelope, e.g PSK signals, a constant modulus algorithm (CMA)-based channel estimation can be applied.
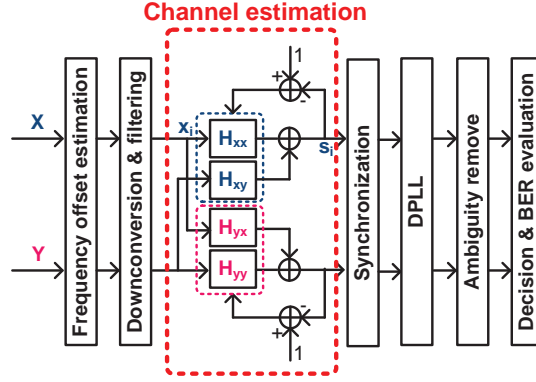
Figure 1.6: RoF access network scenario with wireless MIMO implementation. CO:
central office. BSs: base stations. RAUs: remote antenna units.

1.4.1   MIMO-OFDM RoF systems enabled by
training-based channel estimation

As mentioned in the previous section, OFDM signal is a promising can-
didate for future hybrid optical fiber-wireless access systems due to its
robustness against frequency selective fading or narrowband interference
in wireless channels. The combination of MIMO with OFDM gives an
attractive solution for WLANs, WWANs and fourth-generation (4G)
mobile cellular wireless systems [44, 50–52]. On the other hand, re-
cent research efforts on high capacity optical baseband transmissions
also turn to OFDM for higher spectral efficiency [53, 54]. To imple-
ment PolMux OFDM in both direct detection (DD) and coherent optical
systems requires DSP-based MIMO channel estimation to mitigate the
linear channel effects including chromatic dispersion (CD), polarization
mode dispersion (PMD), polarization dependent loss (PDL) and cross-
polarization interference [55–59]. In general, the synthesized channel
can be estimated by using preamble or training symbols known to both
the transmitter and receiver, which develops many numerical techniques
to perform channel estimation.

Inspired by the usage of MIMO-OFDM in both wireless and fiber-
optic transmission systems, we look into its potential in hybrid optical
fiber-wireless system to further capacity enhancement. By accommo-
dating the channel estimation method based on training sequences pro-
posed in [59] to RoF and wireless MIMO systems, we successfully prove

Figure 1.7: Block diagram of the digital signal processing used in the CMA-based MIMO signal receiver.

and experimentally demonstrate the possibility of using this method to equalize the linear effects both from the fiber and the wireless transmission. In this thesis, **PAPER 11** reports a 2×2 MIMO-OFDM transmission in an optical WDM fiber-wireless access system, while PolMux MIMO-OFDM signal transmissions with detailed explanation of the training-based channel estimation method are reported in **PAPER 12** and **PAPER 13**.

1.4.2   CMA-based blind channel estimation for MIMO-QPSK RoF systems

Single carrier signals, which normally don't require complex electronics like an arbitrary waveform generator (ArWG) to generate, should also be considered in the MIMO RoF systems. On the other hand, a training-based channel estimation method often needs a large number of overhead symbols to extract the channel response, resulting in the decrease of the net data rate in the system. Furthermore, to obtain preamble or training symbols in the receiver, precise synchronization or timing recovery is essentially necessary [54,60] since preamble-based approaches are all decision-directed. Considering most of synchronization algorithms cannot give a satisfying performance as spatial-correlation exists in the MIMO case [61], blind channel estimation without resorting to the preamble or training symbols can be very practically promising for MIMO signal demodulation in reality. Therefore, we implement a blind channel estimation to demodulate the spatial-correlated MIMO signals

employing the well-known CMA at the DSP receiver [62]. Figure 1.7 shows the structure of the channel estimator based on a lattice filter with transfer functions H_{xx}, H_{xy}, H_{yx} and H_{yy}, which represents the inverse spatial-correlated matrix of the MIMO channel. Each filter block is implemented in the time domain as a finite impulse response (FIR) filter with optimized number of taps. We use CMA to perform blind filter adaption, which minimize the time averaged error

$$\varepsilon_{CMA} = \overline{1 - |S_i|^2} \tag{1.1}$$

implying the mean distance of equalized symbols S_i from the constant unit circle in the complex plane. The filter coefficients are adapted according to the algorithm iterations to minimize ε_{CMA}. In **PAPER 14**, we report a MIMO-QPSK RoF transmission based on such channel estimation.

1.5 State-of-the-Art

In this section, we review the state-of-the-art related to the research topics of this Ph.D. thesis, which are divided into two categories: high-speed mm-wave photonic-wireless communication links and MIMO technology in hybrid optical fiber-wireless systems.

1.5.1 Mm-wave photonic-wireless communication links

Mm-wave signal, by its definition, means an RF signal of wavelength within 1 mm to 10 mm in free space, equivalent to a frequency between 30 GHz and 300 GHz. Due to the spectrum congestion, future high capacity wireless link will unlikely concentrate on the frequency range of below 60 GHz. Therefore, this section will review the recent research front-line of mm-wave communications with carrier frequencies of 60 GHz and above.

For 60 GHz fiber-wireless systems, many research groups have proposed and demonstrated optical mm-wave generation and transmission using different techniques for different scenarios. Gigabit capacity transmissions employing ASK signals in the 60 GHz have been reported for wireless and wireline networks convergence [63–73], multiband transmission [74,75], duplex RoF systems [76,77] and HD video delivery [78,79]. In terms of data rate, a photonic mm-wave transmission of 12.5 Gbit/s over 3.1 m wireless distance was demonstrated [80]. To date, this is the

highest capacity reported in the 60 GHz band using ASK modulation, to my best knowledge. Nevertheless, considering practical issues such as regulations on spectral allocation in the 60 GHz, higher spectral efficiency becomes necessary to achieve equivalent capacity. Therefore, more and more recent research efforts primarily focus on the higher spectral efficient OFDM signals rather than signal carrier signals, for transmission with the 7 GHz unlicensed bandwidth. Point-to-point high speed 60 GHz wireless system demonstrations employing OFDM signals have been reported for single-band [29,39,40,81–84], multiband [85] and bidirectional transmissions [86,87]. To my best knowledge, a most recent report on a 40 Gbit/s transmission over 10 m wireless distance within 7 GHz available bandwidth achieved by using OFDM modulation, adaptive bit-loading and an I/Q imbalance compensation algorithm, is the highest capacity point-to-point wireless link in 60 GHz up to this moment [88].

More and more research attentions are now attracted by the W-band (75-110 GHz) because of its broader available bandwidth for communication purpose. Similarly, both single carrier and multi-carrier signals are investigated in this frequency range. For single carrier modulations, 20 Gbit/s and 25 Gbit/s ASK transmissions in the W-band with the help of uni-traveling carrier photodiode (UTC-PD) and ED with record-high modulation (26 GHz) and video bandwidths (37 GHz) are respectively reported in [89] and [90]. Employing coherent technology in RoF systems gives the possibility of using higher order modulation formats like QPSK and 16QAM. An three-orthogonal-channel QPSK RoF system with overall data rate of up to 40 Gbit/s was demonstrated without wireless transmission [33]. Currently, a transmission of 37.38 Gbit/s QPSK signal with 40 GHz bandwidth over 20 km SMF and 0.3 m air was achieved with the help of a ADC of 30 GHz (80 GSa/s) and a 45 GHz bandwidth (120 GSa/s) [91]. The same authors further improved the wireless distance to 7.5 m by employing Cassegrain-type antennas of 50 dBi gain [92]. Furthermore, a 40 Gbit/s 16QAM was transmitted over 0.3 m wireless distance without using any mm-wave amplifiers in the link [93]. To date, more research works with record high capacity wireless transmissions in both 60 GHz band and W-band combine high-order modulation formats, multiple frequency bands and SDM schemes like MIMO technologies to further increase the overall speed. These works are to be discussed in the next section.

Carrier frequencies around 300 GHz where there is almost no limi-

tation in terms of available bandwidth are also investigated for wireless communications. Therefore, ASK signal is typically used in this frequency range. Data rates of 16 Gbps and 28 Gbps are reported with wireless transmission of 0.5 m [94, 95]. Efforts have also been made to use complex signal formats in the 300 GHz range. A 29.9 Gbit/s QPSK signal transmitted over up to 0.2 m wireless is reported in [96]. Furthermore, simultaneous transmissions of 5 Gbaud QPSK signals in both 100 GHz and 300 GHz carriers were experimentally demonstrated [97].

Most recently, a single-input single-output (SISO) photonic wireless link with a record data rate of 100 Gbit/s 16QAM signal transmission over 20 m wireless distance was reported with carrier frequency at 237.5 GHz [98], which was achieved by employing a mode-locked laser (MLL), a UTC-PD, a pair of cylindrical horn antennas with plano-convex dielectric lens of 86 dBi combined gain and an electronic mm-wave receiver with active monolithic integrated circuit (MMIC).

1.5.2 MIMO technology for fiber-wireless transmission systems

Today, MIMO technology has been widely adopted in wireless communication systems. First simulational studies revealing the potential large capacities of multi-antenna systems were done in the 1980s [99], and followed research works explored the systems from an analytical point of view [100–102]. Since then, MIMO technology has began to attract increasing interests for wireless systems.

In the field of optical transmission systems, MIMO was first considered for free space optical communications [103–105], before drawing the interests of the society of fiber-optic systems for modal multiplexing and inter-symbol interference (ISI) equalization in multimode fiber (MMF) fiber links [106–108]. Since then, increasing research efforts have been put into PolMux coherent optical transmissions, when MIMO began to be widely considered for fiber polarization demultiplexing [55–59, 109].

For hybrid fiber-wireless systems, early simulation works have been conducted towards integrating MIMO-OFDM techniques with RoF [110, 111] and DWDM systems [112]. The MIMO-RoF using 16QAM-OFDM is detailed analyzed and demonstrated with separate fibers for each RAU, in which the wireless transmission distance is up to 8 m with a optimum antenna separation of 1 meter [47].

Training-based MIMO channel estimation has been explored at 60 GHz and 100 GHz RoF systems. Recently, RoF systems with wireless MIMO

transmissions of 5 Gbit/s OOK and 27.15 Gbit/s 16QAM signals are respectively demonstrated employing training sequences [113–115]. For multi-carrier modulation formats, more than 50 Gbit/s MIMO-OFDM fiber-wireless transmissions over 4 m wireless in the 60 GHz band are reported [116,117]. Most recently, a PolMux MIMO-OFDM signal transmission over 40 km fiber and 5 m wireless distance with data rate of 30.67 Gbit/s at 100 GHz is reported, which also uses training-based channel estimation [118].

On the other hand, efforts are also paid to blind channel estimation without training symbols to eliminate synchronization requirements. CMA-based channel estimation has been widely used for MIMO-QPSK system in 40 GHz band [119], 60 GHz band [120] as well as W-band [121–126]. In [121, 122], remote RoF distribution and coherent heterodyne up-conversion is applied to a 20 Gbaud QPSK signal, which is transmitted over 20 km SMF plus a 0.9 m wireless MIMO link. In [123–126], localized incoherent heterodyne beating with free-running lasers are employed after optical baseband QPSK signal transmission in the fiber, resulting in data rates of up to 108 Gbit/s with single channel and 120 Gbit/s with multi-channel signals, respectively. Furthermore, a 112 Gbit/s PolMux-16QAM signal transmission over 400 km SMF plus a 0.5 m wireless 2×2 MIMO link at 35 GHz is also successfully demonstrated with CMA-based channel estimation [127]. Most recently, one more dimension of multiplexing using antenna horizontal- and vertical-polarizations is proposed to enhance the performance of wireless MIMO system in a fiber-wireless link [128].

1.6   Contributions of the thesis beyond the State-of-the-Art

In this section, I highlight the achievements of my Ph.D. project to show how my thesis has significantly extended the state-of-the-art of high capacity hybrid optical fiber-wireless communication systems by employing coherent and incoherent photonic mm-wave generation schemes, single- and multi-carrier advanced modulation formats, coherent heterodyne and incoherent envelope detection techniques, as well as wireless spatial division multiplexing with MIMO technologies. The achievements are divided into two topics in conjunction with the discussed state-of-the-art including high speed mm-wave communications and RoF systems using wireless MIMO technologies.

Table 1.1: Main experimental contributions to the state-of-the-art of mm-wave communications reported in this thesis.

PAPER No.	Mod. format	Data rate (Gbit/s)	Frequency range (GHz)	Fiber links	Wireless distance (m)
1	ASK	0.5	87-88	20km NZDSF	0.5
2	QPSK	25	75-100	22.8km SMF	2.13
3	16QAM & PolMux	100	75-100	–	1.2
4	3-band QPSK-OFDM	8.3/ch	79.25-94.25	22.8km SMF	2
5	4-band 16QAM-OFDM	9.6/ch	78.9-93.3	–	1.3
6	3-band 16QAM-OFDM	42.13	78.5-93.5	–	0.6
7	16QAM-OFDM	1.48	79.08-79.92	22.8km SMF	2.3
8	ASK	2.5	57.5-62.5	25km SMF	6
9	DL: QPSK	16	73.4-89.4	26km SMF	1
	UL: ASK	1.25	86.35-88.85	+100m MMF	1
10	DL: QPSK	16	73.4-89.4	26km+10km	15
	UL: ASK	1.25	86.35-88.85	SMF	5

1.6.1   High capacity mm-wave photonic-wireless communications

Table 1.1 gathers the main experimental achievements in the topic of mm-wave communications during this Ph.D. project. It shows the employed modulation formats, achieved data rates, RF carrier frequencies, transmitted fiber links and wireless distances. These research works performed during my Ph.D. have led to the demonstrations of mm-wave communication links achieving data rates and transmission distances that are part of today's state-of-the-art.

A detailed W-band channel characterizations including path loss, directivity, phase noise and the first fiber-wireless transmission demon-

stration in the framework of the Ph.D. project is reported in **PAPER 1**. Through this work, the W-band channel was evaluated for benchmarking its feasibility of high capacity data transmissions. My works presented in **PAPER 2** and **PAPER 3** improves previous results in [33, 93] in terms of capacity, BER performances and achieved wireless distances. In particular, **PAPER 3** reports on the new wireless capacity record at the time being with an overall wireless data rate of 100 Gbit/s, setting a milestone in the research of high capacity fiber-wireless systems. **PAPER 4-6** presents W-band transmissions of single- and multi-band complex OFDM signals by employing an optical frequency comb generator (OFC), indicating a potential improvements in spectral efficiency compared with single carrier modulations. An initial effort for bidirectional W-band fiber-wireless implementation by emulating a uplink transmission is presented in **PAPER 7**. Novelty of this paper is the re-modulation and further fiber propagation of the down-converted IF signal at the wireless receiver after the W-band link. In collaboration with Nanophotonic Technology Center (NTC) in Polytechnic University of Valencia, we reported in **PAPER 8** the use of optical frequency comb for centralized up-conversion of DWDM signals to simultaneously support multi-band, multi-user with both wireless and wireline services.

PAPER 9 starts to consider the implementation of bidirectional W-band fiber-wireless transmissions for the first time. A simple structured WAP that fulfills the requirements of multi-gigabit asymmetrical downloading and uploading is proposed by employing digital coherent receiver in the downlink and incoherent ED in the uplink. **PAPER 10** further extend the W-band bidirectional transmission by introducing a wireless bridge between two segment of fiber-optic systems to realize a seamless fiber-wireless-fiber integration. Additionally, by employing an active wireless transmitter, up to 15 meters transmission is successfully demonstrated for the first time.

1.6.2 RoF systems with wireless MIMO technologies

A summary of the experimental achievements in the topic of MIMO RoF systems during this Ph.D. project is presented in Table 1.2, which shows the optical multiplexing schemes with modulation formats, achieved data rates, RF carrier frequencies, overall spectral efficiency and demonstrated wireless distances. The ideas of transparently translating the fiber-optic WDM and PolMux into the 2×2 MIMO systems enabled by both training symbols and CMA blind equalization, are novel for the

Table 1.2: Summary of experimental achievements in MIMO RoF systems reported in this thesis.

PAPER No.	Technology	Data rate (Gbit/s)	Carrier frequency (GHz)	Spectral efficiency (bit/s/Hz)	Wireless distance (m)
11	WDM-MIMO-OFDM	0.397	5.65	1.27	1
12	PolMux-MIMO-OFDM	0.797	5.65	1.27	3
13	PolMux-MIMO-OFDM	1.59	5.65	2.52	1
14	PolMux-MIMO-QPSK	5	5.4	4	2

time being and have been proved to be promising solutions for higher capacity and carrier frequencies in later research works [117, 125].

PAPER 11 reports on the first experimental demonstration of an all-VCSEL WDM-MIMO-OFDM RoF system at 5.6 GHz enabled by training-based channel estimation algorithm. A net rate of 397 Mbit/s 16QAM-OFDM signal transmission is recovered after the fiber-wireless transmission. To further increase the spectral efficiency of a single optical wavelength channel RoF system, PolMux-MIMO-OFDM transmissions are proposed and demonstrated. A 797 Mbit/s 4QAM-OFDM transmission over 22.8 km SMF and 3 m wireless MIMO link is reported in **PAPER 12**, while **PAPER 13** presents a transmission of 1.59 Gbit/s 16QAM-OFDM over 22.8 SMF plus 1 m wireless link. Net spectral efficiency of 1.27 bit/s/Hz and 2.52 bit/s/Hz are respectively achieved.

PAPER 14 reports an experimental demonstration of PolMux-MIMO-QPSK transmission with a line rate of 5 Gbit/s and a spectral efficiency of 4 bit/s/Hz, enabled by CMA-based blind channel estimation. This is the first report on CMA-based PolMux RoF plus wireless 2×2 MIMO transmission demonstration, to the best of my knowledge.

Chapter 2

Description of Papers

This thesis is based on a set of papers already published or accepted for publication in peer-reviewed journals and conference proceedings. These papers present the results obtained during the course of my doctoral studies, combining theoretical analysis, simulational and experimental evaluations. These papers are grouped into two categories: generation and transmission of mm-wave signals in high capacity hybrid optical fiber-wireless systems (**PAPER 1** to **PAPER 10**) and MIMO multiplexing technology in RoF access systems (**PAPER 11** to **PAPER 14**).

2.1 High capacity mm-wave links in hybrid optical fiber-wireless systems

PAPER 1 presents a detailed experimental investigation of a hybrid optical-fiber wireless communication system operating in the W-band (75-110 GHz). Frequency up- and down-conversion for the W-band signal generation and detection are both performed by electrical means by using a frequency sexupler and a narrowband mixer. Detailed measurements of W-band wireless channel properties such as channel loss, frequency response, phase noise, and capacity are presented and discussed. Finally, a 500 Mbit/s ASK signal transmission over a 20 km NZDSF link and 0.5 m wireless distance is experimentally demonstrated for the purpose of performance analysis.

Contributions: Xiaodan performed the experiment and measurements planning, experiment set up, data acquisition and signal demodulation. Prepared manuscript.

In **PAPER 2**, we demonstrate a photonic up-converted fiber-wireless system with 25 Gbit/s QPSK signal transmission in the W-band for in-building wireless networks. The W-band radio-over-fiber (RoF) signal is generated and distributed to the remote antenna unit (RAU) by launching two free-running lasers with 87.5 GHz separation into a 22.8 km SMF from the central office (CO). One laser carries 12.5 Gbaud optical baseband QPSK data, and the other acts as a carrier frequency generating laser. The two signals are heterodyne mixed at a photodetector after fiber transmission, and the baseband QPSK signal is transparently up-converted to the W-band. Up to 2.13 m air transmission is demonstrated. At the receiver, a double stage frequency down-conversion are performed in electrical and digital domain, respectively. bit-error-rate (BER) performance well below the 2×10^{-3} forward error correction (FEC) limit is achieved after offline DSP equalization and signal demodulation. Theoretical analysis and simulations focusing on the optical signal power ratio for heterodyne mixing are also presented, showing a consistency with the experimental results.

Contributions: Proposing the idea. Experiment design, theoretical analysis of photonic up-conversion and electrical down-conversion, measurements planning, W-band wireless link setup and optimization, data acquisition and signal processing. Prepared manuscript.

PAPER 3 reports on an experimental demonstration of a dual channel photonic wireless link in the W-band with a overall capacity of 100 Gbit/s, employing PolMux in optical fiber and spatial multiplexing in wireless. An optical 12.5 Gbaud PolMux 16-QAM baseband signal is up-converted to the W-band by incoherent heterodyne mixing with a second free-running laser at a fast response photodiode (PD) in the wireless transmitter. At the receiver, the signal is firstly electrically down-converted to an intermediate frequency (IF) centered at 13.5 GHz, before being sampled by a 80 GSa/s ADC for offline DSP down-conversion and signal demodulation. The measured wireless distances are up to 2 meters and 1.2 meters for one polarization channel and both channels, respectively. BER performances below the 7% overhead FEC limit of 2×10^{-3} are achieved in all transmission cases. This paper sets a milestone in hybrid optical fiber-wireless communication systems by reaching the 100 Gbit/s capacity for the first time.

Contributions: Proposing the idea. Experiment design, theoretical

analysis of photonic up-conversion and electrical down-conversion, measurements planning, PolMux emulator and W-band wireless link setup and optimization, data acquisition and signal processing. Prepared manuscript.

PAPER 4 presents a scalable high-speed W-band fiber wireless communication system. Three-channel baseband QPSK-OFDM signals with data rates of 8.3-Gb/s/ch are generated in a 15-GHz bandwidth by employing an optical frequency comb generator. The baseband signals are seamlessly translated from the optical to the wireless domain by incoherent up-conversion method. The W-band wireless carrier is generated with a second free-running laser. After wireless transmission, a W-band electronic down-converter and a digital signal processing-based receiver are used. The three-channel QPSK-OFDM W-band wireless signals are transmitted over 0.5- and 2-m air distance with and without 22.8-km SMF, respectively, with achieved performance below the forward error correction (FEC) limit of 2×10^{-3}.

Contributions: Designed and built the experimental setup of optical heterodyning up-conversion, W-band wireless transmission link and the two-stage RF down-conversion. System optimization. Assisted with manuscript preparation.

In **PAPER 5**, a photonic generation and wireless transmission of single and multi-channel orthogonal frequency-division multiplexing (OFDM) modulated signals in the 75-110 GHz band is experimentally demonstrated employing I/Q electro-optical modulation and optical heterodyne up-conversion. A theoretical description on receiver signal-to-noise ratio (SNR) in the line-of-sight (LOS) wireless transmission is also presented. The wireless transmission of 16QAM-OFDM signals is demonstrated with a BER performance within the FEC limits. Firstly, signals of 19.1 Gb/s in 6.3 GHz bandwidth are transmitted over up to 1.3-m wireless distance. After that, an optical comb generator is further employed to support different channels, allowing the cost and energy efficiency of the system to be increased and supporting different users in the system. Four channels at 9.6 Gb/s/ch in 14.4-GHz bandwidth are generated and transmitted over up to 1.3 m wireless distance. The transmission of a 9.6-Gb/s single channel signal occupying 3.2-GHz bandwidth over 22.8 km of standard SMF and 0.6 m of wireless distance is

also demonstrated in the multiband system.

Contributions: Designed and built the experimental setup of optical heterodyning up-conversion, W-band wireless transmission link and the two-stage RF down-conversion. System optimization. Assisted with manuscript preparation.

PAPER 6 reports on an extended work with similar system architecture with the works presented in **PAPER 4** and **PAPER 5**. By using an improved DSP channel estimation algorithm, photonics-wireless transmission of 8.9 Gbit/s, 26.7 Gbit/s and 42.13 Gbit/s 16QAM-OFDM W-band signals are successfully demonstrated, with achieved bit-error-rate (BER) performance below the FEC limit.

Contributions: Designed and built the experimental setup of optical heterodyning up-conversion, W-band wireless transmission link and the two-stage RF down-conversion. System optimization. Assisted with manuscript preparation.

In **PAPER 7**, we propose and experimentally emulate a uplink fiber-wireless transmission in the W-band. The W-band OFDM signal is generated photonically with heterodyne up-conversion. After wireless transmission and electrical down-conversion, the intermediate frequency (IF) signal is re-modulated onto the lightwave for a further transmission over 22.8 km SMF. Both a 740.8 Mbit/s QPSK-OFDM signal and a 1.48 Gbit/s 16QAM-OFDM signal transmitted over the fiber-wireless link can be demodulated with a BER performance well below the FEC limit. This work is our first step towards the bidirectional transmissions in hybrid optical fiber-wireless systems.

Contributions: Proposed the idea of uplink transmission in the W-band. Experiment design and measurements planning, data acquisition and signal processing. Prepared manuscript.

PAPER 8 reports on a dense wavelength division multiplexing (DWDM) fiber-wireless access system in the 60 GHz band that enables smooth integration between the fiber-optic networks and the high speed wireless networks. By employing an centralized optical frequency comb (OFC), both the wireline and the wireless services for each DWDM user can be simultaneously supported. Besides, each baseband channel can be trans-

parently replicated to multiple RF bands for different wireless standards,
which can be flexibly filtered at the end user to select the on-demand
band, depending on the applications. For demonstration, a 2.5 Gbit/s
ASK signal is transmitted through the system and successfully achieve
a bit-error-rate (BER) performance well below the 7% overhead FEC
limit of BER 2×10^{-3} for both the wireline and the 60 GHz wireless
signals after 25 km SMF plus up to 6 m wireless link.

Contributions: Proposed the original idea. Experiment planning,
setup and optimization, data acquisition and signal processing. Pre-
pared manuscript.

PAPER 9 presents our first experimental demonstration of a bidirec-
tional transmission link in W-Band for hybrid access networks. In the
downlink, a 16 Gbit/s QPSK single sideband (SSB) RoF signal is gen-
erated at the CO and distributed to a simple structured wireless access
point (WAP) for coherent photonic heterodyne mixing. Electrical down-
conversion are used in the downlink receiver and offline DSP evaluation
is performed. In the uplink direction, the frequency up-conversion of
a 1.25 Gbit/s ASK signal is conducted in electrical domain by using
the same frequency sexupler as reported in **PAPER 1**, while the down-
conversion is performed by a envelope detector. In both directions, fiber-
wireless transmissions over a 26 km SMF and a 100 m MMF plus up to
1 m air distance are successfully achieved.

Contributions: Proposed the original idea. Experiment planning,
setup and optimization, data acquisition and signal processing. Pre-
pared manuscript.

In **PAPER 10**, we demonstrate a bidirectional wireless bridge, or a
fiber-wireless-fiber link, in the W-band enabling the seamless conver-
gence between the wireless and fiber-optic access networks. In the
downlink, a 16 Gbit/s QPSK signal is photonically up-converted at the
wireless transmitter and electrically down-converted at the wireless re-
ceiver. The down-converted signal is re-modulated on to the lightwave
and transmit further through the fiber-optic system. In the uplink,
both up-and down-conversion are performed by electrical means. Fur-
thermore, we investigate both passive and active wireless transmitters
in this work for both downlink and uplink transmissions. With an active
wireless transmitter, fiber-wireless-fiber transmissions over 26 km SMF,

up to 15 meters wireless distance, and a final 10 km SMF are success-
fully achieved with a BER below the 7% FEC limit in the downlink. In
the uplink, the wireless distance is limited to 5 meters due to physical
constrains in the lab. However, further extension of the wireless distance
is promising.

Contributions: Proposed the original idea. Experiment planning,
setup and optimization, data acquisition and signal processing. Pre-
pared manuscript.

2.2 MIMO multiplexing implementation in RoF systems

In **PAPER 11** we propose and demonstrate the first experimental re-
sults of fiber-wireless transmissions of a 2×2 MIMO-OFDM RoF signal
for WDM-PON system using all-VCSELs optical sources. Error free
transmission are achieved over a 20 km NZDSF and a 2 meter 2×2
wireless MIMO link for RoF signals of 4QAM-OFDM at 198.5 Mbit/s
and 16QAM-OFDM at 397 Mbit/s. We investigate the effects of various
wireless transmission distances and antenna separations to evaluate the
robustness of the MIMO-OFDM channel estimation algorithm based on
training symbols. No penalty was observed when varying the antenna
separation of the sub-elements of the MIMO-OFDM signal with a 1 m
wireless distance. This work is potentially an attractive candidate for
future femto-cell networks especially for in-door office environments.

Contributions: Design and build the wireless MIMO link, system op-
timization and data acquisition. Assisted with manuscript preparation.

PAPER 12 presents a 2×2 MIMO wireless over fiber transmission
system by seamlessly translation of 4QAM-OFDM on dual polarization
states at 795.5 Mbit/s net data rate using digital training-based channel
estimation. The OFDM signals are arranged in frames of 10 symbols,
out of which 3 are training symbols used for synchronization and channel
estimation. A cyclic prefix with 0.1 symbol length is added in each
symbol. An external cavity laser (ECL) operating at 1550 nm is used as
laser source. The signal is successfully transmitted over 22.8 km SMF
with wireless distance up to 3 m. This work proves that a training-based
scheme can be developed to estimate the combined effects from both the

fiber PolMux and the wireless MIMO transmission channel.

Contributions: Idea of converging PolMux & MIMO-OFDM, training-based channel estimation. Build the wireless MIMO link. Prepared manuscript.

PAPER 13 presents an extended work of **PAPER 12** by proposing a spectral efficient radio over WDM-PON system by combining optical PolMux and wireless MIMO multiplexing techniques. A detailed description of the training-based zero forcing (ZF) channel estimation algorithm compensating both the polarization rotation and wireless multipath fading is provided. For demonstration, a 795.5 Mb/s net data rate QPSK-OFDM signal with error free ($< 1 \times 10^{-5}$) performance and a 1.59 Gb/s net data rate 16QAM-OFDM signal with BER performance of 1.2×10^{-2} are achieved after transmission in 22.8 km SMF followed by 3 m and 1 m air distances, respectively.

Contributions: Idea of converging PolMux & MIMO. Design and build the wireless MIMO link. Signal processing. Assisted with manuscript preparation.

In **PAPER 14**, we report an experimentally demonstration a 5 Gbit/s fiber-wireless transmission system combining optical PolMux and wireless MIMO spatial multiplexing technologies. The optical-wireless channel throughput is enhanced by achieving a 4b/s/Hz spectral efficiency. Based on the implementation of constant modulus algorithm (CMA), the 2×2 MIMO wireless channel is characterized and adaptively equalized for signal demodulation. The performance of the CMA-based channel adaptation is studied and it is revealed that the algorithm is particularly advantageous to the MIMO wireless system due to the inter-channel delay insensitivity. The hybrid transmission performance after a 26 km SMF plus up to 2 m wireless MIMO link is investigated.

Contributions: Idea of converging PolMux & MIMO. Design and build the wireless MIMO link. Signal processing. Prepared manuscript.

Chapter 3

Conclusion

3.1 Conclusions

The increasing demand for higher wireless bandwidth continually places tremendous pressure on the "last mile" network infrastructures. This thesis addresses the implementation and performance evaluation of high speed hybrid optical fiber-wireless communication links for access networks. The research results presented in this thesis are pioneering in two main areas: firstly, in the high capacity millimeter-wave (mm-wave) photonic-wireless transmission systems using high-order modulation signals and coherent heterodyne digital receivers. Transmission of up to 100 Gbit/s wireless signal at a carrier frequency of 100 GHz was experimentally demonstrated. Secondly, in the seamless translation of WDM/PolMux RoF transmissions into wireless MIMO systems with both OFDM and QPSK signal formats. All in all, these achievements in this thesis have shown great potential to fulfill the requirements of high capacity and high spectral efficiency of next generation hybrid optical fiber-wireless networks.

3.1.1 High capacity mm-wave fiber-wireless communication systems

Along the way of this Ph.D. project, there is a continuous research focus on the different methods for the generation, transmission and detection of large bandwidth, high frequency photonic-wireless signals with high spectral efficiency. Both the electrical up-conversion method (**PAPER 1**, **PAPER 9** and **PAPER 10**) and photonic frequency

up-conversion methods (**PAPER 2-10**) for the generation of mm-wave signals are investigated. Among the photonic generation techniques, I study the heterodyne mixing up-conversion with both incoherent free-running lasers in **PAPER 2-8**, and with coherent optical sources in **PAPER 9** and **PAPER 10**.

In terms of modulation formats, this thesis covers the simple ASK modulation in **PAPER 1** and **PAPER 8-10**, single carrier QPSK signal in **PAPER 2**, **PAPER 9** and **PAPER 10**, 16QAM signal in **PAPER 3**, as well as the multi-carrier OFDM signals in **PAPER 4-7**.

With respect to wireless capacity, a time being record 100 Gbit/s 16QAM signal transmission is successfully demonstrated in **PAPER 3**. Furthermore, transmission of multi-channel OFDM signals with a overall net rate of 42.13 Gbit/s is reported in **PAPER 6**.

Finally, from an architecture point of view, the thesis stresses down-link transmissions in **PAPER 1-6** and **PAPER 8**, uplink transmission in **PAPER 7** and bidirectional transmissions in **PAPER 9** and **10**, for practical implementations of hybrid optical fiber-wireless systems.

3.1.2 MIMO multiplexing for RoF system

RoF systems enabled by wireless MIMO multiplexing technologies are shown in this thesis to be a prospective candidate for next generation fiber-wireless access networks. By seamlessly translating fiber WDM/PolMux RoF signals into wireless MIMO systems, overall system coverage, robustness and throughput can be enhanced. **PAPER 11** presents the first experimental demonstration of a WDM-MIMO-OFDM RoF system based on directly-modulated VCSELs. Instead, integrations of PolMux RoF systems with wireless MIMO technology are studies in **PAPER 12**, **PAPER 13** and **PAPER 14**.

Different modulation formats are enabled by different channel estimation methods in MIMO systems. For multi-carrier OFDM signals, training-based channel estimation method providing lower computational complexity and better performance is employed in **PAPER 11**, **PAPER 12** and **PAPER 13**. On the other hand, for single carrier signal like QPSK, a blind channel estimation based on CMA can eliminate the requirement of synchronization and increase net data rate without sacrificing signal bandwidth for training symbols. The experimental demonstration with MIMO-QPSK transmission is reported in **PAPER 14**.

3.2   Future Work

In spite of the encouraging and substantial research accomplishments in
the very recent years, there are still many issues need to be identified
and studied in the future in the research direction of high speed optical
fiber-wireless communications. In this section I would like to provide
my vision of the future work that could be pursued in the area of high
capacity hybrid optical fiber-wireless systems, on top of the research
achievements presented in this thesis.

3.2.1   Real-time implementation of high capacity photonic-wireless links

So far to the best of my knowledge, all the reported front-line wireless
transmission demonstrations with high order modulation formats are
enabled by offline DSP demodulation, which is still one step away from
real-time implementation. Therefore, research efforts on real-time high
speed wireless transmissions with the help of field-programmable gate
array (FPGAs) or application-specific integrated circuits (ASICs) are
foreseen to be under intensive research years from now.

A milestone in the real-time implementation of a digital coherent
receiver was a 90 nm CMOS ASIC with a 20 GSa/s ADC and DSP for
40 Gbit/s PolMux-QPSK demodulation, accomplished by Nortel Net-
works (now Ciena Corporation) in 2008 [129], who achieved 100 Gbit/s
ASIC PolMux-QPSK architecture by both dual sub-carrier implemen-
tation and single carrier implementation in 2009 [130]. In 2011, AT&T
labs reported on a single-carrier coherent 112 Gbit/s PolMux-QPSK
real-time transmission employing a state-of-the-art ASIC with 56GS/s
ADC/DSP [131]. Although current demonstrations only focus on base-
band coherent optical transmissions, these technology advances indi-
cate a promising future realization of real-time high capacity photonic-
wireless transmissions.

3.2.2   Towards Terabit/s wireless communication links

Technology roadmap studies show that the demand of bandwidth for
both wireline and wireless services is growing with tremendous rates,
and no end of this progress is in sight. Therefore, it is necessary to look
ahead for even faster solutions in wireless systems. There are mainly
two directions of research line: moving the carrier frequency further up

to sub-THz or even THz range for broader bandwidth, and continuing with the concept of "parallelism" which is widely adopted in fiber-optic systems, by implementing more parallel channels in wireless MIMO systems.

The current capacity record of a single-input single-output (SISO) wireless link is 100 Gbit/s with a carrier frequency of 237.5 GHz [98], which brings the potential to double the capacity by employing MIMO technology. We have enough confidence to believe that the next milestone of Terabit/s wireless transmission can be achieved in the coming years.

Paper 1: Experimental characterization of a hybrid fiber-wireless transmission link in the 75 to 110 GHz band

Experimental characterization of a hybrid fiber-wireless transmission link in the 75 to 110 GHz band

Xiaodan Pang
Xianbin Yu
Technical University of Denmark
DTU Fotonik, DK-2800
Kongens Lyngby, Denmark
E-mail: xipa@fotonik.dtu.dk

Ying Zhao
Tsinghua University
Department of Electronic Engineering
10084, Beijing, China

Lei Deng
Hua-Zhong University of Science and Technology
School of Optoelectronics Science and
   Engineering
Wuhan, China

Darko Zibar
Idelfonso Tafur Monroy
Technical University of Denmark
DTU Fotonik, DK-2800
Kongens Lyngby, Denmark

Abstract. We present a detailed experimental investigation of a hybrid optical-fiber wireless communication system operating at the 75 to 110 GHz (*W*-band) for meeting the emerging demands in short-range wireless applications. Measured *W*-band wireless channel properties such as channel loss, frequency response, phase noise, and capacity are reported. Our proposed system performs a sextuple frequency up-conversion after 20 km of fiber transmission, followed by a *W*-band wireless link. A 500 Mbit/s amplitude shift keying signal transmission is experimentally demonstrated for performance analysis purposes. © *2012 Society of Photo-Optical Instrumentation Engineers (SPIE).* [DOI: 10.1117/1.OE.51.4.045004]

1 Introduction

The seamless convergence of wireless and fiber-optic networks requires wireless links with increased capacity to keep the pace with high-speed fiber-optic communication systems.[1,2] Millimeter-wave (mm-wave) technology is a promising approach to satisfy the high-capacity requirement for the future wireless access networks. The applications and use of the 60-GHz band are well studied and reported in the literature.[3,4] Nevertheless, the underexploited higher-frequency range from 100 to 300 GHz is becoming a timely relevant research topic due to its capability to offer an even wider bandwidth for even faster gigabit-class wireless access rate. Recently, many efforts have contributed to achieving data transmission in the *W*-band wireless systems, including mm-wave generation and modulation techniques, transmission performance tests, and analysis.[5–7] In most of these works, although they provide details of their experiment configurations, there is limited reported details and studies on the wireless channel characteristics, with less studies considering the combined optical fiber-wireless channel situation. In particular, due to the atmosphere absorption and high free-space loss of mm-wave carrier, the mm-wave wireless transmission distance is highly limited. In this context, the well-known radio-over-fiber (RoF) technology, which integrates optical and wireless systems, provides a solution to increase the coverage while maintaining the mobility of the broadband services in the local area networking scenario.
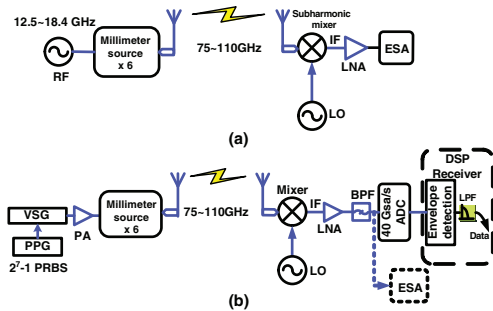
In this paper, we experimentally demonstrate a RoF system with a 75 to 100 GHz wireless link. A *K*-band RF signal modulated with data, is up-converted to *W*-band by a six-time frequency multiplicator. Using this method, 100-GHz photodetector (PD) and *W*-band amplifiers at the transmitter and receiver, which will increase the operational complexity and system cost, are not needed, as we target short-range high-capacity wireless link with potential reduced complexity. The characteristics of the wireless link are detailed tested and analyzed in terms of frequency response and emission distance. These characteristics are used as basic-considerations for the optimum design of our *W*-band wireless link. Furthermore, up to 500 Mbit/s amplitude shift keying (ASK) data traffic transmission over 20-km optical fiber and 50-cm wireless link is used for our experimental demonstrations and analysis.

2 Experimental Setups

In order to characterize the *W*-band wireless channel, two subsystems are first built, as shown in Fig. 1. The characteristics measurements of the 100-GHz wireless analogue channel are performed in Fig. 1(a). In our experiment, a 12.5 to 18.4 GHz (*K*-band) RF signal is generated, followed by a sextuple millimeter source (Agilent E8257DS15) to up-convert the signal into the 75 to 110 GHz.

After that, a wireless link is established between a pair of *W*-band horn antennas of a 24-dBi gain and less than 4 deg half-power beam width. The receiving antenna is directly connected to a sub harmonic mixer for frequency down-conversion. The local oscillator (LO) signal is 18 times multiplied in the sub harmonic mixer and then mixed with

Fig. 1 Schematics of subsystems: (a) *W*-band analogue channel characteristics test; (b) wireless link transmission test (PA: power amplifier, LNA: low-noise amplifier).

the received *W*-band signal. In this way, the *W*-band signals are down-converted to intermediate frequency (IF) at the output of the sub harmonic. Furthermore, a bandpass filter (BPF) is placed after the mixer to filter other harmonics noise due to the imperfect operation of the mixer. Subsequently, the characteristics of the IF signal such as signal power, spectrum, and phase noise are analyzed with an electrical spectrum analyzer (ESA). In the second subsystem as shown in Fig. 1(b), a pseudo random bit sequence (PRBS) of length $2^7 - 1$ is generated by a pulse pattern generator (PPG) and up-converted to *K*-band at a vector signal generator (VSG). The up-converted RF signal is transmitted over the wireless link. The received IF signal is sampled by a 40 GSa/s analog digital converter (ADC) and then demodulated by a digital signal processing (DSP) receiver using envelop detection scheme.

Figure 2 shows the schematic diagram of our experimental setup of a RoF system including a 75 to 110 GHz wireless link. A DFB laser of 10-MHz linewidth with central wavelength of 1550 nm is fed into a Mach-Zehnder Modulator (MZM) with 15-GHz bandwidth, where a *K*-band RF signal carrying ASK data traffic is intensity-modulated onto the optical carrier. After 20-km non-zero dispersion shifted fiber (NZDSF, NZD+, zero dispersion at 1540 nm) and a low-noise Erbium-doped fiber amplifier (EDFA), the *K*-band RF signal is recovered by a photodiode (PD) before

up-conversion and transmission over the *W*-band wireless link. Similarly, a DSP receiver is used to demodulate the received signals after ADC. It is noted that the 20-km NZDSF and preamp EDFA are used to minimize the impact of fiber dispersion and nonlinear effect on the generated mm-wave signals due to the high nonlinearity of the up-conversion process.
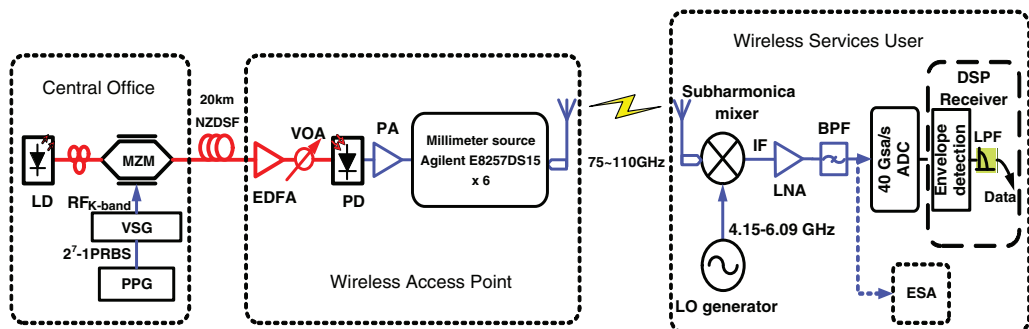
3 Results

3.1 *Wireless Link Characteristics*

Figure 3 shows the *W*-band channel response by measuring the received IF power as a function of signal frequency in terms of different wireless distances. We can see that, in general, the received power decreases with the increase of RF frequency in a given distance. It also shows that when the two horn antennas are placed close to each other and the wireless distance is assumed to be zero, the received power is significantly decreased in certain RF frequencies. By taking into account the type of antennas used in the experiment, far-field propagation takes places at air distances more than 36.8 cm. Therefore, near-field coupling may introduce such unpredictable behavior.
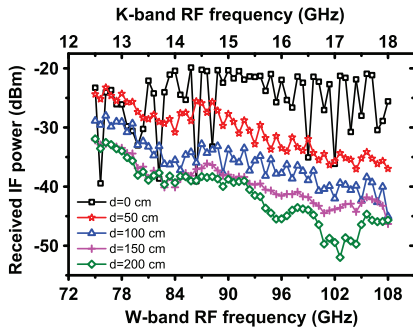
The relative wireless channel loss as a function of distance is measured and shown in Fig. 4(a). In this measurement, the source RF is set to be 16.6 GHz, corresponding 99.6 GHz after up-conversion. From Fig. 3 it can be seen that at this frequency there is no severe destructive interference at all distances. Because of the complexity of direct measuring the *W*-band RF signal power, the IF power at the receiver is measured based on the linear performance of the LNA. Therefore, the received power at ~0-cm wireless distance is set as a reference level. From the figure it can be seen that the wireless loss increments are 6, 10, and 14 dB when the wireless distance increasing from 1 m to 2, 3, and 4 m, respectively, showing a consistency with the corresponding theoretically calculated values 6.021, 9.542, and 12.04 dB for the same distance increments. The 2-dB difference between the theoretical and measured value for increasing wireless distance from 1 to 4 m is attributed to a slight alignment error when the antenna separation becomes large.

Figure 4(b) shows the impact of the alignment between the transmitting and receiving antennas on the received power. During this measurement the distance between the

Fig. 2 Experimental setup for a radio-over-fiber system plus a *W*-band wireless link (LD: laser diode, IM: intensity modulator, VOA: variable optical attenuator, PD: photodiode).
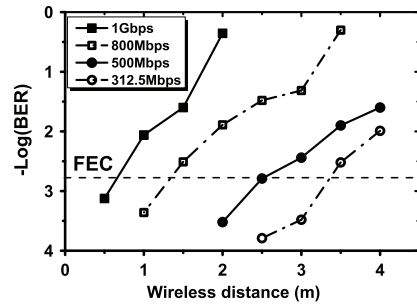
Fig. 3 The *W*-band channel frequency response in terms of different wireless distances.

Fig. 5 Measured bit error-rate performance against the wireless distance without optical links.

two antennas is fixed at 40 cm. We only change the alignment angle between the axes of two antenna's horns to measure the changing of received IF power. It is observed that the ultimate performance of the wireless link is extremely related to the optimum of alignment. From the figure it can be seen that when the alignment angle is increased from 0 to 45 deg, the power penalty in received signal is around 34 dB.

3.2 Wireless Data Transmission

In this subexperiment, the transmission performance of the wireless channel is evaluated. The subsystem setup is shown in Fig. 1(b). According to the Fig. 3, the mixer has the best frequency response when the input RF frequency is 14.6 GHz, which corresponds to the *W*-band frequency of 87.6 GHz. Moreover, the LO frequency is set to 4.813 GHz, which results in an output IF of 960 MHz (for 1 Gbps transmission, LO is set to 4.803 GHz, corresponding IF is 1140 MHz). However, the transmitted data rate is therefore limited by the narrow bandwidth of the received IF signal. Figure 5 shows the measured bit error rate (BER) performance under different data rates and the wireless distances between the antennas. We begin our measurement from 50 cm distance, at which error-free demodulations are achieved at data rates of 800 Mbit/s and lower, while 1 Gbit/s transmission has a BER of 7.5×10^{-4}. Assuming the forward error correction (FEC) limit of 2×10^{-3}, transmissions at all the measured bit rates are
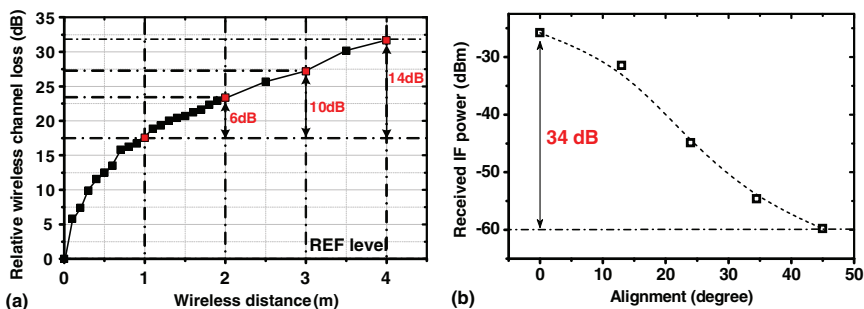
well below this limit. In the experiment, $\sim 10^5$ sampled bits were used to analyze the BER performance offline. Meanwhile, we can notice that as the distance and bit rate increase, the BER performance goes worse.

3.3 Radio-Over-Fiber System

After characterizing the wireless channel properties and the data transmission performance of the *W*-band link, a RoF experimental system is established. The wireless distance is fixed at 50 cm, and the alignment of antenna's horns is optimized during our measurement. A phase noise characterization is first studied by transmitting a signal frequency RF carrier through the system and compared with the received IF signal after up-conversion and down-conversion. Figure 6 shows the comparison of the phase noise curves between the transmitted and the received RF signal. It can be seen that the phase noise increases approximately 25 dBc · Hz^{-1} after the transmission. This is introduced by the frequency nonlinear up-/down-conversions, fiber transmission, and phase noise of the LO signal. From the figure we can also see that the phase noise level of the received IF signal is below −60 dBc · Hz^{-1} between 100 Hz and 1 kHz and well below −70 dBc · Hz^{-1} above 1 kHz. This phase noise floor is considerably well for the demonstrated ASK data transmission at 500 Mbit/s.[8,9]

System transmission test is demonstrated using the same input RF signal (14.6 GHz, corresponding to 87.6-GHz wire-

Fig. 4 (a) Wireless channel loss versus wireless distance ($RF_{W-band} = 99.6$ GHz); (b) Received signal power versus alignment between sending and receiving antennas (Source power = 0 dBm, $RF_{W-band} = 99.6$ GHz, wireless distance = 40 cm).
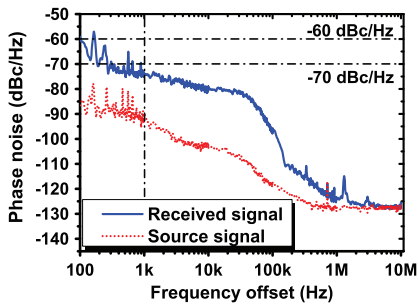
Fig. 6 Measured upper-sideband phase noise of the 14.6-GHz source and up-converted 87.6-GHz signals.
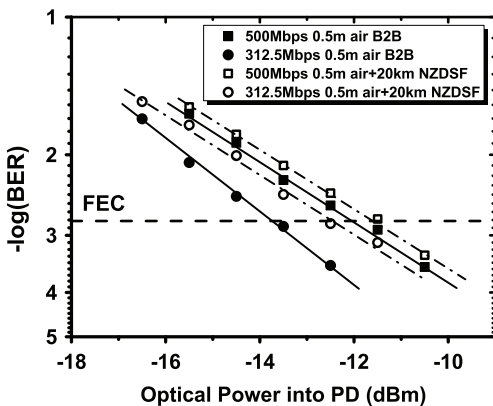

Fig. 7 Measured bit error-rate for 500 and 312.5 Mbps with and without 20-km fiber link transmissions.

less signal) with the previous transmission test in the subsystem [Fig. 1(b)]. In the experiment, the wireless distance is set to 50 cm. The BER performance as a function of the received optical power for 500 and 312.5 Mbit/s data rates in both with and without 20 km fiber transmission are shown in Fig. 7. It can be observed that there was approximately 1-dB receiver penalty between optical back-to-back with 0.5-m wireless transmission and 20-km NZDSF transmission to achieve a BER of 2×10^{-3}.

4 Conclusions

In this report, we experimentally demonstrated a millimeter-wave wireless link operating at 75 to 100 GHz frequency band. Detailed characteristics of this W-band wireless channel were first analyzed in terms of frequency response, phase noise, emission distance, directivity, etc. in order to estimate and optimize the channel performance for data transmission. 3.5 m for 312.5 Mbit/s, and less than 1 m for 1 Gbit/s wireless 100 GHz transmission were successfully demonstrated to achieve BER performance below the FEC limit. Furthermore, by employing the RoF technology, 500-Mbps composite transmission performance over 20-km NZDSF and the wireless channel was also presented. Our results show the importance of

characterizing the hybrid optical-fiber wireless channel for 75- to 110-GHz operation; the data-system experiment shows the potential of high-capacity short-range wireless access systems. Further work is ongoing on comparison of our experimental results and theoretical modeling.

References

1. T. Kleine-Ostmann and T. Nagatsuma, "A review on terahertz communications research," *J. Infrared Millimet. Terahertz Waves* **32**(2), 143–171 (2011).
2. J. Wells, "Faster than fiber: the future of multi-gb/s wireless," *IEEE Microw. Mag.* **10**(3), 104–112 (2009).
3. H. S. Chung et al. "Transmission of multiple HD-TV signals over a wired/wireless line millimeter-wave link with 60 GHz," *J. Lightwave Technol.* **25**(11), 3413–3418 (2007).
4. M. Beltrn et al., "60 GHz DCM and BPSK ultra-wideband radio-over-fiber with 5 m wireless transmission at 1.44 Gbps," *2010 36'th European Conference and Exhibition on Optical Communication (ECOC)*, Paper Th.9.B.3, Turin, Italy.
5. C. W. Chow et al.,"100 GHz ultra-wideband (UWB) fiber-to-the-antenna (FTTA) system for in-building and in-home networks," *Opt. Express* **18**(2), 473–478 (2010).
6. A. Hirata, M. Harada, and T. Nagatsuma, "120-GHz wireless link using photonic techniques for generation, modulation, and emission of millimeter-wave signals," *J. Lightwave Technol.* **21**(10), 2145–2153 (2003).
7. R. Sambaraju et al., "Up to 40 Gb/s wireless signal generation and demodulation in 75-110 GHz band using photonic technique," *IEEE Topical Meeting on Microwave Photonics (MWP), 2010* (1October, Montreal, Quebec, Canada, (2010).
8. E. Rotholz, "Phase noise of mixer," *Electron. Lett.* **20**(19), 786–787 (1984).
9. G. Qi et al., "Phase-noise analysis of optically generated millimeter-wave signals with external optical modulation techniques," *J. Lightwave Technol.* **24**(12), 4861–4875 (2006).

Xiaodan Pang received a BSc degree in optical information science and technology from Shandong University, Jinan, China, in 2008, and an MSc degree in photonics from Royal Institute of Technology, Stockholm, Sweden, in 2010. He is currently pursuing a PhD degree in optical communications engineering at DTU Fotonik, Technical University of Denmark. His research interests are in the area of hybrid optical fiber-wireless communication systems.

Xianbin Yu received a PhD from Zhejiang University, Hangzhou, China, in 2005. From October 2005 to October 2007, he was a postdoctoral researcher with Tsinghua University, Beijing, China. In November 2007, he became a postdoctoral research fellow with DTU Fotonik, Technical University of Denmark, Lyngby, Denmark, where he is currently an assistant professor. He co-authored one book chapter and over 60 peer-reviewed international journal and conference papers. His research interests are in the areas of microwave photonics, optical-fiber communications, wireless-over-fiber, ultrafast photonic wireless signal processing, and ultrahigh-speed short-range access technologies.

Ying Zhao was born in Beijing, China, in 1984. He received a BS in electronic engineering from Peking University, Beijing, China, in 2007. He is currently working toward a PhD at the Department of Electronic Engineering, Tsinghua University and he is also a guest PhD student of the Department of Photonics Engineering, Technical University of Denmark. His current areas of interest are high-speed optical communications and radio-over-fiber technology.

Lei Deng received BS and MS degrees in optoelectronics and information engineering from Huazhong University of Science and Technology, Wuhan, China, in 2006 and 2008, respectively. He is a PhD candidate at the same university. Now he is in the Technical University of Denmark as a guest PhD student. His research interests include fiber-optic communications, advanced modulation formats, and OFDM in radio-over-fiber (RoF) systems and next-generation passive optical network (PON) systems.

Darko Zibar received the MSc degree in telecommunication in 2004 from the Technical University of Denmark and the PhD degree in 2007 from the Department of Communications, Optics and Materials, COM_DTU within the field of optical communications. He was a visiting researcher with Optoelectronic Research Group at the University of California, Santa Barbara (UCSB) from January 2006 to August 2006. From February 2009 until July 2009, he was visiting researcher with Nokia-Siemens Networks. Currently, he is employed at DTU Fotonik, Technical University of Denmark as the assistant professor. His research interests are in the area of coherent optical communication, with the emphasis on digital demodulation and compensation techniques. He is a recipient of the Best Student Paper Award at the IEEE Microwave Photonics Conference (MWP) 2006 as well as Villum Kann Rasmussen postdoctoral research grant in 2007.

Idelfonso Tafur Monroy is currently professor and head of the metro-access and short range communications group of DTU Fotonik at the Technical University of Denmark. He received a MSc degree from the Bonch-Bruevitch Institute of Communications, St. Petersburg, Russia, in 1992. He received a Technology Licenciate degree from the Royal Institute of Technology, Stockholm, Sweden, in 1996. In 1999 he received a PhD degree from the Electrical Engineering Department of the Eindhoven University of Technology, the Netherlands and worked as an assistant professor until 2006. He is currently involved in the ICT European projects GiGaWaM and EURO-FOS and is the technical coordinator of the ICT-CHRON project. His research interests are in hybrid optical-wireless communication systems, high-capacity optical fiber communications, digital signal processing for baseband, and radio-over-fiber links, application of nanophotonic technologies in the metropolitan and access segments of optical networks as well as in short-range optical-wireless communication links.

Paper 2: 25 Gbit/s QPSK Hybrid Fiber-Wireless Transmission in the W-Band (75-110 GHz) With Remote Antenna Unit for In-Building Wireless Networks

Xiaodan Pang, Antonio Caballero, Anton Dogadaev, Valeria Arlunno, Lei Deng, Robert Borkowski, Jesper S. Pedersen, Darko Zibar, Xianbin Yu, and Idelfonso Tafur Monroy, "25 Gbit/s QPSK Hybrid Fiber-Wireless Transmission in the W-Band (75-110 GHz) With Remote Antenna Unit for In-Building Wireless Networks," *IEEE Photonics Journal*, vol. 4, pp. 691-698, 2012.

25 Gbit/s QPSK Hybrid Fiber-Wireless Transmission in the W-Band (75–110 GHz) With Remote Antenna Unit for In-Building Wireless Networks

Xiaodan Pang, Student Member, IEEE
Antonio Caballero
Anton Dogadaev
Valeria Arlunno
Lei Deng
Robert Borkowski
Jesper S. Pedersen
Darko Zibar, Member, IEEE
Xianbin Yu, Member, IEEE
Idelfonso Tafur Monroy, Member, IEEE

25 Gbit/s QPSK Hybrid Fiber-Wireless Transmission in the W-Band (75–110 GHz) With Remote Antenna Unit for In-Building Wireless Networks

Xiaodan Pang,[1] *Student Member, IEEE*, **Antonio Caballero,**[1] **Anton Dogadaev,**[1]
Valeria Arlunno,[1] **Lei Deng,**[2] **Robert Borkowski,**[1] **Jesper S. Pedersen,**[1]
Darko Zibar,[1] *Member, IEEE*, **Xianbin Yu,**[1] *Member, IEEE*, **and**
Idelfonso Tafur Monroy,[1] *Member, IEEE*

[1]DTU Fotonik, Department of Photonics Engineering, Technical University of Denmark,
2800 Kgs. Lyngby, Denmark
[2]School of Optoelectronics Science and Engineering, HuaZhong University of Science and Technology,
Wuhan 430074, China

Abstract: In this paper, we demonstrate a photonic up-converted 25 Gbit/s fiber-wireless quadrature phase shift-keying (QPSK) data transmission link at the W-band (75–110 GHz). By launching two free-running lasers spaced at 87.5 GHz into a standard single-mode fiber (SSMF) at the central office, a W-band radio-over-fiber (RoF) signal is generated and distributed to the remote antenna unit (RAU). One laser carries 12.5 Gbaud optical baseband QPSK data, and the other acts as a carrier frequency generating laser. The two signals are heterodyne mixed at a photodetector in the RAU, and the baseband QPSK signal is transparently up-converted to the W-band. After the wireless transmission, the received signal is first down-converted to an intermediate frequency (IF) at 13.5 GHz at an electrical balanced mixer before being sampled and converted to the digital domain. A digital-signal-processing (DSP)-based receiver is employed for offline digital down-conversion and signal demodulation. We successfully demonstrate a 25 Gbit/s QPSK wireless data transmission link over a 22.8 km SSMF plus up to 2.13 m air distance with a bit-error-rate performance below the 2×10^{-3} forward error correction (FEC) limit. The proposed system may have the potential for the integration of the in-building wireless networks with the fiber access networks, e.g., fiber-to-the-building (FTTB).

Index Terms: Microwave photonics, radio over fiber, optical communications.

1. Introduction

The emergence of mobile devices such as multifunction mobile phones and tablets accompanied with future bandwidth intensive applications, e.g., 3-D Internet and Hi-Vision/Ultra High Definition TV data (more than 24 Gbit/s) [1], has become one of the drivers for demanding wireless data capacity on the scale of tens of gigabits per second. It is highly desirable that the future wireless links will possess the same capacity with the optical fibers to realize the seamless hybrid fiber-wireless access over the last mile [2]. Radio-over-fiber (RoF) communication systems are considered to be one of the most promising candidates to provide ultrabroadband services while maintaining high mobility in this
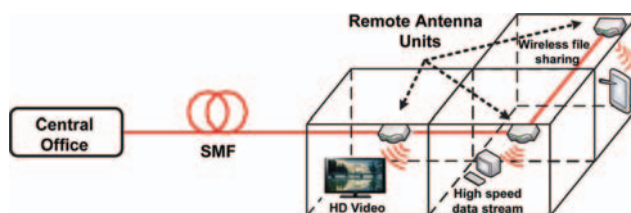
Fig. 1. Hybrid fiber-wireless access system for multiapplications in-building environment.

context. As shown in Fig. 1, an in-building hybrid fiber-wireless access system implemented via RoF technology provides an elegant solution for flexible multiservice wireless access. A key point in such scenario is that the remote antenna units (RAUs) should keep a simple, passive and compact structure, leading to a low-cost implementation [3], [4].

Meanwhile, there are mainly two approaches to achieve tens of gigabits per second wireless capacity. One possible solution is to increase the wireless spectral efficiency to enlarge the data throughput over the same bandwidth [5]. However, it will largely increase the signal-to-noise ratio (SNR) requirement, as well as the receiver complexity. Another straightforward solution is to raise the carrier frequency to higher frequency bands, e.g., millimeter-wave (MMW) range (30–300 GHz), where a broader bandwidth is available. Currently, the frequency bands below 100 GHz have limited unlicensed bandwidth left for wireless transmission [6]. In recent years, a number of multigigabit hybrid fiber-wireless links operating at the 60 GHz band are investigated and reported [5], [7], [8]. Nevertheless, the under-exploited higher frequency range at 100 GHz and above is becoming a timely relevant research topic for its wider bandwidth availability.

Recently, the W-band (75–110 GHz) is attracting increasing attention due to its potential to provide the requested high capacity [6]. The Federal Communications Commission (FCC) has opened the commercial use of spectra in the 71–75.5 GHz, 81–86 GHz, 92–100 GHz, and 102–109.5 GHz bands [9], which are recommended for high-speed wireless communications. Analysis and measurements on W-band signal generation, detection, and wireless transmission properties are under intensive investigation. In terms of signal generation and detection scheme, W-band channel properties measurements and signal transmissions based on electronically frequency up and down-conversion are reported in [10]–[12], while an up to 40 Gbit/s wireless signal transmission in the W-band using both photonic generation and detection without air transmission is demonstrated and detailed analyzed [13], [14]. Specifically, an ultrabroadband photonic down-converter based on optical comb generation that can operate from microwave up to 100 GHz has recently been introduced [15]. Considering the wireless distance, data rate, and signal formats transmitted in the W-band, to date, 10 Gbit/s transmission over 400 m single-mode fiber (SMF) plus 120 m wireless distance with simple amplitude shift-keying (ASK) modulation is reported [16], while an error-free (1×10^{-12}) 20 Gbit/s on–off-keying (OOK) signal transmission through 25 km SMF and 20 cm wireless is demonstrated [17]. To achieve higher spectral efficiency, quadrature phase shift-keying (QPSK) and 16-quadrature amplitude modulation (16-QAM) have also been used to obtain 20 Gbit/s [18] and 40 Gbit/s [19] in the W-band. In [18] and [19], a coherent optical heterodyning method is used to generate the W-band wireless carrier, and transmission performance below forward error correction (FEC) limit of 2×10^{-3} is achieved with 30 mm wireless distance. By using an optical frequency comb generator, a three-channel 8.3 Gbit/s/ch optical orthogonal frequency-division-multiplexing (OOFDM) transmission over 22.8 km SMF with up to 2 m air distance is reported in [20]. More recently, an up to 100 Gbit/s line rate wireless transmission in the W-band with air distance of 1.2 m by combining optical polarization multiplexing and wireless spatial multiplexing has been demonstrated; however, there are only a few meters of fiber transmission [21]. Nevertheless, considering the integration of the in-building wireless networks with the existing optical fiber access networks, e.g., fiber-to-the-building (FTTB) networks, a system with a better compromise between fiber transmission distance, wireless coverage, and data rate need to be further developed.
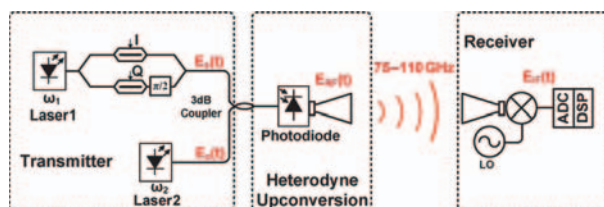
Fig. 2. Block diagram of hybrid optical fiber-wireless system using incoherent heterodyne up-conversion and electrical and digital down-conversion.

In this paper, we propose and experimentally demonstrate a hybrid fiber-wireless link at the W-band which can be potentially used for integrating the in-building wireless access networks with the optical fiber access networks, as shown in Fig. 1. By using photonic up-conversion technique with two free-running laser heterodyning (incoherent method), the proposed system seamlessly converts an optical baseband signal into the W-band. For demonstration, a 25 Gbit/s QPSK signal occupying a bandwidth of 25 GHz centered at 87.5 GHz is transmitted. A W-band low-noise amplifier (LNA) and a broadband balanced mixer are employed at the receiver for down-converting the received signal to an intermediate frequency (IF) centering at 13.5 GHz, and a digital-signal-processing (DSP)-based signal demodulator is implemented for digital down-conversion, I/Q separation, synchronization, equalization, and signal demodulation. The data transmitted after 22.8 km SMF plus 2.3 m wireless are successfully recovered with a bit-rate-ratio (BER) performance well below the FEC limit of 2×10^{-3}. The RAU in this proposed downlink system consists of only a fast responsive photodetector and a W-band horn antenna, therefore fulfilling the passive, simplicity, and low-cost requirements. When considering the bidirectional transmission, an electrical local oscillator (LO) may also be needed in the RAU for a low-cost optical modulation in the uplink.

2. Principle of Incoherent Heterodyne Up-Conversion and Two Stage Down-Conversion

Fig. 2 shows the block diagram of the proposed system. The W-band signal is generated by heterodyning mixing the baseband optical signal with a second free-running lightwave at the photodetector. At the receiver, the W-band signal is first down-converted electrically to an IF and then sampled and digitally converted down to the baseband.

At the transmitter, the inphase and quadrature branches of the I/Q modulator are, respectively, modulated by two binary data sequences $I(t)$ and $Q(t)$. The baseband optical QPSK signal $\hat{E}_s(t)$ and the carrier frequency generating laser $\hat{E}_c(t)$ can be represented as

$$\hat{E}_s(t) = \sqrt{P_s} \cdot [I(t) + jQ(t)] \cdot e^{[-j(\omega_s t + \phi_s(t))]} \cdot \hat{e}_s \tag{1}$$

$$\hat{E}_c(t) = \sqrt{P_c} \cdot e^{[-j(\omega_c t + \phi_c(t))]} \cdot \hat{e}_c \tag{2}$$

where P_s, ω_s, and $\phi_s(t)$ represent the optical power, angular frequency, and phase of the signal laser, respectively, and P_c, ω_c and $\phi_c(t)$ represent the carrier generating laser. $\hat{e}_s$ and $\hat{e}_c$ are the optical polarization unit vectors. The combined signal is beating at a photodiode for heterodyne up-conversion, and the output signal $E_{out}(t)$ can be described as

$$E_{out}(t) \propto |E_s(t) + jE_c(t)|^2 = P_s + P_c + E_{RF}(t)$$

$$E_{RF}(t) = 2\sqrt{P_s P_c} \cdot [I(t) \cdot \sin(\triangle \omega t + \triangle \phi(t)) + Q(t) \cdot \cos(\triangle \omega t + \triangle \phi(t))] \cdot \hat{e}_s \hat{e}_c$$

$$\triangle \omega = \omega_c - \omega_s, \quad \triangle \phi(t) = \phi_c(t) - \phi_s(t) \tag{3}$$

where $E_{RF}(t)$ represents the generated RF signal transmitted into the air with carrier frequency of $\triangle \omega$. At the receiver, an electrical sinusoidal LO signal is mixed with the received RF signal at a
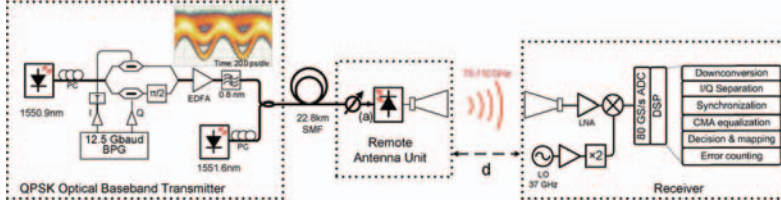
Fig. 3. Experimental setup for hybrid fiber-wireless transmission of 25 Gbit/s QPSK signals in the W-band. BPG: Binary pattern generator. (The eye diagram of the QPSK baseband signal is shown in the inset.)

balanced mixer. The LO signal with power P_{LO}, angular frequency ω_{LO}, and phase $\phi_{LO}(t)$ is expressed as $E_{LO}(t) = \sqrt{P_{LO}} \cdot \cos(\omega_{LO}t + \phi_{LO}(t))$. Then, the W-band signal is down-converted into an IF signal, which is expressed as

$$E_{IF}(t) = \langle E_{RF}(t) \cdot E_{LO}(t) \rangle$$
$$= \sqrt{P_s P_c P_{LO}} \cdot [I(t) \cdot \sin(\triangle\omega_{IF}t + \triangle\phi_{IF}(t)) + Q(t) \cdot \cos(\triangle\omega_{IF}t + \triangle\phi_{IF}(t))] \cdot \hat{e}_s \hat{e}_c$$
$$\triangle\omega_{IF} = \omega_{LO} - (\omega_c - \omega_s), \quad \triangle\phi_{IF}(t) = \phi_{LO}(t) - (\phi_c(t) - \phi_s(t)). \qquad (4)$$

The angle brackets denote low-pass filtering used for rejecting the components at $\triangle\omega + \omega_{LO}$. From the equation, it can be seen that he phase noise of the signal laser, carrier laser and LO signal are all included in $\triangle\phi_{IF}(t)$. The IF signal is then sampled and converted to digital domain, where the second stage down-conversion takes place. Assuming the sampling period of the analog-to-digital conversion (ADC) is T_s, the output signal after down-conversion and low-pass filtering can be expressed as

$$E_{Rx}(nT_s) = \langle E_{IF}(nT_s) \cdot e^{j\triangle\omega_{IF}nT_s} \rangle$$
$$= \frac{1}{2}\sqrt{P_s P_c P_{LO}} \cdot [I(nT_s) \cdot \sin(\triangle\phi_{IF}(nT_s)) - jI(nT_s) \cdot \cos(\triangle\phi_{IF}(nT_s)) + Q(nT_s)$$
$$\cdot \cos(\triangle\phi_{IF}(nT_s)) + jQ(nT_s) \cdot \sin(\triangle\phi_{IF}(nT_s))] \cdot \hat{e}_s \hat{e}_c$$
$$= -\frac{1}{2}j\sqrt{P_s P_c P_{LO}} \cdot (I(nT_s) + jQ(nT_s)) \cdot e^{(j\triangle\phi_{IF}(nT_s))} \cdot \hat{e}_s \hat{e}_c. \qquad (5)$$

It is noted that the system loss is not considered in the expressions. As shown in (5), the term $I(nT_s) + jQ(nT_s)$ is our desired QPSK signal, while the $exp(j\triangle\phi_{IF}(nT_s))$ item contains all the phase noise accumulated during the transmission, which is to be corrected during DSP demodulation [13]. The efficiency of the phase noise correction depends on the signal linewidth, which should be kept as narrow as possible by using narrow linewidth lasers for the heterodyne up-conversion [14]. It is also shown that maximum value of the signal power is achieved when the polarization states $\hat{e}_s$ and $\hat{e}_c$ are aligned.

3. Experimental Setup

Fig. 3 shows the schematic of the experimental setup. A optical carrier emitted from an external cavity laser (ECL, $\lambda_1 = 1552.0$ nm) with 100 kHz linewidth is fed into a integrated LiNbO3 I/Q modulator, where two independent 12.5 Gbaud binary data streams (pseudo-random bit sequence (PRBS) of length $2^{15} - 1$) modulate the phase of the optical carrier, resulting in a 25 Gbit/s optical baseband QPSK signal at the output of the modulator. An erbium-doped fiber amplifier (EDFA) is employed for amplification, and an optical bandpass filter (OBPF) with 0.8 nm bandwidth is used to filter the out-of-band noise. Subsequently, the optical QPSK signal is combined with an unmodulated CW optical carrier from a second ECL ($\lambda_2 = 1551.3$ nm) with 100 kHz linewidth, corresponding to a 0.7 nm difference from the central wavelength of the baseband QPSK signal.
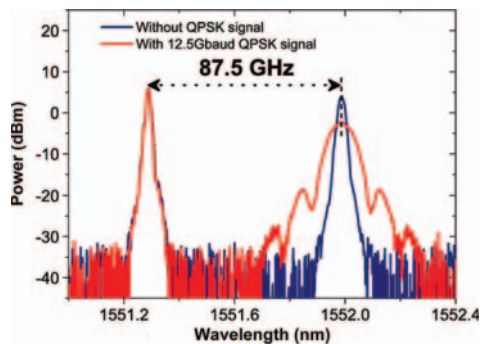
Fig. 4. Optical spectra at the input of the photodetector [point (a) in Fig. 3] with and without the QPSK data modulation.

The combined QPSK signal and the unmodulated CW carrier can be then transmitted to a RAU where they are heterodyne mixed at a 100 GHz photodetector (u²t XPDV4120R). Optical transmission through 22.8 km of standard single-mode fiber (SSMF) is evaluated during the experiment. As the combined signal can be considered as a single sideband (SSB) RoF signal, the periodical RF power fading in a conventional double sideband (DSB) modulated RoF system caused by the fiber dispersion no longer exists [7]. Fig. 4 shows the optical spectra of the combined signal at point (a) in Fig. 3. The signal after the photodetection is an electrical QPSK signal at the W-band of a 25 GHz total bandwidth with the central frequency at 87.5 GHz, which is fed to a rectangular W-band horn antenna with 24 dBi gain. After wireless transmission, the W-band QPSK signal is received by a second W-band rectangular horn antenna with 25 dBi gain. The received signal is amplified by a 25 dB gain LNA (Radiometer Physics W-LNA) with a noise figure of 4.5 dB. Subsequently, an electrical down-conversion is performed at a W-band balanced mixer driven by a 74 GHz sinusoidal LO obtained after frequency doubling from a 37 GHz signal synthesizer (Rohde & Schwarz SMF 100A), and the signal located in the 75–100 GHz band is translated to a IF of 1–26 GHz with a central frequency at 13.5 GHz. The IF signal is sampled at 80 GS/s by a digital signal analyzer with 32 GHz real time bandwidth (Agilent DSAX93204A) and demodulated by offline DSP. The DSP algorithm consists of frequency down conversion, I/Q separation, synchronization, equalization, data recovery by symbol mapping, and BER tester. In the equalization module, due to the inherent constant envelop nature of the QPSK signal, a five-tap constant-modulus algorithm (CMA) pre-equalizer is first employed for blind channel equalization, followed by a carrier-phase recovery process and a post-equalization in the form of a nonlinear decision feedback equalizer (DFE). A more detailed description of the receiver can be found in [14]. We can clearly observe the performance improvement by comparing the received signal constellations with/without the CMA equalization for the 25 Gbit/s W-band QPSK signal shown in Fig. 5.

4. Experimental Results and Discussions

An optimal ratio between the carrier generating signal power P_c and the baseband QPSK signal power P_s before the combining and heterodyning is first evaluated with respect to BER performance. Fig. 6 illustrates the measured BER performance and the theoretical equivalent isotropic radiated power (EIRP) as a function of the power ratio between P_c and P_s. We can observe that the best BER performance occurs when the carrier power equals to the signal power, where the maximum signal EIRP is generated. This performance is also in accordance with that shown in (3), as the maximum RF signal power can only be obtained if P_c and P_s are equal when the combined optical power is kept constant.
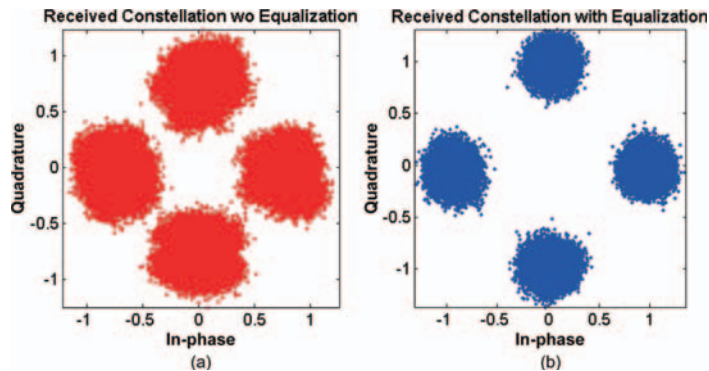
Fig. 5. Received constellations of 25 Gbit/s W-band QPSK signal after 0.5 m of air transmission. (a) Without CMA equalization. (b) With CMA equalization.
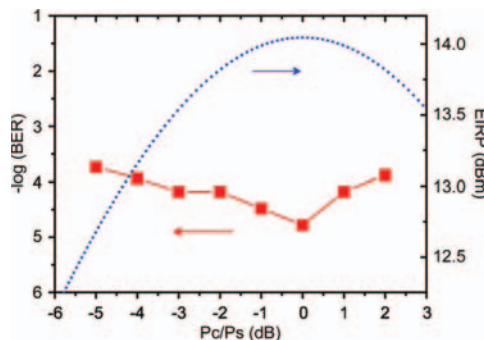

Fig. 6. Measured BER performance and simulated EIRP as a function of power ratio between the carrier generating signal and the baseband QPSK signal (P_c/P_s) with constant 1.5 dBm combined power at the PD after 1 m of wireless transmission.

After fixing the operational power ratio at the optimal value, the evaluation of the system transmission properties is performed. Fig. 7 illustrates the error-vector-magnitude (EVM) of the demodulated signal as a function of the transmitted wireless distance with the corresponding signal constellations shown in the insets. By fixing the received optical power by the PD at 1.5 dBm, it can be seen that a gradually degradation of EVM performance with the increase of the wireless transmission distance. At 50 cm, the received signal has an EVM of 26% and the clusters in the constellation are small and clearly separated, while the value becomes 53% with the distance increasing to 120 cm, and the corresponding constellation becomes disseminated, which is due to the decreased SNR at the receiver, as well as the decreased accuracy of the antenna alignment.

Fig. 8 displays the system BER performances as a function of the received optical power at the PD [point (a) in Fig. 3] with wireless distances at 1 and 2.13 m for both without optical fiber and with 22.8 km SMF transmission. It is noted that the SNR of the received IF signal is quite limited by the responsivity of the PD ($\sim$0.3 A/W at 87.5 GHz), the saturation level of the W-band LNA (-20 dBm maximum input power) and the low conversion efficiency of the broadband electrical mixer. However, considering a 7% FEC overhead can potentially be effective for BER of 2×10^{-3}, we can observe that for both the 1 m and 2.13 m wireless cases, the BERs are well below this limit.
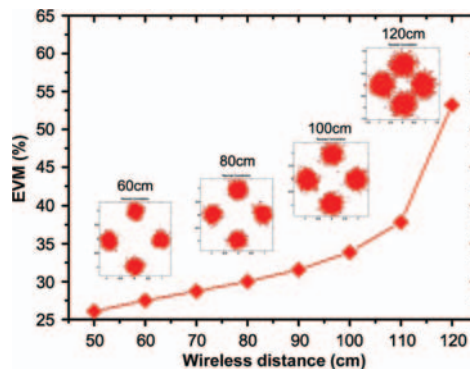
Fig. 7. EVM versus wireless distance with 1.5 dBm optical power at the PD (corresponding constellations are shown in the insets).
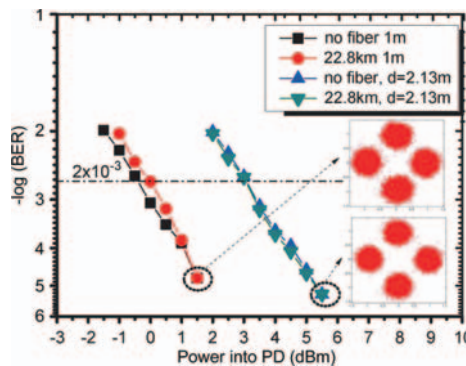

Fig. 8. BER as a function of received optical power at the PD for wireless distances at 1 and 2.13 m. (Insets: the received constellations after 1 m and 2.13 m wireless plus 22.8 km SMF transmission.)

Receiver sensitivities at the FEC limit are 0 dBm and 3 dBm for the 1 and 2 m wireless distance, respectively. It can be seen that all the measured curves are quite linear with respect to the power change, which is almost only due to change of SNR at the receiver, as the CMA equalizer can correct a certain degree of distortion introduced during the transmission. Moreover, because of the uncorrelated phase relation between the carrier and the baseband signal, the relative phase delay caused by the fiber dispersion only has effect on the baseband signal itself. It is observed that the 22.8 km SMF induces less than a 0.5 dB penalty for both cases, which confirms the possibility for integrating the proposed system with the FTTB networks.

5. Conclusion

We have demonstrated a 25 Gbit/s hybrid fiber-wireless transmission system in the W-band with 22.8 km SSMF plus up to 2.13 m of air distance. The W-band QPSK signal is generated by transparent photonic up-conversion using incoherent heterodyning between two free-running lasers. Electrical down-conversion combined with DSP receiver makes the system robust against phase noise and distortion. The RAU structure consisting of only a fast responsive PD and a transmitter

antenna is kept passive and simple to maintain its flexibility. Thus, this system may have the potential to be used in the integration of the in-building distribution networks with the fiber access networks like FTTB systems.

References

[1] T. Nagatsuma, T. Takada, H.-J. Song, K. Ajito, N. Kukutsu, and Y. Kado, "Millimeter- and THz-wave photonics towards 100-Gbit/s wireless transmission," in *Proc. 23rd Annu. Meeting IEEE Photon. Soc.*, 2010, pp. 385–386.

[2] J. Wells, "Faster than fiber: The future of multi-G/s wireless," *IEEE Microw. Mag.*, vol. 10, no. 3, pp. 104–112, May 2009.

[3] L. Deng, X. Pang, Y. Zhao, M. B. Othman, J. B. Jensen, D. Zibar, X. Yu, D. Liu, and I. Tafur Monroy, "2 × 2 MIMO-OFDM gigabit fiber-wireless access system based on polarization division multiplexed WDM-PON," *Opt. Exp.*, vol. 20, no. 4, pp. 4369–4375, Feb. 2012.

[4] C. W. Chow, F. M. Kuo, J. W. Shi, C. H. Yeh, Y. F. Wu, C. H. Wang, Y. T. Li, and C. L. Pan, "100 GHz ultra-wideband (UWB) fiber-to-the-antenna (FTTA) system for in-building and in-home networks," *Opt. Exp.*, vol. 18, no. 2, pp. 473–478, Jan. 2010.

[5] C.-T. Lin, J. Chen, W.-J. Jiang, L.-Y. Wang He, P.-T. Shih, C.-H. Ho, and S. Chi, "Ultra-high data-rate 60 GHz radio-over-fiber systems employing optical frequency multiplication and adaptive OFDM formats," presented at the Optical Fiber Commun. Conf. Expo., Nat. Fiber Optic Engineers Conf., Los Angeles, CA, 2011, Paper OThJ6.

[6] D. Zibar, A. Caballero Jambrina, X. Yu, X. Pang, A. K. Dogadaev, and I. Tafur Monroy, "Hybrid optical fibre-wireless links at the 75–110 GHz band supporting 100 Gbps transmission capacities," in *Proc MWP/APMP*, Singapore, Nov. 2011, pp. 445–449.

[7] H.-C. Chien, Y.-T. Hsueh, A. Chowdhury, J. Yu, and G.-K. Chang, "Optical millimeter-wave generation and transmission without carrier suppression for single- and multi-band wireless over fiber applications," *J. Lightw. Technol.*, vol. 28, no. 16, pp. 2230–2237, Aug. 2010.

[8] M. Weiss, A. Stohr, F. Lecoche, and B. Charbonnier, "27 Gbit/s photonic wireless 60 GHz transmission system using 16-QAM OFDM," in *Proc. Int. Topical Meeting MWP*, 2009, pp. 1–3.

[9] FCC online table of frequency allocations. [Online]. Available: www.fcc.gov/oet/spectrum/table/fcctable.pdf

[10] X. Pang, X. Yu, Y. Zhao, L. Deng, D. Zibar, and I. Tafur Monroy, "Channel measurements for an optical fiber-wireless transmission system in the 75–110 GHz band," in *Proc. Int. Topical Meeting Microw. Photon. Conf. Microw. Photon.*, 2011, pp. 21–24.

[11] Y. Zhao, L. Deng, X. Pang, X. Yu, X. Zheng, H. Zhang, and I. Tafur Monroy, "Digital predistortion of 75–110 GHz W-band frequency multiplier for fiber wireless short range access systems," *Opt. Exp.*, vol. 19, no. 26, pp. B18–B25, Dec. 2011.

[12] R. W. Ridgway, D. W. Nippa, and S. Yen, "Data transmission using differential phase-shift keying on a 92 GHz carrier," *IEEE Trans. Microw. Theory Tech.*, vol. 58, no. 11, pp. 3117–3126, Nov. 2010.

[13] D. Zibar, R. Sambaraju, A. Caballero, J. Herrera, U. Westergren, A. Walber, J. B. Jensen, J. Marti, and I. Tafur Monroy, "High-capacity wireless signal generation and demodulation in 75- to 110-GHz band employing all-optical OFDM," *IEEE Photon. Technol. Lett.*, vol. 23, no. 12, pp. 810–812, Jun. 2011.

[14] A. Caballero Jambrina, D. Zibar, R. Sambaraju, J. Marti, and I. Tafur Monroy, "High-capacity 60 GHz and 75–110 GHz band links employing all-optical OFDM generation and digital coherent detection," *J. Lightw. Technol.*, vol. 30, no. 1, pp. 147–155, Jan. 2012.

[15] Y. Zhao, X. Pang, L. Deng, X. Yu, X. Zheng, and I. Tafur Monroy, "Ultra-broadband photonic harmonic mixer based on optical comb generation," *IEEE Photon. Technol. Lett.*, vol. 24, no. 1, pp. 16–18, Jan. 2012.

[16] A. Hirata, H. Takahashi, R. Yamaguchi, T. Kosugi, K. Murata, T. Nagatsuma, N. Kukutsu, and Y. Kado, "Transmission characteristics of 120-GHz-band wireless link using radio-on-fiber technologies," *J. Lightw. Technol.*, vol. 26, no. 15, pp. 2338–2344, Aug. 2008.

[17] F.-M. Kuo, C.-B. Huang, J.-W. Shi, N.-W. Chen, H.-P. Chuang, J. E. Bowers, and C.-L. Pan, "Remotely up-converted 20-Gbit/s error-free wireless on–off-keying data transmission at W-band using an ultra-wideband photonic transmitter-mixer," *IEEE Photon. J.*, vol. 3, no. 2, pp. 209–219, Apr. 2011.

[18] A. Kanno, K. Inagaki, I. Morohashi, T. Sakamoto, T. Kuri, I. Hosako, T. Kawanishi, Y. Yoshida, and K.-I. Kitayama, "20-Gb/s QPSK W-band (75–110 GHz) wireless link in free space using radio-over-fiber technique," *IEICE Electron. Exp.*, vol. 8, no. 8, pp. 612–617, 2011.

[19] A. Kanno, K. Inagaki, I. Morohashi, T. Sakamoto, T. Kuri, I. Hosako, T. Kawanishi, Y. Yoshida, and K.-I. Kitayama, "40 Gb/s W-band (75–110 GHz) 16-QAM radio-over-fiber signal generation and its wireless transmission," *Opt. Exp.*, vol. 19, no. 26, pp. B56–B63, Dec. 2011.

[20] L. Deng, M. Beltran, X. Pang, X. Zhang, V. Arlunno, Y. Zhao, A. Caballero Jambrina, A. K. Dogadaev, X. Yu, R. Llorente, D. Liu, and I. Tafur Monroy, "Fiber wireless transmission of 8.3-Gb/s/ch QPSK-OFDM signals in 75–110-GHz band," *IEEE Photon. Technol. Lett.*, vol. 24, no. 5, pp. 383–385, Mar. 2012.

[21] X. Pang, A. Caballero Jambrina, A. Dogadaev, V. Arlunno, R. Borkowski, J. Pedersen, L. Deng, F. Karinou, F. Roubeau, D. Zibar, X. Yu, and I. Tafur Monroy, "100 Gbit/s hybrid optical fiber-wireless link in the W-band (75–110 GHz)," *Opt. Exp.*, vol. 19, no. 25, pp. 24 944–24 949, Dec. 2011.

Paper 3: 100 Gbit/s hybrid optical fiber-wireless link in the W-band (75-110 GHz)

Xiaodan Pang, Antonio Caballero, Anton Dogadaev, Valeria Arlunno, Robert Borkowski, Jesper S. Pedersen, Lei Deng, Fotini Karinou, Fabien Roubeau, Darko Zibar, Xianbin Yu, and Idelfonso Tafur Monroy, "100 Gbit/s hybrid optical fiber-wireless link in the W-band (75-110 GHz)," *Optics Express*, vol. 19, pp. 24944-24949, 2011.

100 Gbit/s hybrid optical fiber-wireless link in the W-band (75–110 GHz)

Xiaodan Pang, Antonio Caballero, Anton Dogadaev, Valeria Arlunno, Robert Borkowski, Jesper S. Pedersen, Lei Deng, Fotini Karinou, Fabien Roubeau, Darko Zibar, Xianbin Yu, [*] **Idelfonso Tafur Monroy**

DTU Fotonik, Department of Photonics Engineering, Technical University of Denmark
2800, Kgs. Lyngby, Denmark
[*]xiyu@fotonik.dtu.dk

Abstract: We experimentally demonstrate an 100 Gbit/s hybrid optical fiber-wireless link by employing photonic heterodyning up-conversion of optical 12.5 Gbaud polarization multiplexed 16-QAM baseband signal with two free running lasers. Bit-error-rate performance below the FEC limit is successfully achieved for air transmission distances up to 120 cm.

© 2011 Optical Society of America

OCIS codes: (060.5625) Radio frequency photonics; (060.2330)Fiber optics communications.

References and links

1. J. Wells, "Faster than fiber: the future of multi-Gb/s wireless," IEEE Microw. Mag. **10**, 104–112 (2009).
2. T. Nagatsuma, T. Takada, H.-J. Song, K. Ajito, N. Kukutsu, and T. Kado, "Millimeter- and THz-wave photonics towards 100-Gbit/s wireless transmission," IEEE Photonic Society's 23rd Annu. Meeting, Denver, CO, Nov. 7–11, 2010, Paper WE4.
3. J. Takeuchi, A. Hirata, H. Takahashi, and N. Kukutsu, "10-Gbit/s bi-directional and 20-Gbit/s uni-directional data transmission over a 120-GHz-band wireless link using a finline ortho-mode transducer," Asia-Pacific Microwave Conference Proceedings (APMC) 195–198 (2010).
4. A. Hirata, R. Yamaguchi, T. Kosugi, H. Takahashi, K. Murata, T. Nagatsuma, N. Kukutsu, Y. Kado, N. Iai, S. Okabe, S. Kimura, H. Ikegawa, H. Nishikawa, T. Nakayama, and T. Inada, "10-Gbit/s wireless link using InP HEMT MMICs for generating 120-GHz-band millimeter-wave signal," IEEE Trans. Microw. Theory Tech. **57**, 1102–1109 (2009).
5. F.-M. Kuo, C.-B. Huang, J.-W. Shi, N.-W. Chen, H.-P. Chuang, J. Bowers, and C.-L. Pan, "Remotely up-converted 20-Gbit/s error free wireless on-off-keying data transmission at w-band using an ultrawideband photonic transmitter-mixer," IEEE Photon. J. **3**, 209–219 (2011).
6. R. Ridgway, D. Nippa, and S. Yen,"Data transmission using differential phase-shift keying on a 92 GHz carrier," IEEE Trans. Microw. Theory Tech. **58**, 3117–3126 (2010).
7. H. Takahashi, T. Kosugi, A. Hirata, K. Murata, and N. Kukutsu, "10-Gbit/s BPSK modulator and demodulator for a 120-GHz-band wireless link, " IEEE Trans. Microw. Theory Tech. **59**, 1361–1368 (2011).
8. A. Kanno, K. Inagaki, I. Morohashi, T. Sakamoto, T. Kuri, I. Hosako, T. Kawanishi, Y. Yoshida, and K.-I. Kitayama, "20-Gb/s QPSK W-band (75-110GHz) wireless link in free space using radio-over-fiber technique," IEICE Electron. Express **8**, 612–617 (2011).
9. A. Kanno, K. Inagaki, I. Morohashi, T. Sakamoto, T. Kuri, I. Hosako, T. Kawanishi, Y. Yoshida, and K.-I. Kitayama, "40 Gb/S W-BAND (75-110 GHZ) 16-QAM Radio-over-fiber signal generation and its wireless transmission" We.10.P1.112, ECOC 2011.
10. D. Zibar, R. Sambaraju, A. Caballero, J. Herrera, U. Westergren, A. Walber, J. B. Jensen, J. Marti, and I. Tafur Monroy, "High-capacity wireless signal generation and demodulation in 75- to 110-GHz band employing all-optical OFDM," IEEE Photon. Technol. Lett. **23**, 810–812 (2011).
11. A. H. Gnauck, P. J. Winzer, S. Chandrasekhar, X. Liu, B. Zhu, and D. W. Peckham, "Spectrally efficient long-haul WDM transmission using 224-Gb/s polarization-multiplexed 16-QAM," J. Lightwave Technol. **29**, 373–377 (2011).

1. Introduction

Hybrid optical fiber-wireless transmission systems with ultrahigh capacities will serve as the key building block to support the next generation truly user-centered networking. Users will create a virtual 'personal atmosphere' of connectivity to the world, that will follow the users whether they are on their workplace, traveling or at home. This user personal atmosphere will be powered by ubiquitous access and control to services and application enabled by seamless broadband wireless-fiber connections to a large range of devices in their near vicinity. To realize the seamless integration of wireless and fiber-optic networks, the wireless links needs to be developed to match the capacity of high-speed fiber-optic communication systems, while preserving transparency to bit-rates and modulation formats [1].

Currently, the W-band (75-110 GHz) has attracted increasing interest as a candidate radio frequency (RF) band to provide wireless communication links with multi-gigabit data transmission. Technology roadmap studies show that there is a conceivable demand in the years to come for 100 Gbit/s wireless capacity links [2]. Among current and emerging applications to use such high capacities are wireless closed-proximity transmission links and short range wireless communications. As an example, transmission of super Hi-Vision format is expected to require a transmission speed of 24 Gbit/s [2]. These trends accompanied by the growing demand for flexible access to cloud services with high speed peripherals motivate us to look for technologies and techniques to realize 100 Gbit/s fiber-wireless transmission links.

Wireless data transmission above 10 Gbit/s with simple amplitude shift-keying modulation (ASK) in the W-band have been demonstrated by mainly using millimeter-wave electronics [3] and hybrid photonic-electronic techniques [4, 5]. More advanced modulation formats in the W-band such as differential phase shift-keying (DPSK), binary/quadrature phase shift-keying (BPSK/QPSK) with data rates of 10 Gbit/s and 20 Gbit/s are reported in [6–8]. Most recently, 40 Gbit/s 16-level quadrature amplitude modulation (16-QAM) wireless transmission in the W-band is presented [9]. We have previously demonstrated 40 Gbit/s signal generation in the W-band by employing photonic up-conversion of all-optical frequency division multiplexed (OFDM) QPSK signals, with detection performed by photonic down conversion supported by digital coherent demodulation [10]. Regarding achieved air transmission distances for bit-rates above 20 Gbit/s in the W-band, so far 20 cm for 20 Gbit/s ASK transmission [5] and 3 cm for 40 Gbit/s 16-QAM transmission [9] are reported. However, both capacity and wireless transmission distance need to be further developed.

In this paper, we report on a hybrid optical fiber-wireless transmission link achieving 100 Gbit/s by transparent photonic up-conversion of a polarization multiplexed (PolMux) 16-QAM optical baseband signal with wireless transmission in the W-band. Bit-error rate (BER) performance below 2×10^{-3} is successfully achieved for wireless transmission distances up to 120 cm. Considering a 7% FEC overhead, error free transmission of an overall net bit rate of 93 Gbit/s can be expected. We believe this is a breakthrough in hybrid optical fiber-wireless transmission systems that open the door for ultra-high capacity short range and close-proximity user-centered networking.

2. Principle of heterodyne up-conversion and two stage down-conversion

In our proposed system, the RF signal is generated by direct heterodyning with two free running lasers. After the wireless transmission, two stage down-conversion is implemented before signal demodulation. First stage is electrically down-converting the RF signal to a lower intermediate frequency (IF) and the second stage is implemented in digital domain using digital signal processing (DSP) method. The block diagram of this architecture is shown in Fig. 1.

At the transmitter, an I/Q modulator is used to generate signals with high level modulation format. The inphase and quadrature branches are respectively modulated with multilevel signals
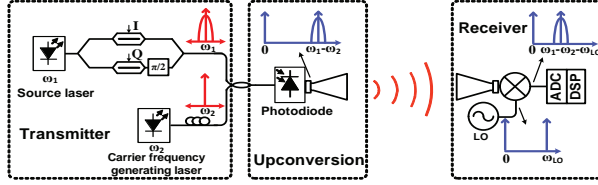
Fig. 1. Block diagram of hybrid optical fiber-wireless system using heterodyne up-conversion and two stage down-conversion.

$I(t)$ and $Q(t)$. The output optical baseband signal at frequency ω_1 from the I/Q modulator is combined with a carrier frequency generating laser with frequency ω_2 before the photodiode. The optical baseband signal $\hat{\mathbf{E}}_s(t)$ and the carrier frequency generating laser signal $\hat{\mathbf{E}}_c(t)$ can be represented as:

$$\hat{\mathbf{E}}_s(t) = \sqrt{P_s} \cdot [I(t) + jQ(t)] \cdot \exp[-j(\omega_1 t + \phi_1(t))] \cdot \hat{\mathbf{e}}_s \qquad (1)$$

$$\hat{\mathbf{E}}_c(t) = \sqrt{P_c} \cdot \exp[-j(\omega_2 t + \phi_2(t))] \cdot \hat{\mathbf{e}}_c \qquad (2)$$

where P_s, P_c are optical power of the signal laser and the carrier frequency generating laser, $\phi_1(t)$ and $\phi_2(t)$ are phases of the signal and carrier frequency generating laser, and $\hat{\mathbf{e}}_s$, $\hat{\mathbf{e}}_c$ are the polarization unit vectors.

After heterodyne beating at the photodiode, the generated electrical signal consists of a baseband component and a RF signal with carrier frequency $\omega_{RF} = |\omega_1 - \omega_2|$. So the RF signal transmitted into the air can be expressed as:

$$E_{RF}(t) = 2\sqrt{P_s P_c} \cdot [I(t)\cos(\omega_{RF} t + \phi_{RF}(t)) + Q(t)\sin(\omega_{RF} t + \phi_{RF}(t))] \cdot \hat{\mathbf{e}}_s \hat{\mathbf{e}}_c \qquad (3)$$

with phase of $\phi_{RF}(t) = \phi_1(t) - \phi_2(t)$. At the receiver, an electrical local oscillator (LO) (Eq. (4)) signal is mixed with the received RF signal at a balanced mixer to firstly down-convert the RF signal into an IF signal. Equation (5) describes the down-converted IF signal.

$$E_{LO}(t) = \sqrt{P_{LO}} \cdot \cos(\omega_{LO} t + \phi_{LO}(t)) \qquad (4)$$

$$E_{IF}(t) = \langle E_{RF}(t) \cdot E_{LO}(t) \rangle = \sqrt{P_s P_c P_{LO}} \cdot [I(t)\cos(\omega_{IF} t + \phi_{IF}(t)) \\ + Q(t)\sin(\omega_{IF} t + \phi_{IF}(t))] \cdot \hat{\mathbf{e}}_s \hat{\mathbf{e}}_c \qquad (5)$$

where angular frequency ω_{IF} equals to $\omega_{RF} - \omega_{LO}$ and phase $\phi_{IF}(t)$ equals to $\phi_{RF}(t) - \phi_{LO}(t)$. The angle brackets denote low-pass filtering used for rejecting the components at $\omega_{RF} + \omega_{LO}$. The IF signal is then converted into the digital domain for digital down-conversion and demodulation. The signal after the digital down-converter can be expressed as:

$$E_{Rx}(t) = \langle E_{IF}(t) \cdot \exp(j\omega_{IF} t) \rangle = \frac{1}{2}\sqrt{P_s P_c P_{LO}} \cdot [I(t) + jQ(t)] \cdot \exp(-j\phi_{IF}(t)) \cdot \hat{\mathbf{e}}_s \hat{\mathbf{e}}_c \qquad (6)$$

It is noted that the system loss is not considered in the expressions. From Eq. (6) we can see that the transmitted baseband signal $I(t) + jQ(t)$ can be recovered at the DSP receiver. The accumulated phase offset and phase noise during transmission is contained in the term $\phi_{IF}(t)$, which can be later corrected in DSP [10]. Maximum value of the RF signal power is achieved when the polarization states $\hat{\mathbf{e}}_s$ and $\hat{\mathbf{e}}_c$ are aligned.

3. Experimental setup

Figure 2 presents the experimental set-up of the W-band wireless link under consideration. We adopt the 16-QAM baseband transmitter proposed in [11]. The ECL feeds a integrated LiNbO3 double-nested Mach-Zehnder modulator (MZM) with V_π of 3.5 V. The in-phase (I) and quadrature (Q) branches of the modulator are driven by 12.5 Gb/s four-level electrical signals.
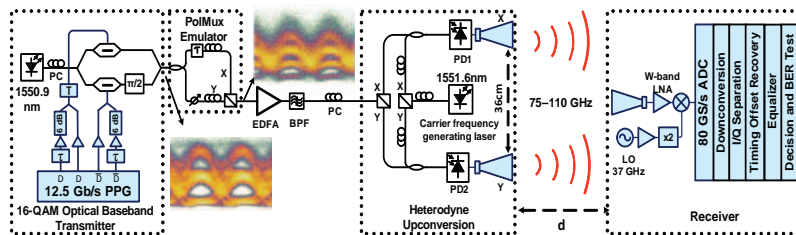
Fig. 2. Experimental setup for generation and detection of 100 Gbit/s PolMux 16-QAM wireless signals in W-band. (The eye diagrams of the 16-QAM signal before and after polarization multiplexing are shown in the inset).

Each four-level signal is derived from two copies of pseudorandom bit sequences (PRBS) of length $2^{15} - 1$, decorrelated with a relative delay of 6 bit periods. The two four-level signals were decorrelated by 33 symbol periods before being applied to the modulator. The output of the modulator is a 16-QAM optical baseband signal with a data rate of 50 Gbit/s, whose capacity is doubled to 100 Gbit/s by implementing polarization multiplexing.

Fig. 3. Optical spectra of the 16-QAM signal and carrier frequency generating laser signal before the photodiode.

Up-conversion to the W-band is performed by direct heterodyning in a fast response 100 GHz bandwidth photodetector (PD, u^{2}t XPDV4120R). An erbium-doped fiber amplifier (EDFA) is used to boost the signal power before heterodyne beating. Heterodyning is performed for each of the polarization states (X and Y) of the optical baseband signal with the correspondent aligned polarization state of an carrier frequency generating laser signal. An ECL with 100 kHz linewidth is used as the carrier frequency generating laser with a wavelength separation of 0.7 nm from the PolMux 16-QAM optical signal, resulting in an 87.5 GHz central carrier frequency for the up-converted W-band wireless signal. Figure 3 shows the optical spectra of the signals before the PD.

At the wireless transmitter side, each up-converted signal, corresponding to the X and Y PolMux components, is fed to a W-band horn antenna with 24 dBi gain. The two transmitter antennas radiate simultaneously facing a receiver antenna. Detection is performed aligning a transmitter-receiver antenna pair at a time by aligning the receiver angle to a given transmitter antenna. No crosstalk is observed from the second antenna due to high directivity of the system. After air transmission, the signals are received by a horn antenna with 25 dBi gain and amplified by a W-band 25 dB gain low-noise amplifier (LNA) (Radiometer Physics W-LNA) with a noise figure of 4.5 dB. Subsequently, electrical down-conversion is performed by using a W-band balanced mixer driven by a 74 GHz sinusoidal LO signal obtained after frequency doubling from a 37 GHz signal synthesizer (Rohde & Schwarz SMF 100A). In this way, the detected wireless signal located in the 75-100 GHz frequency region is translated to the 1-26 GHz band with a central frequency around 13.5 GHz. Analog-to-digital conversion is performed by an
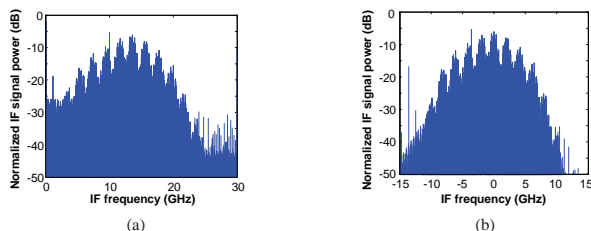
Fig. 4. Electrical spectra of (a) received IF signal and (b) after digital down-conversion and filtering.
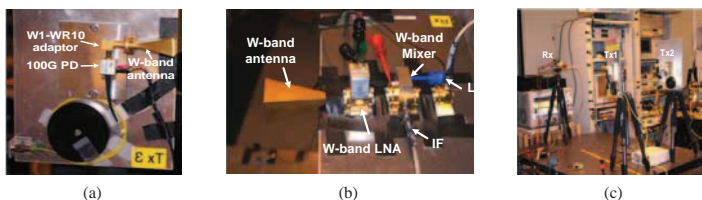

Fig. 5. (a). Wireless transmitter: High-speed photodetector and W-band horn antenna; (b) Wireless receiver: W-band antenna, LNA, mixer (c) Global view of the wireless link setup with both the wireless transmitter and receiver.

80 GS/s real-time digital sampling oscilloscope (DSO, Agilent DSAX93204A) with 32 GHz analog bandwidth. Offline signal demodulation is performed by a DSP-based receiver, consisting of frequency down conversion, I/Q separation, carrier recovery and filtering, equalizer, symbol decision and BER tester [10]. Figure 4a and Figure 4b shows the electrical spectra of the received IF signal and the signal after digital down-conversion and low pass filtering with cutoff frequency of $0.75 \times$baud rate, respectively. From the figures it can be seen that there are narrow lobes within the main lobes of the signal spectra, resulting from the delayed PRBS at the 16-QAM baseband transmitter as well as the fast frequency shifting after heterodyning beating up-conversion. The photographs of the wireless transmitter, receiver and the whole wireless setup are shown in Fig. 5a, 5b and 5c, respectively.

4.   Results and discussions

Bit-error rate (BER) measurements are performed for both cases of single polarization (without polarization multiplexing) and PolMux 16-QAM signals achieving total bit rate of 50 Gbit/s and 100 Gbit/s respectively, with total number of 320000 bits for error counting. The BER results are shown in Fig. 6 as a function of the received optical power into the photodiodes for a given air transmission distance d.

   For the single polarization 16-QAM case, Fig. 6a presents the BER results for transmission distances of 50 cm, 150 cm and up to 200 cm. As we can see from Fig. 6a, considering a 7% FEC overhead can potentially be effective for BER of 2×10^{-3}, error free transmission of net data rate of 46.5 Gbit/s is achieved for all air transmission cases. For the case of PolMux, the separation between the two transmitting antennas is 36 cm (see Fig. 2) while air transmission is measured for a distance d to the receiver antenna of 50 cm, 75 cm and 120 cm. Longer transmission distances were hampered by power budget limitation. The BER performance of 100 Gbit/s PolMux 16-QAM signal is shown in Fig. 6b, by averaging the BER of both X and
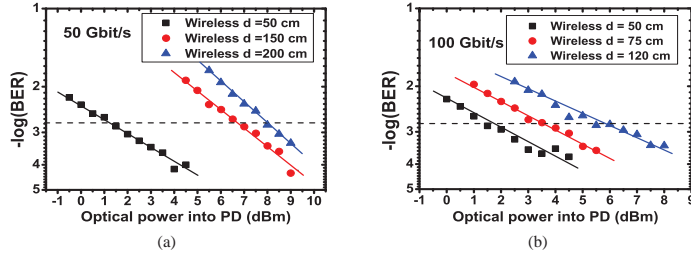
Fig. 6. Measured BER curves versus optical power into photodiode for: (a) 50 Gbit/s single polarization 16-QAM, (b) 100 Gbit/s PolMux 16-QAM.
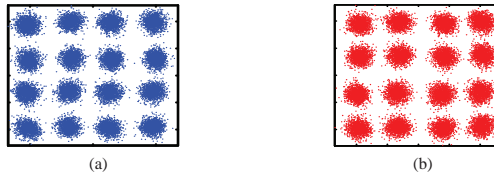

Fig. 7. Constellations of received signals of (a) X-branch and (b) Y-branch after 120 cm wireless transmission (8 dBm input power into PD).

Y branches. From the figure we can observe that a BER value below 2×10^{-3} is achieved at 1.5 dBm, 3.5 dBm and 5.5 dBm received optical power at PD for air transmission distance of 50 cm, 75 cm and 120 cm, corresponding to radiated RF power of ∼-23 dBm, -19 dBm and -15 dBm, respectively. It is noted that far field propagation takes places at air distances more than 36.8 cm by taking into account the type of antennas used in the experiment.

Comparing the BER performance at the BER of 2×10^{-3} for 50 cm air transmission of single polarization in Fig. 6a and PolMux in Fig. 6b, we attribute the observed 0.5 dB optical power penalty to imperfect separation of the two polarization states in the beam splitter used in the up-conversion stage. Figure 6b also indicates the required optical power to achieve 2×10^{-3} BER at 120 cm is 6 dBm, corresponding to an equivalent isotropically radiated power (EIRP) of 12.5 dBm. We believe that longer air transmission distances can be achieved by using a W-band power amplifier at the transmitter and a higher gain LNA at the receiver side. Figure 7 shows the received 16-QAM constellations of the X and Y branches after 120 cm wireless transmission at 8 dBm optical power, with BER of 3.2×10^{-4} and 3.1×10^{-4}, respectively.

5. Conclusion

100 Gbit/s wireless transmission in the 75-110 GHz band employing photonic generation is successfully demonstrated with air transmission distance of 120 cm. A dual-polarization 16-QAM baseband optical signal is up-converted by optically heterodyning with a free-running optical carrier generating laser to generate 100 Gbit/s at 87.5 GHz center wireless carrier frequency. This is the highest achieved capacity for a W-band wireless link, to our best knowledge.

Acknowledgment

Paper 4: Fiber Wireless Transmission of 8.3 Gb/s/ch QPSK-OFDM Signals in 75-110 GHz Band

Lei Deng, Marta Beltrán, **Xiaodan Pang**, Xu Zhang, Valeria Arlunno, Ying Zhao, Antonio Caballero, Anton Dogadaev, Xianbin Yu, Roberto Llorente, Deming Liu, Idelfonso Tafur Monroy, "Fiber Wireless Transmission of 8.3 Gb/s/ch QPSK-OFDM Signals in 75-110 GHz Band," *IEEE Photonics Technology Letters*, vol. 24, pp. 383-385, 2012.

Fiber Wireless Transmission of 8.3-Gb/s/ch QPSK-OFDM Signals in 75–110-GHz Band

Lei Deng, *Student Member, IEEE*, Marta Beltrán, *Member, IEEE*, Xiaodan Pang, Xu Zhang, Valeria Arlunno, Ying Zhao, Antonio Caballero, Anton Dogadaev, Xianbin Yu, *Member, IEEE*, Roberto Llorente, *Member, IEEE*, Deming Liu, and Idelfonso Tafur Monroy, *Member, IEEE*

Abstract—In this letter, we present a scalable high-speed W-band (75–110-GHz) fiber wireless communication system. By using an optical frequency comb generator, three-channel 8.3-Gb/s/ch optical orthogonal frequency-division-multiplexing (OOFDM) baseband signals in a 15-GHz bandwidth are seamlessly translated from the optical to the wireless domain. The W-band wireless carrier is generated from heterodyne mixing the OOFDM baseband signal with a free-running laser. A W-band electronic down-converter and a digital signal processing-based receiver are used. Three-channel QPSK-OFDM W-band wireless signals are transmitted over 0.5- and 2-m air distance with and without 22.8-km single-mode fiber, respectively, with achieved performance below the forward error correction limit.

Index Terms—Digital signal processing, microwave photonics, optical frequency comb generator, optical orthogonal frequency-division multiplexing (OOFDM), wireless communication.

I. Introduction

THE bandwidth demand of wireless applications, such as super Hi-Vision/Ultra High Definition TV data (more than 24 Gb/s) [1], is unprecedentedly growing, so it is highly desirable that next generation hybrid wireless-optical systems can bring the capacities from optical links into radio links, to realize the seamless integration of wireless and fiber-optic network [2], while preserving transparency to bit rates and modulation formats. Among some millimeter-wave frequency bands of interest, the W-band (75–110 GHz) has

lower atmospheric propagation loss and a broader transmission window compared for example to the 60 GHz and 120 GHz [2], and recently is attracting increasing attention. There are several GHz unregulated bandwidths in the W-band, which could be potentially used to provide for us high capacity wireless links.

To date, 10 Gb/s [3] and 20 Gb/s [4] with amplitude shift-keying modulation (ASK) W-band transmission systems have been reported. To achieve higher capacity, spectral efficient modulation techniques such as quadrature phase-shift keying (QPSK) and 16-quadrature amplitude modulation (QAM) have also been used to obtain 20 Gb/s [5] and 40 Gb/s [6] in the W-band wireless links. In these schemes, hybrid photonic-electronic up-conversion (coherent method) is used to generate the W-band wireless carrier, and 20 cm "error free" (1×10^{-12}) wireless transmission in [4] and 30 mm wireless transmission with achieved performance below the forward error correction (FEC) limit in [5], [6] are demonstrated. Recently, a photonic up/down-conversion (incoherent method) with RF/bit-rate transparency has also been proposed for a 40 Gb/s W-band system, however, without wireless transmission [7].

In this letter, we report on a scalable system by combining OOFDM and coherent all-optical frequency division multiplexed techniques to achieve high capacity wireless communications in the 75–110 GHz band. By using photonic up-conversion technique (incoherent method), the proposed system seamlessly converts a high-speed optical OFDM baseband signal into the W-band. This scheme is fully transparent to modulation format and bit-rate, as well as fully scalable to the RF carrier frequency. Furthermore, we measure fiber wireless transmission performance and demonstrate the scalability of the proposed system.

II. Experimental Setup

The experiment setup of the proposed W-band wireless transmission system is shown in Fig. 1. At the QPSK-OOFDM transmitter, a 100 kHz linewidth optical carrier emitted from an external cavity laser (ECL, $\lambda_1 = 1549.942$ nm) is modulated by an optical frequency comb generator employing an overdriven Mach-Zehnder modulator (MZM). The MZM is biased in its nonlinear region by equalizing the power of the central 3 comb lines. A 25 GHz bandwidth reflective fiber Bragg grating (FBG) is used to further rectify 3 lines by filtering out high-order sidebands. The frequency spacing of
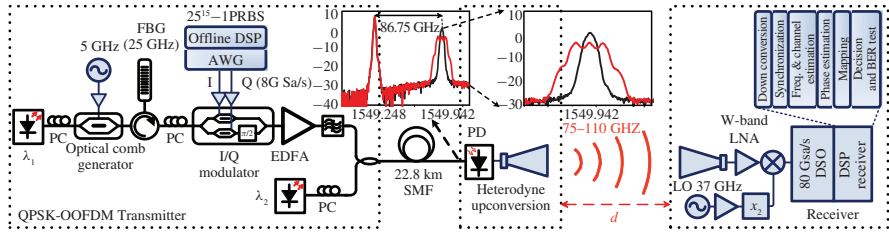
Fig. 1. Experimental setup for the W-band QPSK-OOFDM wireless signal over fiber transmission system. (The optical spectra of optical baseband signal (single-channel and three-channel) with optical LO before the PD are shown in the insets.) PC: polarization controller; DSO: digital sampling oscilloscope.
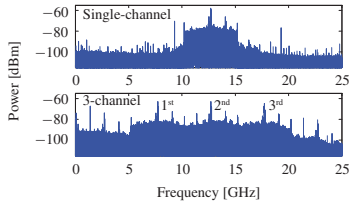

Fig. 2. Electrical spectra of QPSK-OFDM signal (single-channel and three-channel) after down-conversion mixer at the receiver.
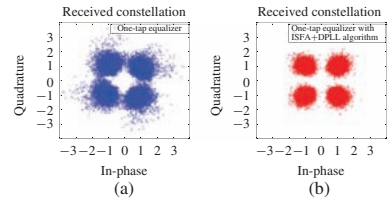

Fig. 3. Received constellations of 8.3-Gb/s W-band signals (single-channel) after 22.8-km SMF and 2-m air distance transmission (a) without ISFA-DPLL (BER of 4×10^{-3}) and (b) with ISFA-DPLL (no error in 38 400 bits).

the comb lines is set to 5 GHz. Subsequently, an arbitrary waveform generator (AWG, Tektronix AWG 7122C) operating at 8 GS/s drives an optical in-phase/quadrature (I/Q) modulator which is biased at its null point to encode all the comb lines with QPSK-OFDM simultaneously. An erbium-doped fiber amplifier (EDFA) and a 0.8 nm bandwidth optical filter in the transmitter are used to compensate the loss of the optical comb generator and the optical I/Q modulator and filter the outband noise. In the signal generation, a data stream with a pseudo-random bit sequence (PRBS) word length of $2^{15}-1$ is mapped onto 128-point inverse fast Fourier transform (IFFT) and 80 QPSK subcarriers (SCs) consists of 4 pilot SCs and 76 data SCs. 10 training symbols in each 267 data symbols are used for time synchronization and channel estimation. The cyclic prefix is 1/10 of the IFFT length so that the OFDM symbol size is 141. At the output of the I/Q modulator, the generated optical signal is seamless, resulting in 3-channel optical OFDM signal at 8.3 Gb/s/ch (8 GS/s × 2 × 76/141 × 257/267) with a total spectral bandwidth of 15 GHz (3 channels × 8 GS/s × 80/128). Because the comb spacing is integral multiple of the OFDM SC spacing, all of the OFDM SCs from different comb lines are orthogonal to each other. It is noted that these 3-channel OFDM signals are correlated, the de-correlation of 3-channel and the effect of inter-channel interference (ICI) between different channels are under further investigation from a practical point of view.

The optical QPSK-OFDM signal is then combined with a 100 kHz linewidth free-running CW laser ($\lambda_2 = 1549.248$ nm) for W-band wireless signals generation [7]. The optical spectra of both single-channel and 3-channel are shown in the insets of Fig. 1. The single-channel signal is tested when the 5 GHz driving RF signal of optical comb generator is off.

After 22.8 km of single mode fiber (SMF) propagation, the combined optical signal is heterodyne mixed in a 100 GHz bandwidth photodiode (PD, u²t XPDV4120R) to generate a W-band wireless signal which is fed to a W-band horn antenna with 24 dBi gain. After air transmission, the signal is detected by a horn antenna with 25 dBi gain and amplified by a W-band 25 dB gain low-noise amplifier (LNA, Radiometer Physics W-LNA). Subsequently, a W-band balanced mixer driven by a 74 GHz sinusoidal local oscillator (LO) signal after frequency doubling from a 37 GHz signal synthesizer (Rohde & Schwarz SMF 100A) is adopted to realize electrical down-conversion. The electrical spectra of QPSK-OFDM intermediate frequency (IF) signals after down-conversion are shown in Fig. 2.

At the receiver side, the IF signal is converted to digital signal by an 80 GS/s real-time digital sampling oscilloscope with 32 GHz analog bandwidth (Agilent DSAX93204A). After that, offline signal demodulation is performed by a digital signal processing (DSP)-based receiver, consisting of frequency down-conversion, time synchronization, frequency and channel estimation, pilot-based phase estimation, data mapping and bit error rate (BER) tester. To eliminate the dispersion and nonlinearity effects induced by fiber and wireless transmission, one-tap equalizer and an effective algorithm combining the intra symbol frequency-domain averaging (ISFA) [8] and digital phase-locked loop (DPLL) are programmed for channel estimation. We can clearly observe the performance improvement by comparing the received constellations with/without ISFA-DPLL for 8.3 Gb/s W-band signals shown in Fig. 3.

III. RESULTS AND DISCUSSION

In the experiment, the millimeter-wave carrier frequency is set to 86.75 GHz to match the central frequency of the mixer.
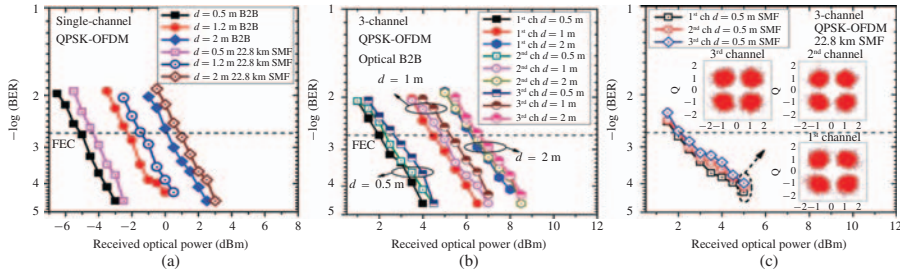
Fig. 4.   (a) Measured BER performance of single-channel QPSK-OFDM signal fiber wireless transmission. (b) Three-channel QPSK-OFDM signal fiber wireless transmission in optical B2B. (c) After 22.8-km SMF. (Insets: the received constellations of different channels in the three-channel case.)

We measure the performance for both cases of single-channel and 3-channel at the data rate of 8.3 Gb/s/ch. After considering the 7% Reed-Solomon FEC overhead, the effective bit rate is 7.719 Gb/s/ch. Fig. 4(a) presents the BER performance versus the received optical power at the PD after different air distances as well as fiber propagation in the single-channel case. It is observed that 22.8 km SMF induces less than 1 dB power penalty at the FEC limit (BER of 2×10^{-3}) for all air transmission cases. Moreover, after fiber transmission, the receiver sensitivity at the FEC limit is achieved at -4.3 dBm, -1.4 dBm and 0.8 dBm for air transmission of 0.5 m, 1.2 m and 2 m, respectively. The signal to noise ratio is decreased as air distance increases, resulting in higher required optical power at the FEC limit.

Fig. 4(b) shows the wireless transmission BER performance of 3-channel QPSK-OFDM W-band signal in the optical back-to-back (B2B) case. We can observe that the receiver sensitivity of the 1st channel to reach the FEC limit is 2 dBm, 4.5 dBm, 6.2 dBm for air transmission of 0.5 m, 1 m and 2 m, respectively, which is 6.3 dB higher than those in the single-channel case. This power penalty is expected, since the optical signal to noise ratio (OSNR) of 3-channel is about 4.5 dB lower than that of single-channel at a given optical power, which is indicated in the optical spectra in Fig. 1. We can also see from Fig. 4(b) that the 3rd channel has 1 dB power penalty compared to the 1st channel. This can be attributed to the bandwidth limitations of the RF components involved. Moreover, the phase ripple and non-flat frequency response destroy the orthogonality of the OFDM subcarriers and introduce inter-symbol interference (ISI). However, these effects cause negligible performance degradation on the 2nd channel by discarding one edge OFDM subcarrier during the BER counter.

Fig. 4(c) shows the BER curves of 3-channel W-band signal after 22.8 km SMF and 0.5 m air transmission. The receiver sensitivity at the FEC limit is obtained at about 1.9 dBm for the 1st channel, and hence the penalty induced by the fiber is negligible compared with the Fig. 4(b). However, the system performance is degraded when the received optical power at the PD is higher than 4 dBm, corresponding to 9.5 dBm optical power at the input of fiber. This can be explained that OFDM signal is sensitive to the nonlinearity of fiber transmission due to the high peak-to-average-power-ratio (PAPR) property.

The received constellations of 3-channel QPSK-OFDM signal are shown in the insets of Fig. 4(c) as well.

IV. CONCLUSION

We have demonstrated a high speed and spectral efficient W-band wireless fiber transmission system based on the OFDM modulation and coherent all-optical frequency division multiplexed techniques. By using ISFA and DPLL as improved channel estimation method, 3-channel 8.3 Gb/s/ch QPSK-OFDM signals at 86.75 GHz are transmitted over 0.5 m and 2 m air distance with and without 22.8 km SMF, respectively. This system provides a promising solution to realize high capacity wireless links, with the advantage of transparency for future wireless/wireline seamless network integration.

REFERENCES

[1] T. Nagatsuma, *et al*, "Millimeter and THz-wave photonics towards 100-Gbit/s wire-less transmission," in *Proc. IEEE Photon. Soc. 23rd Annu. Meet.*, Denver, CO, Nov. 2010, pp. 385–386, paper WE4.
[2] J. Wells, "Faster than fiber: The future of multi-Gb/s wireless," *IEEE Microw. Mag.*, vol. 10, no. 3, pp. 104–112, May 2009.
[3] A. Hirata, T. Furuta, H. Ito, and T. Nagatsuma, "10-Gb/s millimeter-wave signal generation using photodiode bias modulation," *J. Lightw. Technol.*, vol. 24, no. 4, pp. 1725–1731, Apr. 2006.
[4] F.-M. Kuo, *et al*, "Remotely up-converted 20-Gbit/s error free wireless on-off-keying data transmission at W-band using an ultrawideband photonic transmitter-mixer," *IEEE Photon. J.*, vol. 3, no. 2, pp. 209–219, Apr. 2011.
[5] A. Kanno, *et al*, "20-Gb/s QPSK W-band (75–110 GHz) wireless link in free space using radio-over-fiber tech-nique," *IEICE Electron. Express*, vol. 8, no. 8, pp. 612–617, Apr. 15, 2011.
[6] A. Kanno, *et al*, "40 Gb/s W-band (75–110 GHz) 16-QAM radio-over-fiber signal generation and its wireless transmission," in *Proc. Eur. Conf. Opt. Commun.*, 2011, pp. 1–3, paper We.10.P1.112.
[7] D. Zibar, *et al*, "High-capacity wireless signal generation and demodulation in 75 to 110-GHz band employing all-optical OFDM," *IEEE Photon. Technol. Lett.*, vol. 23, no. 12, pp. 810–812, Jun. 1, 2011.
[8] X. Liu and F. Buchali, "Intra-symbol frequency-domain averaging based channel estimation for coherent optical OFDM," *Opt. Express*, vol. 16, no. 26, pp. 21944–21957, Dec. 15, 2008.

Paper 5: Single- and Multiband OFDM Photonic Wireless Links in the 75-110 GHz Band Employing Optical Combs

Single- and Multiband OFDM Photonic Wireless Links in the 75−110 GHz Band Employing Optical Combs

M. Beltrán, Member, IEEE
L. Deng, Student Member, IEEE
X. Pang
X. Zhang
V. Arlunno
Y. Zhao
X. Yu, Member, IEEE
R. Llorente, Member, IEEE
D. Liu
I. Tafur Monroy, Member, IEEE

Single- and Multiband OFDM Photonic Wireless Links in the 75−110 GHz Band Employing Optical Combs

M. Beltrán,[1] *Member, IEEE*, **L. Deng,**[2] *Student Member, IEEE*,
X. Pang,[3] **X. Zhang,**[3] **V. Arlunno,**[3] **Y. Zhao,**[3] **X. Yu,**[3] *Member, IEEE*,
R. Llorente,[1] *Member, IEEE*, **D. Liu,**[2] **and I. Tafur Monroy,**[3] *Member, IEEE*

[1]Valencia Nanophotonics Technology Center, Universidad Politécnica de Valencia,
46022 Valencia, Spain
[2]College of Optoelectronics Science and Engineering, HuaZhong University of Science and
Technology, Wuhan 430074, China
[3]DTU Fotonik, Department of Photonics Engineering, Technical University of Denmark,
2800 Kgs. Lyngby, Denmark

Abstract: The photonic generation of electrical orthogonal frequency-division multiplexing (OFDM) modulated wireless signals in the 75−110 GHz band is experimentally demonstrated employing in-phase/quadrature electrooptical modulation and optical heterodyn upconversion. The wireless transmission of 16-quadrature-amplitude-modulation OFDM signals is demonstrated with a bit error rate performance within the forward error correction limits. Signals of 19.1 Gb/s in 6.3-GHz bandwidth are transmitted over up to 1.3-m wireless distance. Optical comb generation is further employed to support different channels, allowing the cost and energy efficiency of the system to be increased and supporting different users in the system. Four channels at 9.6 Gb/s/ch in 14.4-GHz bandwidth are generated and transmitted over up to 1.3-m wireless distance. The transmission of a 9.6-Gb/s single-channel signal occupying 3.2-GHz bandwidth over 22.8 km of standard single-mode fiber and 0.6 m of wireless distance is also demonstrated in the multiband system.

Index Terms: Microwave photonics signal processing, frequency combs, heterodyning, fiber optics systems, orthogonal frequency division multiplexing.

1. Introduction

Wireless communication links supporting very high capacity are required to provide access network services such as 10-gigabit Ethernet (10 Gb/s), Super Hi-Vision (SHV)/Ultra High Definition (UHD) TV data (> 24 Gb/s), OC-768/STM-256 data (43 Gb/s), and 100-gigabit Ethernet (100 Gb/s), and also for close-proximity bulk data transfer [1]. Millimeter-wave wireless systems at around 60 GHz and higher frequencies can provide bandwidth enough to easily support multi-Gb/s communications, being a potential solution for future seamless integrated optical/wireless access, as well as for mobile backhauling [2]. The 60-GHz band has been widely studied as a wide bandwidth has been regulated in many countries for unlicensed use with a high equivalent isotropic radiated power

TABLE 1

Photonic Wireless Systems in the 75−110 GHz Band (MLL: Mode-locked laser, NBUTC-PD: Near-ballistic uni-travelling-carrier photodiode, IQ: In-phase/quadrature electrooptical modulator, DP-QPSK: Dual-polarization QPSK modulator, MZM: Mach–Zehnder modulator)

Mod. format	Data rate (Gb/s)	Frequency range (GHz)	Fiber length (km)	Wireless distance (m)	Technology		Ref.
					Transmitter	Receiver	
OOK	20 BER<10^{-12}	85.5−100.5	25	0.2	MLL+NBUTC-PD	Power detector	[10]
Optical QPSK-OFDM	40 BER<10^{-2}	70−95	−	−	MZM comb+IQ+ECL heterodyning	Optical detection	[13]
16-QAM	40 BER<2·10^{-3}	82.5−102.5	−	0.03	Two-tone optical generator+DP-QPSK +UTC-PD	Electrical heterodyne	[11]
16-QAM PolMux	100 BER<2·10^{-3}	75−100	−	1.2	IQ+ECL heterodyning	Electrical heterodyne	[12]
Three-band QPSK-OFDM	8.3 /ch BER<2·10^{-3}	79.25−94.25	22.8 0.01	0.5 2	MZM comb+IQ+ECL heterodyning	Electrical heterodyne	[22]
Three-band 16-QAM-OFDM	15.1 /ch BER<2·10^{-3}	78.5−93.5	0.01	0.6	IQ+MZM comb+ECL heterodyning	Electrical heterodyne	[23]
16-QAM-OFDM	19.1 BER<2·10^{-3}	77.4−83.8	0.01	1.3	IQ+ECL heterodyning	Electrical heterodyne	This work
Four-band 16-QAM-OFDM	9.6 /ch BER<2·10^{-3}	78.9−93.3	0.01	1.3	IQ+PM comb+ECL heterodyning	Electrical heterodyne	This work

(EIRP) of higher than 40 dBm allowed [3]. A number of standards in the 60-GHz band have recently been proposed, including WirelessHD, ECMA-387, IEEE 802.15.3c, and WiGig. These technologies target to provide up to 7-Gb/s data rates at short-range indoor wireless distances of up to 10 m. Standard devices of 60 GHz are also available for wireless display connectivity, for HD audio/video streaming from the consumer electronics, personal computing, and portable devices to HDTVs. In addition, other higher frequency millimeter-wave bands can potentially offer larger bandwidths to support higher capacities, as well as lower atmospheric loss to extend wireless transmission distances as compared to the 60-GHz band [4]. Of particular interest, the 71−76/81−86 GHz paired band has been allocated for commercial use in the United States, Europe, and other countries, and permits point-to-point communications over distances of several kilometers. Commercial equipment is easily available in the 71−76/81−86 GHz band supporting 1.25-Gb/s Gigabit Ethernet connectivity. Electronic-based millimeter-wave wireless links at frequencies higher than 100 GHz have also been demonstrated providing up to 20 Gb/s with polarization multiplexing (PolMux) over the kilometer distance [5].

Radio-over-fiber technology combined with millimeter-wave wireless systems is seen as a fast deployable and cost-effective solution for providing seamless integrated optical/wireless access at > 10 Gb/s [2]. Radio-over-fiber systems operating within 7-GHz bandwidth in the 60-GHz band have been reported to provide capacities higher than 10 Gb/s when spectrally efficient electrical orthogonal frequency-division multiplexing (OFDM) modulation based on quadrature amplitude modulation (QAM) and electrooptical modulation for upconversion are employed, such as 27 Gb/s for 2.5-m wireless distance employing 16-QAM-OFDM [6], 21 Gb/s for 500-m standard single-mode fiber (SSMF) transmission and 10-m (or 2.5 m in bidirectional system) wireless transmission employing 8-QAM-OFDM [7], 26.5 Gb/s for 100-km SSMF and 3-m wireless distance employing adaptive-level QAM-OFDM in amplified long-reach networks [8], and 50 Gb/s for 4-m wireless distance employing 16-QAM-OFDM and multiple-input multiple-output (MIMO) spatial multiplexing [9]. In addition, radio-over-fiber systems in the 75−110 GHz band (W-band) are recently attracting increasing interest to deliver 40 Gb/s and beyond. A number of photonic wireless transmission systems in the 75−110 GHz band have been demonstrated, as summarized in Table 1. A system providing error-free 20 Gb/s with on–off keying (OOK) modulation and simple RF power detection has

been demonstrated including 25 km of fiber transmission [10]. Spectral efficient modulation formats have also been employed, at 20 Gb/s and 40 Gb/s based on quadrature phase-shift keying (QPSK) and 16-QAM formats, respectively [11], and up to 100 Gb/s based on 16-QAM with PolMux [12]. A system based on optical OFDM with optical detection has also been demonstrated [13]. For fixed wireless access over the kilometer distance, photonic wireless links in the $75-110$ GHz band have been reported at < 10 Gb/s employing differential phase-shift keying modulation [14]. Finally, millimeter-wave systems operating at frequencies higher than 110 GHz based on photonic generation have been demonstrated to provide error-free > 20 Gb/s at 300 GHz with OOK modulation [5].

Photonic millimeter-wave wireless links have been reported using the wide RF bandwidth in a single channel. A different approach is to allocate multiple channels of lower data rate signals to serve different users in the system. The multiband approach also enables flexible bandwidth allocation by aggregating channels, thus relaxing the power and bandwidth requirements of electrooptical equipment such as digital-to-analog/analog-to-digital converters (DAC/ADC) for energy-efficient and cost-effective systems. Combined optical access and wireless transmission of multiband OFDM-based signals in the 60-GHz band has been demonstrated based on subcarrier multiplexing (SCM) [3]. Wavelength division multiplexing (WDM) architectures can also be employed, where multiple wavelengths produced by an optical frequency comb or by a continuous-wave laser array support the different channels [15].

A number of approaches have been demonstrated for optical comb generation. Mode-locked lasers provide stable and sharp spectral components over a wide bandwidth with low noise qualities. In addition, optical frequency combs based on electrooptic modulators driven by large-amplitude sinusoidal signals permit arbitrary wavelength spacing by adjusting the frequency of the sinusoidal signals [16]–[18]. Although this technique can provide a relatively flat optical comb, it can be limited by the insertion loss of the modulator together with the modulation efficiency. Finally, gain-switched pulsed lasers can be employed for simple and cost-efficient multicarrier generation [19]. Additionally, the number of comb wavelengths can be increased without influencing optical bandwidth by applying an adequate time-domain periodic multiphase modulation on the laser pulse train [20].

In this paper, we experimentally demonstrate the optical generation, wireless transmission, and electrical heterodyn detection of multiband OFDM-based wireless signals in the $75-110$ GHz band. The proposed system has the following advantages: 1) Electrical OFDM modulation with a high number of subcarriers has been widely used in optical and wireless communications systems to benefit from its high spectral efficiency, flexibility, and robustness against fiber dispersion impairments and wireless multipath fading [3], [21]. 2) Seamless allocation of multiple channels in the wide RF bandwidth is demonstrated enabled by optical comb generation [22]. 3) Optical heterodyn mixing enables seamless optical frequency upconversion, highly scalable in RF frequency [13]. The phase and frequency drift originated from the wireless signal generation, and detection is compensated by baseband digital signal processing (DSP) at the receiver, thus avoiding the need for phase-locking techniques. Based on this approach, we have demonstrated the combined SSMF and wireless transmission of a three-channel QPSK-OFDM signal at 8.3 Gb/s/ch with a bandwidth of 5 GHz/ch (15-GHz total RF bandwidth) [22], as summarized in Table 1. The wireless transmission of three-channel signals has also been demonstrated employing 16-QAM-OFDM [23], as summarized in Table 1. In this paper, the wireless transmission of four-channel 16-QAM-OFDM signals [24] is compared with that of the signal generated in a single-band system, with a bit error rate (BER) performance within the standard forward error correction (FEC) limit of $2 \cdot 10^{-3}$, as summarized in Table 1. After removing the 7% overhead for FEC, the effective data rates are 17.8 Gb/s and 8.9 Gb/s/ch with a spectral efficiency of 2.8 b/s/Hz and 2.8 b/s/Hz/ch, respectively.

2. Theoretical Description

Considering the line-of-sight (LOS) case in the wireless link, the signal-to-noise ratio (SNR) at the receiver side can be calculated in dB using the link power budget equation [25]

$$\text{SNR} = P_T + G_T + G_R - L_{FS} - L_I - (N_o + 10\log(B) + NF) \tag{1}$$
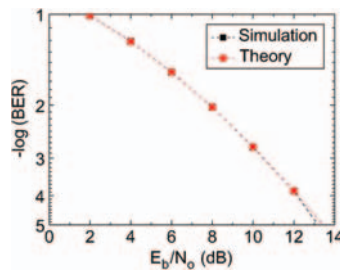
Fig. 1. Bit error probability curve for 16-QAM-OFDM in AWGN.

where P_T is the transmitter power, G_T and G_R are the transmitter and receiver antenna gain, respectively, I_L is the implementation loss of the link, N_0 is the thermal noise in 1 Hz of bandwidth, B is the system bandwidth, and NF is the noise figure of the receiver. L_{FS} represents the free space loss as given by $L_{FS} = 20\log(4\pi fd/c)$, where c is the light speed, f is the signal frequency, and d is the wireless distance in the far field.

For link budget analysis, the most important aspect of a given modulation technique is the SNR necessary for a receiver to achieve a specified level of reliability in terms of BER. BER is a function of the energy per bit relative to the noise power E_b/N_o. In the additive white Gaussian noise (AWGN) channel, single carrier and OFDM have approximately the same performance in terms of E_b/N_o, and the theoretical BER of 16-QAM-OFDM is shown in Fig. 1 [25]. The corresponding curve simulated for the 16-QAM-OFDM signal employed in the experimental work exhibits slight differences with the theoretical curve, as shown in Fig. 1. Note that E_b/N_o is independent of the system data rate R_b. SNR and E_b/N_o can be related by

$$SNR = (E_b/N_o) \cdot (R_b/B). \tag{2}$$

In addition, considering the resistance load and the responsivity of the photodetector employed in the experimental work, P_T can be related to the received optical power P_{opt} by

$$P_T(\text{dBm}) = 2P_{\text{opt}}(\text{dBm}) - 22. \tag{3}$$

3. Experimental Setup

Fig. 2 shows the schematic of the experimental setup. At the optical OFDM transmitter, a baseband OFDM signal is generated employing a two-channel arbitrary waveform generator (Tektronix AWG7122C) and in-phase/quadrature (IQ) electrooptical modulation. The OFDM signal comprises a data stream consisting of a pseudorandom bit sequence (PRBS) of length $2^{15} - 1$ mapped onto 72 16-QAM subcarriers, which, together with eight pilot subcarriers, one zero power dc subcarrier, and 47 zero-power edge subcarriers, are converted to the time domain via an inverse fast Fourier transform (IFFT) of size 128. A cyclic prefix of length 13 samples is employed, resulting in an OFDM symbol size of 141. To facilitate OFDM frame synchronization and channel estimation, ten training symbols are inserted at the beginning of each OFDM frame that contains 150 data symbols. The real and imaginary parts of the complex OFDM signal are clipped and converted to analog signals at the outputs of the AWG. The two filtered signals are amplified and applied to an IQ modulator connected to an external-cavity laser (ECL) at $\lambda_1 = 1549.9$ nm with 100-kHz linewidth. The IQ modulator reduces to half the bandwidth requirement of the DAC, although it introduces high transmission loss as it is biased at the minimum transmission point. In this way, an optical OFDM signal is generated, which is amplified by an erbium-doped fiber amplifier (EDFA). An optical bandpass filter with 0.8-nm bandwidth is employed to filter noise.

The optical OFDM signal is expanded by optical comb generation based on an electrooptic phase modulator (PM) [16] to form five OFDM channels. The output from the comb is further filtered by a
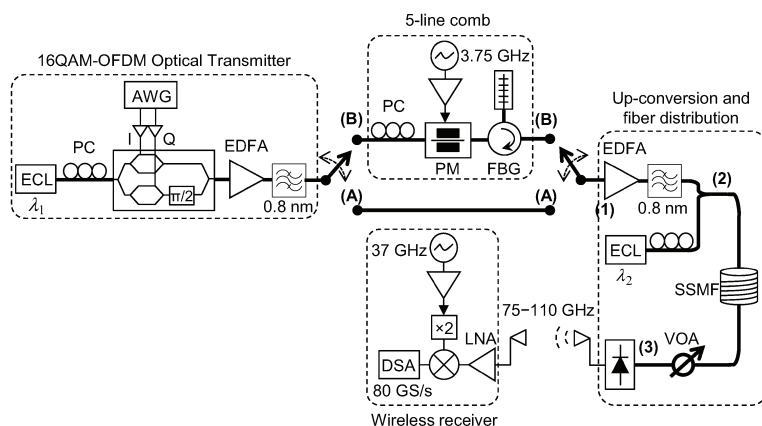
Fig. 2. Experimental setup of an OFDM photonic wireless system in the 75−110 GHz band. Configuration (A): single-band system. Configuration (B): multiband system employing optical comb generation. PC: Polarization controller, VOA: Variable optical attenuator.
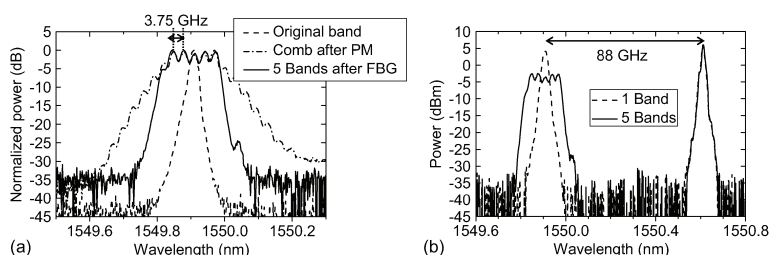

Fig. 3. (a) Optical spectra measured at various points in Fig. 2. (b) Optical spectra measured at point (2) in Fig. 2. (Resolution bandwidth: 0.01 nm).

fiber Bragg grating (FBG) with 25-GHz bandwidth operating in reflection to reduce crosstalk penalty from the edge comb lines, as shown in Fig. 3(a). The comb wavelength spacing is set to 3.75 GHz to minimize crosstalk penalty while maximizing spectral efficiency. It should be noted that the optical comb repeats the same OFDM signal. The effect of crosstalk when independent data bit streams are coded for each OFDM channel should be further investigated for the application in reality. This could be done by using different optical carriers and modulate each of them in a different I/Q modulator by each OFDM data signal. The modulated optical carriers would then be optically combined to generate an optical multiband OFDM signal, as shown in [15]. Decorrelation of adjacent channels at least has usually been considered for emulation of a real system, e.g., by employing frequency shifting and optical delay [21] or two modulators for odd and even channels [15].

To perform optical frequency upconversion, the optical OFDM signal at point (1) in Fig. 2 is amplified and combined with an unmodulated continuous-wave optical carrier from an ECL with 100-kHz linewidth at λ_2 located at the desired RF carrier apart. Fig. 3(b) shows the spectrum of the combined signal at point (2) in Fig. 2. The combined signal is transmitted over fiber to a remote antenna site where the optical ODFM signal and the unmodulated carrier are heterodyn mixed in a 100-GHz photodetector (u^{2}t Photonics, XPDV4120R). The photodetected signal is an OFDM signal

at the desired RF carrier in the $75-110$ GHz band, which is fed to a rectangular horn antenna in the $75-110$ GHz band with 24-dBi gain.

After wireless transmission, the RF OFDM signal is received by a similar antenna with 25-dBi gain and amplified by a low-noise amplifier (LNA; Radiometer Physics, $75-105$ GHz) with 25-dB gain. An electrical mixer ($75-110$ GHz RF and $1-36$ GHz IF) driven by a local oscillator (LO) signal at 74 GHz is employed for frequency downconversion. The LO signal is generated by frequency doubling a 37-GHz signal from a signal generator (Rohde&Schwarz, SMF100A). The down-converted signal is digitized by a digital signal analyzer at 80 GS/s with 32-GHz real-time bandwidth (Agilent, DSAX93204A) and demodulated by offline DSP.

In the receiver DSP, each OFDM channel is demodulated individually after frequency downconversion and low-pass filtering (LPF). For each baseband OFDM channel, time synchronization, frequency and channel estimation, pilot-assisted phase estimation, data recovery by symbol mapping and serialization, and BER test are performed. To mitigate the dispersion and nonlinearity effects induced by fiber and wireless transmission, one-tap equalizer and an effective algorithm combining intrasymbol frequency-domain averaging [26] and digital phase-locked loop are employed for channel estimation. The effect of the algorithm can be observed in the constellation diagrams in [23]. The pilot-assisted phase estimation consists of estimating the common phase error due to the laser phase noise, as described in [27]. BER is evaluated by counting the number of errors considering 42 912 bits. Note that the frequency/phase estimation algorithm (frequency and channel estimation and pilot-assisted phase estimation) can track the frequency jitter of the ECL lasers provided that a maximum frequency offset is not exceeded; otherwise, advanced algorithms may be employed [13].

4. Transmission Performance

The feasibility of the photonic generation and wireless transmission of 16-QAM-OFDM signals in the 75–110 GHz band has been evaluated. The performance of single-band signals generated by IQ modulation and optical heterodyn upconversion, configuration (A) in Fig. 2 is first evaluated. Wireless transmission performance is further evaluated when the RF bandwidth is used in multiple channels employing optical comb generation, configuration (B) in Fig. 2. The performance of the single-channel signal in the multiband system when the RF signal driving the PM in Fig. 2 is off is also evaluated.

4.1. Single-Band System

In the single-band system, configuration (A) in Fig. 2, the AWG operates at 10 GS/s, resulting in an optical OFDM signal at 19.14 Gb/s $(10 \text{ GS/s} \cdot \log_2(16) \cdot 72/141 \cdot 150/160)$ with a bandwidth of 6.328 GHz $(10 \text{ GS/s} \cdot 81/128)$. Two antialiasing LPF with 3.4-GHz bandwidth are employed at the AWG outputs. The RF carrier frequency is set at 80.6 GHz by tuning λ_2 in Fig. 2.

Fig. 4(a) shows the BER performance of the 19.14-Gb/s single-band 16-QAM-OFDM signal as a function of the received optical power at point (3) in Fig. 2 for different wireless transmission distances compared with the theoretical slope for 16-QAM-OFDM in AWGN. The receiver sensitivities at the FEC limit of $2 \cdot 10^{-3}$ are -2.1 dBm, -0.7 dBm, and 1.7 dBm for 0.5 m, 0.75 m, and 1.3 m of wireless distance, respectively. Fig. 4(b) shows received constellations confirming the BER performance shown in Fig. 4(a). The electrical spectrum of the 19.14-Gb/s signal after digitization at the receiver is shown in Fig. 4(c).

The difference in the receiver sensitivity at 0.5 m and 0.75 m or at 0.75 m and 1.3 m is near the theoretical values of 1.75 dB or 2.4 dB, respectively. From (1) and (3), the difference in the received optical power P_{opt} required for a given BER at different wireless distance due to the increased free space loss L_{FS} is given by $\Delta P_{opt} = \Delta L_{FS}/2$. In addition, the signal does not exhibit an apparent BER floor, and it is not expected to be significantly limited by the residual phase error after pilot-assisted phase estimation considering an estimated phase error variance of 0.0179 rad^2 for a combined laser linewidth of 200 kHz and a symbol rate of 70.2 MSymbol/s [28].
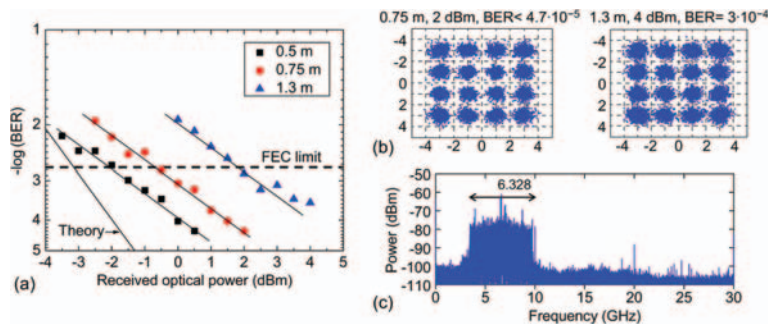
Fig. 4. (a) BER performance of the 19.14 Gb/s single-band system, configuration (A) in Fig. 2, as a function of the received optical power and wireless distance. (b) Constellation diagrams. (c) Electrical spectrum after digitization at the receiver at 2 dBm received optical power and 0.75 m wireless distance.
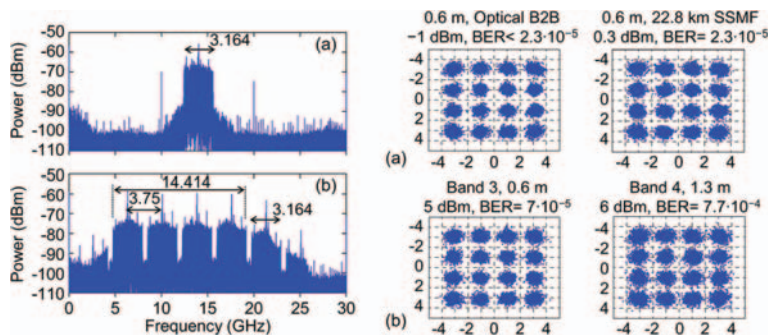

Fig. 5. Electrical spectra after digitization at the receiver at 4.5 dBm received optical power for optical B2B and 0.6 m wireless distance, and constellation diagrams, for configuration (B) in Fig. 2. (a) 9.57 Gb/s single-band OFDM signal. (b) 9.57 Gb/s/ch four-band OFDM signal.

4.2. Multiband System

In the multiband system, configuration (B) in Fig. 2, the AWG operates at 5 GS/s, resulting in an optical OFDM signal at 9.57 Gb/s $(5 \text{ GS/s} \cdot \log_2(16) \cdot 72/141 \cdot 150/160)$ with a bandwidth of 3.164 GHz $(5 \text{ GS/s} \cdot 81/128)$. Two antialiasing LPF with 2.5-GHz bandwidth are employed at the AWG outputs. The RF carrier frequency is set at 88 GHz by tuning λ_2 in Fig. 2.

Up to four RF OFDM bands out of the five optical OFDM bands can be demodulated within the FEC limits due to the frequency response of the photodetector. BER performance of the four OFDM channels at 9.57 Gb/s/ch has been evaluated and compared with the performance of the 9.57-Gb/s single-band OFDM signal. The performance of the single-band OFDM signal is evaluated when the RF signal driving the PM in Fig. 2 is off. Fig. 5 shows the electrical spectra of the single- and four-band OFDM signals after digitization at the receiver. Received constellations are also shown in Fig. 5, confirming the BER performance shown in Fig. 6. Fig. 6 shows the measured BER as a function of the received optical power at point (3) in Fig. 2. Fig. 6(a) shows BER performance of the 9.57-Gb/s single-band 16-QAM-OFDM signal for combined optical and wireless transmission compared with the theoretical slope for 16-QAM-OFDM in AWGN. The receiver sensitivity at the FEC limit of $2 \cdot 10^{-3}$ is -4.2 dBm and -0.6 dBm for optical back-to-back (B2B) and 0.6 m and 1.3 m
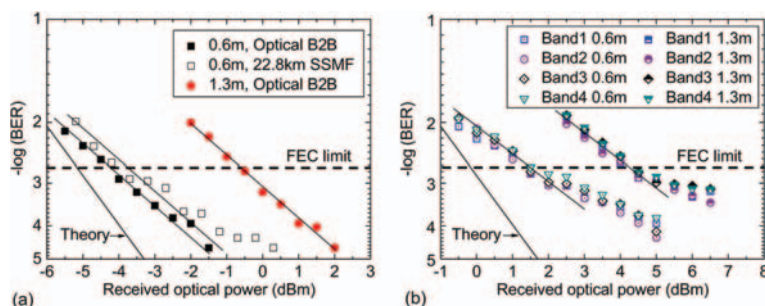
Fig. 6. BER performance of the multiband system, configuration (B) in Fig. 2, as a function of received optical power. (a) 9.57 Gb/s single-band OFDM signal as a function of optical and wireless transmission distance. (b) 9.57 Gb/s/ch four-band OFDM signal as a function of wireless distance for optical B2B.

of wireless distance, respectively. As compared with the 9.57-Gb/s single-band OFDM signal in Fig. 6(a), the 19.14-Gb/s single-band OFDM signal in Fig. 4(a) exhibits 2.7-dB and 2.3-dB penalty in receiver sensitivity, respectively. Theoretically, it is expected that the single-band OFDM signal in Fig. 4(a) at twice the data rate and bandwidth have a near 1.5-dB receiver sensitivity penalty compared with the single-band OFDM signal in Fig. 6(a), as given by $10\log(2)/2$ from (1), (2), and (3). The difference between theory and experiment may be mainly ascribed to the higher optical SNR penalty due to residual laser phase noise, which is expected for the lower symbol rate signal in Fig. 6(a) with an estimated phase error variance of 0.0358 rad^2 [28]. The BER curves in Figs. 4(a) and 6(a) have similar slopes. In addition, optical transmission over 22.8 km of SSMF induces 0.4-dB receiver sensitivity penalty for 0.6-m wireless distance. BER is degraded for received optical power higher than 0.3 dBm due to fiber nonlinearity, corresponding to an optical power of 5.8 dBm at the input of the fiber. The fiber nonlinearity is the reason that the BER is not below the FEC limit for combined 22.8-km SSMF and 1.3-m wireless distance.

Fig. 6(b) shows the wireless transmission performance of the four OFDM bands for optical B2B compared with the theoretical slope for 16-QAM-OFDM in AWGN. There is negligible power penalty among the different OFDM bands when one OFDM subcarrier in the second band is removed during BER evaluation. The receiver sensitivity at the FEC limit of $2 \cdot 10^{-3}$ is 1.5 dBm and 4.3 dBm for 0.6 m and 1.3 m of wireless distance, respectively. The optical comb reduces the optical SNR; the maximum power spectral density decreases by $6.6-7.6$ dB, as shown in Fig. 3(b), thus inducing a receiver sensitivity penalty of 5.7 dB and 4.9 dB for 0.6 m and 1.3 m of wireless distance, respectively. The four-band BER in Fig. 6(b) slope more gradually with received optical power than the single-band BER in Fig. 6(a) due to the increased optical noise. Although the SNR is dominated by electrical noise, decreasing the received optical power increases the BER, the optical noise affects performance. Reducing the channel spacing would increase the optical noise, thus reducing the slope, as shown in [23]. Furthermore, BER is degraded for received optical power higher than 5 dBm and 6 dBm due to receiver saturation. In addition, although it is expected that BER is degraded due to fiber nonlinearity from a higher received optical power for the multiband OFDM signal compared with the single-band OFDM signal [23], the BER is not below the FEC limit for combined 22.8-km SSMF and 0.6- or 1.3-m wireless distance.

Fig. 6 also indicates that the required received optical power to achieve BER $< 2 \cdot 10^{-3}$ is up to 5 dBm, corresponding to a maximum transmitter power of -12 dBm and a maximum EIRP of 12 dBm. The received RF power is approximately -36 dBm and -36.5 dBm for 2-dBm and 5-dBm received optical power at 0.6 m and 1.3 m of wireless distance, respectively. The wireless distance could be extended by employing a W-band high-power amplifier at the transmitter and a higher gain LNA at the receiver side.

As expected, the difference in the receiver sensitivity at 0.6 m and 1.3 m in Fig. 6(a) and in Fig. 6(b) is near 3.4 dB, as given by $\Delta P_{\rm opt} = \Delta L_{FS}/2$.

The herein demonstrated system supports four channels in 14.4-GHz total bandwidth with 4.3-dBm receiver optical sensitivity for 1.3-m wireless distance as compared with three channels in 11.2-GHz or 9.4-GHz total bandwidth with 2.8 dBm or 3.2 dBm, respectively [23].

The demonstrated single-band transmission could be suitable for delivering 10-Gigabit Ethernet signals [see Fig. 6(a)] or UHDTV signals [see Fig. 4(a)] to a single user. Although with higher complexity and lower performance, the multiband system [see Fig. 6(b)] could be suitable for providing multiuser or higher capacity access, e.g., up to four 10-Gigabit Ethernet users and up to two UHDTV users or one OC-768/STM-256 user by aggregating channels.

5. Conclusion

The photonic generation and wireless transmission of electrical 16-QAM-OFDM signals in the $75-110$ GHz band has been experimentally demonstrated using a single RF band and when the RF bandwidth is used in multiple channels. A single-band system at 17.8-Gb/s effective data rate in 6.3-GHz bandwidth has been demonstrated up to 1.3 m of wireless distance. This signal exhibits up to 2.7-dB penalty in receiver optical sensitivity as compared with a single band at 8.9 Gb/s effective data rate in 3.2-GHz bandwidth in a system supporting multiband generation. The transmission of the 8.9-Gb/s signal over combined 22.8-km SSMF and 0.6-m wireless distance has also been demonstrated. The transmission of up to four channels at an effective data rate of 8.9 Gb/s/ch in 14.4-GHz bandwidth has been demonstrated up to 1.3 m of wireless distance employing an optical comb. The proposed multiband radio-over-fiber approach can provide a cost- and power-efficient solution for high-capacity hybrid wireless/optical links supporting multiple users with flexible bandwidth allocation.

References

[1] T. Nagatsuma, T. Takada, H.-J. Song, K. Ajito, N. Kukutsu, and Y. Kado, "Millimeter- and THz-wave photonics towards 100-Gb/s wireless transmission," in *Proc. IEEE 23rd Annu. Meet. Photon. Soc.*, 2010, pp. 385–386.
[2] A. Stöhr, "10 Gb/s wireless transmission using millimeter-wave over optical fiber systems," presented at the Proc. Opt. Fiber Commun. Conf., Los Angeles, CA, 2011, Paper OTuO3.
[3] M. Beltrán, J. B. Jensen, X. Yu, R. Llorente, R. Rodes, M. Ortsiefer, C. Neumeyr, and I. Tafur Monroy, "Performance of a 60-GHz DCM-OFDM and BPSK-impulse ultra-wideband system with radio-over-fiber and wireless transmission employing a directly-modulated VCSEL," *IEEE J. Sel. Areas Commun.*, vol. 29, no. 6, pp. 1295–1303, Jun. 2011.
[4] J. Wells, "Faster than fiber: The future of multi-Gb/s wireless," *IEEE Microw. Mag.*, vol. 10, no. 3, pp. 104–112, May 2009.
[5] T. Nagatsuma, "Photonic generation of millimeter waves and its applications," presented at the Proc. Opt. Fiber Commun. Conf., Los Angeles, CA, 2012, Paper OM2B.7.
[6] M. Weiss, A. Stöhr, F. Lecoche, and B. Charbonnier, "27 Gb/s photonic wireless 60 GHz transmission system using 16-QAM OFDM," *Proc. Int. Top. Meet. Microw. Photon.*, pp. 1–3, 2009.
[7] P.-T. Shih, A. Ngoma, C.-T. Lin, F. Annunziata, J. Chen, J. George, M. Sauer, and S. Chi, "2 × 21 Gbps symmetrical full-duplex transmission of OFDM wireless signals over a bidirectional IMDD radio-over-fiber system at 60 GHz," presented at the Proc. Eur. Conf. Opt. Commun., Torino, Italy, 2010, Paper Th.9.B.4.
[8] C. Wei, C. Lin, M. Chao, W. Jiang, and C. Ho, "Long-reach 26.54-Gbps OFDM RoF system at 60 GHz over 100-km fiber and 3-m wireless transmission employing phase noise compensation and bit-loading algorithms," presented at the Proc. Eur. Conf. Opt. Commun., Geneva, Switzerland, 2011, Paper We.7.C.5.
[9] C.-H. Ho, R. Sambaraju, W.-J. Jiang, T. H. Lu, C.-Y. Wang, H. Yang, W.-Y. Lee, C.-T. Lin, C.-C. Wei, S. Chi, and A. Ng'oma, "50-Gb/s radio-over-fiber system employing MIMO and OFDM modulation at 60 GHz," presented at the Proc. Opt. Fiber Commun. Conf., Los Angeles, CA, 2012, Paper OM2B.3.
[10] F.-M. Kuo, C.-B. Huang, J.-W. Shi, N.-W. Chen, H.-P. Chuang, J. Bowers, and C.-L. Pan, "Remotely up-converted 20-Gb/s error-free wireless on–off-keying data transmission at W-band using an ultrawideband photonic transmitter-mixer," *IEEE Photon. J.*, vol. 3, no. 2, pp. 209–219, Apr. 2011.
[11] A. Kanno, K. Inagaki, I. Morohashi, T. Sakamoto, T. Kuri, I. Hosako, T. Kawanishi, Y. Yoshida, and K. Kitayama, "40 Gb/s W-band (75–110 GHz) 16-QAM radio-over-fiber signal generation and its wireless transmission," *Opt. Exp.*, vol. 19, no. 26, pp. B56–B63, Dec. 2011.
[12] X. Pang, A. Caballero, A. Dogadaev, V. Arlunno, R. Borkowski, J. S. Pedersen, L. Deng, F. Karinou, F. Roubeau, D. Zibar, X. Yu, and I. Tafur Monroy, "100 Gb/s hybrid optical fiber-wireless link in the W-band (75–110 GHz)," *Opt. Exp.*, vol. 19, no. 25, pp. 24944–24949, Dec. 2011.
[13] D. Zibar, R. Sambaraju, A. Caballero, J. Herrera, U. Westergren, A. Walber, J. B. Jensen, J. Marti, and I. Tafur Monroy, "High-capacity wireless signal generation and demodulation in 75- to 110-GHz band employing all-optical OFDM," *IEEE Photon. Technol. Lett.*, vol. 23, no. 12, pp. 810–812, Jun. 2011.
[14] R.-W. Ridgway, D.-W. Nippa, and S. Yen, "Data transmission using differential phase-shift keying on a 92 GHz carrier," *IEEE Trans. Microw. Theory Tech.*, vol. 58, no. 11, pp. 3117–3126, Nov. 2010.

[15] R. Freund, G. Bosco, L. Oxenlwe, M. Winter, A. D. Ellis, M. Nölle, C. Schmidt-Langhorst, R. Ludwig, C. Schubert, A. Carena, P. Poggiolini, M. Galili, H. C. H. Mulvad, D. Hillerkuss, R. Schmogrow, W. Freude, J. Leuthold, F. C. G. Gunning, J. Zhao, P. Frascella, S. K. Ibrahim, and N. M. Suibhne, "Single- and multi-carrier techniques to build up Tb/s per channel transmission systems," presented at the Proc. Int. Conf. Transparent Opt. Netw., Munich, Germany, 2010, Paper Tu.D1.4.

[16] Z. Jiang, D. E. Leaird, and A. M. Weiner, "Optical processing based on spectral line-by-line pulse shaping on a phase-modulated CW laser," *IEEE J. Quantum Electron.*, vol. 42, no. 7, pp. 657–665, Jul. 2006.

[17] I. Morohashi, T. Sakamoto, H. Sotobayashi, T. Kawanishi, and I. Hosako, "Broadband wavelength-tunable ultrashort pulse source using a Mach–Zehnder modulator and dispersion-flattened dispersion-decreasing fiber," *Opt. Lett.*, vol. 34, no. 15, pp. 2297–2299, Aug. 2009.

[18] J. Yu, Z. Dong, and N. Chi, "Generation, transmission and coherent detection of 11.2 Tb/s (112 × 100Gb/s) single source optical OFDM superchannel," presented at the Proc. Opt. Fiber Commun. Conf., Los Angeles, CA, 2011, Paper PDPA6.

[19] P. M. Anandarajah, R. Maher, Y. Q. Xu, S. Latkowski, J. O'Carroll, S. G. Murdoch, R. Phelan, J. O'Gorman, and L. P. Barry, "Generation of coherent multicarrier signals by gain switching of discrete mode lasers," *IEEE Photon. J.*, vol. 3, no. 1, pp. 112–122, Feb. 2011.

[20] M. Beltrán, J. Caraquitena, R. Llorente, and J. Marti, "Reconfigurable multiwavelength source based on electrooptic phase modulation of a pulsed laser," *IEEE Photon. Technol. Lett.*, vol. 23, no. 16, pp. 1175–1177, Aug. 2011.

[21] X. Liu, S. Chandrasekhar, B. Zhu, P. J. Winzer, A. H. Gnauck, and D. W. Peckham, "Transmission of a 448-Gb/s reduced-guard-interval CO-OFDM signal with a 60-GHz optical bandwidth over 2000 km of ULAF and five 80-GHz-grid ROADMs," presented at the Proc. Opt. Fiber Commun. Conf., San Diego, CA, 2010, Paper PDPC2.

[22] L. Deng, M. Beltrán, X. Pang, X. Zhang, V. Arlunno, Y. Zhao, A. Caballero, A. Dogadaev, X. Yu, R. Llorente, D. Liu, and I. Tafur Monroy, "Fiber wireless transmission of 8.3-Gb/s/ch QPSK-OFDM signals in 75-110-GHz band," *IEEE Photon. Technol. Lett.*, vol. 24, no. 5, pp. 383–385, Mar. 2012.

[23] L. Deng, D. Liu, X. Pang, X. Zhang, V. Arlunno, Y. Zhao, A. Caballero, A. K. Dogadaev, X. Yu, I. T. Monroy, M. Beltrán, and R. Llorente, "42.13 Gb/s 16QAM-OFDM photonics-wireless transmission in 75-110 GHz band," *Progr. Electromagn. Res.*, vol. 126, pp. 449–461, Mar. 2012.

[24] M. Beltrán, L. Deng, X. Pang, X. Zhang, V. Arlunno, Y. Zhao, X. Yu, R. Llorente, D. Liu, and I. Tafur Monroy, "38.2-Gb/s optical-wireless transmission in 75–110 GHz based on electrical OFDM with optical comb expansion," presented at the Proc. Opt. Fiber Commun. Conf., Los Angeles, CA, 2012, Paper OM2B.2.

[25] J. G. Proakis, *Digital Communications*, 4th ed.   New York: McGraw-Hill, 2001.

[26] X. Liu and F. Buchali, "Intra-symbol frequency-domain averaging based channel estimation for coherent optical OFDM," *Opt. Exp.*, vol. 16, no. 26, pp. 21944–21957, Dec. 2008.

[27] W. Shieh and I. Djordjevic, *OFDM for Optical Communications.*   San Diego, CA: Academic, 2010.

[28] X. Yi, W. Shieh, and Y. Ma, "Phase noise effects on high spectral efficiency coherent optical OFDM transmission," *J. Lightw. Technol.*, vol. 26, no. 10, pp. 1309–1316, May 2008.

Paper 6: 42.13 Gbit/s 16QAM-OFDM Photonics-Wireless Transmission in 75-110 GHz Band

Lei Deng, Deming Liu, **Xiaodan Pang**, Xu Zhang, Valeria Arlunno, Ying Zhao, Antonio Caballero, Anton Dogadaev, Xianbin Yu, Idelfonso Tafur Monroy, Marta Beltrán, Roberto Llorente, "42.13 Gbit/s 16QAM-OFDM Photonics-Wireless Transmission in 75-110 GHz Band," *Progress In Electromagnetics Research*, vol. 126, pp. 449-461, 2012.

42.13 GBIT/S 16QAM-OFDM PHOTONICS-WIRELESS TRANSMISSION IN 75–110 GHz BAND

L. Deng[1],[*], D. M. Liu[1], X. D. Pang[2], X. Zhang[2], V. Arlunno[2], Y. Zhao[2], A. Caballero[2], A. K. Dogadaev[2], X. B. Yu[2], I. T. Monroy[2], M. Beltrán[3], and R. Llorente[3]

[1]College of Optoelectronics Science and Engineering, Huazhong University of Science and Technology, Wuhan 430074, China

[2]DTU Fotonik, Department of Photonics Engineering, Technical University of Denmark, Kgs. Lyngby DK-2800, Denmark

[3]Valencia Nanophotonics Technology Center, Universidad Politcnica de Valencia, Valencia 46022, Spain

Abstract—We present a simple architecture for realizing high capacity W-band (75–110 GHz) photonics-wireless system. 42.13 Gbit/s 16QAM-OFDM optical baseband signal is obtained in a seamless 15 GHz spectral bandwidth by using an optical frequency comb generator, resulting in a spectral efficiency of 2.808 bits/s/Hz. Transparent photonic heterodyne up-conversion based on two free-running lasers is employed to synthesize the W-band wireless signal. In the experiment, we program an improved DSP receiver and successfully demonstrate photonics-wireless transmission of 8.9 Gbit/s, 26.7 Gbit/s and 42.13 Gbit/s 16QAM-OOFDM W-band signals, with achieved bit-error-rate (BER) performance below the forward error correction (FEC) limit.

1. INTRODUCTION

Due to the explosive bandwidth growth expected from the emerging wireless applications such as 3-D face-to-face communication and super Hi-Vision/Ultra High Definition TV data (more than 24 Gbit/s) [1], wireless communication links with very large capacity (towards 100 Gbit/s) are envisioned. However, current microwave wireless systems can provide only tens of Mbit/s because of regulatory constraints [2–4]. An alternative solution is to shift the carrier frequency

to the millimeter-wave bands, where several GHz unregulated available bandwidths are able to potentially provide very high capacity. Compared to 60 GHz [5, 6] and 120 GHz bands, the unregulated W-band (75–110 GHz) is recently attracting increasing research interests due to less air absorption loss and larger available frequency window [7, 8]. Furthermore, radio over fiber techniques in the W-band fiber-wireless system are expected to enable not only broadband services and wide wireless coverage, but also seamless integration of wireless links into future optical networks.

As a highly spectral efficient and flexible modulation technique, orthogonal frequency division multiplexing (OFDM) has been widely used in current wireless system [9, 10], since it is robust against fiber dispersion effects (chromatic dispersion and polarization mode dispersion) in optical fiber channels and wireless multipath fading in wireless channels. In the 60 GHz band, OFDM technique has already been used to realize 27 Gbit/s [11] and 28 Gbit/s [12] 16-quadrature amplitude modulation (QAM)-OFDM fiber-wireless links with coherent optical up-conversion at a modulator. In the W-band, quadrature phase-shift keying (QPSK) and 16-QAM have also been used to achieve 20 Gbit/s [13] and 40 Gbit/s [14] wireless links. So far, no high speed OFDM W-band wireless transmission system has been reported. In these reported 60 GHz band and W-band schemes, hybrid photonic-electronic up-conversion (coherent method) is used to generate the high wireless carrier frequency, and 2.5 m wireless transmission with achieved performance slightly above the forward error correction (FEC) limit in [11] and 30 mm wireless transmission with achieved performance below the FEC limit in [13, 14] are demonstrated. Recently, a photonic up/down-conversion (incoherent method) with RF/bit-rate transparency has also been proposed for a 40 Gbit/s OFDM W-band system without air transmission [15]. The wireless transmission demonstration of very high speed OFDM W-band signals will therefore contribute to the needed development of ultra-broadband wireless communication technology.

In this paper, we present for the first time, a high speed and scalable photonics-wireless transmission system in 75–110 GHz by combining the spectral efficient OFDM modulation and coherent optical frequency division multiplexing techniques. By using optical heterodyne mixing of a high-speed optical OFDM baseband signal with a free-running laser, the system can seamlessly generate a high capacity W-band wireless signal, while preserving transparency to bit rates, modulation format and RF carrier. A digital signal processing (DSP) based receiver benefits us with significant complexity reduction and increased flexibility. Furthermore, 0.6 m photonics-

wireless transmission of 42.13 Gbit/s OOFDM signal is successfully achieved in the experiment. We also demonstrate the capacity and bandwidth scalability of the proposed system.
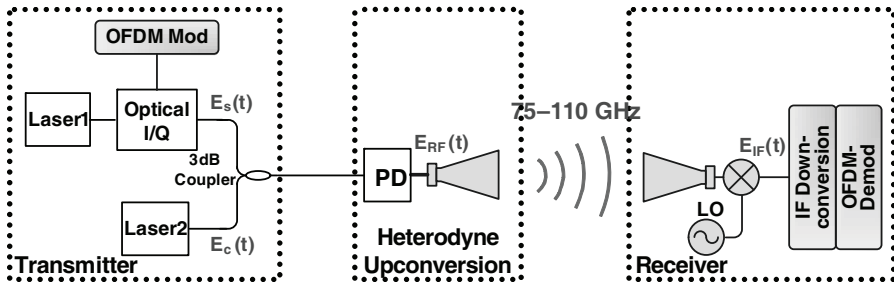
2. PRINCIPLE OF HETERODYNE UP-CONVERSION AND DOWN-CONVERSION

The block diagram of the proposed system is shown in Fig. 1. In the transmitter, the optical in-phase/quadrature-modulated OFDM signal is heterodyne mixed with a free running laser to generate the W-band wireless signal. The baseband electrical OFDM signal $E_{\mathrm{OFDM}}(t)$, the optical OFDM signal $E_s(t)$ and the beating laser $E_c(t)$ can be represented as:

$$E_{\mathrm{OFDM}}(t) = I(t) + jQ(t),$$
$$E_s(t) = \sqrt{P_s} \cdot E_{\mathrm{OFDM}}(t) \cdot \exp[-j(\omega_s t + \phi_s(t))],$$
$$E_c(t) = \sqrt{P_c} \cdot \exp[-j(\omega_c t + \phi_c(t))], \quad (1)$$

where $I(t)$ and $Q(t)$ are the real and image part of the electrical baseband OFDM signal. P_s, ω_s and $\phi_s(t)$ represent the optical power, angular frequency and phase of the signal laser respectively, so as P_c, ω_c and $\phi_c(t)$ for the beating laser. The combined signal is beating at a photodiode for heterodyne up-conversion, and the output signal $E(t)$ could be described as:

$$E(t) \ \propto \ |E_s(t) + jE_c(t)|^2 = P_s + P_c + E_{\mathrm{RF}}(t),$$
$$E_{\mathrm{RF}}(t) = 2\sqrt{P_s P_c} \cdot [I(t) \cdot \sin(\triangle\omega t + \triangle\phi(t))$$
$$+ Q(t) \cdot \cos(\triangle\omega t + \triangle\phi(t))],$$
$$\triangle\omega = \omega_c - \omega_s, \quad \triangle\phi(t) = \phi_c(t) - \phi_s(t), \quad (2)$$

Figure 1. The block diagram of the proposed photonics-wireless system.

where $E_{\mathrm{RF}}(t)$ represents the generated W-band signal with carrier frequency of $\triangle\omega$, and the phase noise of signal laser and beating laser are included in $\triangle\phi(t)$. By using a horn antenna, the W-band wireless signal is detected after air transmission. A W-band balanced mixer and a sinusoidal LO signal are used for electrical down-conversion. The LO signal is expressed as $E_{\mathrm{LO}}(t) = \sqrt{P_{\mathrm{LO}}} \cdot \cos(\omega_{\mathrm{LO}}t + \phi_{\mathrm{LO}}(t))$, here P_{LO}, ω_{LO} and $\phi_{\mathrm{LO}}(t)$ represent the power, angular frequency and phase of the LO signal, respectively. After the electrical down-conversion, the generated intermediate frequency (IF) signal can be described as:

$$
\begin{aligned}
E_{\mathrm{IF}}(t) &= \langle E_{\mathrm{RF}}(t) \cdot E_{\mathrm{LO}}(t) \rangle \\
&= \sqrt{P_s P_c P_{\mathrm{LO}}} \cdot [I(t) \cdot \sin(\triangle\omega_{\mathrm{IF}}t + \triangle\phi_{\mathrm{IF}}(t)) \\
&\quad + Q(t) \cdot \cos(\triangle\omega_{\mathrm{IF}}t + \triangle\phi_{\mathrm{IF}}(t))], \\
\triangle\omega_{\mathrm{IF}} &= \omega_{\mathrm{LO}} - (\omega_c - \omega_s), \quad \triangle\phi_{\mathrm{IF}}(t) = \phi_{\mathrm{LO}}(t) - (\phi_c(t) - \phi_s(t)), \ (3)
\end{aligned}
$$

where $\triangle\omega_{\mathrm{IF}}$ and $\triangle\phi_{\mathrm{IF}}(t)$ represent the angular frequency and phase of the IF carrier signal. The phase noise of the signal laser, beating laser and LO signal are all included in $\triangle\phi_{\mathrm{IF}}(t)$. After electrical down-conversion, 2-steps demodulation algorithms are performed in our DSP receiver. In the first step, IF frequency down-conversion is implemented by multiplying IF signal $E_{\mathrm{IF}}(t)$ by $\exp(-j\triangle\omega_{\mathrm{IF}}t)$, as expressed in Eq. (4). A low-pass filter is used to filter out the high-order items, and the generated signal $E_1(t)'$ is described in Eq. (4) as well.

$$
\begin{aligned}
E_1(t) &= E_{\mathrm{IF}}(t) \cdot \exp(-j\triangle\omega_{\mathrm{IF}}t), \\
E_1(t)' &= \frac{1}{2}\sqrt{P_s P_c P_{\mathrm{LO}}} \cdot [I(t) \cdot \sin(\triangle\phi_{\mathrm{IF}}(t)) - jI(t) \cdot \cos(\triangle\phi_{\mathrm{IF}}(t)) \\
&\quad + Q(t) \cdot \cos(\triangle\phi_{\mathrm{IF}}(t)) + jQ(t) \cdot \sin(\triangle\phi_{\mathrm{IF}}(t))] \\
&= -\frac{1}{2}j\sqrt{P_s P_c P_{\mathrm{LO}}} \cdot (I(t) + jQ(t)) \cdot \exp(j\triangle\phi_{\mathrm{IF}}(t)). \qquad (4)
\end{aligned}
$$

As shown in Eq. (4), the $I(t) + jQ(t)$ item is the desired OFDM signal, and the $\exp(j\triangle\phi_{\mathrm{IF}}(t))$ item is the phase noise which need to be removed. Therefore, in the second step, frequency and channel estimation and pilot-based phase noise estimation algorithms are used for the OFDM demodulation in our experiment.
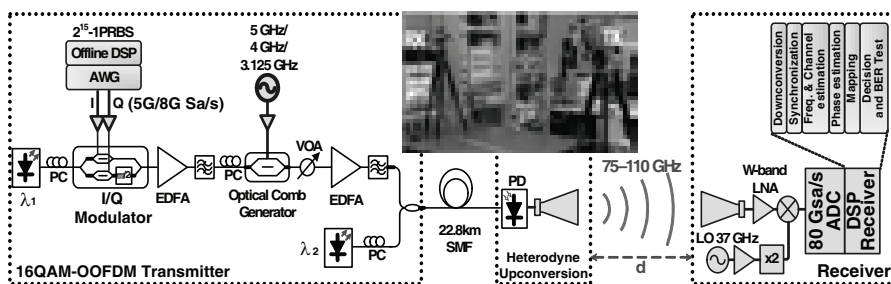
3. EXPERIMENTAL SETUP

Figure 2 shows the experimental setup of the proposed high capacity 16QAM-OFDM W-band wireless transmission system. At the 16QAM-OOFDM transmitter, an arbitrary waveform generator (AWG, Tektronix AWG 7122C) is performed to generate the OFDM

waveform. In the signal generator, a data stream with a pseudo-random bit sequence (PRBS) length of $2^{15} - 1$ is mapped onto 72 16-QAM subcarriers, which are converted into the time domain together with 8 pilot subcarriers, one unfilled DC subcarrier, and 47 unfilled edge subcarriers by applying 128-point inverse fast Fourier transform (IFFT) [16]. The cyclic prefix is 1/10 of the IFFT length resulting in an OFDM symbol size of 141. To facilitate time synchronization and channel estimation, 10 training symbols are inserted at the beginning of each OFDM frame that contains 150 data symbols. The real and imaginary parts of the OFDM signal are clipped and converted to analog signals by two D/A converters operating at 5 GS/s with a D/A resolution of 10 bits. The generated OFDM signals are filtered by two antialiasing low-pass filters (LPFs) with 2.5 GHz bandwidth, and then used to modulate a 100 kHz-linewidth continuous-wave (CW) external cavity laser (ECL, λ_1 = 1552.886 nm) at an optical in-phase/quadrature (I/Q) modulator biased at its null point. An optical OFDM signal at a net data rate of 9.57 Gbit/s ($5\,\text{GSa/s} \times 4 \times 72 \div 141 \times 150 \div 160$) with a bandwidth of 3.164 GHz ($5\,\text{GSa/s} \times 81 \div 128$) is formed. An erbium-doped fiber amplifier (EDFA) and an optical filter with 0.8 nm bandwidth are used to compensate the loss of optical I/Q modulator and filter out the outband noise, respectively.

Subsequently, the optical OFDM signal is launched into an optical frequency comb generator employing an overdriven Mach-Zehnder modulator (MZM). The MZM is biased in its nonlinear region by equalizing the power of the central 3 comb lines. The frequency spacing of the comb lines is set to 3.125 GHz, 4 GHz and 5 GHz for scalability testing. In the case of 4 GHz comb spectral spacing, 72 OFDM
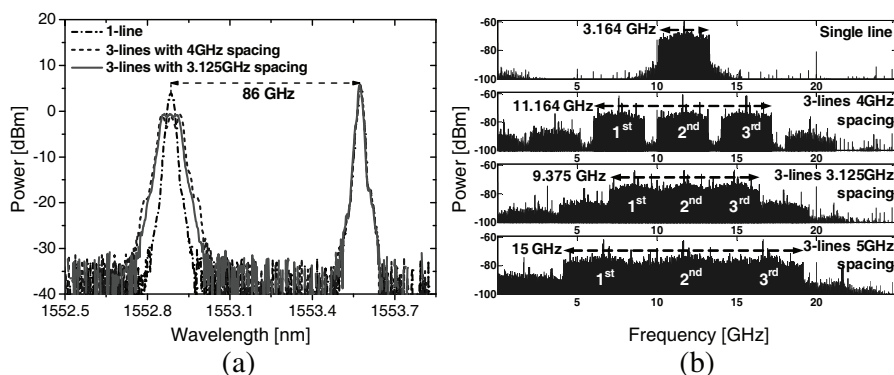

Figure 2. Experimental setup for the proposed 16QAM-OOFDM W-band transmission system. Inset photograph: Global view of the wireless link setup with wireless transmitter (TX) and receiver (RX). AWG: Arbitrary waveform generator. PC: Polarization controller. VOA: Variable optical attenuator.

subcarriers are adopted in each comb-line to obtain an optical OFDM signal at 28.72 Gbit/s (3lines×5 GSa/s×4×72÷141×150÷160) with a spectral bandwidth of 11.164 GHz (5 GSa/s×81÷128+2×4 GHz). In the case of 3.125 GHz spacing, one edge subcarrier of the OFDM signal in each comb-line is deleted to avoid the inter-symbol interference (ISI), resulting in an optical OFDM signal at 28.32 Gb/s with a spectral bandwidth of 9.375 GHz (3lines × 5 GSa/s × 80 ÷ 128). In the case of 5 GHz spacing, the sampling rate of AWG is set to 8 GSa/s, and 71 OFDM subcarriers are adopted in each comb-line to obtain an optical OFDM signal at 45.31 Gbit/s (3lines × 8 GSa/s × 4 × 71 ÷ 141 × 150 ÷ 160) with a spectral bandwidth of 15 GHz (3lines×8 GSa/s×80÷128). The generated optical signal at the output of optical comb generator is seamless in the case of 3.125 GHz and 5 GHz spectral spacing, because the comb spacing is integral multiple of the OFDM subcarrier spacing and all of the OFDM subcarriers from different comb lines are orthogonal to each other. The second EDFA and optical filter with 0.8 nm bandwidth are used to compensate the insertion loss of the optical comb generator and to eliminate the high-order modulation sidebands. It is noted that these 3-lines OFDM signals are correlated, and the de-correlation of 3-lines and the effect of inter-channel interference (ICI) between different lines are under further investigation from a practical point of view.

The optical 3-lines 16QAM-OFDM signal is then combined with a 100 kHz linewidth free-running CW laser (λ_2 = 1553.574 nm)
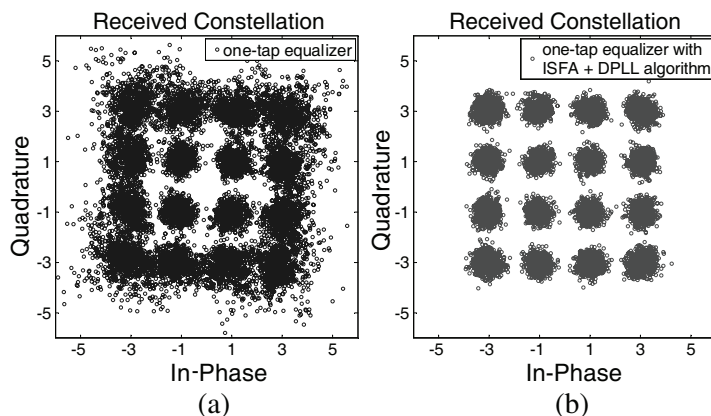

Figure 3. (a) The optical spectra of optical baseband signal (single-line, 3-lines with 3.125 GHz spacing and 4 GHz spacing) and local oscillator (LO). (b) Electrical spectra of 16QAM-OOFDM signal (single-line, 3-lines with 3.125 GHz, 4 GHz and 5 GHz spacing) after down-conversion mixer.

for optical transparent generation of W-band wireless signals. The measured optical spectra of single-line, 3-lines with 3.125 GHz and 4 GHz spacing at the input of the photodiode are shown in the Fig. 3(a). After 22.8 km of standard single mode fiber (SSMF) propagation, the combined optical signal is heterodyne mixed in a 100 GHz bandwidth photodiode (PD, u^2t XPDV4120R) at the remote antenna site to generate a W-band wireless signal, which is then fed to a W-band horn antenna with 24 dBi gain. A photograph of the global view of the wireless link is inserted in Fig. 2 as well. After air transmission, the signal is detected by a horn antenna with 25 dBi gain and amplified by a W-band 25 dB gain low-noise amplifier (LNA, Radiometer Physics W-LAN). A W-band balanced mixer driven by a 74 GHz sinusoidal LO signal after frequency doubling from a 37 GHz signal synthesizer (Rohde & Schwarz SMF 100A) is employed for electrical down-conversion. The electrical spectra of intermediate frequency (IF) signals after down-conversion for single-line, 3-lines with 3.125 GHz, 4 GHz and 5 GHz spacing are shown in Fig. 3(b).

An 80 GSa/s real-time sampling oscilloscope with 32 GHz analog bandwidth (Agilent DSAX93204A) is used to capture the IF signals. Offline signal demodulation is then performed by a DSP-based receiver consisting of frequency down-conversion, time synchronization, frequency and channel estimation, pilot-based phase estimation, data mapping and bit error rate (BER) tester. Furthermore, we program one-tap equalizer and an effective channel estimation algorithm by combining the intra symbol frequency-domain averaging (ISFA) [17, 18]

Figure 4. Received constellations of 9.57 Gbit/s (single-line) W-band signal after 22.8 km SMF and 0.65 m air distance transmission without ISFA-DPLL (BER of 1.49×10^{-2}) and with ISFA-DPLL (BER of 2.33×10^{-5}).
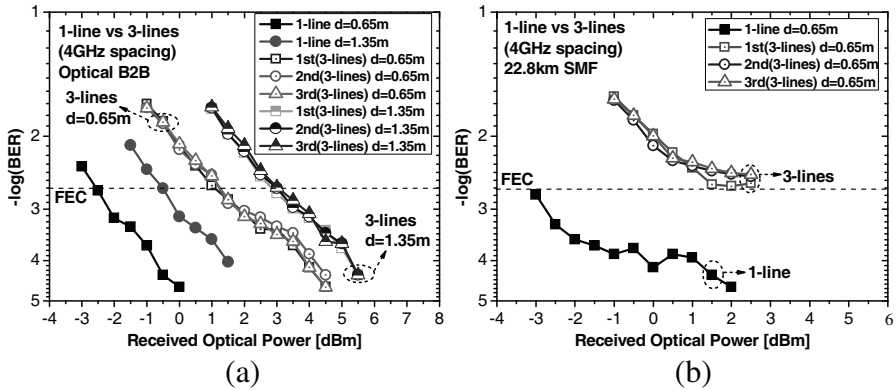
and digital phase-locked loop (DPLL) to mitigate the dispersion and nonlinearity (e.g., four-wave mixing) effects induced by fiber and wireless transmission. We can clearly observe the performance improvement by comparing the received constellations with/without ISFA-DPLL for 9.57 Gb/s (single-line) 16QAM-OFDM W-band signal after 22.8 km SMF and 0.65 m air transmission in Fig. 4.

4. EXPERIMENTAL RESULTS AND DISCUSSIONS

The millimeter-wave carrier frequency is set to 86 GHz in our experiment to match the central operation frequency of the electrical mixer. To test the system scalability, we measure the performance for single line, 3-lines with 3.125 GHz, 4 GHz and 5 GHz spacing at bit rates of 9.57 Gbit/s, 28.32 Gbit/s, 28.72 Gbit/s and 45.31 Gbit/s, respectively. After considering the 7% Reed-Solomon forward-error correction (FEC) overhead, the effective net bit rate is 8.9 Gbit/s, 26.33 Gbit/s, 26.7 Gbit/s, and 42.13 Gbit/s, respectively.

Figure 5(a) shows the measured BER in terms of the received optical power into the PD after different air transmission distances in optical back-to-back (B2B) for both single-line and 3-lines with 4 GHz spacing. In the case of single-line, the 4 GHz driving RF signal at optical frequency comb generator is off. We can observe that the receiver sensitivity at the FEC limit (BER of 2×10^{-3}) is achieved at -2.5 dBm and -0.5 dBm for air transmission of 0.65 m and 1.35 m, respectively. The signal to noise ratio decreases as air distance

Figure 5. Measured BER performance of 8.9 Gbit/s (single-line) and 26.7 Gbit/s (3-lines with 4 GHz spacing) 16QAM-OFDM W-band wireless transmission without (a) and with (b) 22.8 km SMF fiber transmission.

increases, resulting in higher required optical power at the FEC limit. For 3-lines with 4 GHz spacing, we can see that the receiver sensitivity of the 1st line to reach the FEC limit is 1 dBm and 2.8 dBm for air transmission of 0.65 m and 1.35 m, respectively. There is negligible power penalty among different lines, and about 3.5 dB power penalty between single line case and 3-lines cases at the same air distance. This power penalty is expected, since the optical signal to noise ratio (OSNR) of 3-lines is about 5 dB lower than that of single-line at a given optical power, as indicated in Fig. 3(a).

(a)

(b)

Figure 6. Measured BER performance of 26.33 Gbit/s 16QAM-OFDM signal (3-lines with 3.125 GHz spacing) wireless transmission in optical B2B (a) and received constellations (b).
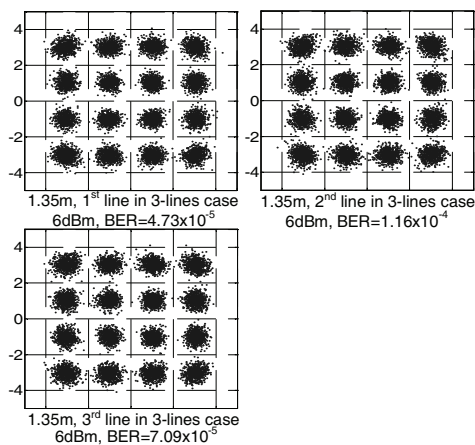
Figure 5(b) presents the BER performance of 8.9 Gbit/s (single-line) and 26.7 Gbit/s (3-lines with 4 GHz spacing) 16QAM-OFDM W-band signal after hybrid 22.8 km SMF and 0.65 m air transmission. Compared to the optical B2B case, the system performance is degraded when the received optical power into the PD is higher than 0 dBm for single-line case and 2 dBm for 3-lines case. This can be explained that OFDM signal is sensitive to the nonlinearity of the fiber and wireless channel due to its high peak-to-average-power-ratio (PAPR).
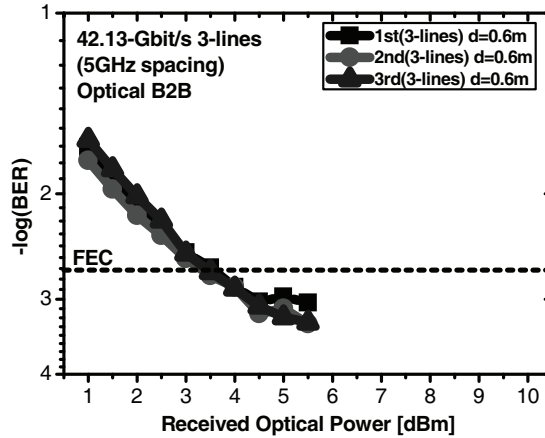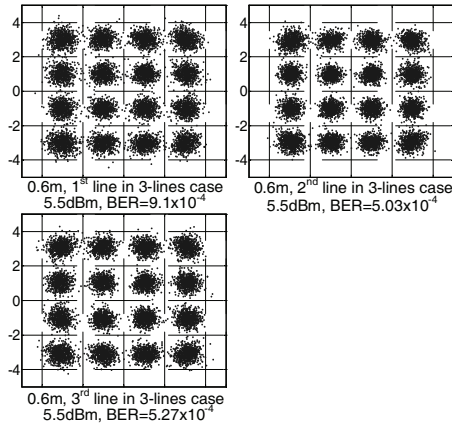

(a)

(b)

Figure 7. Measured BER performance of 42.13 Gbit/s 16QAM-OFDM signal (3-lines with 5 GHz spacing) wireless transmission in optical B2B (a) and received constellations (b).

Figure 6(a) and Fig. 7(a) depict the BER curves of 26.33 Gbit/s (3-lines with 3.125 GHz spacing) and 42.13 Gbit/s (3-lines with 5 GHz spacing) W-band signal wireless transmissions. For 3-lines with 3.125 GHz spacing, we can see that the receiver sensitivity of the 1st line to reach the FEC limit is 1.9 dBm and 3.2 dBm for air transmission of 0.6 m and 1.35 m, respectively. 0.9 dB power penalty compared to 3-lines with 4 GHz spacing is attributed to the phase ripple and non-flat frequency response, which degrade the orthogonality of the OFDM subcarriers and introduce inter-symbol interference (ISI). In the case of 3-lines with 5 GHz spacing, we successfully achieve BER performance below the FEC limit for 42.13 Gbit/s 16QAM-OFDM W-band signal after 0.6 m air transmission in the experiment. The receiver sensitivity of the 1st line is 3.5 dBm, and there is negligible power penalty among different comb lines. The received constellations of 26.33 Gbit/s and 42.13 Gbit/s W-band signals are shown in the Fig. 6(b) and Fig. 7(b) as well.

5. CONCLUSION

We have presented a high speed OOFDM photonics-wireless transmission system in 75–110 GHz employing photonic technologies. To our best knowledge, this is the first attempt to combine OFDM modulation and coherent optical frequency division multiplexed techniques to implement a W-band wireless signal up to 42.13 Gbit/s. By developing intra symbol frequency-domain averaging (ISFA) and digital phase-locked loop (DPLL) as an improved channel estimation method, 42.13 Gbit/s 16QAM-OFDM signals at 86 GHz are successfully transmitted over 0.6 m air distance. The proposed system provides for us a promising solution to bring the capacities in optical links to radio links, to realize the seamless integration of high speed wireless and fiber-optic networks.

REFERENCES

1. Nagatsuma, T., T. Tkakda, H.-J. Song, K. Ajito, N. Kukutsu, and Y. Kado, "Millimeter- and THz-wave photonics towards 100-Gbit/s wireless transmission," *Proc. of IEEE Photonics Society's 23th Annual Meeting*, 385–386, Denver, Colorado, USA, 2010.

2. Ni, W., N. Nakajima, and S. Zhang, "A broadband compact folded monopole antenna for WLAN/WIMAX communication applications," *Journal of Electromagnetic Waves and Applications*, Vol. 24, No. 7, 921–930, 2010.

3. Soltani, S., M. N. Azarmanesh, E. Valikhanloo, and P. Lotfi, "Design of a simple single-feed dual-orthogonal-linearly-polarized slot antenna for concurrent 3.5 GHz WIMAX and 5 GHz WLAN access point," *Jouranl of Electromagnetic Waves and Applications*, Vol. 24, No. 13, 1741–1750, 2010.

4. Ren, X.-S., Y.-Z. Yin, W. Hu, and Y.-Q. Wei, "Compact tri-band rectangular ring patch antenna with asymmetrical strips for WLAN/WIMAX applications," *Jouranl of Electromagnetic Waves and Applications*, Vol. 24, No. 13, 1829–1838, 2010.

5. Yang, B., X.-F. Jin, X.-M. Zhang, H. Chi, and S. L. Zheng, "Photonic generation of 60 GHz millimeter-wave by frequency quadrupling based on a mode-locking SOA fiber ring laser with a low modulation depth MZM," *Jouranl of Electromagnetic Waves and Applications*, Vol. 24, No. 13, 1773–1782, 2010.

6. Navarro-Cia, M., V. T. Landivar, M. Beruete, and M. S. Ayza, "A slow light fishnet-like absorber in the millimeter-wave range," *Progress In Electromagnetics Research*, Vol. 118, 287–301, 2011.

7. Wells, J., "Faster than fiber: The future of multi-Gb/s wireless," *IEEE Microw. Mag.*, Vol. 10, No. 3, 104–112, 2009.

8. Thakur, J. P., W.-G. Kim, and Y.-H. Kim, "Large aperture low aberration aspheric dielectric lens antenna for W-band quasioptics," *Progress In Electromagnetics Research*, Vol. 103, 57–65, 2010.

9. Nee, V. R. and R. Prasad, *OFDM Wireless Multimedia Communications*, Artech House, Boston, 2000.

10. Prasad, R., *OFDM for Wireless Communications Systems*, Artech House, Boston, 2004.

11. Weiss, M., A. Stohr, F. Lecoche, and B. Charbonnier, "27 Gbit/s photonic wireless 60 GHz transmission system using 16-QAM OFDM," *Proc. of International Topical Meeting on Microwave Photonics*, 1–3, Valencia, Spain, 2009.

12. Lin, C.-T, E.-Z. Wong, W.-J. Jiang, P.-T. Shin, J. Chen, and S. Chi, "28-Gb/s 16-QAM OFDM radio-over-fiber system within 7-GHz license-free band at 60 GHz employing all-optical up-conversion," *Proc. of Conference on Lasers and Electro-optics and Conference on Quantum Electronics and Laser Science CLEO/QELS*, 1–2, Baltimore, MD, USA, 2009.

13. Kanno, A., K. Inagaki, I. Morohashi, T. Sakamoto, T. Kuri, I. Hosako, T. Kawanishi, Y. Yoshida, and K.-I. Kitayama, "20-Gb/s QPSK W-band (75–110 GHz) wireless link in free space using radio-over-fiber technique," *IEICE Electron. Express*, Vol. 8, No. 8, 612–617, 2011.

14. Kanno, A., K. Inagaki, I. Morohashi, T. Sakamoto, T. Kuri, I. Hosako, T. Kawanishi, Y. Yoshida, and K.-I. Kitayama, "40 Gb/s W-band (75–110 GHz) 16-QAM radio-over-fiber signal generation and its wireless transmission," *Opt. Express*, Vol. 19, No. 26, B56–B63, 2011.

15. Zibar, D., R. Sambaraju, A. Caballero, J. Herrera, U. Westergren, A. Walber, J. B. Jensen, J. Marti, and I. T. Monroy, "High-capacity wireless signal generation and demodulation in 75- to 110-GHz band employing all-optical OFDM," *IEEE Photon. Technol. Lett.*, Vol. 23, No. 12, 810–812, 2011.

16. You, Y.-H. and J. B. Kim, "Pilot and data symbol-aided frequency estimation for UWB-OFDM," *Progress In Electromagnetics Research*, Vol. 90, 205–217, 2009.

17. Lee, Y.-D., D.-H. Park and H.-K. Song, "Improved channel estimation and MAI-Robust schemes for wireless OFDMA system," *Progress In Electromagnetics Research*, Vol. 81, 213–223, 2008.

18. Liu, X. and F. Buchali, "Intra-symbol frequency-domain averaging based channel estimation for coherent optical OFDM," *Opt. Express*, Vol. 16, No. 26, 21944–21957, 2008.

Paper 7: Uplink transmission in the W-band (75-110 GHz) for hybrid optical fiber-wireless access networks

Xiaodan Pang, Lei Deng, Anton Dogadaev, Xu Zhang, Xianbin Yu, Idelfonso Tafur Monroy, "Uplink transmission in the W-band (75-110 GHz) for hybrid optical fiber-wireless access networks," *Microwave and Optical Technology Letters*, vol. 55, pp. 1033-1036, 2013.

$$\theta_1 + \theta_2 - \phi/2 = \pi/2, \tag{6}$$

$$\theta_3 + \theta_4 - \phi/2 = \pi/2. \tag{7}$$

The equivalent circuit of the filter is similar to a parallel-coupled half-wavelength resonator filter, so the same design method is available.

3. DESIGN EXAMPLE

A F4B substrate with a relative dielectric constant of 2.45, a thickness of 0.8 mm, and a loss tangent of 0.001 is chosen for the filter design. The corresponding parameters are listed below

$\theta_1 = 70.6^\circ,\ \theta_2 = 14.55^\circ,\ \theta_3 = 40.11^\circ,\ \theta_4 = 45.04^\circ,\ \phi = -9.7^\circ,$
$K_{12} = K_{34} = 4.45,\ J_{23} = 0.0012,$
$Z_0 = 52.18\ \Omega,\ Z_{0e} = 57.32\ \Omega,\ Z_{0o} = 47.9\ \Omega.$

Figure 4 illustrates the measured and simulated results of the filter. The designed center frequency is at 2.426 GHz with a fraction bandwidth of 13.81% while the measured one is at 2.38 GHz with a fraction bandwidth of 13.45%. The first harmonic passband is presented at about $3f_0$. The simulated minimum insertion loss in the passband is 0.56 dB, while the measured one is 0.84 dB. The difference is mainly caused by the extra mismatch of the SMA connector in the measurement. Two transmission zeroes are located at 1.43 and 2.98 GHz which have greatly improved the roll-off rate. The implemented filter is compact which has a dimension of $0.33\lambda_g$ by $0.21\lambda_g$. Geometric parameters of the filter are listed in Figure 1.

4. CONCLUSION

A bandpass filter using inductive coupled resonators is investigated. The equivalent circuit of the filter is analyzed. Based on the analysis, a fourth-order bandpass filter is fabricated which shows compact size and good stopband rejection. The design concept is validated as the measured result agrees well with the simulation.

REFERENCES

1. J.-R. Lee, J.-H. Cho, and S.-W. Yun, New compact bandpass filter using microstrip λ/4 resonators with open stub inverter, IEEE Microwave Wireless Compon Lett 10 (2000), 526–527.
2. C.-H. Wang, Y.-S. Lin, and C. H. Chen, Novel inductance-incorporated microstrip coupled-line bandpass filters with two attenuation poles, In: IEEE MTT-S International Microwave Symposium Digest, Fort Worth, TX, 2004, 1979–1982.
3. W.-H. Tu, Compact double-mode cross-coupled microstrip bandpass filter with tunable transmission zeros, IET Microwave Antennas Propag 2 (2008), 373–377.
4. X.-Ch. Zhang, Zh.-Y. Yu, and J. Xu, Design of microstrip dual-mode filters based on source-load coupling, IEEE Microwave Wireless Compon Lett 18 (2008), 677–679.
5. L. Li and Z.-F. Li, Application of inductive source-load coupling in microstrip dual-mode filter design, Electron Lett 46 (2010), 141–142.
6. L. Athukorala and D. Budimir, Design of open-loop dual-mode microstrip filters, Prog Electromagn Res Lett 19 (2010), 179–185.
7. X. Y. Zhang, J.-X. Chen, Q. Xue, and S.-M. Li, Dual-band bandpass filters using stub-loaded resonators, IEEE Microwave Wireless Compon Lett 17 (2007), 583–585.
8. J.-S. Hong and W. Tang, Dual-band filter based on non-degenerate dual-mode slow-wave open-loop resonators, In: IEEE MTT-S International Microwave Symposium Digest, Boston, MA, 2009, 861–864.
9. J.-S. Hong and M.J. Lancaster, Microstrip filters for RF/microwave applications, Wiley, New York, NY, 2001.
10. M. Makimoto and S. Yamashita, Bandpass filters using parallel coupled stripline stepped impedance resonators, IEEE Trans Microwave Theory Tech 28 (1980), 1413–1417.

UPLINK TRANSMISSION IN THE W-BAND (75–110 GHz) FOR HYBRID OPTICAL FIBER-WIRELESS ACCESS NETWORKS

Xiaodan Pang,[1] Lei Deng,[1,2] Anton Dogadaev,[1] Xu Zhang,[1] Xianbin Yu,[1] and Idelfonso Tafur Monroy[1]
[1] Department of Photonics Engineering, Technical University of Denmark, Kgs. Lyngby, Denmark; Corresponding author: xipa@fotonik.dtu.dk
[2] School of Optoelectronics Science and Engineering, Huazhong University of Science and Technology, Wuhan, China

ABSTRACT: *We report on an experimental, W-band, uplink for hybrid fiber-wireless systems which enables high speed communication from the wireless end users to the central server. Overall system performances for an OFDM signal format are discussed in detail.* © 2013 Wiley Periodicals, Inc. Microwave Opt Technol Lett 55:1033–1036, 2013; View this article online at wileyonlinelibrary.com. DOI 10.1002/mop.27476

1. INTRODUCTION

Driven by the increasing demand for bandwidth intensive applications such as interactive 3D video, as well as the emergence of the multifunctional portable devices as smart phones and tablet computers [1], the Federal Communications Commission (FCC) has opened the commercial use of spectra in the 71–75.5 GHz, 81–86 GHz, 92–100 GHz, and 102–109.5 GHz bands [2], which are recommended for multigigabit capacity wireless communications. On the other hand, radio-over-fiber (RoF) technology provides an elegant solution to deliver ubiquitous wireless services through the centralized servers with low-cost and bandwidth-abundant fiber-optic connectivity. In this context, the W-band (75–110 GHz) hybrid fiber-wireless systems are under intensive research [3–5]. To maximize the spectral efficiency, a W-band OFDM data downlink transmission with multiple frequency bands is recently reported [6, 7].

Meanwhile, to keep up with the increasing large-volume instant video uploads, gigabit/s wireless capacity in the uplink direction, from the wireless end users to the central server, can be expected soon on demand [1]. In order to simultaneously support multiple users with gigabit/s capacity per user, combining OFDM signal with frequency division multiple access (FDMA) scheme in the W-band hybrid fiber-wireless networks can be potentially a feasible solution. Figure 1 displays a typical indoor wireless access environment, where multiple end user

Figure 1 A typical indoor scenario with multiple wireless uplink applications using FDMA scheme. [Color figure can be viewed in the online issue, which is available at wileyonlinelibrary.com]

devices share the offered bandwidth. Depending on different scenarios, the user number and bandwidth per user can be flexibly allocated.

In this article, we present an experimental study of the proposed W-band hybrid fiber-wireless system in the uplink direction. A W-band OFDM signal undergoes air transmission, antenna detection followed by electrical down-conversion to an intermediate frequency (IF), re-modulation onto an optical carrier, fiber transmission and is recovered at the receiver end by offline digital signal processing (DSP). Electrical down-conversion before optical re-modulation has the following advantages: (1) Ultra-broadband optical modulator working up to W-band is no longer needed; (2) The period of the periodical RF power fading along transmission induced by the fiber dispersion is effectively prolonged due to a lower carrier frequency used for fiber transport [8]; (3) The down-converted IF signal can fit within the 50 GHz WDM grid, enabling a potential integration with future WDM-PON networks. A proof-of-concept demonstration of a single channel 1.48 Gbit/s 16QAM-OFDM signal (occupying 840 MHz bandwidth) transmission over up to 2.3 m air distance plus 22.8 km SSMF is presented.
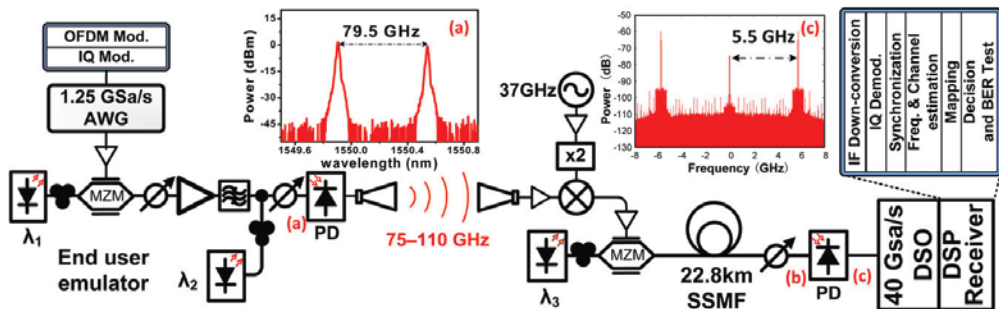
2. EXPERIMENTAL SETUP

The schematic diagram of the experimental setup is shown in Figure 2. A electrical OFDM signal is generated by offline DSP and converted to an analog signal by a 1.25 GS/s arbitrary waveform generator (AWG). In the offline DSP, a data stream consisting of a pseudo-random bit sequence (PRBS) of length

2^{15}-1 is mapped onto 129 subcarriers, of which 64 subcarriers carry real QPSK/16QAM data and one is unfilled DC subcarrier. The remaining 64 subcarriers are the complex conjugate of the aforementioned 64 subcarriers to enforce Hermitian symmetry in the input facet of 192-point IFFT. The cyclic prefix is 1/10 of the IFFT length resulting in an OFDM symbol size of 211. For frame synchronization and channel estimation, three training symbols are inserted at the beginning of each OFDM frame that contains 130 data symbols, resulting in a net data rate of 740.8 Mbit/s for QPSK and 1.48 Gbit/s (1.25 GS/s × 4 × 64/211 × 127/130) for 16QAM with a total bandwidth of 840 MHz (1.25 GS/s × 129/192). The generated OFDM signal is used to modulate a 100 kHz-linewidth external cavity laser (ECL, λ_1 = 1550.548 nm) at a Mach–Zehnder Modulator (MZM). After amplification and filtering, the optical OFDM signal is combined with a second 100 kHz-linewidth ECL (λ_2 = 1549.896 nm) for heterodyne up-conversion (see inset at point (a) in Fig. 2) at a fast response photodetector (PD). The generated OFDM signal centered at 81.5 GHz is launched to the air by a 25 dBi gain W-band horn antenna, emulating the wireless signal of the end user.

After the wireless transmission, the signal is picked up by a second 25 dBi gain horn antenna and amplified by an electrical low noise amplifier (LNA) with 4.5 dB noise factor before fed into a broadband mixer, where the signal is mixed with a 74 GHz local oscillator (LO), resulting in an IF signal centered at 7.5 GHz. An ECL (λ_3 = 1550.0 nm) is intensity modulated by the IF signal at a second MZM and launched into a 22.8 km SSMF. A 10 G PD is employed to recover the IF signal (inset at point(c) in Fig. 2), which is sampled by a 40 GS/s digital sampling oscilloscope (DSO) with 13 GHz real time bandwidth and demodulated by offline DSP. The DSP receiver consists of frequency down-conversion, low-pass filtering, synchronization, channel estimation, data recovery by symbol mapping and serialization, and a BER counter. In particular, a one-tap equalizer, an intra-symbol frequency-domain averaging algorithm and a digital phase-locked loop (DPLL) are used for channel estimation to eliminate dispersion and nonlinearity effects induced during the wireless and fiber transmission. BER is evaluated by counting the number of errors considering 65,536 bits.

3. EXPERIMENTAL RESULTS

The quality of the W-band signal generated by the end user emulator is firstly evaluated and used as a basic reference. In this measurement, the down-converted electrical IF signal is

Figure 2 Experimental setup of the W-band uplink hybrid fiber-wireless system. Insets: Optical spectra at point (a) and electrical spectra at point (c). [Color figure can be viewed in the online issue, which is available at wileyonlinelibrary.com]
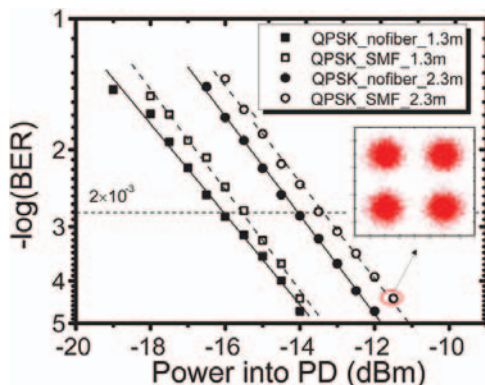
Figure 3 BER performance at different EIRPs for QPSK-OFDM and 16QAM-OFDM after 1.3 m and 2.3 m wireless transmission

directly sampled and demodulated without re-modulation onto an optical carrier. The BER performance at different equivalent isotropic radiated powers (EIRPs) for the QPSK/16QAM-OFDM signals after 1.3 m and 2.3 m wireless transmission is shown in Figure 3. For both QPSK-OFDM and 16QAM-OFDM signal, the BER performance well below the 2×10^{-3} forward error correction (FEC) limit can be achieved. No error is detected at EIRP of 7 dBm and 11 dBm for the QPSK and 16QAM at 2.3 m wireless distance, respectively.

After the primary evaluation, the system transmission performance is tested with a fixed value of EIRP set at 11 dBm for both the QPSK and 16QAM signals. Figure 4 displays the BER as a function of the received optical power (RoP) at the PD (point (b) in Fig. 2) for the 740.8 Mbit/s QPSK-OFDM signal before and after the 22.8 km SSMF transmission. For all cases, the measured BER is well below the FEC limit and no error is detected for 65,536 bits when the RoP is more than −11 dBm.

In Figure 4, it shows that optical fiber transmission over the 22.8 km link induces 0.5 dB receiver sensitivity penalty at the FEC limit, which indicates that no severe RF power fading is taking place. The constellation diagram of the received signal after 2.3 m wireless plus 22.8 km SSMF transmission is shown in the inset of Figure 4, which is clearly separated and no distortion is observed.

The measured BER performance versus the RoP at the PD for the 1.48 Gbit/s 16QAM-OFDM signal transmission is shown in Figure 5. Similarly, it can be seen from Figure 5 that BER values are achieved below the FEC limit for both the 1.3 m and 2.3 m wireless plus the 22.8 km fiber transmissions. However, in the case of 2.3 m wireless transmission, there appears a slight error floor above −8 dBm. This phenomenon can be attributed to the limited SNR of the down-converted IF signal after re-modulating onto the lightwave with the transmitted 11 dBm EIRP, as shown in Figure 3. Moreover, respectively 1 dB and 2 dB power penalty at the FEC limit is induced by the 22.8 km SSMF for 1.3 m and 2.3 m wireless cases. This is mainly due to the fact that the accuracy of the channel estimation algorithm in the DSP receiver, particularly the intra-symbol frequency-domain averaging algorithm and the DPLL, degrades with decrease of signal SNR. A slight signal distortion can be noticed from the received signal constellation shown in the inset of Figure 5.

4. CONCLUSION

We experimentally demonstrated a W-band hybrid fiber-wireless uplink access system that has the potential to provide high-speed connectivity from the wireless end user to the central server. The proposed system is enabled by an electrical down-conversion stage that eliminates the requirement for ultra-broadband optical modulators, and also largely reduces the effect of the dispersion-induced periodical RF fading. A proof-of-concept demonstration of a single channel 1.48 Gbit/s 16QAM-OFDM transmission within a bandwidth of 840 MHz is performed and its system performance is evaluated. Considering the newly allocated 20.5 GHz bandwidth in the 75–110 GHz band by the FCC, up to 24 users with 1.48 Gbit/s/user can be simultaneously supported by a FDMA scheme. As the down-converted IF signal
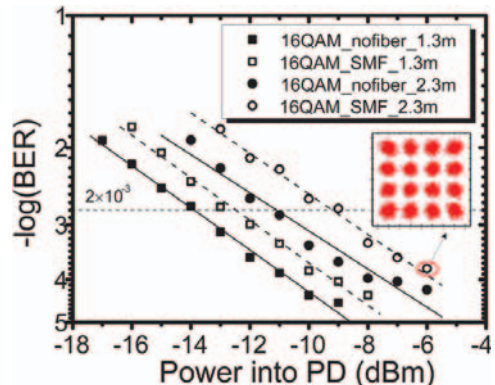

Figure 4 BER performance of the QPSK-OFDM signal as a function of the RoP at the PD (point (b) in Fig. 2) w/wo 22.8 km SSMF at 11 dBm EIRP. Inset: received signal constellation after 2.3 m wireless and 22.8 km SSMF transmission. [Color figure can be viewed in the online issue, which is available at wileyonlinelibrary.com]

Figure 5 BER of the 16QAM-OFDM signal versus the RoP at the PD (point (b) in Fig. 2) w/wo 22.8 km SSMF at 11 dBm EIRP. Inset: received constellation after 2.3 m wireless and 22.8 km SSMF transmission. [Color figure can be viewed in the online issue, which is available at wileyonlinelibrary.com]

can be fit within the 50 GHz WDM grid, the system has the potential to be integrated with the future WDM-PON networks.

REFERENCES

1. Cisco VNI Global Mobile Data Traffic Forecast 2010–2016, [Online], Available at: http://www.cisco.com/en/US/solutions/collateral/ns341/ns525/ns537/ns705/ns827/white_paper_c11-520862.pdf
2. FCC online table of frequency allocations, [Online], Available: http://transition.fcc.gov/oet/spectrum/table/fcctable.pdf
3. A. Kanno, K. Inagaki, I. Morohashi, T. Sakamoto, T. Kuri, I. Hosako, T. Kawanishi, Y. Yoshida, and K.-I. Kitayama, 40 Gb/s W-band (75–110 GHz) 16-QAM radio-over-fiber signal generation and its wireless transmission, Opt Express 19 (2011), B56–B63.
4. X. Pang, A. Caballero, A. Dogadaev, V. Arlunno, L. Deng, R. Borkowski, J. Pedersen, D. Zibar, X. Yu, and I.T. Monroy, 25 Gbit/s QPSK hybrid fiber-wireless transmission in the W-band (75–110 GHz) with remote antenna unit for in-building wireless networks, IEEE Photonics J 4 (2012), 691–698.
5. X. Pang, A. Caballero, A. Dogadaev, V. Arlunno, R. Borkowski, J. Pedersen, L. Deng, F. Karinou, F. Roubeau, D. Zibar, X. Yu, and I.T. Monroy, 100 Gbit/s hybrid optical fiber-wireless link in the W-band (75–110 GHz), Opt Express 19 (2011), 24944–24949.
6. L. Deng, M. Beltrán, X. Pang, X. Zhang, V. Arlunno, Y. Zhao, A. Caballero, A. Dogadaev, X. Yu, R. Llorente, D. Liu, and I.T. Monroy, Fiber wireless transmission of 8.3-Gb/s/ch QPSK-OFDM signals in 75–110 GHz band, IEEE Photonics Technol Lett 24 (2012), 383–385.
7. L. Deng, D. Liu, X. Pang, X. Zhang, V. Arlunno, Y. Zhao, A. Caballero, A.K. Dogadaev, X. Yu, I.T. Monroy, M. Beltrán, and R. Llorente, 42.13 Gbit/s 16qam-OFDM photonics-wireless transmission in 75-110 GHz band, Prog Electromagn Res 126 (2012), 449–461.
8. H.-C. Chien, Y.-T. Hsueh, A. Chowdhury, J. Yu, and G.-K. Chang, Optical millimeter-wave generation and transmission without carrier suppression for single and multiband wireless over fiber applications, J Lightwave Technol 28 (2010), 2230–2237.

BROADBAND SCHIFFMAN PHASE SHIFTER USING COUPLED SUSPENDED LINES WITH TUNING SEPTUMS

Seungyeoup Rhee
Department of Electronic Communication, Chonnam National University, Yeosu, South Korea; Corresponding author: ysrsy@chonnam.ac.kr

ABSTRACT: *A novel design of 90° Schiffman phase shifter using coupled suspended lines with tuning septums is presented for broadband operations. In this design, the 90° Schiffman phase shifter is realized with a high impedance ratio, which cannot be implemented using conventional coupled lines. © 2013 Wiley Periodicals, Inc. Microwave Opt Technol Lett 55:1036–1038, 2013; View this article online at wileyonlinelibrary.com. DOI 10.1002/mop.27494*

1. INTRODUCTION

The original Schiffman phase shifter is the most attractive of all phase shifters [1–4]. It has a very simple structure that consists of a transmission lines and a coupled section. The main disadvantage of the conventional Schiffman phase shifter is its narrow band property due to a low impedance ratio (the ratio of even mode impedance to odd mode impedance in the coupled section) in the general coupled lines. To achieve a larger bandwidth, it is necessary to use tightly coupled lines with a high impedance ratio.

Various techniques to overcome this disadvantage have been reported. Recently, the bandwidth has been improved by using dentate microstrip [1] and a slot in the cavity under the coupled line [1]. However, these structures are so complex and have many design parameters, which makes fabrication difficult.

In this letter, a novel design of 90° Schiffman phase shifter using coupled suspended lines with tuning septums is presented for broadband operations. The proposed broadband 90° Schiffman phase shifter is realized with high impedance ratio, which cannot be implemented using the pure coupled lines.

2. DESIGN

Figure 1 shows the structure of the proposed standard 90° Schiffman phase shifter using coupled suspended lines with tuning septums beneath the coupled lines. The maximum of differential phase shift, in terms of impedance ratio, is derived in [2] as

$$\Delta\phi_{\max} = K\tan^{-1}\sqrt{\frac{K\rho - 2\sqrt{\rho}}{2\sqrt{\rho} - K}} - \cos^{-1}\left(\frac{\rho + 1 - K\sqrt{\rho}}{\rho - 1}\right) \quad (1)$$

where K denotes the ratio of the length of the uniform transmission line to the coupled one. Figure 2 shows one design curve based on impedance ratio and space gap between coupled lines with respect to $\Delta\phi_{\max}$.

By referring to the design curve of the 90° Schiffman phase shifter, an impedance ratio is chosen to ensure an optimal bandwidth and it is checked whether this ratio is possible with coupled lines. If the limit of the spacing gap (S) with conventional PCB process is 0.2 mm, then $\Delta\phi_{\max} \geq 5.0°$ cannot be achieved with conventional coupled lines, according to the results of Figure 2.

However, using coupled suspended lines with tuning septums, a Schiffman phase shifter with $\Delta\phi_{\max} \geq 5.0°$ is possible because S is greater than 0.2 mm, the limit of the spacing gap as mentioned above. In this letter, the ratio 3.0 is chosen because it cannot be implemented with conventional coupled lines and its ratio is the optimal value obtained from Eq. (1) for designing a 90° Schiffman phase shifter with ±5.0° phase deviation.

Accordingly, the even and odd mode impedances of the coupled lines are determined as $Z_{\text{oe}} = 50\sqrt{\rho} = 86.6$ Ω and $Z_{\text{oo}} = 50/\sqrt{\rho} = 28.9$ Ω. To achieve such even and odd mode impedances at 2.4 GHz, the width of the coupled lines and the space gap between the coupled lines were determined as 1.05 and 0.13 mm on a FR4 substrate with a relative dielectric constant of 4.4 and a thickness of 1 mm. In fact, the coupled microstrip line with 0.13 mm gap is difficult to fabricate because of manufacturing limitations. If the septums ($t = 3.0$ mm) is placed in the ground beneath coupled lines, the above even and odd impedance can be implemented using the coupled line with a 1.4 mm width and 0.2 mm gap. The transmission line widths of the input and output ports are the same, i.e., both 1.7 mm for 50-Ω impedance matching. The performance of the proposed phase shifter is predicted through the parametric studies carried out by Zeland IE3D software.

Paper 8: DWDM Fiber-Wireless Access System with Centralized Optical Frequency Comb-based RF Carrier Generation

Xiaodan Pang, Marta Beltrán, José Sánchez, Eloy Pellicer, J.J. Vegas Olmos, Roberto Llorente, Idelfonso Tafur Monroy, "DWDM Fiber-Wireless Access System with Centralized Optical Frequency Comb-based RF Carrier Generation," *The Optical Fiber Communication Conference and Exposition and the National Fiber Optic Engineers Conference, OFC/NFOEC'13*, Anaheim, CA, USA, 2013, paper JTh2A.56.

DWDM Fiber-Wireless Access System with Centralized Optical Frequency Comb-based RF Carrier Generation

Xiaodan Pang[1], Marta Beltrán[2], José Sánchez[2], Eloy Pellicer[2], J.J. Vegas Olmos[1], Roberto Llorente[2], and Idelfonso Tafur Monroy[1]

1) DTU Fotonik, Technical University of Denmark, Oersteds Plads 358, 2800 Kgs. Lyngby, Denmark
xipa@fotonik.dtu.dk
2) Valencia Nanophotonics Technology Center, Universidad Politécnica de Valencia, 46022 Valencia, Spain

Abstract: We propose and experimentally demonstrate an optical wireless DWDM system at 60 GHz with optical incoherent heterodyne up-conversion using an optical frequency comb. Multiple users with wireline and wireless services are simultaneously supported.
OCIS codes: (060.2330) Fiber optics communications; (060.5625) Radio frequency photonics; (060.2840) Heterodyne

1. Introduction

Wireless communication is an area that has witnessed substantial technology advancement in the past two decades. End-users have benefited from such advances and a large fragment of our economy is growing around broadband communication services, such as social networking, cloud computing, e-health systems, video streaming, gaming and so on. Capacity improvements in both optical networks and wireless systems have been based on incremental refinements of existing technologies. However, it is becoming evident that this growth model may not provide the projected future capacity – conservative estimations project a 18-fold increase between 2011 and 2016 in global mobile data traffic. Furthermore, the average smartphone will generate 2.6 GB of traffic per month in 2016, a 17-fold increase over the 2011 average of 150 MB per month. Aggregate smartphone traffic in 2016 will be 50 times greater than it is today, with a compounded annual growth rate of 119 percent [1]. Current technologies will not support such traffic growth, since wireless bands are already saturated. Millimeter-wave at 60 GHz band is viewed as a promising candidate with its 7 GHz spectrum available for radio communication (57-64 GHz) [2, 3].

On the other hand, seamless convergence between fiber-optic and wireless networks in the "last mile" has a great potential for delivering data services to the end-users with more flexibility and mobility [4]. In optical access networks, wavelength division multiplexing (WDM) technique is considered as a promising candidate as it can increase the total throughput as well as ensure the scalability of the network by allocating wavelengths to each end user [5, 6]. However, when integrating the conventional radio-over-fiber (RoF) signals at 60 GHz and above with the dense WDM (DWDM) system with 50 GHz or 25 GHz channel spacing, the signal carriers will be filtered out by the arrayed waveguide gratings (AWG). Meanwhile, the fiber chromatic dispersion induced double-side band RoF signal power fading will further limit the flexibility of the system. In this paper, we propose an optical fiber-wireless DWDM access system using optical incoherent heterodyne up-conversion by employing an centralized optical frequency comb (OFC)-based local oscillator (LO). As the carrier signals are added after the AWG, no adaptation to the baseband DWDM signals is needed and the system flexibility is preserved. The proposed system has the potential to simultaneously support multiple users with both wireline and wireless broadband services.

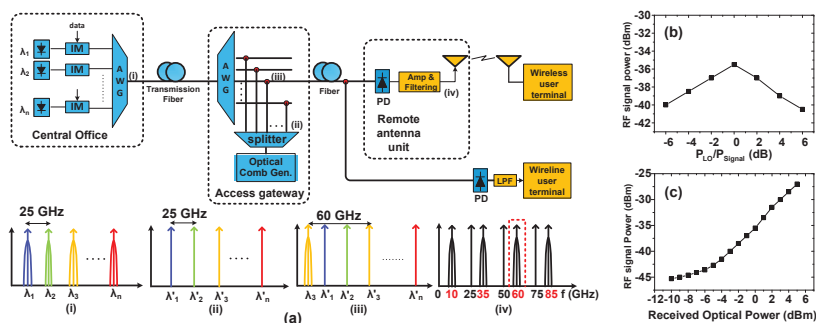## 2. Architecture of the optical wireless DWDM network

Figure 1. (a). Conceptual diagram of the proposed optical wireless DWDM system using optical frequency comb-based incoherent heterodyne up-conversion. (b). Measured 60 GHz RF power vs. ratio of LO power and signal power. (c). RF power vs. optical power when $P_{LO}/P_{signal} = 0$ dB

Figure 1 shows the conceptual diagram of the proposed optical fiber-wireless DWDM access system. In the central office, multiple CW lightwaves from λ_1 to λ_n separated by 25 GHz are used to carry the baseband data (Inset (i) in Fig. 1 (a)). An AWG aggregates the signals into a transmission fiber. A second AWG at the access gateway is used to separate the wavelengths that are assigned to specific users. An optical frequency comb from λ_1' to λ_n' with 25 GHz frequency separation is employed as a local oscillator (LO) and combined with each incoming signal. Since the shift between λ and λ' is 10 GHz, we observe a 60 GHz separation between the corresponding comb line and the signal, shown in Inset (ii) and (iii) in Fig. 1. The combined signals are then sent to the wireline/wireless end-users. For the wireline user, the baseband signal is directly detected by a low frequency PD followed by a low-pass filter (LPF). For wireless applications, the signal is sent to the remote antenna unit (RAU), where the heterodyne mixing is performed at a fast-response PD. As shown in Inset (iv) in Fig. 1, the baseband signal is simultaneously up-converted to different RF bands including X-band, K_a-band, V-band and W-band. Signal amplification and filtering are performed to select the on-demand RF band based on the user applications.

An initial characterization of the generated RF signal at 60 GHz is firstly carried out. We use two free-running CW lasers with < 100 kHz linewidth to perform the incoherent heterodyning mixing. Fig. 1 (b) shows the generated RF power as a function of the power ratio between the two lasers. The optimal power ratio between the two lasers is found at 0 dB, meaning that when the two lasers gives equal power, the RF signal is maximized. This result is consistent with our previous theoretical analysis [7]. The RF power with respect to the combined optical power is shown in Fig. 1 (c), where the lasers power ratio is optimized.
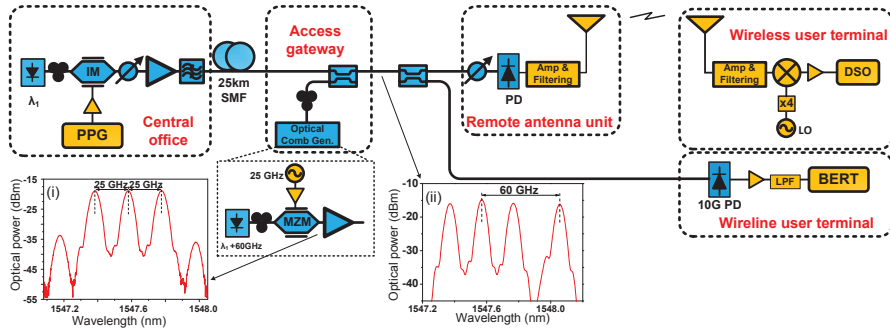
3. Experimental setup and results

Figure 2. Experimental setup. PPG: pulse-pattern generator; BERT: bit-error-ratio tester; DSO: digital storage oscilloscope; LPF: low-pass filter.

Figure 2 shows the experimental setup for a single optical channel. A CW lightwave emitted from a Distributed Feedback Laser (DFB, λ_1=1548.05 nm) with < 100 kHz linewidth is modulated via an intensity modulator (IM) driven by a 2.5 Gb/s pseudo-random binary sequence (PRBS) electrical signal of length 2^7-1 to generate an On/OFF keying (OOK) optical baseband signal. An erbium-doped fiber amplifier (EDFA) is employed for amplification, and an optical bandpass filter (OBPF) with 0.8 nm bandwidth is used to filter the out-of-band noise. After that, the signal is transmitted to the access gateway via a 25 km standard single mode fiber (SSMF) link. A second DFB laser (λ_2=1547.57 nm) with < 100 kHz linewidth is launched into an OFC generator employing an overdriven Mach-Zehnder modulator (MZM). The MZM is biased in its nonlinear region by equalizing the power of the central 3 comb lines that are separated by 25 GHz (Fig. 2. (i)). After amplification the OFC is combined with the baseband signal at a 3 dB coupler. The separation between the signal and the center comb line is 60 GHz, as shown in Fig. 2. (ii). The signal is then split into two paths, one going directly to the wireline user terminal where a low frequency PD performs O/E conversion of the baseband signal before sending it to the bit-error-ratio tester (BERT) for BER evaluation; the other transmitting to the RAU where the signals heterodyne mixing takes place at a 60 GHz PD. Following photodetection and amplification, a RF filter with 3 dB bandwidth ranging from 56.26 - 62 GHz is used to select the up-converted signal centered at 60 GHz. The filtered RF signal then feeds a standard V-band horn antenna of 20 dBi for up to 6 m wireless transmission. An identical horn antenna is used to pick up the signal at the receiver.

In order to detect the RF signal transparently to modulation formats, an electrical mixer is used to perform the down-conversion. A 14 GHz signal generator and a frequency multiplier by 4 are employed to generate the LO signal for down-conversion. The transmitted RF signal centered at 60 GHz is then converted to an intermediate frequency (IF) at 4 GHz. The analog to digital conversion (A/D) is realized in a digital storage scope with 40 GS/s
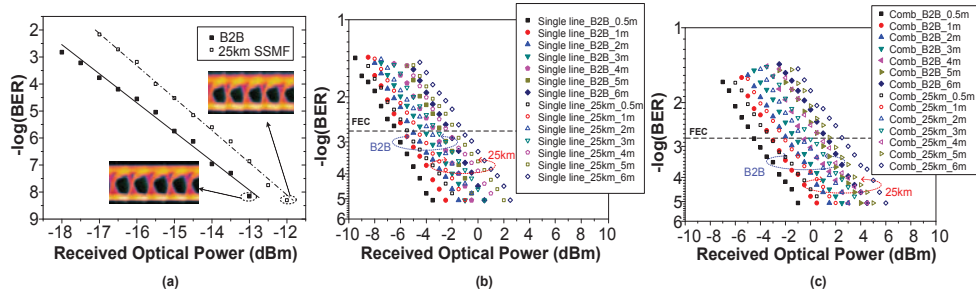
Figure 3. BER curves for (a) baseband signal; (b) the 60 GHz wireless signal in the case of single line LO; (c) the 60 GHz wireless signal in the case of optical frequency comb-based LO

and 13 GHz bandwidth. The signal demodulation is performed by offline digital signal processing (DSP). To overcome the frequency jitter that usually occurs with optical incoherent heterodyne mixing, a digital self-heterodyning is firstly performed to further down-convert the IF signal to baseband in the digital domain. The signal then passes a LPF followed by the decision and BER evaluation.

First, the performance of the baseband signal received by the wireline user terminal is evaluated. Figure 3 (a) shows the BER curve of the baseband signal before and after the 25 km SSMF link. Negligible shape distortion of the received eye diagram is seen after the fiber transmission. A power penalty of less than 1 dB is observed coming from the fiber dispersion. We then evaluate the wireless transmission performance. To begin with, we firstly assess the case that the LO is a single optical line instead of the OFC by switching off the 25 GHz generator. The BER curves of different wireless distances from 0.5 m till up to 6 m for both B2B and after 25 km SSMF are shown in Fig. 3 (b). We can see that for all cases the BER performance yield values below the FEC limit of 2×10^{-3} without an apparent BER floor. Compared with B2B, the penalty after 25 km SSMF transmission at the FEC limit is around 2 dB for all wireless distances. After this, we substitute the LO with the OFC generator, while keeping the peak power of each comb line the same level with the single line case. Figure 3 (c) shows the BER performance of the cases that OFC-based LO is employed for signal up-conversion. Similarly, for all cases with and without 25 km SSMF transmission plus up to 6 meters wireless transmission, BERs of well below the FEC limit are achieved. Compared with the single-line LO case, we observe around 3.5 dB difference in performance in terms of sensitivity at the FEC limit. This difference is from the power of the adjacent comb lines, which are filtered out before the wireless transmission. For the case of 25 km SSMF plus 6 meters wireless transmission, the requirement for the received optical power at the BER of 2×10^{-3} is 2.5 dBm.

4. Conclusion

We have proposed an optical fiber-wireless DWDM access system that simultaneously provides wireline and wireless broadband services with no adaptation to the baseband signals while preserving the system flexibility. The 60 GHz mm-wave is generated using the optical incoherent heterodyne up-conversion method with an optical frequency comb-based LO. A 60 GHz signal has been experimentally generated with a LO of 3 comb lines with 25 GHz separation mixing with a 2.5 Gbit/s OOK optical baseband signal. Signal transmission through a 25 km SSMF and up to 6 meters air distances is successfully received with a BER performance well below 2×10^{-3}. The optical power penalty for the 60 GHz mm-wave signal after SMF transmission is around 2 dB.

References

[1] "Cisco Visual Networking Index: Forecast and Methodology, 2011-2016," Cisco White Paper, May, 2012, [Available: Online]
[2] J. Yu et al., "A Novel Architecture to Provide Super-Broadband Optical Wireless Access Service," OFC/NFOEC 2012, paper JTh2A.70.
[3] W.J. Jiang et al., "40 Gb/s RoF Signal Transmission with 10 m Wireless Distance at 60 GHz," OFC/NFOEC 2012, paper OTu2H.1.
[4] D. Zibar et al., "Hybrid Optical Fibre-Wireless links at the 75–110 GHz Band Supporting 100 Gbps Transmission Capacities," MWP 2011, paper 3005.
[5] T. Tashiro et al., "40 km fiber transmission of time domain multiplexed MIMO RF signals for RoF-DAS over WDM-PON," OFC/NFOEC 2012, paper OTu2H.4.
[6] K. Prince et al., "Converged Wireline and Wireless Access Over a 78-km Deployed Fiber Long-Reach WDM PON," IEEE PTL, **21**, pp. 1274-1276, (2009).
[7] X. Pang et al., "25 Gbit/s QPSK Hybrid Fiber-Wireless Transmission in the W-Band (75–110 GHz) With Remote Antenna Unit for In-Building Wireless Networks," Photonics Journal, IEEE, **4**, pp. 691-698, (2012)

Paper 9: A Multi-gigabit W-Band Bidirectional Seamless Fiber-Wireless Transmission System with Simple Structured Access Point

A Multi-gigabit W-Band Bidirectional Seamless Fiber-Wireless Transmission System with Simple Structured Access Point

Xiaodan Pang, J.J. Vegas Olmos, Alexander Lebedev, Idelfonso Tafur Monroy

Department of Photonics Engineering, Technical University of Denmark, Kgs. Lyngby, 2800, Denmark,
xipa@fotonik.dtu.dk

Abstract *We propose a simple wireless access point for hybrid access networks and experimentally demonstrate bidirectional operation in W-Band. Photonic up-conversion and electrical down-conversion are used in the downlink, while in the uplink both up- and down-conversion are conducted by electrical means.*
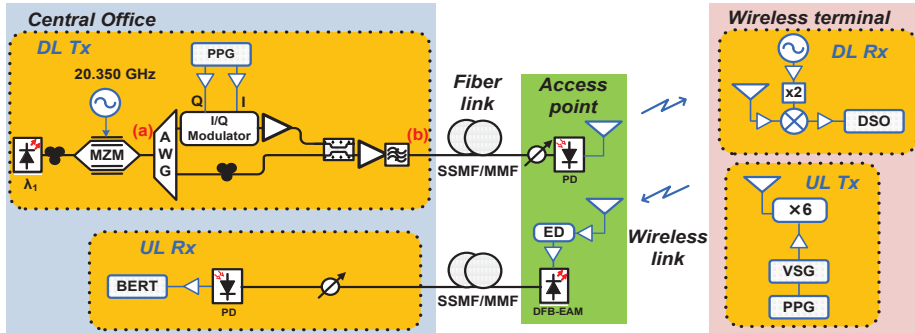
Introduction

Hybrid fiber-wireless transmission systems can serve as the key building block to support many services and applications that can bring conveniences to our daily life. Services like e-health monitoring, distance e-education and holographic video conferencing all rely on machine to machine communication, employing wired or wireless physical media. With the recent maturity and popularity of portable devices like tables and smartphones, services in wireless are normally preferred by end-users. Due to the high bandwidth demand for these applications, conventional wireless bands won't be able to support enough capacity in the near future. Therefore, using wireless carriers at higher frequency bands with broader transmission bandwidth, e.g. millimeter-wave (mm-wave) region is becoming necessary [1].

Recently, experimental demonstrations on high-speed downlink (DL) fiber-wireless transmission in the V-band (50-75 GHz), W-band (75-110 GHz) and higher frequency bands have been reported [2-8]. From a practical architectural point of view, considerations on bidirectional mm-wave over fiber transmissions have also been stressed in the Ka-band (26.5-40 GHz), V-band and E-band (60-90 GHz) [9-14]. In this paper, we go beyond the state-of-the-art by evaluating a bidirectional fiber-wireless link in the W-band for multi-gigabit access purposes, with focus on simplicity, as well as our study is complementary to ongoing research efforts. Furthermore, with the decreased coverage of mm-wave signals, a larger number of wireless access points can be expected in the future indoor access network scenarios. Thus simplicity of the access point structure should also be considered as a key factor in designing the next generation fiber-wireless access networks.

In this paper, we report on an experimental demonstration of a simple structured, high-capacity bidirectional fiber-wireless system in the W-band that can provide multi-gigabit services for access networks. In the DL, a 16 Gbit/s quadrature phase shift keying (QPSK) signal can be recovered after transmitting over the fiber-wireless link, while a 1.25 Gbit/s amplitude shifted keying (ASK) signal in the uplink (UL) direction are simultaneously supported. A fiber link consisting of mixed single / multi-mode fiber (SMF/MMF) is assessed, representing the fiber-wireless

Fig. 1: Experimental setup. MZM: Mach-Zehnder modulator. AWG: arrayed waveguide grating. PPG: pulse pattern generator. DSO: digital storage scope. VSG: vector signal generator. ED: envelope detector. DFB-EAM: distributed feedback laser – electroabsorption modulator. BERT: bit-error-rate tester.
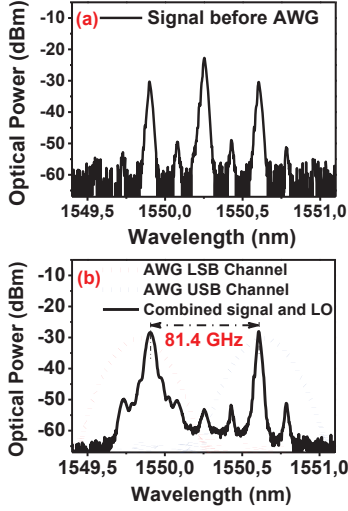
Fig. 2: Optical spectra of DL measured after photonic generation (a) and before fiber transmission (b).

Fig. 3: (a) DL BER vs. received optical power. (b) Corresponding received signal constellations.

services delivery in the indoor access network scenarios.

Experimental setup

Figure 1 presents the experimental setup of the proposed bidirectional fiber-wireless system. In the downlink transmitter (DL Tx), a continuous-wave (CW) lightwave at 1550.2 nm from an external cavity laser (ECL) is fed into a Mach-Zehnder modulator (MZM). The MZM driven by a 20.35 GHz modulation signal can generate the fourth order harmonics at the modulator output [15]. An arrayed waveguide grating (AWG) with 50 GHz channel grids is used to block the optical central carrier while separating the upper / lower sideband (USB / LSB). The LSB is launched into an integrated LiNbO3 dual parallel MZM driven by a two-channel 8 Gbaud pseudo-random binary sequences (PRBS) with a word length of 2^{15}-1, resulting in an overall 16 Gbit/s QPSK signal at the output. The USB separating from the LSB with 81.4 GHz is polarization aligned and combined with the LSB branch at a 3 dB coupler, acting as a carrier generating signal later for the optical heterodyne up-conversion. The optical spectra before the AWG and after signal combining are shown in Fig. 2 (a) and (b), respectively. After a mixed SMF/MMF transmission, the signal is up-converted at a 100 GHz photodetector (PD) and radiated to the air by a 25 dBi horn antenna. At the receiver side, the received signal is firstly amplified by a 40 dB gain low noise amplifier (LNA), before being electrically down-converted

and sampled by a 40 GSa/s digital storage oscilloscope (DSO) for offline signal processing and demodulation.

In the UL direction, a 1.25 Gbit/s electrical signal from the PPG is firstly up-converted to 14.6 GHz by a vector signal generator (VSG) before feeding to an electrical frequency sextupler, which generates an 87.6 GHz ASK signal. The signal is then radiated by a 24 dBi horn antenna. At the access point, the signal is picked up by an identical antenna and then fed to a zero-biased Schottky diode performing a function of an envelope detector (ED) for down-conversion from W-band to baseband. The baseband signal is then directly modulated onto lightwave by a distributed feedback laser - electroabsorption modulators (DFB-EAM). After transmission through the same fiber link, the signal is recovered by a 10 G PD and the transmission is evaluated in real time by a bit-error-rate tester (BERT).

Experimental results

In this work, optical transmissions over 26 km SMF and 100 m MMF in both directions are evaluated. In the DL, the received QPSK signal after fiber plus up to 1 m wireless transmission can be demodulated within the 7% FEC limit of 2×10^{-3}. Figure 3(a) shows the measured BER as a function of received optical power at the PD, for transmission cases of different combination

(a)

(b)

Fig. 4: (a) UL BER vs. received optical power.
(b) Corresponding received signal eye diagrams

of fiber types and lengths. The receiver sensitivity at the FEC limit is -5 dBm and -2.5 dBm for 0.5 m and 1 m wireless transmission without fiber links, respectively. Optical transmission over the 26 km SMF and 100m MMF induce ~0.5 dB receiver sensitivity penalty for both wireless cases. Further extension of wireless transmission distance is limited by the radiated signal power at the transmitter. Therefore, it can be expected to further increase the wireless distance by using active access point with mm-wave signal power amplifiers. Examples of recovered constellations for 0.5 m and 1 m wireless are shown in Fig. 3(b). Certain distortion can be observed for the 0.5 m wireless constellation, which is attributed to certain degree of saturation of the W-band LNA at the wireless receiver. On contrast, for 1 m wireless transmission, the distortion is no longer observed, however a slight decrease in the receiver's signal to noise ratio (SNR) can be seen. In spite of the trade-off between SNR and signal distortion, the clusters in the constellations for both cases are clearly separated.

The BER performance for the UL direction is presented in Fig. 4(a). Error free (BER<10^{-9}) transmission can be achieved in all tested cases.

The receiver sensitivity is -16 dBm and -15.5 dBm for optical back-to-back (OB2B) plus 0.5 m and 1 m wireless transmission. The sensitivity penalty induced by fiber transmission is less than 1 dB. Corresponding eye diagrams before and after fiber transmission at -14 dBm received optical power for both wireless distances are shown in Fig. 4(b). Despite the distortion in the eye shapes after fiber transmission, the eye openings are still clear to recover the transmitted data at the receiver.

Conclusions

We have proposed and experimentally demonstrated in this paper a bidirectional fiber-wireless system in the W-band. Signal transmission over a fiber-wireless link consisting of 26 km SMF, 100 m MMF and up to 1 m wireless is evaluated in both directions. In the DL, 16 Gbit/s QPSK signal is transmitted and recovered with BER well below FEC limit of 2×10^{-3}. For the UL, error free (BER<10^{-9}) transmission of 1.25 Gbit/s ASK signal is achieved. The proposed system with a simple structured access point has a high transparency and scalability to system data rates, which could be considered as a candidate in future seamless fiber-wireless access networks.

Acknowledgements

References

[1] T. Nagatsuma et al., Proc. 23rd Annu. Meeting IEEE Photon. Soc., We4 (2010).
[2] M. Weiss et al., Proc. MWP'09, PDP (2009).
[3] W. Jiang et al., Proc. OFC'12, OTu2H.1 (2012).
[4] A. Kanno et al., Opt. Exp. **19**, B56 (2011).
[5] X. Pang et al., IEEE Photon. J. **4**, 691 (2011).
[6] X. Pang et al., Opt. Exp. **19**, 24994 (2011).
[7] J. Zhang et al., IEEE Photon. Technol. Lett. **25**, 780 (2013).
[8] S. Koenig et al., Proc. OFC'13, PDP5B.4 (2013).
[9] Y. Yang et al., Proc. ECOC'12, P3.12 (2002).
[10] A. H. M. R. Islam et al., IEEE Photon. J. **4** 1956 (2012).
[11] T. Sono et al., Proc. MWP'06, W 15 (2006).
[12] S. Zou et al., Proc. ECOC'12, P6.16 (2012).
[13] C. Ye et al., Proc. OFC'13, OM3D.7 (2013).
[14] X. Li et al., IEEE Photon. J. **5,** 7900107 (2013).
[15] H. Kikuchi et al., IEEE Trans. Microw. Theory Techn., **55**, 1964 (2007).

Paper 10: A 15-meter Multi-Gigabit W-band Bidirectional Wireless Bridge in Fiber-Optic Access Networks

Xiaodan Pang, J.J. Vegas Olmos, Alexander Lebedev, Idelfonso Tafur Monroy, "A 15-meter Multi-Gigabit W-band Bidirectional Wireless Bridge in Fiber-Optic Access Networks," *IEEE International Topical Meeting on Microwave Photonics, MWP'13*, accepted for presentation.

A 15-meter Multi-Gigabit W-band Bidirectional Wireless Bridge in Fiber-Optic Access Networks

Xiaodan Pang, J.J. Vegas Olmos*, Alexander Lebedev, Idelfonso Tafur Monroy

DTU Fotonik, Department of Photonics Engineering
Technical University of Denmark
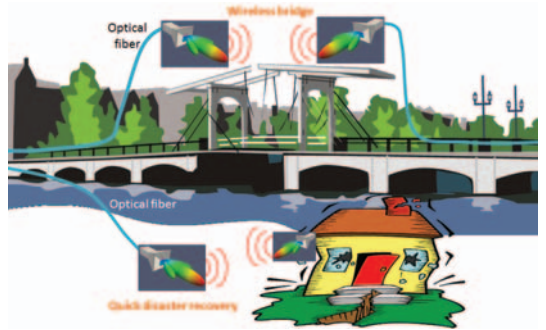Kgs. Lyngby, 2800, Denmark
*jjvo@fotonik.dtu.dk

Abstract—**We present a bidirectional wireless bridge in the W-band enabling the seamless convergence between the wireless and fiber-optic access networks. In the downlink, a 16 Gbit/s QPSK signal is photonically up-converted at the wireless transmitter and electrically down-converted at the wireless receiver. The down-converted signal is re-modulated on to the lightwave and transmit further through the fiber-optic system. In the uplink, both up-and down-conversion are performed by electrical means. Furthermore, we investigate both passive and active wireless transmitters in this work for both downlink and uplink transmissions. With an active wireless transmitter, up to 15 meters wireless transmission is successfully achieved with a BER below the 7% FEC limit in the downlink.**

Keywords— radio-over-fiber; w-band communications; optical access network

I. INTRODUCTION

Hybrid photonic-wireless systems are envisaged to seamlessly provide high-capacity connections over multiple scenarios, such as bridges, indoor distribution and distribution antenna systems, among others. Radio-over-fiber (RoF) techniques are supporting to bridge the gap between the large capacity of optical fibers and the flexibility of wireless transmission [1, 2]. Currently, two main trends are impacting the RoF field: migration towards higher frequency bands and increase of the channel capacity. Frequency bands below 10 GHz are already overcrowded, and therefore, open systems are looking for more spacious transmission bands such as 60 GHz [3-5], 75-110 GHz [6-9] and even sub-THz [10]. The W-band (75-110 GHz) is attractive because of its wide frequency bands, and seems to be an accepted good choice for transmission capacities in the order of multi-gigabits. The increase of the channel capacity is simultaneously impacting the field in the form of utilization of advanced modulation formats instead of the dominating approaches as on-off keying of the optical segment.

However, a main limitation of RoF systems is the poor conversion efficiency of the opto-electro-opto processes; namely, the efficiency of photodiodes and modulators. This efficiency shortcoming, in practical terms, introduces a limitation in the wireless range achieved by most experimental demonstrations of RoF systems, sometimes in the order of few centimeters or meters. This limitation may not affect scenarios such as short distance communications in data centers or

Fig. 1: Network scenarios based on hybrid photonic-wireless links, such as wireless bridges and quick disaster recovery systems.

indoor distributed antenna systems. However, scenarios such as disaster recovery, ad hoc last mile systems, or corporate communications as shown in Fig. 1, require transmission distances in the order of tens of meters.

In this paper, we show an active transmitter enabling wireless transmission up to 15 meters. The overall system consists of a bidirectional hybrid photonic-wireless link, comprising a fiber link, a wireless bridge, and a final fiber link. The paper is organized as follows: in Section II, we show the experimental setup of the proposed bidirectional wireless-fiber bridge. The experimental results for both passive and active wireless transmission are presented and discussed in Section III. Finally, conclusions are given in Section IV.

II. EXPERIMENTAL SETUP

Figure 2 presents the experimental setup of the proposed bidirectional wireless bridge for fiber-optic access systems. At the downlink (DL) transmitter, an continuous-wave (CW) lightwave at 1550.2 nm from an external cavity laser (ECL 1) is fed into a Mach-Zehnder modulator (MZM). By driving the MZM with a 20.35 GHz modulation signal and adjusting the applied bias voltage to the modulator, the second order harmonics of the driving signal can be generated at the modulator output [11]. After the MZM placed an arrayed waveguide grating (AWG) with 50 GHz channel grids, which is used to block the optical central carrier while separating the
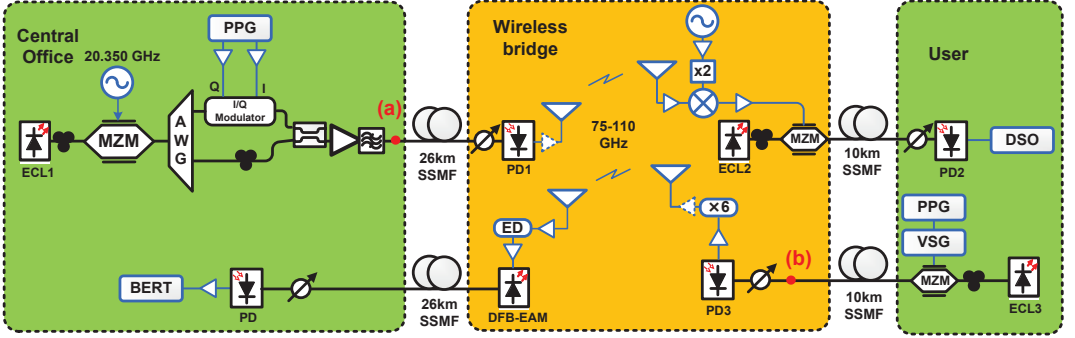
Fig. 2: Experimental setup. ECL: external cavity laser. MZM: Mach-Zehnder modulator. AWG: arrayed waveguide grating. PPG: pulse pattern generator. PD: photodetector. DSO: digital storage scope. VSG: vector signal generator. ED: envelope detector. DFB-EAM: distributed feedback laser - electroabsorption modulator. BERT: bit-error-rate tester.
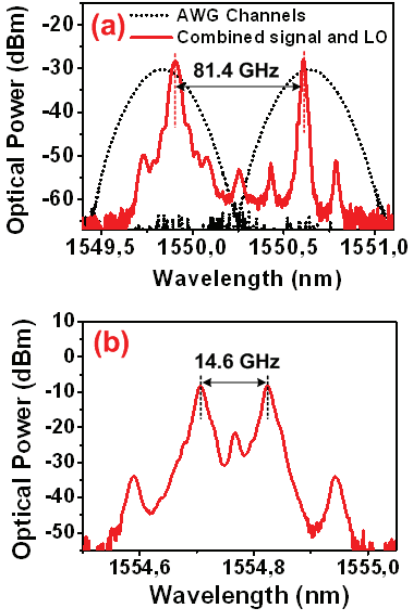

Fig. 3: Optical spectra measured at downlink point (a) and uplink point (b) in Fig. 2.

upper / lower sidebands (USB / LSB). The frequency separation between the USB and LSB is 81.4 GHz. The LSB is launched into a integrated LiNbO3 dual-parallel MZM driven by a two-channel 8 Gbaud pseudo-random binary sequences (PRBS) with a word length of 2^{15}-1, resulting in an overall 16 Gbit/s QPSK signal at the output. On the other hand, the USB is polarization aligned and combined with the LSB at a 3 dB coupler, acting as a carrier generating local oscillator (LO)

later for the optical heterodyne up-conversion. The optical spectra of the AWG channels and the combined signal is shown in Fig. 3 (a). At the output of the DL transmitter, the combined signal and LO forming a single side-band (SSB) RoF signal is launched into a 26 km standard single mode fiber (SSMF). After transmission, the signal is up-converted to a W-band RF signal at a 100 GHz photodetector. (PD 1). In this experiment, we test wireless transmissions both with and without a W-band power amplifier (PA) before radiating the signal to the air, representing the active and the passive wireless transmitter cases. A wireless bridge is established between a pair of 25 dBi horn antennas. At the receiver, the received signal is firstly amplified by a 40 dB gain low noise amplifier (LNA), before being electrically down-converted to a intermediate frequency (IF) centered at 6.4 GHz at a W-band balanced mixer. The IF signal is then re-modulated onto lightwave at a second MZM and transmitted a final 10 km SSMF. At the receiver, the IF-over-fiber signal is converted back to electrical domain at a second PD and sampled by a 40 GSa/s digital storage oscilloscope (DSO) for offline signal processing and demodulation.

In the uplink (UL) direction, a 1.25 Gbit/s electrical signal from a pulse pattern generator (PPG) is firstly up-converted to a IF at 7.3 GHz by a vector signal generator (VSG). Then the IF signal is modulated at the minimum transmission point of a MZM, forming a carrier suppressed-double sideband (CS-DSB) IF-over-fiber signal, the optical spectrum of which is shown in Fig. 3 (b). The signal transmits over the same 10 km SSMF as used in the DL before being converted back to electrical at a PD. After that the IF signal is fed to an electrical frequency sextupler, which up-converts the signal to an 81.6 GHz amplitude shifted-keying (ASK). Detailed characterization of the frequency sextupler can be found in [12]. Similarly, both the active and passive wireless transmitters are tested, by adding or skipping the W-band PA. The signal is then radiated by a 24 dBi horn antenna. At the wireless receiver, the signal is picked up by an identical antenna and then fed to a zero-biased Schottky diode performing a function of an envelope detector (ED) down-converting the W-band signal directly to baseband.
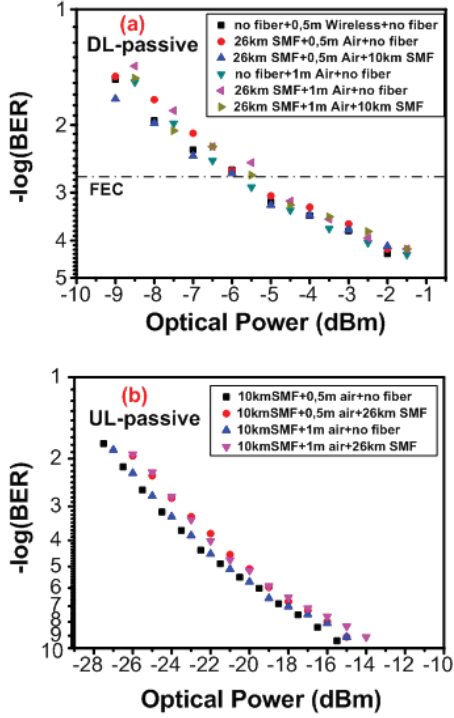
Fig. 4: Measured BER vs. received optical power in the (a) DL and (b) UL, with passive wireless transmitter.

Fig. 5: Measured BER vs. received optical power in the (a) DL and (b) UL, with active wireless transmitter.

The down-converted signal is directly modulated onto lightwave at an distributed feedback laser - electroabsorption modulator (DFB-EAM). After transmitting the same 26 km SSMF fiber link as the DL, the signal is recovered by a 10 G PD and the transmission is evaluated in real time by a bit-error-rate tester (BERT).

III. RESULTS AND DISCUSSION

A. Passive wireless transmitter

The transmission performance of the system is experimentally evaluated by means of bit-error-rates (BERs). In the first step, we skip the W-band PA at the transmitter in both DL and UL directions, benchmarking the transmission performance of the passive wireless transmission case. Figure 4(a) and (b) shows the measured BER curves in both DL and UL in such case. We evaluate the BERs as a function of the received optical power at PD after the last piece of fiber transmission. The wireless power in both directions are adjusted to give the best performance for each wireless distance during the measurements, which means maximizing the signal-to-noise ratio (SNR), while minimizing the signal distortion caused by the LNA saturation at the wireless receiver.

In the DL, as shown in Fig. 4(a), the received QPSK signal after the compounded 36 km SSMF plus the wireless bridge can be recovered within the 7% forward error correction (FEC) limit of 2×10^{-3}. Due to the low radiated RF power in this passive case, the transmitted air distances of the wireless bridge are limited to 1 m. The receiver sensitivity at the FEC limit is -5.5 dBm and -6 dBm for 0.5 m and 1 m wireless transmission without fiber links, respectively. Negligible penalty (<0.5 dB) is observed after transmission over both the first 26 km and the final 10 km fiber links. For the UL, Error free (BER<10^{-9}) transmission can be achieved in all tested cases. The receiver sensitivity at BER of 10^{-9} is -15.5 dBm and -15 dBm for 0.5 m and 1 m wireless transmission with only the first 10 km SSMF fiber link. ~1 dB penalty is introduced by the final 26 km SSMF transmission, which can also be regarded as negligible.

B. Active wireless transmitter

After benchmarking the passive wireless transmission case, we add a W-band PA of 14 dB gain to the wireless transmitter to boost the radiated RF power. By doing this the wireless coverage is highly increased. In the DL direction, we succeeded reaching up to 15 meters wireless transmission with received BER performance within the 7% FEC limit. Figure 5(a) presents the BER performances of the DL

**10km SMF+0.5m Air +26km SMF
Passive wireless Tx**

**10km SMF+1m Air +26km SMF
Passive wireless Tx**

**10km SMF+5m Air +26km SMF
Active wireless Tx**

Fig. 6: Received UL signal eye diagrams at error free (BER<10^{-9}) transmission points.

transmission with wireless distance of 2 m, 5 m, 10 m and 15 m. With only the first 26 km SSMF and the wireless link, the receiver sensitivities at the FEC limit are -9.5 dBm, -7 dBm, -5 dBm and -3 dBm. These performance differences are due to the different SNR at the receiver for different wireless distances. The final 10 km SSMF transmission induces <0.5 dB penalty in all wireless distances. It is noted that longer transmission distances are limited by the frequency selective fading induced by multipath effect in the indoor experimental environment rather than wireless power. Therefore further efforts to mitigate this issue will be necessary.

In the UL direction, the transmission demonstration in the active case is limited to 5 meters due to the physical constrains of the laboratory condition. According to the measured BER curves shown in Fig. 5(b), BER of 10^{-9} can be reached with received power larger than -14 dBm, despite a slight error floor is observed due to the slightly distortion induced by the W-band PA. Again, no penalty of the sensitivity is induced after the final 26 km SSMF transmission. The received eye diagrams after the total 36 km SSMF and 0.5 m / 1 m air transmission in the passive case and 5 m transmission in the active case are shown in Fig. 6. We can see that in the passive case the eye diagrams are clear and open without being distorted, while after adding the W-band PA in the active wireless transmitter case, a certain level of distortion in the eye diagram can be

observed. In spite of certain degradation induced by the active transmitter, achieving transmission over long distance of up to 15 meters can be expected, as the wireless signal has a large enough power margin. Moreover, the UL signal is more immune to frequency selective fading in the indoor environment due to its narrower bandwidth compared with the DL signal.

IV. CONCLUSIONS

This paper has shown an experimental demonstration of a bidirectional hybrid photonic-wireless link with a 81.4 GHz W-band wireless transmission. Two different transmitters are shown, passive and active, the latter enabling a wireless transmission of 15 meters. The fiber guided sections compounded a total of 36 km. The demonstrated channel capacity is 16 Gbit/s, although higher capacity can be achieved since the W-band has more available bandwidth. Both the downlink and the uplink reach error free performance without perceptible error flour, which indicates that the capacity higher bound is yet to be reached.

REFERENCES

[1] T. Nagatsuma et al., "Millimeter- and THz-wave Photonics Towards 100-Gbit/s Wireless Transmission," *Proc. 23rd Annu. Meeting IEEE Photon. Soc.*, We4 2010.

[2] JJ Vegas Olmos et al., "Reconfigurable radio-over-fiber networks: Multiple-access functionality directly over the optical layer," *IEEE Trans. Microw. Theory Techn.*, vol. 58, pp. 3001-3010, 2010.

[3] M. Weiss et al., "27 Gbit/s photonic wireless 60 GHz transmission system using 16-QAM OFDM," *Proc. MWP'09*, PDP, 2009.

[4] W. Jiang et al., "40 Gb/s RoF Signal Transmission with 10 m Wireless Distance at 60 GHz," in *OFC/NFOEC* 2012, paper OTu2H.1.

[5] C. Ho et al., "50-Gb/s Radio-over-Fiber System Employing MIMO and OFDM Modulation at 60 GHz," in *OFC/NFOEC* 2012, paper OM2B.3.

[6] A. Kanno et al., "40 Gb/s W-band (75-110 GHz) 16-QAM radio-over-fiber signal generation and its wireless transmission," *Opt. Exp.*, vol. 19, pp. B56–B63, Dec. 2011.

[7] L. Deng et al., "42.13 Gbit/s 16qam-OFDM photonics-wireless transmission in 75-110 GHz band," *Progress In Electromagnetics Research*, vol. 126, pp. 449-461, 2012.

[8] X. Pang et al., "100 Gbit/s hybrid optical fiber-wireless link in the W-band (75-110 GHz)," *Opt. Exp.*, vol. 19, pp. 24944-24949, Dec. 2011.

[9] J. Zhang et al., "Multichannel 120-Gb/s Data Transmission Over 2 x 2 MIMO Fiber-Wireless Link at W-Band," *IEEE Photon. Technol. Lett.*, vol.25, no.8, pp.780,783, 2013

[10] S. Koenig et al., "100 Gbit/s Wireless Link with mm-Wave Photonics," in *OFC/NFOEC* 2013, paper PDP5B.4.

[11] H. Kiuchi et al., "High Extinction Ratio Mach–Zehnder Modulator Applied to a Highly Stable Optical Signal Generator," *IEEE Trans. Microw. Theory Techn.*, vol.55, pp.1964, 2007.

[12] X. Pang et al., "Experimental characterization of a hybrid fiber-wireless transmission link in the 75 to 110 GHz band," *Opt. Eng.*, vol. 51, pp. 045004-1-045004-5, 2012.

Paper 11: MIMO-OFDM WDM PON with DM-VCSEL for Femtocells Application

Maisara B. Othman, Lei Deng, **Xiaodan Pang**, J. Caminos, W. Kozuch, K. Prince, Xianbin Yu, Jesper B. Jensen, and Idelfonso Tafur Monroy, "MIMO-OFDM WDM PON with DM-VCSEL for Femtocells Application," *Optics Express*, vol. 19, pp. B537-B542, 2011.

MIMO-OFDM WDM PON with DM-VCSEL for femtocells application

M. B. Othman,[1,2,*] Lei Deng,[1] Xiaodan Pang,[1] J. Caminos,[1] W. Kozuch,[1] K. Prince,[1] Xianbin Yu,[1] Jesper Bevensee Jensen,[1] and I. Tafur Monroy[1]

[1]DTU Fotonik, Department of Photonics Engineering, Technical University of Denmark, DK-2800, Kgs. Lyngby, Denmark
[2]Department of Communication Engineering, Faculty of Electrical and Electronic Engineering, UTHM, 86400 Parit Raja, Batu Pahat, Johor, Malaysia
[*]mabio@fotonik.dtu.dk

Abstract: We report on experimental demonstration of 2x2 MIMO-OFDM 5.6-GHz radio over fiber signaling over 20 km WDM-PON with directly modulated (DM) VCSELs for femtocells application. MIMO-OFDM algorithms effectively compensate for impairments in the wireless link. Error-free signal demodulation of 64 subcarrier 4-QAM signals modulated at 198.5 Mb/s net data rate is achieved after fiber and 2 m indoor wireless transmission. We report BER of 7×10^{-3} at the receiver for 16-QAM signals modulated at 397 Mb/s after 1 m of wireless transmission. Performance dependence on different wireless transmission path lengths, antenna separation, and number of subcarriers have been investigated.

OCIS codes: (060.0060) Fiber optics and optical communications; (060.5625) Radio frequency photonics.

References and links

1. A. J. Cooper, "Fiber/Radio for the provision of cordless/mobile telephony services in the access network," Electron. Lett. **26**(24), 2054–2056 (1990).
2. M. Sauer, A. Kobyakov, and J. George, "Radio over fiber for picocellular network architectures," J. Lightwave Technol. **25**(11), 3301–3320 (2007).
3. I. Harjula, A. Ramirez, F. Martinez, D. Zorrilla, M. Katz, and V. Polo, "Practical issues in the combining of MIMO techniques and RoF in OFDM/A systems," Proc. of the 7th WSEAS, 244–248 (2008).
4. V. Tarokh, *New Directions in Wireless Communications Research*, Chap. 2 (Springer, 2009).
5. W. Shieh and I. Djordjevic, *OFDM for Optical Communication*, Chaps. 1, 4, 12 (Elsevier, 2010).
6. J. Zhang and G. de la Roche, *Femtocells: Technologies and Deployment*, Chaps. 2, 4, 9 (Wiley, 2010).
7. S. L. Jansen, I. Morita, T. C. Schenk, and H. Tanaka, "Long-haul transmission of 16x52.5 Gbits/s polarization-division multiplexed OFDM enabled by MIMO processing (Invited)," J. Opt. Netw. **7**(2), 173–182 (2008).
8. S. R. Saunders, S. Carlaw, A. Giustina, R. R. Bhat, V. S. Rao, and R. Siegberg, *Femtocells: Opportunities and Challenges for Business and Technology* (Wiley, 2009).
9. A. J. Paulraj, D. A. Gore, R. U. Nabar, and H. Bolcskei, "An overview of MIMO communications - a key to gigabit wireless," Proc. IEEE **92**(2), 198–218 (2004).
10. J. H. Winters, "Smart antennas for wireless systems," IEEE Personal Commun. **5**(1), 23–27 (1998).
11. K. Iwatsuki, T. Tashiro, K. Hara, T. Taniguchi, J.- Kani, N. Yoshimoto, K. Miyamoto, T. Nishiumi, T. Higashino, K. Tsukamoto, and S. Komaki, "Broadband Ubiquitous Femto-cell Network with DAS over WDM-PON (invited paper)," Proc. SPIE **7958**, 79580I (2011).
12. K. Tsukamoto, T. Nishiumi, T. Yamagami, T. Higashino, S. Komaki, R. Kubo, T. Taniguchi, J.-I. Kani, N. Yoshimoto, H. Kimura, and K. Iwatsuki, "Convergence of WDM Access and Ubiquitous Antenna Architecture for Broadband Wireless Services," PIERS Online **6**(4), 385–389 (2010).
13. W.-S. Tsai, H.-H. Lu, S.-J. Tzeng, T.-S. Chien, S.-H. Chen, and Y.-C. Chi, "Bidirectional dense wavelength-division multiplexing passive optical network based on injection-locked vertical cavity surface-emitting lasers and a data comparator," Opt. Eng. **45**(9), 095003 (2006).
14. E. Kapon and A. Sirbu, "Long-wavelength VCSELs: Power-efficient answer," Nat. Photonics **3**(1), 27–29 (2009).
15. R. Rodes, J. B. Jensen, D. Zibar, C. Neumeyr, E. Roenneberg, J. Rosskopf, M. Ortsiefer, and I. T. Monroy, "All-VCSEL based digital coherent detection link for multi Gbit/s WDM passive optical networks," Opt. Express **18**(24), 24969–24974 (2010).
16. S. Nema, A. Goel, and R. P. Singh, "Integrated DWDM and MIMO-OFDM System for 4G High Capacity Mobile Communication," Signal Process. Int. J. **3**(5), 132–143 (2010).
17. A. Kobyakov, M. Sauer, A. Ng'oma, and J. H. Winters, "Effect of Optical Loss and Antenna Separation in 2x2 MIMO Fiber-Radio Systems," IEEE Trans. Antenn. Propag. **58**(1), 187–194 (2010).

18. M. B. Othman, L. Deng, X. Pang, J. Caminos, W. Kozuch, K. Prince, J. B. Jensen, and I. T. Monroy, "Directly-modulated VCSELs for 2×2 MIMO-OFDM radio over fiber in WDM-PON," ECOC (2011).
19. Y. S. Cho, J. Kim, W. Y. Yang, and C.-G. Kang, *MIMO-OFDM Wireless Communication with MATLAB*, Chap. 6 (Wiley, 2010).
20. X. Liu and F. Buchali, "A novel channel estimation method for PDM-OFDM enabling improved tolerance to WDM nonlinearity," OFC/NFOEC (2009).
21. M. Beltran, J. B. Jensen, R. Llorente, and I. Tafur Monroy, "Experimental Analysis of 60-GHz VCSEL and ECL Photonic Generation and Transmission of Impulse-Radio Ultra-Wideband Signals," IEEE Photon. Technol. Lett. **23**(15), 1055–1057 (2011).

1. Introduction

Wireless networks based on radio over fiber (RoF) technologies have been proposed as a promising cost effective solution to meet ever increasing user demands for high data rate and mobility. Since it was first demonstrated for cordless and mobile telephone services in 1990 [1], extensive research has been carried out to investigate its limitation and develop new high performance RoF technologies. Multiple input multiple output (MIMO) is widely used to increase wireless bit rates [2] and improve larger area coverage than traditional single input single output (SISO) antennas. Such multiple antenna techniques, however, present a challenge for RoF systems, which have to ensure clean transmission of multiple signals between elements of the antenna array, and must mitigate signal path impairments which introduce crosstalk, attenuation and multipath fading [3]. Sophisticated receiver algorithms have to be implemented and receiver components synchronization needs to be very accurate to overcome these path-dependent effects [4].

Orthogonal frequency division multiplexing (OFDM) has emerged as one of the leading modulation techniques in the wireless domain. The combination of OFDM with MIMO provides an attractive solution because OFDM potentially offers high spectral efficiency and resilience to multipath fading. Specifically, MIMO-OFDM signals can be processed using relatively straightforward matrix algebra, and seems to be a promising candidate for RoF system because of the simultaneous compensation of multipath fading in wireless channels and dispersion effects in optical fiber links [5]. Furthermore, OFDM is a future candidate for femtocell application [6] because the interference can be reduced by using more frequency resources. In addition, for multi-carrier systems like OFDM, a large computational complexity will be introduced by using the classical MIMO channel estimation method based on the butterfly structure because an adaptive filter needs to be assigned for each OFDM subcarrier. Consequently, a training-based channel estimation method has the relatively low computational complexity at the receiver [7] and draws more interest in analyzing multi-carrier systems.

The goal of femtocells is to provide reliable communication using existing broadband internet connection and improve the indoor coverage [8]. Femtocells provide many benefits in terms of cost, power, capacity and scalability [6]. However, there are many challenges in the deployment of femtocell such as network architecture, allocation of spectrum resources and the avoidance of electromagnetic interference. One of the main impairments of wireless channels is frequency selective fading. It is especially so in intense multipath environments where the behaviour of the channel differs between different frequencies. This is particularly true in indoor and urban environments. The combination of the throughput enhancement [9] and path diversity [10] offered by MIMO technologies with the robustness of OFDM against frequency selective fading is regarded a very promising basis for femtocell multi-user wireless transmission applications [6]. A small sized femtocell access point (FAP) is usually located in a home or office where it also linked to a broadband internet connection as shown in Fig. 1. The recent explosive growth of the internet has triggered the introduction of a broadband access network based on fiber to-the-office (FTTO) and fiber-to-the-home (FTTH). Therefore, the increasing of wireless demands makes RoF as an enabling technology to support femtocell in the WDM network [11] for FTTH and FTTO network.

Wavelength division multiplexed passive optical network (WDM-PON) systems can transparently deliver radio frequency signaling required to support hybrid fixed and wireless access networking systems. WDM-PON technology is therefore expected to further improve

the throughput in the wireless service area covered by RoF-MIMO antennas [12]. Previously, distributed feedback (DFB) laser diodes have been suggested for use in WDM-PON but have only gained limited industry attention because of the high cost [13]. Directly modulated
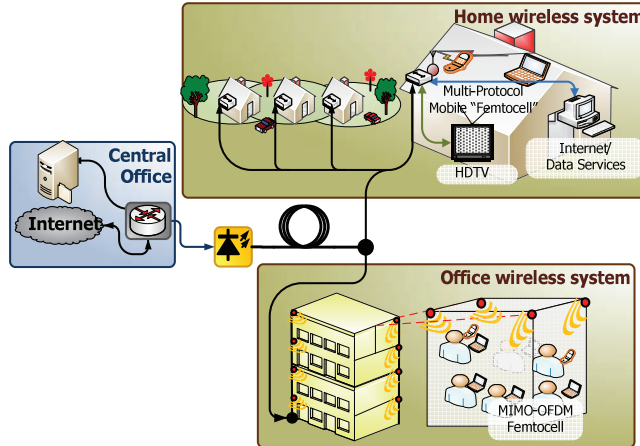

Fig. 1. Femtocell in home and office environment for radio over fiber network.

vertical-cavity surface-emitting lasers (VCSELs) have emerged as an attractive solution for WDM-PON due to the cost effective production, low power consumption [14], and low threshold and driving current operation [15]. Simulation work regarding integration of MIMO-OFDM technology with RoF has been presented in [3], and regarding integration of dense wavelength division multiplexing (DWDM) with MIMO-OFDM in [16]. The experimental work in [17] demonstrates the MIMO RoF concepts, but implemented separate fibers for each remote access unit (RAU).

Previously in [18], we have successfully demonstrated DM-VCSEL 2 x 2 MIMO OFDM over WDM-PON. The OFDM-MIMO training sequence algorithm are applied to compensate the receiver complexity will be further described in this paper. We give an overview of the experimental setup and present the performance evaluation and discussion. Additionally we add investigations of the influence on performance by the number of subcarriers in the OFDM signals, and we present initial experimental results of 16-QAM OFDM-MIMO at 397 Mb/s.

2. OFDM-MIMO training sequence algorithm

Multiple transmit-and-receive antennas in OFDM systems can improve communication quality and capacity. For the OFDM systems with multiple transmitter antennas, each tone at each receiver antenna is associated with multiple channel parameters, which makes channel estimation difficult. Fortunately, channel parameters for different tones of each channel are correlated and the channel estimators are based on this correlation. Several channel estimation schemes have been proposed for the OFDM systems with multiple transmit-and-receive antennas for space diversity, or (MIMO) systems for wireless data access [19]. Channel estimation is important for signal demodulation in MIMO systems, in particular when a large number of subcarriers and advanced multiplexing technique are employed. The training-based channel estimation method is computationally efficient because of its simple expression [20]. However, their transmission efficiencies are reduced due to required overhead of training symbols such as preamble or pilot tones that are transmitted in addition to data symbol. In our work we allocated three training symbols in each of the frame. We implemented different

training symbols for each sub-element of the MIMO-OFDM signal. This enables estimation on the receiver side of the MIMO wireless channel response using this MIMO-OFDM algorithm.

3. Experimental setup

Experimental setup of the system is illustrated in Fig. 2. In the central office (CO), two different real valued 64-subcarrier 4-QAM OFDM baseband signals with 198.5 Mb/s net data rate (excluding the training symbols) and 312 MHz of bandwidth are generated by an arbitrary waveform generator (ArbWaveGen). The OFDM symbols are arranged in frames of 10 symbols. The first 3 symbols implement the training sequence, and 10% cyclic prefix is added. A dual channel baseband MIMO-OFDM signal is generated in the ArbWaveGen, which is then up- converted to a 5.65 GHz radio frequency (RF) carrier; the signal in one arm is up-converted using a mixer and the other arm implements RF up-conversion using the vector signal generator (VSG).
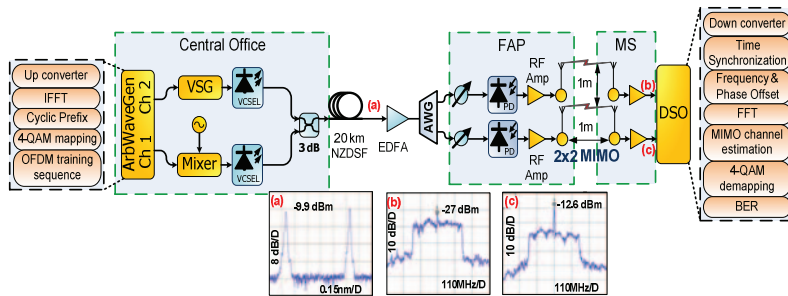

Fig. 2. Experiment setup for all-VCSELs for WDM-PON with 4-QAM OFDM signals over 20 km NZDSF and 2x2 wireless MIMO. RF carrier frequency of 5.65 GHz was used for both branches of the MIMO channel.

Different training sequences are used for each sub-element of the MIMO-OFDM signal; this enables estimation of the MIMO wireless channel response. The electrical MIMO-OFDM signals directly modulate two VCSELs operating at different bias levels to generate different wavelengths of 1535.29 nm and 1536.09 nm. The two optical signals are combined using a 3 dB coupler; they propagate through 20 km non- zero dispersion shifted fiber (NZDSF). The NZDSF is employed due to improved dispersion performance in the PON system [21]. The optical spectrum of the CO transmitter output is shown in Fig. 2(a). After 20 km NZDSF transmission, the downstream WDM signals are divided using an arrayed waveguide grating (AWG). After the photodetector, RF amplifiers boost the signal with 20 dB gain, at the FAP antenna. The wireless signals propagate through 1 meter distance. Elements of the 2x2 antenna array implemented at both femtocell access point (FAP) and mobile station (MS) are vertically spaced by 1 meter; vertical polarization is implemented for the wireless link for femtocell network. At the MS receiver, the signals are captured by two antennas and amplified with a 20 dB gain electrical amplifier. The RF OFDM signals are sampled by a digital sampling scope (DSO), with 20 Gs/s sampling rate. The electrical MIMO-OFDM spectrum is shown in Fig. 2(b) for the VSG and Fig. 2(c) for the mixer.

A digital signal processing (DSP) enabled receiver at the MS uses the different training sequences implemented on sub-elements of the MIMO-OFDM wireless transmission to identify the MIMO signals radiated from each antenna element, and demodulates the OFDM signals. Signal down-conversion, time synchronization, frequency and phase offset removal and fast Fourier transform (FFT) processing are implemented in DSP. Compensation for crosstalk and multipath fading is done using a minimum-mean-square-error (MMSE) algorithm. The bit error rate (BER) is calculated after symbol demapping. Transmission quality was assessed using BER sensitivity to received optical power metric. We consider a

BER of 2×10^{-3}, since forward error correction (FEC) techniques may be applied to obtain error free transmission when the 7% of FEC overhead are taken into account.

4. Results and discussion

Figure 3 presents BER results obtained as the MIMO signal propagates through the system: we distinguish between signal elements upconverted using mixer (solid symbols) and VSG (hollow symbols). Figure 3(a) presents BER variation with received optical power (ROP) at different wireless distances between FAP and MS; results are assessed at 1 m (circle), 2 m (square) and 3 m (triangle). We fixed the separation spacing between the elements of the FAP and MS antenna arrays at 1 meter. The insets show received constellation diagrams observed at the MS; clear 4-QAM OFDM constellations are obtained. The increasing of power penalty is observed as wireless transmission distance increases. With a fixed transmit power, the increased path loss associated with longer wireless transmission lengths results in reduced receiver signal to noise ratio (SNR), leading to increased BER. This agrees well with experimental observations. The MIMO-OFDM signal could be received error free after 2 meters of wireless transmission. This can be clearly seen from the 4-QAM OFDM constellation diagram in Fig. 3(a). After 3 meters wireless transmission, the signals could still be demodulated with a BER below FEC limit of 2×10^{-3}. We observe that the increase of the distance between FAP and MS reduces the performance.

Fig. 3. Showing variation of (a) BER with ROP after fiber transmission, at various distances between RAU and MS: and (b) BER with ROP after fiber transmission, for different antenna separation, with fixed 1 meter distance between RAU and MS. (c) BER with ROP with 4-QAM modulation using different subcarriers: (d) BER with ROP for 4-QAM and 16-QAM modulation scheme with 64 subcarriers and fixed 1 meter distance between RAU and MS. MIMO signal elements which are upconverted using mixer (solid symbols) and VSG (hollow symbols) are identified. Insets show constellation obtained at FEC limit (BER = 2×10^{-3}).

After fiber transmission, the effect of antenna separation on performance is assessed by varying the spacing between the elements of the FAP and MS antenna arrays, while preserving 1 m transmission distance between FAP and MS. The results obtained with antenna spacing of 0.5 m (square), 1 m (circle) and 1.5 m (diamond) are presented in Fig. 3(b). We observed similar performance without any penalty for all separations for both

channels in Fig. 3(b). This is shows that the good transmission was obtained at different antenna separation higher than 0.5m. 4-QAM constellation diagrams for 0.5 m antenna separation are shown for both channels in the Fig. 3(b); these obtained at BER $2x10^{-3}$.

Figure 3(c) shows the different number of subcarriers transmitted in the system over wireless transmission with 4-QAM modulation scheme. The 64 subcarriers represent by (square), 128 subcarriers (circle) and 256 subcarriers (triangle). Theoretically increasing the number of subcarriers should be able to give better performance in a sense that we will be able to handle larger delay spreads. This statement can be supported by looking at the Fig. 3(c) when the number of subcarriers increased from 64 to 128 the ROP performance become better. But several typical implementation problems arise with a large number of subcarriers. When we have large numbers of subcarriers, we have to assign the subcarrier frequencies very close to each other with same amount of bandwidth. We know that the receiver needs to synchronize itself to the carrier frequency very well, otherwise a comparatively small carrier frequency offset may cause a large frequency mismatch between neighboring subcarriers. When the subcarrier spacing is very small, the receiver synchronization components need to be very accurate, which is still not possible with low-cost RF hardware [4]. We observe that at 256 subcarriers, the performance is degraded. We attribute this degradation to a combination of RoF nonlinearities and receiver synchronization to the narrowly spaced subcarriers. Thus, a reasonable trade-off between the subcarrier spacing and the number of subcarriers must be achieved.

A performance comparison between different modulation scheme also been done in this experiment. Figure 3(d) shows the performance evaluation of 4-QAM (square) and 16-QAM (triangle). The insets show received constellation diagrams observed at the MS; 16-QAM OFDM constellations are obtained at BER of 7x10-3 with 397Mb/s net data rate. At higher amplitudes, the constellation symbols are dispersed widely compared with the one at the center because the nonlinearity of the VCSELs. The BER curves for 16-QAM also do not reach the standard FEC limit because the higher the modulation format requires higher power to increase the signal to noise ratio (SNR).

5. Conclusions

We have presented the MIMO-OFDM signal distribution in a WDM-PON system using DM-VCSELs optical sources with wireless MIMO transmission. This provides potentially a cost effective solution for future femtocells access networks. MIMO-OFDM algorithms effectively compensate for impairments in the wireless link. We also investigate the effects of various wireless transmission path lengths, antenna separation, various number of subcarriers in OFDM and different modulation schemes to see the ability of the MIMO-OFDM algorithm to estimate the MIMO wireless channel response. We report error free transmission after 20 km NZDSF and 2 meter 2x2 wireless MIMO-OFDM. The 4-QAM signals modulated at 198.5Mb/s net data rate with 5.65 GHz radio over fiber signaling transmission for WDM-PON system. For 16-QAM, after 1m wireless transmission a BER of $7x10^{-3}$ is reported at the receiver. MIMO-OFDM has a good potential to be implemented for indoor systems because the complexity at the receiver side can be reduced with training sequence algorithm. The maximum number of subcarriers that are allowed in this system is 128 because of the tradeoff between the subcarrier spacing and the number of subcarriers must be achieved. However, for higher modulation technique, powerful receiver algorithm is required to synchronize the signals and higher power to drive the transmission signal. Future work needs to be done for the upstream to demonstrate the bidirectional WDM PON with MIMO in femtocell application. We believe this work can be a potentially attractive candidate for future femtocells network especially for indoor office environment.

Paper 12: Seamless Translation of Optical Fiber PolMux-OFDM into a 2×2 MIMO Wireless Transmission Enabled by Digital Training-Based Fiber-Wireless Channel Estimation

Xiaodan Pang, Lei Deng, Ying Zhao, Maisara B. Othman, Xianbin Yu, Jesper B. Jensen, Darko Zibar, and Idelfonso Tafur Monroy, "Seamless Translation of Optical Fiber PolMux-OFDM into a 2×2 MIMO Wireless Transmission Enabled by Digital Training-Based Fiber-Wireless Channel Estimation," *In Proc. Asia Communications and Photonics Conference and Exhibition, ACP'11*, Shanghai, China, 2011, paper 83090C-1.

Seamless Translation of Optical Fiber PolMux-OFDM into a 2×2 MIMO Wireless Transmission Enabled by Digital Training-Based Fiber-Wireless Channel Estimation

Xiaodan Pang[*a], Ying Zhao[b], Lei Deng[c], M. B. Othman[a], Xianbin Yu[a], J. B. Jensen[a], D. Zibar[a] and I.T. Monroy[a]

[a]DTU Fotonik, Technical University of Denmark, DK-2800, Kgs. Lyngby, Denmark
[b]Department of Electronic Engineering, Tsinghua University, 10084, Beijing, China
[c]School of Optoelectronics Science and Engineering, HuaZhong University of Science and Technology, Wuhan, China

ABSTRACT

We propose and demonstrate a 2×2 multiple-input multiple-output (MIMO) wireless over fiber transmission system. Seamless translation of two orthogonal frequency division multiplexing (OFDM) signals on dual optical polarization states into wireless MIMO transmission at 795.5 Mbit/s net data rate is enabled by using digital training-based channel estimation. A net spectral efficiency of 2.55 bit/s/Hz is achieved.

Keywords: radio frequency photonics, wireless communication, polarization multiplexing, MIMO, OFDM

1. INTRODUCTION

Hybrid optical fiber-wireless transmission systems will play an important part in the next generation user-centered access networking. This truly user-centered network will be powered by free access to services and applications enabled by seamless broadband fiber-wireless connections to various devices nearby. To realize the seamless integration of wireless and fiber-optic networks, the wireless links needs to be developed to preserve transparency to bit-rates and modulation formats.[1]

Orthogonal frequency division multiplexing (OFDM) is a promising candidate signal format for future hybrid optical fiber-wireless access systems. This is because of the inherent high chromatic dispersion tolerance of OFDM signals in optical fibers and its robustness against frequency selective fading or narrowband interference in wireless channels.[2,3] More interestingly, the spectral efficiency in fiber links can be further increased by polarization multiplexing (PolMux).[4] Research on baseband PolMux OFDM transmission has been reported.[5,6] In wireless channels, multiple-input multiple-output (MIMO) technique provides an attractive solution to increase capacity for bandwidth limited systems.[7] Meanwhile, the well-known radio-over-fiber (RoF) technology, which combines optical fiber and wireless techniques, provides a good solution to increase the coverage while maintaining the mobility of the broadband services in the local area networking scenarios. Based on these reasons, a RoF system combining optical PolMux, wireless MIMO and OFDM data format is able to fulfill the requirements of robustness, high flexibility and high spectral efficiency for providing broadband services in local networks. So far, in reported work focusing on PolMux wireless MIMO systems, only simple modulation format like on-off keying (OOK) is used.[7]

In addition, for multi-carrier systems like OFDM, a large computational complexity will be introduced by using the classical MIMO channel estimation method based on the butterfly structure because an adaptive filter needs to be assigned for each OFDM subcarrier. Consequently, a training-based channel estimation method has the relatively low computational complexity at the receiver[5] and draws more interests in analyzing multi-carrier systems.

---

* Send correspondence to Xiaodan Pang: E-mail: xipa@fotonik.dtu.dk, Telephone: +45 4525 7375

In this paper, we experimentally demonstrate a proof-of-concept hybrid fiber wireless system. A PolMux 4-quadrature amplitude modulation (4-QAM) OFDM RoF signal is seamlessly translated into a 2×2 MIMO wireless transmission. By using training sequence-based OFDM-MIMO channel estimation, transmitted wireless signal in both branches are successfully demodulated and a net spectral efficiency of 2.55 bit/s/Hz is achieved.
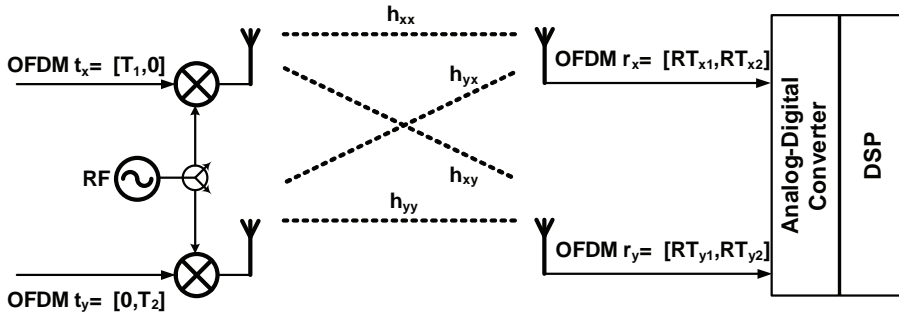

Figure 1. Block diagram of a wireless MIMO Channel

2. TRAINING-BASED CHANNEL ESTIMATION FOR OFDM-MIMO

In optical fiber-wireless MIMO systems, accurate channel estimation is important for signal demodulation. This is because it is the prerequisite for designing the channel equalizer in the digital domain at the receiver. In particular, when a large number of sub-carriers and advanced multiplexing technique are employed, more accurate channel estimation is required. Figure 1 shows the block diagram of a wireless MIMO OFDM channel.

In our proposed PolMux-MIMO system, the total fiber-wireless channel response for a MIMO-OFDM signal can be described as:

$$
\begin{bmatrix} r_x \\ r_y \end{bmatrix} = \begin{bmatrix} h_{xx} & h_{yx} \\ h_{xy} & h_{yy} \end{bmatrix} \times \begin{bmatrix} t_x \\ t_y \end{bmatrix}
\tag{1}
$$

where t_x and t_x respectively stands for the transmitted signal in X and Y branch, and t_y and r_y are the received X and Y branch signal at the receiver. The 2×2 matrix in the equation describes the response of the fiber-wireless MIMO channel, including both the polarization mixing in the fiber and the crosstalk during wireless transmission. To obtain the parameters in the channel transfer matrix is the purpose of the channel estimation.

In order to derive this channel transfer matrix parameters, we transmit a pair of time-interleaved training sequences $T_X = [T_1, 0]^T$, $T_Y = [0, T_2]^T$ in the OFDM signal of the two tributaries, respectively. By precisely controlling the synchronization between the two branches' signals during the fiber-wireless transmission, assuming there is no difference in the arrival time of the two transmitted signals to the receivers in the two branches, the received training sequences in two consecutive training durations can be described as

$$
\begin{bmatrix} RT_{x1} & RT_{x2} \\ RT_{y1} & RT_{y2} \end{bmatrix} = \begin{bmatrix} h_{xx} & h_{yx} \\ h_{xy} & h_{yy} \end{bmatrix} \times \begin{bmatrix} T_1 & 0 \\ 0 & T_2 \end{bmatrix}
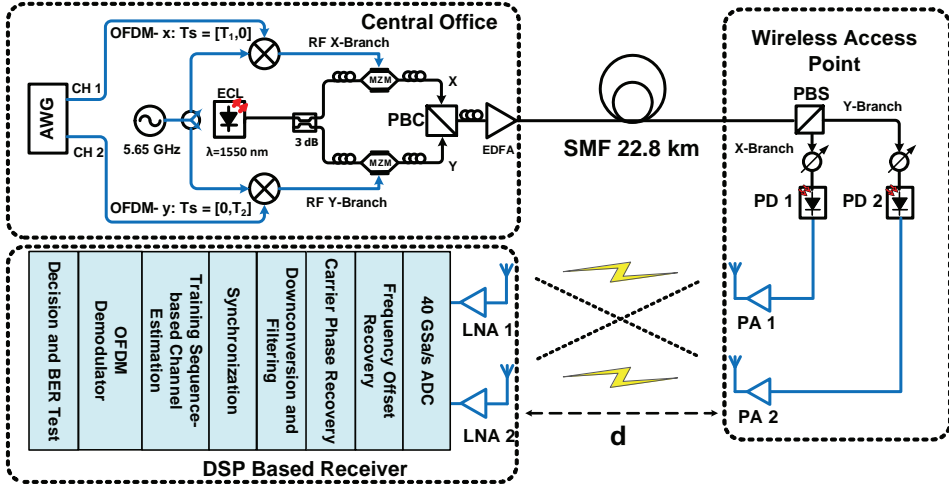\tag{2}
$$

Figure 2. Experimental set-up (AWG: Arbitrary waveform generator; ECL: External cavity laser; MZM: Mach-Zehnder modulator; PBC/PBS: Polarization beam combiner/splitter; PA: Power amplifier; LNA: Low-noise amplifier)

in which RT_{x1} and RT_{x2} stands for the received training symbol from X branch at the first and second training durations respectively. So are the RT_{y1} and RT_{y2} for the Y branch. As these received training symbols can be directly obtained at the receiver side after transmission, the channel transfer matrix then can be easily calculated as

$$\begin{bmatrix} h_{xx} & h_{yx} \\ h_{xy} & h_{yy} \end{bmatrix} = \begin{bmatrix} RT_{x1}/T_1 & RT_{x2}/T_2 \\ RT_{y1}/T_1 & RT_{y2}/T_2 \end{bmatrix} \tag{3}$$

This training-based channel estimation method is computationally efficient because of its simple expression.[8] On the other hand, when implementing this channel estimation method into practice, especially in the wireless MIMO systems, strict synchronization between the two channels is required. By using this method, the MIMO-OFDM signals demodulation algorithm can be implemented digitally.

3. EXPERIMENTAL SETUP

The experimental setup for the PolMux RoF plus wireless 2×2 MIMO system is shown in figure 2. At the RoF signal transmitter, a 1.25 GSa/s arbitrary waveform generator (AWG) is used to generate two baseband real-valued 4-QAM OFDM signals with 64 sub-carriers by an up-sampling factor of 4. The OFDM signals have bandwidth of 625 MHz, corresponding to a gross data rate of 625 Mbit/s in each branch. The signals are arranged in frames of 10 symbols, out of which 3 are training symbols used for synchronization and channel estimation purpose. An cyclic prefix with 0.1 symbol length is added in each symbol. Therefore the signal in each X branch and Y branch has a net data rate of 397.7 Mbit/s. These two OFDM signals with time-interleaved training sequences are then separately up-converted to 5.65 GHz.

A narrow line width external cavity laser (ECL) with central wavelength at 1550 nm is used as the lightwave source. The output optical signal is equally divided into two optical tributaries at a 3 dB coupler. By using

two Mach-Zehnder modulators (MZM) which are biased at their linear points, the two RoF OFDM signals are modulated onto the optical carriers at each of the two branches. After that, by using two polarization controllers to align the polarization states of the signals at the two branches to the X and Y inputs of a polarization beam combiner (PBC), which are designed orthogonal with each other, the two signals are polarization multiplexed at the output of the PBC. A polarization controller placing after the PBC is used for roughly controlling the polarization state of the signal. The output signal then has a net data rate of 795.5 Mbit/s and thus a net spectral efficiency of 2.55 bit/s/Hz is achieved. In fact, the spectral efficiency of this system is expected to be further increased if an AWG with a higher sample rate is employed and higher level modulation formats are to be used.

After being amplified by a booster erbium-doped fiber amplifier (EDFA), the PolMux RoF OFDM signal transmits through a 22.8 km standard signal mode fiber (SSMF). At the wireless access point, the optical signal is divided back to X and Y polarizations by a polarization beam splitter (PBS). After electrical amplification, the optical signals of these two tributaries are converted into the RF domain by two photodiodes (PD), separately, and then fed to two transmitter antennas. At the user side, two receiver antennas, placed with the same separation as the transmitter antennas, form a 2×2 wireless MIMO system. The received signals are then delivered to a 40 GS/s analog-digital convertor (ADC), where the analog signals are converted into the digital domain. A digital signal processing (DSP) based receiver, consisting of frequency and phase recovery, frequency down-conversion, training based MIMO-OFDM channel estimation and OFDM demodulation modules, is used to demodulate the received signals and evaluate bit error rate (BER).

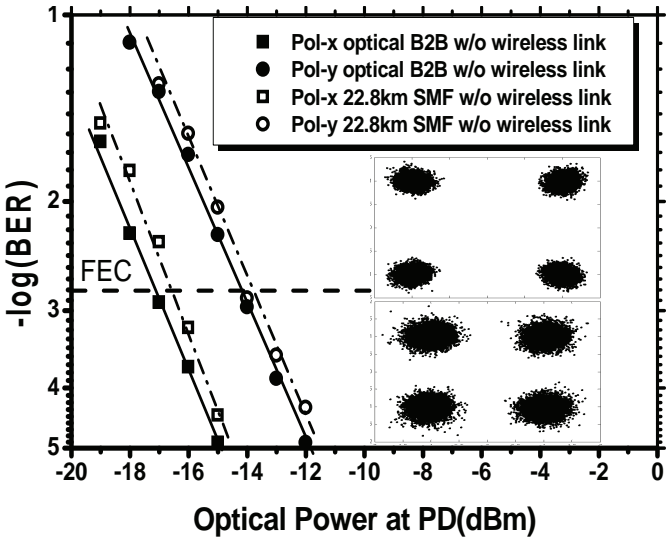Figure 3. BER as a function of optical power at PD without wireless links (upper constellation: X polarization branch after 22.8 km SMF; lower constellation: Y polarization branch)

4. RESULTS

Figure 3 shows the tested bit-error-rate (BER) curves for the two channels' RoF signals in both optical back-to-back and after 22.8 km single mode fiber transmission without any wireless through the air. Considering the

FEC limit at a BER of 2×10^{-3}, from the figure it can be seen that there is around 3 dB difference between X and Y polarization signals. This difference is attributed to the fact that the performances of the components used during the experiment, particularly the responsivity of the two photodiodes used in the two branches are different. Apart from the difference in the performance of components, we can see that the penalty between back-to-back and fiber transmission in both branches are less than 1 dB at the FEC limit. The reason for such small penalty is that at low bit rate the dispersion effect in the fiber is almost negligible. Moreover, it can also be seen from the inserts of figure 3 that the received constellations of optical signals after fiber transmission in X branch (upper) and Y branch (below) are both clear.
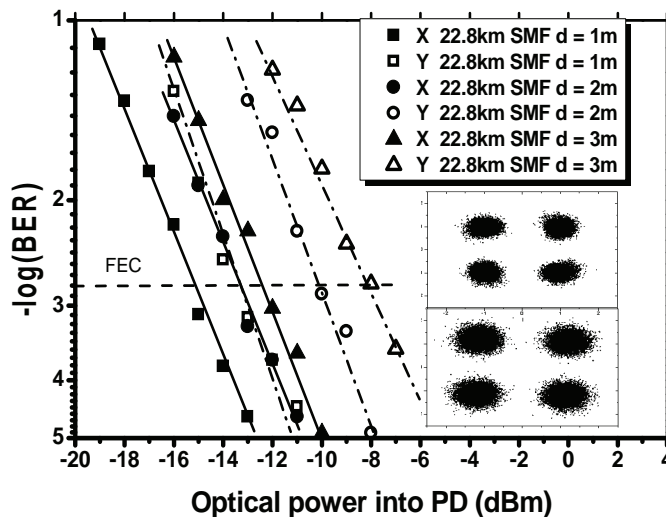

Figure 4. BER as a function of optical power at PD for different wireless distances (upper constellation: X branch at 1 m; lower constellation: Y branch at 1 m)

The BER curves as a function of the received optical power at the photodiode after 22.8 km fiber for different wireless transmission distances are shown in figure 4. From the figure we can see that both X and Y channels achieve up to 3 m wireless transmission with BER well below the FEC limit. Moreover, the power differences between the BER curves achieving FEC limit at 1 meter wireless and 2 meters wireless are smaller than the differences between 2 meters and 3 meters wireless, for both X and Y branches. We attribute this phenomena to the more accurate channel estimation when the crosstalk angle from reference angle becomes smaller, which exceeds the influence of the decreased received RF power. The constellations of received signals after 1 m wireless transmission for X and Y branches are also shown in the insert of figure 4. It can be seen that the clusters in the constellations are still clearly separated.

5. CONCLUSION

We propose an hybrid fiber-wireless system which seamlessly translate the optical PolMux OFDM signal into a wireless MIMO channel. The combination of the PolMux and MIMO technologies enables data transmission with a net spectral efficiency of 2.55 bit/s/Hz. Furthermore, a training-based scheme is digitally developed to estimate the polarization multiplexed MIMO transmission channel. A net data rate of 795.5 Mbps OFDM

signal transmission over 22.8 km SMF plus 3 m wireless distance is successfully demodulated at the receiver for demonstration purpose. This experimental result is believed to be the first step in our ultrahigh capacity fiber-wireless system research. Therefore, higher bit rate with larger bandwidth at higher frequency band together with more advanced modulation formats can be expected in our future works.

REFERENCES

[1] J. Wells, "Faster than fiber: the future of multi-Gb/s wireless," IEEE Microw. Mag, vol. 10, no. 3, pp. 104-112, 2009.

[2] Chow, C.W.; Yeh, C.H.; Wang, C.H.; Wu, C.L.; Chi, S.; Chinlon Lin; , "Studies of OFDM signal for broadband optical access networks," Selected Areas in Communications, IEEE Journal on , vol.28, no.6, pp.800-807, Aug. 2010

[3] Kumar, G.J.R.; Shaji, K.S.; , "Low complexity algorithm for channel estimation of UWB MIMO-OFDM wireless fading channels," Emerging Trends in Robotics and Communication Technologies (INTERACT), 2010 International Conference on , vol., no., pp.125-128, 3-5 Dec. 2010

[4] Alfiad, M.S.; Kuschnerov, M.; Jansen, S.L.; Wuth, T.; van den Borne, D.; de Waardt, H.; , "Transmission of 11 × 224-Gb/s POLMUX-RZ-16QAM over 1500 km of LongLine and pure-silica SMF," Optical Communication (ECOC), 2010 36th European Conference and Exhibition on , vol., no., pp.1-3, 19-23 Sept. 2010

[5] S.L. Jansen; I. Morita; T.C. Schenk; H. Tanaka, "Long-haul transmission of 16×52.5 Gbits/s polarization-division multiplexed OFDM enabled by MIMO processing", J. Opt. Netw., vol. 7, pp. 173-182, 2008.

[6] Cvijetic, N.; Prasad, N.; Dayou Qian; Ting Wang; , "Block-Diagonal MIMO Equalization for Polarization-Multiplexed OFDM Transmission With Direct Detection," Photonics Technology Letters, IEEE , vol.23, no.12, pp.792-794, June15, 2011

[7] Shu-Hao Fan; Hung-Chang Chien; Chowdhury, A.; Cheng Liu; Wei Jian; Yu-Ting Hsueh; Gee-Kung Chang; , "A novel radio-over-fiber system using the xy-MIMO wireless technique for enhanced radio spectral efficiency," Optical Communication (ECOC), 2010 36th European Conference and Exhibition on , vol., no., pp.1-3, 19-23 Sept. 2010

[8] Xiang Liu; F. Buchali, "A novel channel estimation method for PDM-OFDM enabling improved tolerance to WDM nonlinearity" *paper OWW5*, OFC/NFOEC'2009.

Paper 13: 2×2 MIMO-OFDM Gigabit Fiber-Wireless Access System Based on Polarization Division Multiplexed WDM-PON

Lei Deng, **Xiaodan Pang**, Ying Zhao, Maisara B. Othman, Jesper B. Jensen, Darko Zibar, Xianbin Yu, Deming Liu, and Idelfonso Tafur Monroy, "2×2 MIMO-OFDM Gigabit Fiber-Wireless Access System Based on Polarization Division Multiplexed WDM-PON," *Optics Express*, vol. 20, pp. 4369-4375, 2012.

2x2 MIMO-OFDM Gigabit fiber-wireless access system based on polarization division multiplexed WDM-PON

Lei Deng,[1,2] Xiaodan Pang,[2] Ying Zhao,[3] M. B. Othman,[2] Jesper Bevensee Jensen,[2] Darko Zibar,[2] Xianbin Yu,[2,4] Deming Liu,[1,*] and Idelfonso Tafur Monroy[2,5]

[1]College of Optoelectronics Science and Engineering, HuaZhong University of Science and Technology, Wuhan 430074, China
[2]DTU Fotonik, Department of Photonics Engineering, Technical University of Denmark, Kgs. Lyngby DK-2800, Denmark
[3]Department of Electronic Engineering, Tsinghua University, 10084, Beijing, China
[4]xiyu@fotonik.dtu.dk
[5]idtm@fotonik.dtu.dk
[*]dmliu@mail.hust.edu.cn

Abstract: We propose a spectral efficient radio over wavelength division multiplexed passive optical network (WDM-PON) system by combining optical polarization division multiplexing (PDM) and wireless multiple input multiple output (MIMO) spatial multiplexing techniques. In our experiment, a training-based zero forcing (ZF) channel estimation algorithm is designed to compensate the polarization rotation and wireless multipath fading. A 797 Mb/s net data rate QPSK-OFDM signal with error free ($<1 \times 10^{-5}$) performance and a 1.59 Gb/s net data rate 16QAM-OFDM signal with BER performance of 1.2×10^{-2} are achieved after transmission of 22.8 km single mode fiber followed by 3 m and 1 m air distances, respectively.

©2012 Optical Society of America

OCIS codes: (060.0060) Fiber optics and optical communications; (060.2360) Fiber optics links and subsystems; (060.5625) Radio frequency photonics.

References and links

1. J. Zhang and G. de la Roche, **Femtocells: Technologies and Deployment** (Wiley, 2010), Chaps. 2, 4, 9.
2. M. Sauer, A. Kobyakov, and J. George, "Radio over fiber for picocellular network architectures," J. Lightwave Technol. **25**(11), 3301–3320 (2007).
3. K. Tsukamoto, T. Nishiumi, T. Yamagami, T. Higashino, S. Komaki, R. Kubo, T. Taniguchi, J.-I. Kani, N. Yoshimoto, H. Kimura, and K. Iwatsuki, "Convergence of WDM access and ubiquitous antenna architecture for broadband wireless services," PIERS Online **6**(4), 385–389 (2010).
4. S. Chen, Q. Yang, Y. Ma, and W. Shieh, "Real-time multi-gigabit receiver for coherent optical MIMO-OFDM signals," J. Lightwave Technol. **27**(16), 3699–3704 (2009).
5. A. Agmon, B. Schrenk, J. Prat, and M. Nazarathy, "Polarization beamforming PON doubling bidirectional throughput," J. Lightwave Technol. **28**(17), 2579–2585 (2010).
6. G. L. Stuber, J. R. Barry, S. W. Mclaughlin, Y. Li, M. A. Ingram, and T. G. Pratt, "Broadband MIMO-OFDM wireless communications," Proc. IEEE **92**(2), 271–294 (2004).
7. W. Shieh and I. Djordjevic, **OFDM for Optical Communications** (Springer, 2009), Chap. 2.
8. S. L. Jansen, I. Morita, T. C. Schenk, and H. Tanaka, "Long-haul transmission of 16x52.5 Gbits/s polarization-division multiplexed OFDM enabled by MIMO processing (Invited)," J. Opt. Netw. **7**(2), 173–182 (2008).
9. A. Kobyakov, M. Sauer, A. Ng'oma, and J. H. Winters, "Effect of optical loss and antenna separation in 2x2 MIMO fiber-radio systems," IEEE Trans. Antenn. Propag. **58**(1), 187–194 (2010).
10. M. B. Othman, L. Deng, X. Pang, J. Caminos, W. Kozuch, K. Prince, J. B. Jensen, and I. T. Monroy, "Directly-modulated VCSELs for 2x2 MIMO-OFDM radio over fiber in WDM-PON," in **37th European Conference and Exhibition on Optical Communication (ECOC)**, 2011 (2011), Paper We.10.P1.119.
11. M. B. Othman, L. Deng, X. Pang, J. Caminos, W. Kozuch, K. Prince, X. Yu, J. B. Jensen, and I. T. Monroy, "MIMO-OFDM WDM PON with DM-VCSEL for femtocells application," Opt. Express **19**(26), B537–B542 (2011).
12. S.-H. Fan, H.-C. Chien, A. Chowdhury, C. Liu, W. Jian, Y.-T. Hsueh, and G.-K. Chang, "A novel radio-over-fiber system using the xy-MIMO wireless technique for enhanced radio spectral efficiency," in **36th European Conference and Exhibition on Optical Communication (ECOC)**, 2010 (2010), Paper Th.9.B.1.

13. X. Liu and F. Buchali, "Intra-symbol frequency-domain averaging based channel estimation for coherent optical OFDM," Opt. Express **16**(26), 21944–21957 (2008).
14. X. Liu, S. Chandrasekhar, B. Zhu, P. J. Winzer, A. H. Gnauck, and D. W. Peckham, "448-Gb/s reduced-guard-interval CO-OFDM transmission over 2000km of ultra-large-area fiber and five 80-GHz-Grid ROADMs," J. Lightwave Technol. **29**(4), 483–490 (2011).

1. Introduction

Recently, known as 'home base station', femtocell network has been attracting more and more attentions due to its improved indoor coverage, increased capacity and reliable communication compared to macrocell network [1]. Radio-over-fiber (RoF) is considered as a promising candidate technology for femtocell networks because it allows for centralization of signal processing and network management, resulting in simple remote antenna unit (RAU) design and therefore low-cost implementation [2]. However, to meet the ever growing demand for high capacity wireless services like video-on-demand and video conferencing, it is highly desirable to develop new technologies for in-building femtocell networks. Wavelength division multiplexed passive optical network (WDM-PON) technology is therefore widely adopted to increase the capacity of RoF networks and the number of base stations serviced by a single central station [3], and the schematic scenario of in-home and in-building femtocell network is shown in Fig. 1. Moreover, to further increase the capacity per-wavelength of the femtocell network system, high spectral efficiency modulation and transmission technologies are highly desired. For instance, optical polarization division multiplexing (PDM) technology [4, 5] is regarded as an appealing solution by transmitting data in two orthogonal polarization modes within the same spectral range. Likewise, wireless multiple-input multiple-output (MIMO) technology is also a promising technology to exploit the spatial dimension by applying multiple antennas at both the transmitter and receiver sides [6].

Due to the inherent high chromatic dispersion tolerance in optical fibers and robustness against frequency selective fading or narrowband interference in wireless channels, orthogonal frequency division multiplexing (OFDM) has been widely used in current RoF systems [7]. Therefore, a RoF system combining OFDM with PDM and MIMO techniques can fulfill requirements of robustness, high flexibility and high spectral efficiency for providing broadband services in femtocell network. In addition, for multi-carrier systems like OFDM, a large computational complexity will be introduced by using the classical MIMO channel estimation method. In contrast, training-based channel estimation has the relatively low computational complexity at the receiver and draws more interests [8].

To date, some work has presented the concept of MIMO RoF system, but implemented separate fibers for each RAU [9]. A 397 Mb/s 16-quadrature amplitude modulation (QAM) OFDM-MIMO signal over WDM-PON system has been demonstrated in [10, 11] using different wavelengths instead of PDM technique for two transmitter antennas. 5 Gb/s PDM wireless MIMO transmission over 60 GHz wireless link has also been reported in [12], however, employing on-off keying (OOK) modulation. Moreover, some high speed PDM-OFDM transmission systems have been realized in [13, 14] without wireless transmission.

In this paper, we demonstrate a 2x2 MIMO-OFDM radio over WDM-PON system based on polarization division multiplexing and wireless MIMO techniques. The MIMO-OFDM training-based zero forcing (ZF) channel estimation algorithm is designed to compensate the optical polarization rotation and the wireless multipath fading. Furthermore, up to 1.59 Gb/s 16-QAM MIMO-OFDM fiber-wireless transmission over 1 m air distance and 22.8 km single mode fiber (SMF) are achieved for broadband wireless services around Gb/s. We also demonstrate the scalability of the proposed system under different signal to noise ratio (SNR), cross channel interference and wireless coverage by changing the wireless distance in our experiment.
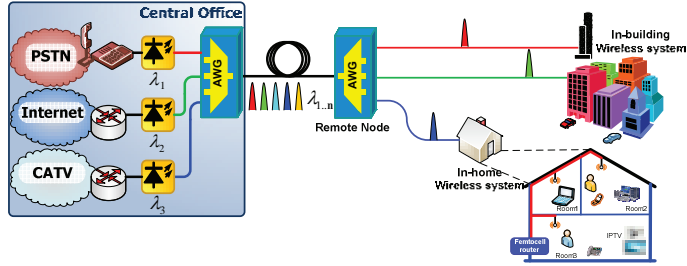
Fig. 1. The schematic scenario of in-home and in-building femtocell network system.

2. Training-based PDM-MIMO-OFDM composite channel estimation

Channel estimation is important for signal demodulation in MIMO system, in particular when a large number of subcarriers and advanced multiplexing technique are employed. In our PDM MIMO-OFDM system, the two orthogonal polarization modes which carry independent OFDM signal will experience a slow polarization rotation, which can be described as:

$$\begin{bmatrix} \mathbf{r_x} \\ \mathbf{r_y} \end{bmatrix} = \mathbf{H_F} \begin{bmatrix} \cos\theta & \sin\theta \\ -\sin\theta & \cos\theta \end{bmatrix} \begin{bmatrix} \mathbf{t_x} \\ \mathbf{t_y} \end{bmatrix}, \tag{1}$$

where $\mathbf{t_x}$ and $\mathbf{r_x}$ are respectively transmitted and received X branch optical signals, so as $\mathbf{t_y}$ and $\mathbf{r_y}$ for Y branch signals. The symbol θ is the rotational angle. $\mathbf{H_F}$ represents the combined effect of fiber chromatic dispersion and polarization dependent loss. In our transmitter, after two photodetectors, two antennas are used to radiate two radio signals, respectively. The wireless channel response could be represented by a matrix $\mathbf{H_{MIMO}}$. Notice that, the polarization rotation in fiber does not change so fast compared to the wireless channel, so it is not difficult to estimate the channel. The hybrid optical and wireless response for our MIMO-OFDM signal can be represented as Eq. (2), where $\mathbf{n_x}$ and $\mathbf{n_y}$ are the random noises, and $\mathbf{h_{xx}}$, $\mathbf{h_{xy}}$, $\mathbf{h_{yx}}$ and $\mathbf{h_{yy}}$ represent the elements in the combined channel response matrix.

$$\begin{bmatrix} \mathbf{r_x} \\ \mathbf{r_y} \end{bmatrix} = \mathbf{H_{MIMO}} \mathbf{H_F} \begin{bmatrix} \cos\theta & \sin\theta \\ -\sin\theta & \cos\theta \end{bmatrix} \begin{bmatrix} \mathbf{t_x} \\ \mathbf{t_y} \end{bmatrix} + \begin{bmatrix} \mathbf{n_x} \\ \mathbf{n_y} \end{bmatrix} = \begin{bmatrix} \mathbf{h_{xx}} & \mathbf{h_{xy}} \\ \mathbf{h_{yx}} & \mathbf{h_{yy}} \end{bmatrix} \begin{bmatrix} \mathbf{t_x} \\ \mathbf{t_y} \end{bmatrix} + \begin{bmatrix} \mathbf{n_x} \\ \mathbf{n_y} \end{bmatrix}. \tag{2}$$

In order to estimate this composite channel transfer matrix at the receiver, we transmit a pair of time-interleaved training sequences $\mathbf{T_X} = [\mathbf{T_1}, 0]^T$, $\mathbf{T_Y} = [0, \mathbf{T_2}]^T$ in the two tributaries. The received training sequences in two consecutive training durations can be expressed as:

$$\begin{bmatrix} \mathbf{RT_{x1}} & \mathbf{RT_{x2}} \\ \mathbf{RT_{y1}} & \mathbf{RT_{y2}} \end{bmatrix} = \begin{bmatrix} \mathbf{h_{xx}} & \mathbf{h_{xy}} \\ \mathbf{h_{yx}} & \mathbf{h_{yy}} \end{bmatrix} \begin{bmatrix} \mathbf{T_1} & 0 \\ 0 & \mathbf{T_2} \end{bmatrix} + \begin{bmatrix} \mathbf{n_{x1}} & \mathbf{n_{x2}} \\ \mathbf{n_{y1}} & \mathbf{n_{y2}} \end{bmatrix}, \tag{3}$$

where $\mathbf{RT_{x1}}$ and $\mathbf{RT_{x2}}$ stand for the received training symbol from X branch at the first and second training duration, respectively, so do $\mathbf{RT_{y1}}$ and $\mathbf{RT_{y2}}$ for the Y branch. And $\mathbf{n_{x1}}$, $\mathbf{n_{x2}}$, $\mathbf{n_{y1}}$ and $\mathbf{n_{y2}}$ are the random noises. The estimated channel transfer matrix then can be easily calculated as Eq. (4). From Eq. (4) we see that even with perfect channel estimation an error term will occur due to the random noises. More advanced algorithm such as minimum mean-squared-error (MMSE) algorithm could be used to improve the performance. However, in our experiment, zero forcing (ZF) instead of MMSE algorithm is used for channel estimation due to its lower computational complexity [4].

$$\begin{bmatrix} \tilde{h}_{xx} & \tilde{h}_{xy} \\ \tilde{h}_{yx} & \tilde{h}_{yy} \end{bmatrix} = \begin{bmatrix} RT_{x1}/T_1 & RT_{x2}/T_2 \\ RT_{y1}/T_1 & RT_{y2}/T_2 \end{bmatrix} = \begin{bmatrix} h_{xx} & h_{xy} \\ h_{yx} & h_{yy} \end{bmatrix} + \begin{bmatrix} n_{x1}/T_1 & n_{x2}/T_2 \\ n_{y1}/T_1 & n_{y2}/T_2 \end{bmatrix}. \tag{4}$$
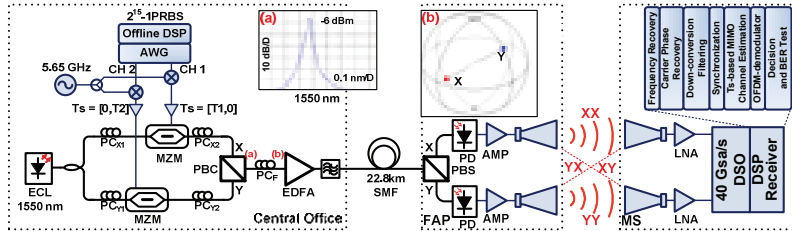

Fig. 2. Experimental setup for the proposed PDM MIMO-OFDM system.

3. Experimental setup

The experimental setup for a single wavelength channel of our proposed MIMO-OFDM signal over PDM WDM-PON system is shown in Fig. 2, for a demonstration purpose. At the central office (CO), a 1.25 GSa/s arbitrary waveform generator (AWG) is performed to generate two-channel baseband real-valued OFDM signals. For each channel, a data stream with a pseudo-random bit sequence (PRBS) length of 2^{15}-1 is mapped onto 129 subcarriers, of which 64 subcarriers carry real QPSK/16-QAM data and one is unfilled DC subcarrier. The remaining 64 subcarriers are the complex conjugate of the aforementioned 64 subcarriers to enforce Hermitian symmetry in the input facet of 256-point inverse fast Fourier transform (IFFT). The cyclic prefix is 1/10 of the IFFT length resulting in an OFDM symbol size of 281. To facilitate time synchronization and MIMO channel estimation, 3 training symbols are inserted at the beginning of each OFDM frame that contains 7 data symbols. Each channel has a net data rate of 398.5 Mb/s (1.25 GSa/s $\times$ 2 $\times$ 64/281 $\times$ 7/10) for QPSK case and 797.1 Mb/s for 16QAM case with a bandwidth of 629.8 MHz (1.25 GSa/s $\times$ 129/256). For simplicity, one frame delay is applied in one channel to decorrelate the two channel signals in the AWG. These two-channel OFDM signals are then separately up-converted to 5.65 GHz. The two RF OFDM signals are used to modulate a 100 kHz-linewidth continuous-wave (CW) external cavity laser (ECL, λ_1 = 1550 nm) at two Mach-Zehnder modulators (MZMs), respectively. A pair of polarization controllers (PCs), namely PC_{X1} and PC_{Y1} are used to optimize the response of the MZMs. PC_{X2} and PC_{Y2} are inserted at the MZMs outputs to align the optical OFDM signal in each channel to the X and Y axis of the following polarization beam combiner (PBC), which then combines the two orthogonal polarizations. Subsequently PC_F is introduced to roughly adjust the polarization of optical signal in the trunk fiber and set the variable power splitting ratio for equal SNR at each transmitter antenna. An erbium-doped fiber amplifer (EDFA) and an optical filter with 0.8 nm bandwidth are used to boost the optical OFDM signal and filter out the outband noise. The optical spectrum and the poincaré sphere of the combined optical signal are shown in the insets of Fig. 2. After excluding the overhead from cyclic prefix and training sequences, the output signal from the PBC is at a net data rate of 797 Mb/s with a spectral efficiency of 1.26 bits/s/Hz for QPSK case and 1.59 Gb/s with a spectral efficiency of 2.52 bits/s/Hz for 16-QAM case.

After 22.8 km of standard single mode fiber (SSMF) propagation, the optical OFDM signal is divided back to X and Y polarizations by a polarization beam splitter (PBS) at the femtocell access point (FAP). By using two 10 GHz bandwidth photodiode (PD), these two tributaries are converted into the RF signals, which are then fed into the FAP antennas after two RF amplifiers with 20 dB gain. After air transmission, these two wireless signals are detected by two receiver antennas and amplified by two 20 dB gain low-noise amplifiers

(LNAs) at the mobile station (MS) receiver. Subsequently, a 40 GSa/s digital sampling oscilloscope (DSO) with 13 GHz analog bandwidth is used to capture these two RF signals. Offline signal demodulation is then performed by a digital signal processing (DSP)-based receiver consisting of frequency and phase recovery, frequency down-conversion, training-based PDM MIMO-OFDM channel estimation, OFDM demodulation modules, data mapping and bit error rate (BER) tester. In our experiment, 80896 bits are calculated for BER test.

Fig. 3. Measured BER performance of Pol-x and Pol-y singal in optical B2B case and 22.8 km SMF fiber transmission case.

Fig. 4. Measured BER performance of PDM MIMO-OFDM signal wireless transmission with 22.8 km SMF fiber transmission.

4. Experimental results and discussions

Figure 3 shows the measured BER in terms of the receiver optical power into the PD in both optical back to back (OB2B) and 22.8 km SMF transmission cases without wireless link. In optical B2B case, we can observe that the receiver sensitivity at the forward-error correction (FEC) limit (BER of 2×10^{-3}) is achieved at −17.2 dBm and −14.3 dBm for the X polarization OFDM signal (Pol-x) and Y polarization OFDM signal (Pol-y), respectively. This 2.9 dB power penalty between Pol-x and Pol-y could be attributed to the different performances of optical and electrical components, particularly the responsivity of the two

photodiodes used in these two branches. Negligible power penalty (around 0.5 dB) is induced after 22.8 km SMF transmission by using training-based MIMO OFDM channel estimation algorithm. The received constellations of Pol-x and Pol-y signal after 22.8 km SMF transmission are shown in the insets of Fig. 3 as well.

Figure 4 presents the wireless transmission BER performance of QPSK-OFDM PDM-MIMO signal after 22.8 km SMF transmission. The separation spacing between the elements of the FAP and MS antenna arrays is fixed at 1 m in the experiment. The received sensitivity at the FEC limit is obtained at −15.2 dBm, −13.4 dBm and −12.5 dBm for the Pol-x signal over air transmission of 1 m, 2 m and 3 m, respectively. The higher required optical power at the FEC limit as air distance increases can be attributed to the increasing cross interference, severer multipath effect and lower SNR. We can also note that larger power penalty is induced between Pol-x and Pol-y for longer air distance. This could be explained by the misalignment between the transmitter and receiver antennas. The received constellations of Pol-x and Pol-y with 3 m air distance and 22.8 km SMF transmission are indicated in the insets of Fig. 4.
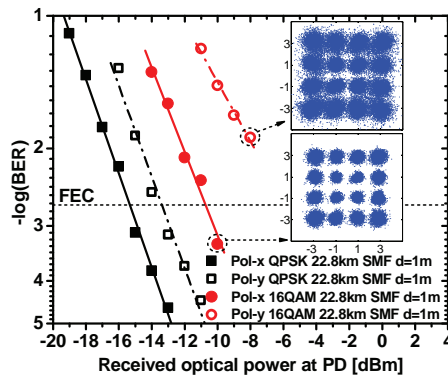

Fig. 5. Measured BER performance of 797 Mb/s QPSK MIMO-OFDM and 1.59 Gb/s 16-QAM MIMO-OFDM signal over 1 m air distance and 22.8 km SMF transmission.

We also test the performance of 1.59 Gb/s 16-QAM MIMO-OFDM signal over 1 m air distance and 22.8 km SMF transmission, as depicted in Fig. 5. We can see that the receiver sensitivity of 16-QAM MIMO-OFDM Pol-x signal to reach the FEC limit is −10.7 dBm. 4.5 dB power penalty compared to QPSK MIMO-OFDM Pol-x wireless transmission can be explained that the constellations states of higher-level modulation format are closer than QPSK, resulting in higher SNR requirement for the same performance. The received constellations of 16-QAM MIMO-OFDM signal are shown in the insets of Fig. 5. The constellation symbols at the higher amplitude are dispersed widely compared to the center ones. This is expected, since OFDM signal is sensitive to the nonlinearity of fiber and wireless transmission due to its high peak-to-average-power-ratio (PAPR). However, we can get BER of 5.01×10^{-4} and 1.28×10^{-2} for 16-QAM MIMO-OFDM Pol-x and Pol-y signal after 1 m air distance and 22.8 km SMF transmission, respectively.

5. Conclusion

We have presented a spectral efficient and WDM-PON compatible MIMO-OFDM access system by combining optical polarization division multiplexing (PDM) and wireless multiple input multiple output (MIMO) spatial multiplexing techniques. Moreover, a training-based zero forcing (ZF) scheme is digitally developed to estimate the polarization multiplexed MIMO transmission channel. A 797 Mb/s net data rate QPSK-OFDM signal and a 1.59 Gb/s

net data rate 16 QAM-OFDM signal at 5.65 GHz RF carrier frequency are transmitted over 3 m and 1 m air distance with 22.8 km single mode fiber, respectively. This system has potential application in future in-door femtocell network supporting Gb/s broadband wireless service.

Acknowledgments

Paper 14: A Spectral Efficient PolMux-QPSK-RoF System with CMA-Based Blind Estimation of a 2 × 2 MIMO Wireless Channel

Xiaodan Pang, Ying Zhao, Lei Deng, Maisara B. Othman, Jesper B. Jensen, Darko Zibar, Xianbin Yu, Deming Liu, and Idelfonso Tafur Monroy, "A Spectral Efficient PolMux-QPSK-RoF System with CMA-Based Blind Estimation of a 2 × 2 MIMO Wireless Channel," *In Proc. IEEE Photonics Conference, IPC'11*, Arlington, VA, USA, 2011, paper TuM2.

A Spectral Efficient PolMux-QPSK-RoF System with CMA-Based Blind Estimation of a 2×2 MIMO Wireless Channel

Xiaodan Pang[*], Ying Zhao[†], Lei Deng[‡], , M. B. Othman[*], Xianbin Yu[*], Jesper B. Jensen[*], I. T. Monroy[*]

[*]Department of Photonics Engineering, Technical University of Denmark, DK-2800, Kgs.Lyngby, Denmark

Email: xipa@fotonik.dtu.dk

[†]Department of Electronic Engineering, Tsinghua University, 10084, Beijing, China

[‡]School of Optoelectronics Science and Engineering, HuaZhong University of Science and Technology, Wuhan, China

Abstract—We experimentally demonstrated a polarization multiplexed (PolMux) RoF system with a 2×2 MIMO wireless link using constant modulus algorithm (CMA) channel estimation. 4 bit/s/Hz spectral efficiency and CMA-enabled 2 dB receiver sensitivity improvement were achieved.

I. INTRODUCTION

Radio-over-fiber (RoF) technology provides a good solution to increase the coverage while maintaining the mobility of the broadband services in the local area network scenario. However, there are challenges when turning this technology into practice, including spectral efficiency, wavelength reuse, wireless channel capacity and components cost [1]. Polarization multiplexing (PolMux) is a promising technique to double the spectral efficiency by transmitting data in two orthogonal polarization modes within the same spectral range. [2]. Furthermore, wireless multiple-input multiple-output (MIMO) technique provides the possibility for bandwidth-limited systems to increase their channel capacity through spatial multiplexing [3]. For the wireless MIMO systems, channel estimation is essential for signal demodulation. Work has been done either using fixed antenna distances [4] or using training-based channel estimation [5]. However, strict synchronizations are required in these methods. In contrast, constant modulus algorithm (CMA) based equalizer is able to make blind estimation when transmitting constant envelope signals, e.g. QPSK [6]. Meanwhile, CMA could also treat the polarization rotation in the fiber together with the wireless crosstalk when combining the PolMux RoF system with MIMO technique.

In this paper we experimentally demonstrate a PolMux-RoF system with a 2×2 MIMO wireless link. By using both PolMux and wireless MIMO, 5 Gbps QPSK signal at 5.4 GHz carrier radio frequency (RF) with spectral efficiency of 4 bit/s/Hz is successfully transmitted through a 10 km SMF plus up to 2 m wireless link. This is the highest wireless capacity reported at this carrier frequency to the best of our knowledge.

II. EXPERIMENTAL SETUP

The experimental setup for our PolMux-MIMO system is shown in Fig. 1. Two 1.25 Gbps pseudorandom bit sequences (PRBS) with a bit length of $2^{15} - 1$ are generated from a
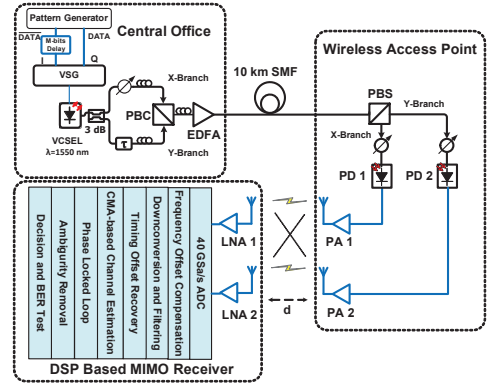

Fig. 1. Experimental set-up (VSG: Vector signal generator; PBC/PBS: Polarization beam combiner/splitter; PA: Power amplifier; LNA: Low-noise amplifier)

pattern generator. These two data sequences are combined and modulated as in-phase and quadrature components at a vector signal generator (VSG) to generate a 2.5 Gbps electrical QPSK signal with 5.4 GHz carrier frequency. The signal is directly modulated on to the lightwave by using a vertical-cavity surface-emitting laser (VCSEL) at central wavelength 1550 nm. After a 3 dB power divider and by adding a delay in one branch, the signals at the two branches become uncorrelated, representing two independent RoF QPSK signals. The two signals are polarization multiplexed at a polarization beam combiner (PBC). The combined PolMux QPSK RoF signal with data rate of 5 Gbps is amplified by a booster Erbium-doped fiber amplifier (EDFA)and transmitted over a 10 km single mode fiber (SMF).

At the wireless access point (WAP), the received signal is aligned to a polarization beam splitter (PBS), which divides the PolMux signal back to X and Y polarization. The RF signals are then recovered by two photodiodes (PD) and fed to two transmitter antennas. The two pairs of transmitter and receiver antennas formed a 2×2 wireless MIMO system. The
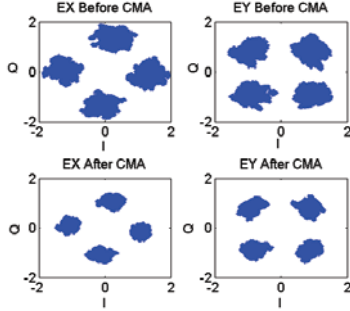
Fig. 2. Received signals' constellations of X and Y branches before (upper) and after (lower) CMA equalization)

separation between the two transmitter antennas is set to 1 meter, so as the separation between the receiver antennas. The two signals received by the receiver antennas are sampled by a 40 GSa/s digital anology converter (ADC) and demodulated by a digital signal processing (DSP) based MIMO receiver.

III. RESULTS

CMA equalizer, which has two input signals with crosstalk from each other, can lock each one component of the equalizer outputs on to each input. Therefore after equalization the crosstalk can be reduced or eliminated. The performance improvement is studied by comparing the received signal quality before and after the CMA processing. As shown in Fig. 2, after back-to-back (B2B) optical PolMux plus 1 m wireless MIMO transmission, the received signals' constellations disseminated due to polarization rotation in optical links and the wireless crosstalk from neighboring transmitter antennas. In contrast, after the optimized CMA equalization, the constellations became much smoother and more compact.

Fig. 3 (a) shows the bit-error rate (BER) as a function of received optical power by the PDs in optical B2B and after 10 km SMF, both with 1 m wireless distance between the transmitting and receiving antennas. Due to the slightly different responsivity of two PDs, the performances have around 0.5 dB penalty between the X and Y branches. Meanwhile, we can observe that there are around 2 dB penalties between 10 km SMF transmission and optical B2B. BER curves for different wireless distances (1 m, 2 m and 3 m) after fiber transmission are shown in Fig. 3 (b). In this figure the BER are calculated for the total 5 Gbps QPSK signals transmitted in both channels. It indicates that there is only 1 dB penalty between 1 m and 1.5 m wireless transmission, while 3 dB when the distance goes up to 2 m, This is because as the attenuation in the air becomes larger, the SNR at the receiver goes lower, so that the system turn to noise-limited,where CMA has limited equalization capability. Considering the FEC limit at a BER of 2×10^{-3}, it is clearly shown that in all measured distances we are able to achieve transmissions with BER well below this limit.
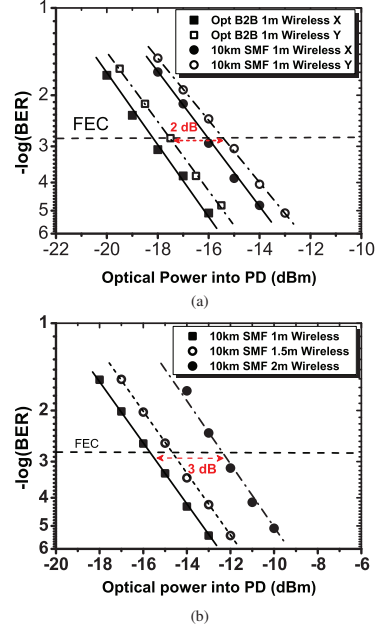

(a)

(b)

Fig. 3. (a) BER as a function of optical power into PD for optical B2B and 10 km SMF transmission, both with 1 m wireless MIMO; (b) BER curves for different wireless distances after 10 km SMF transmission

IV. CONCLUSION

We experimentally demonstrated a VCSEL-based RoF system by combining PolMux and wireless MIMO techniques to increase the spectral efficiency. A CMA-based digital equalizer was proposed to implement blind estimation of a wireless MIMO channel. In the experiment, a 2 m wireless and 10 km SMF transmission of 5.4 GHz QPSK with data rate up to 5 Gbps, and hence 4 bit/s/Hz spectral efficiency was successfully achieved. The performance improvement by the CMA equalizer in its supportable wireless distance makes our spectral efficient MIMO system an attractive solution for providing short range wireless services.

REFERENCES

[1] L. Christina et al., *paper OWP5*, OFC/NFOEC'2009.
[2] A. Sano et al., "Ultra-High Capacity WDM Transmission Using Spectrally-Efficient PDM 16-QAM Modulation and C- and Extended L-Band Wideband Optical Amplification", J. of Lightw. Tech., vol. 29, no.4, pp.578-586, Feb.15, 2011.
[3] M. A. Jensen; J.W. Wallace, "A review of antennas and propagation for MIMO wireless communications", IEEE Trans. on Antennas and Propagation, vol.52, no.11, pp.2810- 2824, Nov. 2004.
[4] Shu-Hao Fan et al., *paper Th.9.B.1*, ECOC 2010.
[5] T.H. Chang; Wei-Cheng Chiang; Y.-W.P. Hong; Chong-Yung Chi, "Training Sequence Design for Discriminatory Channel Estimation in Wireless MIMO Systems", IEEE Transactions on Signal Processing , vol.58, no.12, pp.6223-6237, Dec. 2010.
[6] P. Johannisson et al., *paper Th.9.A.3* ECOC 2010

Bibliography

[1] "Internet World Stats," 2012. [Online].
   Available: www.internetworldstats.com

[2] "Cisco Visual Networking Index: Forecast and Methodology, 2012-2017," May 29, 2013. [Online].
   Available: www.cisco.com

[3] "Cisco Visual Networking Index: Global Mobile Data Traffic Forecast Update, 2012¨C2017," February 6, 2013. [Online].
   Available: www.cisco.com

[4] J. E. Berthold, L. Y. Ong, "Next-Generation Optical Network Architecture and Multidomain Issues," *Proc. of the IEEE*, vol. 100, no. 5, pp. 1130-1139, 2012

[5] E. Wong, "Next-Generation Broadband Access Networks and Technologies," *J. Lightw. Technol.*, vol. 30, no. 4, pp. 597-608, 2012

[6] J.-i. Kani, F. Bourgart, A. Cui, A. Rafel, M. Campbell, R. Davey, and S. Rodrigues, "Next-Generation PON—Part I: Technology Roadmap and General Requirements," *IEEE Commun. Mag.*, vol. 47, no. 11, pp. 43–49, Nov. 2009.

[7] L. Kazovsky, W.-T. Shaw, D. Gutierrez, N. Cheng, and S.-W. Wong, "Next-generation optical access networks," *J. Lightw. Technol.*, vol. 25, no. 11, pp. 3428–3442, Nov. 2007.

[8] K. Prince, *Converged wireline and wireless signal distribution in optical fiber access networks*, PhD Thesis, DTU Fotonik, 2010. ISBN 87-92062-43-1.

[9] T. Nagatsuma, T. Takada, H.-J. Song, K. Ajito, N. Kukutsu, and Y. Kado, "Millimeter- and THz-wave photonics towards 100-Gbit/s

wireless transmission," *IEEE Photonic Society's 23rd Annu. Meeting*, Denver, CO, Nov. 7-11, 2010, paper WE4.

[10] R. Fisher, "60 GHz WPAN Standardization within IEEE 802.15.3c," *International Symposium on Signals, Systems and Electronics, ISSSE'07*, pp. 103-105, 2007

[11] "WirelessHD Specification Version 1.1 Overview," *WirelessHD white paper*, 2010. [Online].
Available: www.wirelesshd.org

[12] ECMA-387 Standard. (2008, Dec.). High Rate 60GHz PHY, MAC and HDMI PAL [Online].
Available: www.ecmainternational.org

[13] "Defining the future of multi-gigabit wireless communication," *WiGig white paper*, 2010. [Online].
Available: wirelessgigabitalliance.org

[14] "Gigabit wireless applications using 60 GHz radios," *Bridgewave whitepaper*, 2006. [Online].
Available: www.bridgewave.com

[15] K. Ramachadran, R. Kokku, R. Mahindra, and S. Rangarajan, "60 GHz Data-Center Networking Wireless $\Rightarrow$ Worry less?" *NEC Technical Report*, 2008.

[16] D. Zibar, A. Caballero Jambrina, X. Yu, X. Pang, A. K. Dogadaev, and I. Tafur Monroy, "Hybrid optical fibre-wireless links at the 75-110 GHz band supporting 100 Gbps transmission capacities," in *International Topical Meeting on Microwave Photonics Conference, MWP'11*, Singapore, November 2011, pp. 445-449.

[17] "FCC online table of frequency allocations." [Online].
Available: www.fcc.gov

[18] J. Yao, "Microwave photonics," *J. Lightwave Technol.* vol. 27, pp. 314-335, 2009.

[19] C. Jastrow, S. Priebe, B. Spitschan, J. Hartmann, M. Jacob, T. Kurner, T. Schrader, T. Kleine-Ostmann, "Wireless digital data transmission at 300 GHz," *Electronics Letters*, vol. 46, no. 9, pp. 661-663, 2010.

[20] A. Hirata, R. Yamaguchi, T. Kosugi, H. Takahashi, K. Murata, T. Nagatsuma, N. Kukutsu, Y. Kado, N. Iai, S. Okabe, S. Kimura, H. Ikegawa, H. Nishikawa, T. Nakayama, T. Inada, "10-Gbit/s Wireless Link Using InP HEMT MMICs for Generating 120-GHz-Band Millimeter-Wave Signal," *IEEE Trans. Microw. Theory Tech.*, vol. 57, no. 5, pp. 1102-1109, 2009.

[21] H.-J. Song, K. Ajito, A. Hirata, A. Wakatsuki, T. Furuta, N. Kukutsu, and T. Nagatsuma, "Multi-gigabit wireless data transmission at over 200-Ghz," in *Proc. 34th International Conference on Infrared, Millimeter and Terahertz Waves, IRMMW-THz'09*, pp. 1-2, 2009.

[22] A. Stohr, S. Babiel, P. Cannard, B. Charbonnier, F. van Dijk, S. Fedderwitz, D. Moodie, L. Pavlovic, L. Ponnampalam, C. Renaud, D. Rogers, V. Rymanov, A. Seeds, A. Steffan, A. Umbach, and M. Weiss, "Millimeter-wave photonic components for broadband wireless systems," *IEEE Trans. Microw. Theory Tech.*, vol. 58, no. 11, pp. 3071-3082, 2010.

[23] J.J. O'Reilly, P.M. Lane, R. Heidemann, R.Hofstetter, "Optical generation of very narrow linewidth millimetre wave signals," *Electronics Letters*, vol. 28, no. 25, pp. 2309-2311, 1992.

[24] D. Wake, C.R. Lima, P.A. Davies, "Optical generation of millimeter-wave signals for fiber-radio systems using a dual-mode DFB semiconductor laser," *IEEE Trans. Microw. Theory Tech.*, vol. 43, no. 9, pp. 2270-2276, 1995.

[25] R.-P. Braun, G. Grosskopf, D. Rohde, F. Schmidt, "Low-phase-noise millimeter-wave generation at 64 GHz and data transmission using optical sideband injection locking," *IEEE Photon. Technol. Lett.*, vol. 10, no. 5, pp. 728¨C730, 1998.

[26] A. Hirata, M.Harada, T. Nagatsuma, "120-GHz wireless link using photonic techniques for generation, modulation, and emission of millimeter-wave signals," *J. Lightw. Technol.*, vol. 21, no. 10, pp. 2145-2153, 2003.

[27] S. Fukushima, C.F.C. Silva, Y. Muramoto, A.J. Seeds, "Optoelectronic millimeter-wave synthesis using an optical frequency comb Generator, optically injection locked lasers, and a unitraveling-carrier photodiode," *J. Lightw. Technol.*, vol. 21, no. 12, pp. 3043- 3051, 2003.

[28] J. Yu, Z. Jia, L. Yi, Y. Su, G.K. Chang, T. Wang, "Optical millimeter-wave generation or up-conversion using external modulators," *IEEE Photon. Technol. Lett.*, vol. 18, no. 1, pp. 265,267, 2006.

[29] W. Jiang, C.T. Lin, A. Ng'oma, P.T. Shih, J. Chen, M. Sauer, F. Annunziata, S. Chi, "Simple 14-Gb/s Short-Range Radio-Over-Fiber System Employing a Single-Electrode MZM for 60-GHz Wireless Applications," *J. Lightw. Technol.*, vol. 28, no. 16, pp. 2238-2246, 2010.

[30] C. Liu, H.C. Chien, Z. Gao, W. Jian, A. Chowdhury, J. Yu; G.K. Chang, "Multi-band 16QAM-OFDM vector signal delivery over 60-GHz DSB-SC optical millimeter-wave through LO enhancement," in *Optical Fiber Communication/National Fiber Optic Engineers Conference, OFC'11*, 2011, paper OThJ2.

[31] A.H.M. Razibul Islam, M. Bakaul, A. Nirmalathas, G.E. Town, "Simplification of millimeter-wave radio-over-fiber system employing heterodyning of uncorrelated optical carriers and self-homodyning of RF signal at the receiver," *Opt. Express*, vol. 20, pp. 5707-5724, 2012.

[32] D. Zibar, R. Sambaraju, R. Alemany, A. Caballero, J. Herrera, I. Tafur Monroy, "Radio-frequency transparent demodulation for broadband hybrid wireless-optical links," *IEEE Photon. Technol. Lett.*, vol. 22, no. 11, pp. 784¨C786, 2010.

[33] A. Caballero, D. Zibar, R. Sambaraju, J. Marti and I. Tafur Monroy, "High-capacity 60 GHz and 75-110 GHz band links employing all-optical OFDM generation and digital coherent detection," *J. Lightw. Technol.*, vol. 30, no. 1, pp. 147-155, 2012.

[34] A. Caballero Jambrina, *High Capacity Radio over Fiber Transmission Links*, PhD Thesis, DTU Fotonik, 2011.

[35] V.R. Nee, and R. Prasad, *OFDM Wireless Multimedia Communications*, Artech House, Boston, 2000.

[36] R. Prasad, *OFDM for Wireless Communications Systems*, Artech House, Boston, 2004.

[37] C.W. Chow, C.H. Yeh, C.H. Wang, C.L. Wu, S. Chi, Lin Chinlon, "Studies of OFDM signal for broadband optical access networks," *IEEE J. Sel. Areas Commun.*, vol. 28, no. 6, pp. 800-807, 2010.

[38] G.J.R. Kumar, K.S. Shaji, "Low complexity algorithm for channel estimation of UWB MIMO-OFDM wireless fading channels," in *International Conference on Emerging Trends in Robotics and Communication Technologies, INTERACT'10*, pp.125-128, 3-5 Dec. 2010.

[39] W. Jiang, C.T. Lin, L.Y. Wang He, C.C. Wei, C. Ho, Y.M. Yang, P.T. Shih, J. Chen, S. Chi, "32.65-Gbps OFDM RoF signal generation at 60GHz employing an adaptive I/Q imbalance correction," in *36th European Conference and Exhibition on Optical Communication, ECOC'10*, 19-23 Sept. 2010, paper Th.9.B.5.

[40] C.C. Wei, C.T. Lin, M.I. Chao, W. Jiang, "Adaptively Modulated OFDM RoF Signals at 60 GHz Over Long-Reach 100-km Transmission Systems Employing Phase Noise Suppression," *IEEE Photon. Technol. Lett.*, vol. 24, no. 1, pp. 49-51, 2012.

[41] N. Guerrero Gonzalez, *Digital Photonic Receivers for Wireless and Wireline Optical Fiber Transmission Links*, PhD Thesis, DTU Fotonik, 2011.

[42] X. Zhang, *Digital Signal Processing for Optical Coherent Communication Systems*, PhD Thesis, DTU Fotonik, 2012.

[43] D. Gesbert, M. Shafi, D. Shiu, P. J. Smith, and A. Naguib, "From theory to practice: An overview of MIMO space-time coded wireless systems," *IEEE J. Sel. Areas Commun.*, vol. 21, no. 3, pp. 281¨C302, 2003.

[44] A. Paulraj, D. A. Gore, R. U. Nabar, and H. H. Böcskei, "An overview of MIMO communications-key to gigabit wireless,",*Proc. IEEE*, vol. 92, no. 2, pp. 198-18, 2004.

[45] T. Higashino, K. Miyamoto, K. Tsukamoto, S. Komaki, T. Tashiro, K. Hara, J. Kani, N. Yoshimoto, and K. Iwatsuki,"A New Confguration of Broadband Wireless Access in Heterogeneous Ubiquitous Antenna and Its Experimental Investigation," *PIERS Proceedings*, 2011.

[46] A.F. Molisch, " MIMO systems with antenna selection - an overview,", *Proceedings Radio and Wireless Conference (RAWCON)*, T2B.1, pp. 167–170, 2003.

[47] A. Kobyakov, M. Sauer, A. Ng'oma, J. H. Winters, "Effect of optical loss and antenna separation in 2×2 multiple input multiple-output fiber-radio systems," *IEEE Trans. Ant. & Prop.*, vol. 58, pp. 187¨C194, 2010.

[48] C.-P. Liu, A. Seeds, "Transmission of MIMO radio signals over fibre using a novel phase quadrature double sideband frequency translation technique," in *Proc. IEEE Microwave Photonics, MWP'08*, pp. 23-26, 2008

[49] Anthony Ng'oma, "Radio-over-Fiber Techniques and Applications for Multi-Gb/s In-Building Wireless Communication," *Access Networks and In-house Communications (ANIC)*, paper ATuB1, 2011.

[50] W. Fan, A. Ghosh, C. Sankaran, P. Fleming, F. Hsieh, S. Benes, "Mobile WiMAX systems: performance and evolution," *IEEE Commun. Mag.*, vol. 46, pp. 41-49, 2008.

[51] H. Bolcskei, " MIMO-OFDM wireless systems: basics, perspectives, and challenges,", *IEEE Wireless Communications*, vol. 13, no.4, pp. 31–37, 2006.

[52] H. Sampath, S. Talwar, J. Tellado, V. Erceg, A.Paulraj, "A fourth-generation MIMO-OFDM broadband wireless system: design, performance, and field trial results," *IEEE Comm. Magazine*, vol. 40 , no.9, pp. 143–149, 2002.

[53] W. Shieh, C. Athaudage, "Coherent optical orthogonal frequency division multiplexing," *Electron. Lett.*, vol. 42, no. 10, pp. 587-589, 2006.

[54] W. Shieh, H. Bao, and Y. Tang, "Coherent optical OFDM: theory and design," *Opt. Express*, vol. 16, pp. 841-59, 2008.

[55] S.L. Jansen, I. Morita, T.C. Schenk, H. Tanaka, "Long-haul transmission of 16×52.5 Gbits/s polarizationdivision multiplexed OFDM enabled by MIMO processing", *J. Opt. Netw.*, vol. 7, pp. 173-182, 2008.

[56] Sander L. Jansen and Itsuro Morita, "Polarization Division-Multiplexed Coherent Optical OFDM Transmission Enabled by MIMO Processing," *High Spectral Density Optical Communication*

Technologies Optical and Fiber Communications Reports, Chapter 8, vol. 6, Part 2, pp. 167-178, Springer, 2010.

[57] X. Liu, F. Buchali, "Intra-symbol frequency-domain averaging based channel estimation for coherent optical OFDM," *Opt. Express* vol. 16, no. 26, pp. 21944-21957, 2008.

[58] X. Liu, F. Buchali, "A novel channel estimation method for PDM-OFDM enabling improved tolerance to WDM nonlinearity," in *Optical Fiber Communication/National Fiber Optic Engineers Conference, OFC'09*, 2009, paper OWW5.

[59] N. Cvijetic, N. Prasad, Q. Dayou, T. Wang, "Block-Diagonal MIMO Equalization for Polarization-Multiplexed OFDM Transmission With Direct Detection," *IEEE Photon. Technol. Lett.*, vol. 23, no. 12, pp. 792-794, 2011.

[60] Y.S. Cho, J. Kim, W.Y. Yang, C.G. Kang, *MIMO-OFDM wireless communications with MATLAB*. John Wiley & Sons (Asia), Singapore, 2010.

[61] C.J. Youn, X. Liu, S. Chandrasekhar, Y. Kwon, J. Kim, J. Choe, K. Choi, E.S. Nam, "An efficient and frequency-offset-tolerant channel estimation and synchronization method for PDM CO-OFDM Transmission," in *36th European Conference and Exhibition on Optical Communication, ECOC'10*, 2010, paper P4.06.

[62] C.R. Johnson, P. Schniter, T.J. Endres, J.D. Behm, D.R. Brown, R.A. Casas, "Blind equalization using the constant modulus criterion: A review," in *Proc. IEEE*, vol. 86, pp. 1927-1950, 1998.

[63] Z. Jia, J. Yu, G. Ellinas, G.K. Chang, "Key enabling technologies for optical-wireless networks: optical millimeter-wave generation, wavelength reuse, and architecture," *J. Lightw. Technol.*, vol. 25, no. 11, pp. 3452-3471, 2007.

[64] J.J. Vegas Olmos, T. Kuri, K. Kitayama, "60-GHz-Band 155-Mb/s and 1.5-Gb/s Baseband Time-Slotted Full-Duplex Radio-Over-Fiber Access Network," *IEEE Photon. Technol. Lett.*, vol. 20, no. 8, pp. 617-619, 2008.

[65] J.J. Vegas Olmos, T. Kuri, T. Sono, K. Tamura, H. Toda, K. Kitayama, "Reconfigurable 2.5-Gb/s Baseband and 60-GHz (155-Mb/s)

Millimeter-Waveband Radio-Over-Fiber (Interleaving) Access Network," *J. Lightw. Technol.*, vol. 26, no. 15, pp. 2506-2512, 2008.

[66] A. Ng'oma, M. Sauer, F. Annunziata, W. J. Jiang, C. T. Lin, J. Chen, P. T. Shih, and S. Chi, "Simple multi-gbps 60 GHz radio-over-fiber links employing optical and electrical data up-conversion and feedforward equalization," in *Optical Fiber Communication/National Fiber Optic Engineers Conference, OFC'09*, 2009, paper OWF2.

[67] A. Chowdhury, H.C. Chien, J. Yu, G.K. Chang, "A novel 50-GHz spaced DWDM 60-GHz millimeter-wave Radio-over-Fiber systems using optical interleaver," in *Optical Fiber Communication/National Fiber Optic Engineers Conference, OFC'09*, 2009, paper OTuB1.

[68] C.P. Tsekrekos, T. Kuri, K. Kitayama, "Simultaneous Transmission of Millimeter-Wave and Baseband Signals Using Wavelength Interleaving and Polarization Multiplexing for an Integrated Reconfigurable Access Network," *IEEE Photon. Technol. Lett.*, vol. 21, no. 21, pp. 1597-1599, 2009.

[69] S.H. Fan, H.C. Chien, Y.T. Hsueh, A. Chowdhury, J. Yu, G.K. Chang, "Simultaneous Transmission of Wireless and Wireline Services Using a Single 60-GHz Radio-Over-Fiber Channel by Coherent Subcarrier Modulation," *IEEE Photon. Technol. Lett.*, vol. 21, no. 16, pp. 1127-1129, 2009.

[70] A. Chowdhury, J. Yu, H.C. Chien, M.F. Huang, T. Wang, G.K. Chang, "Spectrally efficient simultaneous delivery of 112Gbps baseband wireline and 60 GHz MM-wave carrying 10Gbps optical wireless signal in radio-over-fiber WDM-PON access systems," in *35th European Conference and Exhibition on Optical Communication, ECOC'09*, 2009, paper 4.5.1.

[71] C.P. Tsekrekos, T. Kuri, K. Kitayama, "Distribution of Millimeter-Wave and Baseband Services Over an Integrated Reconfigurable Access Network Platform," *J. Lightw. Technol.*, vol. 28, no. 19, pp. 2783-2790, 2010.

[72] J.J. Vegas Olmos, T. Kuri, K. Kitayama, "Reconfigurable Radio-Over-Fiber Networks: Multiple-Access Functionality Directly Over the Optical Layer," *IEEE Trans. Microw. Theory Techn.*, vol. 58, no. 11, pp. 3001-3010, 2010.

[73] C. Lim, C. Pulikkaseril, K.L. Lee, "A Study on LCoS-Based Remote Nodes for 60 GHz Fiber-Wireless Links," *J. Lightw. Technol.*, vol. 30, no. 19, pp. 3110-3117, 2012.

[74] H.C. Chien, Y.T. Hsueh, A. Chowdhury, J. Yu, G.K. Chang, "Optical Millimeter-Wave Generation and Transmission Without Carrier Suppression for Single- and Multi-Band Wireless Over Fiber Applications," *J. Lightw. Technol.*, vol. 28, no. 16, pp. 2230-2237, 2010.

[75] Y.T. Hsueh, Z. Jia, H.C. Chien, A. Chowdhury, J. Yu, G.K. Chang, "Multiband 60-GHz Wireless Over Fiber Access System With High Dispersion Tolerance Using Frequency Tripling Technique," *J. Lightw. Technol.*, vol. 29, no. 8, pp. 1105-1111, 2011.

[76] Z. Jia, J. Yu, Y.T. Hsueh, H.C. Chien, G.K. Chang, "Demonstration of a symmetric bidirectional 60-GHz radio-over-fiber transport system at 2.5-Gb/s over a single 25-km SMF-28," in *34th European Conference and Exhibition on Optical Communication, ECOC'08*, 2008, paper Tu.3.F.5.

[77] Z. Cao, J. Yu, L. Chen, Q. Shu, "Reversely Modulated Optical Single Sideband Scheme and Its Application in a 60-GHz Full Duplex ROF System," *IEEE Photon. Technol. Lett.*, vol. 24, no. 10, pp. 827-829, 2012.

[78] A. Chowdhury, K. Chuang, H.C. Chien, D. Yeh, J. Yu; G.K. Chang, "Field demonstration of Bi-directional millimeter wave RoF systems inter-operable with 60 GHz multi-gigabit CMOS transceivers for in-building HD video and data delivery," in *Optical Fiber Communication/National Fiber Optic Engineers Conference, OFC'11*, 2011, paper OThJ3.

[79] A. Lebedev, T.T. Pham, M. Beltrán, X. Yu, A. Ukhanova, R. Llorente, I. Tafur Monroy, S. Forchhammer, "Optimization of high-definition video coding and hybrid fiber-wireless transmission in the 60 GHz band," *Opt. Express* vol. 19, pp. B895-B904, 2011.

[80] M. Weiß, M. Huchard, A. Stöhr, B. Charbonnier, S. Fedderwitz, D. Jäger, "60-GHz Photonic Millimeter-Wave Link for Short- to Medium-Range Wireless Transmission Up to 12.5 Gb/s," *J. Lightw. Technol.*, vol. 26, no. 15, pp. 2424-2429, 2008.

[81] M. Weiss, A. Stoehr, F. Lecoche, B. Charbonnier, "27 Gbit/s Photonic Wireless 60 GHz Transmission System using 16-QAM OFDM," *International Topical Meeting on Microwave Photonics, MWP'09*, 2009, post deadline paper.

[82] C.T. Lin, J. Chen, W. Jiang, L.Y. Wang He, P.T. Shih, C.H. Ho, S. Chi "Ultra-high data-rate 60 GHz radio-over-fiber systems employing optical frequency multiplication and adaptive OFDM formats," in *Optical Fiber Communication/National Fiber Optic Engineers Conference, OFC'11*, 2011, paper. ThJ6.

[83] C.T. Lin, S.Y. Jian, A. Ng'oma, C.H. Ho, W. Jiang, C.C. Wei, J. Chen, "35-Gb/s 32-QAM Radio-over-Fiber system employing single-sideband single-carrier modulation at 60 GHz," in *Proc. International Topical Meeting on Microwave Photonics, MWP'11*, pp. 246-249, 2011

[84] A. Ng'oma, C.T. Lin, L.Y. Wang He, W. Jiang, F. Annunziata, J. Chen, P.T. Shih, J. George, S. Chi, "31 Gbps RoF system employing adaptive bit-loading OFDM modulation at 60 GHz," in *Optical Fiber Communication/National Fiber Optic Engineers Conference, OFC'11*, 2011, paper OWT7.

[85] C. Liu, H.C. Chien, Z. Gao, W. Jian, A. Chowdhury, J. Yu, G.K. Chang, "Multi-band 16QAM-OFDM vector signal delivery over 60-GHz DSB-SC optical millimeter-wave through LO enhancement," in *Optical Fiber Communication/National Fiber Optic Engineers Conference, OFC'11*, 2011, paper OThJ2.

[86] Y.T. Hsueh, C. Liu, S.H. Fan, J. Yu, G.K, Chang, "A novel full-duplex testbed demonstration of converged all-band 60-GHz radio-over-fiber access architecture," in *Optical Fiber Communication/National Fiber Optic Engineers Conference, OFC'12*, 2012, paper OTu2H.5.

[87] P.T. Shih, A. Ng'oma, C.T. Lin, F. Annunziata, J. Chen, J. George, M. Sauer, S. Chi, "2×21 Gbps symmetrical full-duplex transmission of OFDM wireless signals over a bidirectional IMDD Radio-over-Fiber system at 60 GHz," in *36th European Conference and Exhibition on Optical Communication, ECOC'08*, 2010, paper Th.9.B.4.

[88] W. Jiang, H. Yang, Y.M. Yang, C.T. Lin, A. Ng'oma, "40 Gb/s RoF signal transmission with 10 m wireless distance at 60 GHz," in *Optical Fiber Communication/National Fiber Optic Engineers Conference, OFC'12*, 2012, paper OTu2H.1.

[89] F.M. Kuo, C.B. Huang, J.W. Shi, N.W. Chen, H.-P. Chuang, J.E. Bowers, C.L. Pan, "Remotely Up-Converted 20-Gbit/s Error-Free Wireless On-Off-Keying Data Transmission at W-Band Using an Ultra-Wideband Photonic Transmitter-Mixer," *IEEE Photon. J.*, vol. 3, no. 2, pp. 209-219, 2011.

[90] F.M. Kuo, J.W. Shi, N.W. Chen, J. Hesler, J. Bowers, "25 Gbit/s Error-Free Wireless On-off-keying Data Transmission at W-band using Ultra-Fast Photonic Transmitter-Mixers and Envelop Detectors," in *Optical Fiber Communication/National Fiber Optic Engineers Conference, OFC'12*, 2012, paper OTh1E.5.

[91] A. Kanno, T. Kuri, I. Hosako, T. Kawanishi, Y. Yasumura, Y. Yoshida, K. Kitayama, "20-Gbaud QPSK RoF and millimeter-wave radio transmission," in *Opto-Electronics and Communications Conference, OECC'12*, pp. 735-736, 2012.

[92] A. Kanno, P.T. Dat, T. Kuri, I. Hosako, T. Kawanishi, Y. Yoshida, Y. Yasumura, K. Kitayama, "20-Gbaud QPSK optical and radio transmission using high-gain antennas for resilient access networks," in *IEEE Photonics Society Summer Topical Meeting Series'12*, pp. 145-146, 2012.

[93] A. Kanno, K. Inagaki, I. Morohashi, T. Sakamoto, T. Kuri, I. Hosako, T. Kawanishi, Y. Yoshida, K. Kitayama, "40 Gb/s W-band (75-110 GHz) 16-QAM radio-over-fiber signal generation and its wireless transmission," *Opt. Express*, vol. 19, pp. B56-B63, 2011.

[94] H.J. Song, T. Nagatsuma, "Present and Future of Terahertz Communications," *IEEE Trans. THz Sci. Technol.*, vol. 1, no. 1, pp. 256-263, 2011.

[95] H.J. Song, K. Ajito, Y. Muramoto, A. Wakatsuki, T. Nagatsuma, N. Kukutsu, "24 Gbit/s data transmission in 300 GHz band for future terahertz communications," *Electron. Lett.*, vol. 48, no. 15, pp. 953-954, 2012.

[96] A. Kanno, I. Morohashi, T. Kuri, I. Hosako, T. Kawanishi, Y. Yasumura, Y. Yoshida, K. Kitayama, "16-Gbaud QPSK Radio Transmission Using Optical Frequency Comb with Recirculating Frequency Shifter for 300-GHz RoF Signal,"in *Proc. International Topical Meeting on Microwave Photonics, MWP'12*, S7.6, 2012.

[97] A. Kanno, T. Kuri, I. Hosako, T. Kawanishi, Y. Yasumura, Y. Yoshida, K. Kitayama, "100-GHz and 300-GHz coherent radio-over-fiber transmission using optical frequency comb source," in *Proc. SPIE 8645, Broadband Access Communication Technologies VII*, 864503, January 4, 2013.

[98] S. Koenig, F. Boes, D. Lopez-Diaz, J. Antes, R. Henneberger, R.M. Schmogrow, D. Hillerkuss, R. Palmer, T. Zwick, C. Koos, W. Freude, O. Ambacher, I. Kallfass, J. Leuthold, "100 Gbit/s Wireless Link with mm-Wave Photonics," in *Optical Fiber Communication/National Fiber Optic Engineers Conference, OFC'13*, 2013, paper PDP5B.4.

[99] J. H. Winters, "On the capacity of radio communications systems with diversity in a Rayleigh fading environments," *IEEE J. Selected Areas Communication*, vol.5, no.5, pp. 871-878, 1987.

[100] J.K. Tugnait, "On blind MIMO channel estimation and blind signal separation in unknown additive noise," *First IEEE Signal Processing Workshop on Signal Processing Advances in Wireless Communications*, pp. 53-56, 16-18 April 1997.

[101] G. J. Foschini, M. J. Gans, "On limits of wireless communications in a fading environment when using multiple antennas," *Wireless Personal Communications*, vol. 6, pp. 311-335, 1998.

[102] I. E. Telatar, "Capacity of multi-antenna Gaussion channels," *European Trans. Communications*, vol. 10 , pp. 585-595, 1999.

[103] S.M. Haas, J.H. Shapiro, "Capacity of the multiple-input, multiple-output Poisson channel," in *Proc. IEEE International Symposium on Information Theory'02*, pp. 167, 2002.

[104] Y.A. Alqudah, M. Kavehrad, "MIMO characterization of indoor wireless optical link using a diffuse-transmission configuration," *IEEE Trans. Commun.*, vol. 51, no. 9, pp. 1554-1560, 2003.

[105] S.G. Wilson, M. Brandt-Pearce, Q. Cao, J. Leveque, "Optical MIMO transmission using Q-ary PPM for atmospheric channels," *37th Asilomar Conference on Signals, Systems and Computers'04*, pp. 1090-1094, 9-12 Nov. 2003.

[106] R.C.J. Hsu, A. Shah, B. Jalali, "Coherent optical multiple-input multiple-output communication over multimode fiber," *IEEE International Topical Meeting on Microwave Photonics, MWP'04*, pp. 5-7, 6-6 Oct. 2004.

[107] D. Lenz, B. Rankov, D. Erni, W. Bachtold, A. Wittneben, "MIMO channel for modal multiplexing in highly overmoded optical waveguides," *International Zurich Seminar on Communications'04*, pp. 196-199, 2004.

[108] A.R. Shah, R.C.J. Hsu, B. Jalali, "ISI equalization for a coherent optical MIMO (COMIMO) system," *Conference on Lasers and Electro-Optics, CLEO'05*, pp. 1348-1350, 22-27 May 2005.

[109] Y. Han, and G. Li, "Coherent optical communication using polarization multiple-input-multiple-output," *Opt. Express*, vol. 13, pp. 7527¨C7534, Sep. 2005.

[110] I. Harjula, A. Ramirez, F. Martinez, D. Zorilla, M. Katz, V. Polo, "Practical issues in the combining of MIMO techniques and RoF in OFDM/A systems," *Proc. of the 7th WSEAS*, pp. 244–248 , 2008.

[111] P. Monteiro, S. Pato, J. Pedro, J. Santos, D. Wake, A. Nkansah, N. Gomes, E. Lopez, A. Gameiro, "Radio-over-fiber as the enabler for joint processing of spatially separated radio signals," *IEEE/LEOS Summer Topical Meeting, LEOSST '09*, pp. 43-44, 20-22 July 2009.

[112] S. Nema, A. Goel, R.P. Singh, "Integrated DWDM and MIMO-OFDM System for 4G High Capacity Mobile Communication," *Signal Processing: an International Journal*, vol. 3, no. 5, 2010.

[113] S.H. Fan, H.C. Chien, A. Chowdhury, C. Liu, W. Jian, Y.T. Hsueh, G.K. Chang, "A novel radio-over-fiber system using the xy-MIMO wireless technique for enhanced radio spectral efficiency," in *36th European Conference and Exhibition on Optical Communication, ECOC'10*, 2010, Paper Th.9.B.1.

[114] C.T. Lin, A. Ng'oma, W.Y. Lee, C.Y. Wang, T.H. Lu, W. Jiang, C.H. Ho, C.C. Wei, J. Chen, S. Chi, "MIMO-enhanced radio-over-fiber system at 60GHz," *37th European Conference and Exhibition on Optical Communication, ECOC'11*, 2011, paper We.10.P1.120.

[115] C.T. Lin, A. Ng'oma, W.Y. Lee, C.C. Wei, C.Y. Wang, T.H. Lu, J. Chen, W. Jiang, C.H. Ho, "2×2 MIMO radio-over-fiber system at 60 GHz employing frequency domain equalization," *Optics Express*, vol. 20, no. 1, pp. 562–567, 2012.

[116] C. Ho, R. Sambaraju, W. Jiang, T.H. Lu, C. Wang, H. Yang, W. Lee, C. Lin, C. Wei, S. Chi, A. Ng'oma, "50-Gb/s Radio-over-Fiber System Employing MIMO and OFDM Modulation at 60 GHz," in *Optical Fiber Communication/National Fiber Optic Engineers Conference, OFC'12*, 2012, paper OM2B.3.

[117] K. Huang, Y. Chiang, C. Lin, C. Wei, C. Ho, F. Wu, Y. Chen, S. Chi, "Simple 2×2 MIMO 60-GHz OFDM RoF System with Single-Electrode MZMs Employing Beating Interference Mitigation and IQ Imbalance Compensation," in *Optical Fiber Communication/National Fiber Optic Engineers Conference, OFC'13*, 2013, paper OTu3D.5.

[118] F. Li, Z. Cao, X. Li, Z. Dong, L. Chen, "Fiber-Wireless Transmission System of PDM-MIMO-OFDM at 100 GHz Frequency," *J. Lightw. Technol.*, vol. 31, no. 14, pp. 2394-2399, 2013.

[119] L. Tao, Z. Dong, J. Yu, N. Chi, J. Zhang, X. Li, Y. Shao, G.K. Chang, "Experimental Demonstration of 48-Gb/s PDM-QPSK Radio-Over-Fiber System Over 40-GHz mm-Wave MIMO Wireless Transmission," *IEEE Photon. Technol. Lett.*, vol. 24, no. 24, pp. 2276-2279, 2012.

[120] C. Liu, A. Yi, M. Zhu, J. Wang, L. Zhang, S. Shin, Z. Dong, H. Chien, J. Yu, C. Su, G. Gu, A. Ng'oma, G.K. Chang, "A Novel Direct-Modulation Envelope-Detection Pol-Mux MIMO RoF System based on Blind Equalization Techniques," in *Optical Fiber Communication/National Fiber Optic Engineers Conference, OFC'13*, 2013, paper OM3D.6.

[121] A. Kanno, T. Kuri, I. Hosako, T. Kawanishi, Y. Yasumura, Y. Yoshida, K. Kitayama, "Optical and Radio Seemless MIMO transmission with 20-Gbaud QPSK," *38th European Conference and Exhibition on Optical Communication, ECOC'12*, 2012, Paper We.3.B.2.

[122] A. Kanno, T. Kuri, I. Hosako, T. Kawanishi, Y. Yoshida, y. yasumura, K. Kitayama, "Coherent Optical and Radio Seamless Transmission Based on DSP-Aided Radio-over-Fiber Technology," in *Optical Fiber Communication/National Fiber Optic Engineers Conference, OFC'13*, 2013, paper OTu3D.7.

[123] X. Li, J. Yu, Z. Dong, Z. Cao, N. Chi, J. Zhang, Y. Shao, L. Tao, "Seamless integration of 57.2-Gb/s signal wireline transmission and 100-GHz wireless delivery," *Opt. Express*, vol. 20, pp. 24364-24369, 2012.

[124] X. Li, Z. Dong, J. Yu, N. Chi, Y. Shao, G.K. Chang, "Fiber-wireless transmission system of 108 Gb/s data over 80 km fiber and 2×2 multiple-input multiple-output wireless links at 100 GHz W-band frequency," *Opt. Lett.*, vol. 37, pp. 5106-5108, 2012.

[125] X. Li, Jianjun Yu, Z. Dong, J. Zhang, N. Chi, Jianguo Yu, "Investigation of interference in multiple-input multiple-output wireless transmission at W band for an optical wireless integration system," *Opt. Lett.* vol. 38, pp. 742-744, 2013.

[126] J. Zhang, J. Yu, N. Chi, Z. Dong, X. Li, G.K. Chang, "Multichannel 120-Gb/s Data Transmission Over 2×2 MIMO Fiber-Wireless Link at W-Band," *IEEE Photon. Technol. Lett.*, vol. 25, no. 8, pp. 780-783, 2013.

[127] Z. Dong, J. Yu, X. Li, G. Chang, Z. Cao, "Integration of 112-Gb/s PDM-16QAM Wireline and Wireless Data Delivery in Millimeter Wave RoF System," in *Optical Fiber Communication/National Fiber Optic Engineers Conference, OFC'13*, 2013, paper OM3D.2.

[128] X. Li, J. Yu, J. Zhang, Z. Dong, N. Chi, "Doubling transmission capacity in optical wireless system by antenna horizontal- and vertical-polarization multiplexing," *Opt. Lett.*, vol. 38, pp. 2125-2127, 2013.

[129] H. Sun, K. T. Wu, and K. Roberts, "Real-time measurement of a 40 Gb/s coherent system," *Opt. Express*, vol. 16, pp. 873-879, 2008.

[130] K. Roberts, M. O'Sullivan, K.T. Wu, H. Sun, A. Awadalla, D. Krause, C. Laperle, "Performance of dual-polarization QPSK for optical transport systems," *J. Lightw. Technol.*, vol. 27, no. 16, pp. 3546-3559, 2009.

[131] M. Birk, P. Gerard, R. Curto, L.E. Nelson, X. Zhou, P. Magill, T.J. Schmidt, C. Malouin, B. Zhang, E. Ibragimov, S. Khatana, M. Glavanovic, R. Lofland, R. Marcoccia, R. Saunders, G. Nicholl, M. Nowell, F. Forghieri, "Realtime single-carrier coherent 100 Gb/s PM-QPSK field trial," *J. Lightw. Technol.*, vol. 29, no. 4, pp. 417-425, 2011.

List of Acronyms

ADC analogue-to-digital conversion

ArWG arbitrary waveform generator

ASICs application-specific integrated circuits

ASK amplitude-shift keying

BER bit-error-rate

BS base stations

CMA constant modulus algorithm

CO central office

CS-**DSB** carrier suppressed-DSB

DD direct detection

DFB distributed-feedback laser

DSB double sideband

DSO digital storage oscilloscope

DSP digital signal processing

DWDM dense wavelength division multiplexing

ED envelope detector

FCC Federal Communications Commission

FEC forward error correction

FPGAs field-programmable gate array

HDMI high-definition multimedia interface

HDTV high-definition TV

IF intermediate frequency

IM/DD intensity modulation / direct detection

ISI inter-symbol interference

LO local oscillator

LOS line-of-sight

LTE long term evolution

MIMO multi-input multi-output

MMF multimode fiber

mm-wave millimeter-wave

MZM Mach-Zehnder modulator

UTC-PD uni-traveling carrier photodiode

NGA next generation access

NGN next generation networks

OFC optical frequency comb

OFDM orthogonal frequency-division multiplexing

OOK on-off keying

O/E opto/electro

PAM pulse amplitude modulation

PD photodiode

PDL polarization dependent loss

PolMux polarization multiplexing

PMD polarization mode dispersion

PSK phase-shift keying

QAM quadrature amplitude modulation

QPSK quadrature PSK

RAU remote antenna units

RF radio frequency

RoF radio-over-fiber

SDM spatial division multiplexing

SNR signal-to-noise ratio

SISO single-input single-output

SSB single sideband

WAP wireless access points

WDM wavelength division multiplexing

WLAN wireless local area network

WPAN wireless personal area network

WWAN wireless wide area network

Xiaodan Pang has worked for his Ph.D. degree in optical communications engineering at DTU Fotonik, Technical University of Denmark from 2010 to 2013. He received M.Sc. degree in photonics from Royal Institute of Technology, Stockholm, Sweden in 2010 and B.Sc. degree in optical information science and technology from Shandong University, Jinan, China in 2008. His research interests include hybrid fiber-wireless communication links, coherent optical transmission systems, radio-over-fiber technology and passive optical networks.

DTU Fotonik
Department of Photonics Engineering